

Electronic Thesis and Dissertation Repository

10-11-2018 2:30 PM

Electroflotation for Treatment of Paint Wastewater: Experiments, Kinetics and Hydrodynamics

Syed Reza Mohtashami, *The University of Western Ontario*

Supervisor: Shang, Julie Q., *The University of Western Ontario*

A thesis submitted in partial fulfillment of the requirements for the Doctor of Philosophy degree in Civil and Environmental Engineering

© Syed Reza Mohtashami 2018

Follow this and additional works at: <https://ir.lib.uwo.ca/etd>



Part of the [Environmental Engineering Commons](#), and the [Other Civil and Environmental Engineering Commons](#)

Recommended Citation

Mohtashami, Syed Reza, "Electroflotation for Treatment of Paint Wastewater: Experiments, Kinetics and Hydrodynamics" (2018). *Electronic Thesis and Dissertation Repository*. 5871.
<https://ir.lib.uwo.ca/etd/5871>

This Dissertation/Thesis is brought to you for free and open access by Scholarship@Western. It has been accepted for inclusion in Electronic Thesis and Dissertation Repository by an authorized administrator of Scholarship@Western. For more information, please contact wlsadmin@uwo.ca.

Abstract

Electroflotation (EF) is a process used to remove suspended particles from water using the gas bubbles generated from the water electrolysis. This dissertation focuses on the fundamental principles and applications of EF in the treatment of industrial wastewaters, and in particular, treatment of automotive paint wastewater. In the first part, an extensive review of applications of electroflotation in the treatment of different categories of industrial wastewaters, including the fundamentals of the process, electrode materials, design aspects and process variables, is conducted. The second part is focusing on the kinetic study, statistical analysis and empirical modeling of available experimental data from batch tests of electroflotation treatment of auto paint wastewater. The kinetics of the TSS (Total Suspended Solids) removal was best described with the second-order rate constants. It was confirmed, statistically, that the initial TSS concentration and Current Density were the most significant process variables. Further, empirical equations of the treatment efficiency were produced. In the third part, an experimental program was carried out in a pilot-scale continuous-flow electroflotation reactor on electroflotation treatment of paint wastewater. The total suspended solids removal was investigated as functions of operational parameters, including the hydraulic retention time (HRT), current density and influent total solids (TS) concentration. The maximum TSS removal rate achieved in the experiments was 95%. It was found that the TSS and turbidity removal rates decrease with the increase of influent TS concentration and are directly related to the applied current density and HRT. The electroflotation system showed to be energy-efficient compared to the commercial systems. In the fourth part of this study, by performing the tracer tests, the hydrodynamics and flow characteristics of the electroflotation reactor were investigated. The experiments were conducted at the various HRTs and under the electric current ON/OFF modes. Because of the presence of stagnant regions in the reactor, the calculated residence times were lower than the theoretical HRTs. It was recommended that by selecting a shorter HRT, better flow characteristics can be achieved. Also, the EF gas bubbles, hydrodynamically, showed to improve the treatment efficiency of the EF reactor.

Keywords: Electroflotation, Auto Paint, Industrial Wastewater, Kinetic Study, Residence Time Distribution, Reaction Rate, Statistical Analysis, Wastewater Treatment, Continuous-flow, Empirical Modeling

Co-Authorship

This thesis was prepared in accordance with the guidelines and regulations for a manuscript format stipulated by the Faculty of Graduate Studies at Western University. The following chapters have been modified and submitted to scientific journals with co-authorships as follows:

Chapter 2 Electroflotation for Treatment of Industrial Wastewaters: A Review

A version of this chapter has been submitted to the Journal of Environmental Processes, Springer in 2018.

The contributions of the co-authors are:

Mohtashami, R.: wrote the draft and final version of the paper.

Shang, J. Q.: revised the paper.

Chapter 3 Electroflotation: Kinetic Study and Data Analysis

A version of this chapter has been published in the Journal of Environmental Processes, Springer in 2018.

The contributions of the co-authors are:

Mohtashami, R.: performed the data analysis and empirical modeling and wrote the draft and final version of the paper.

Shang, J. Q.: supervised the experimental project and revised the paper.

Xu, Y.: conducted the laboratory experiments and revised the paper

Chapter 4 Continuous-Flow Electroflotation of Automotive Paint Wastewater

A version of this chapter has been submitted to the Journal Cleaner Production, Elsevier in 2018.

The contributions of the co-authors are:

Mohtashami, R.: conducted the experimental study, performed the data analysis and empirical modeling and wrote the draft and final version of the paper.

Shang, J. Q.: revised the paper.

Chapter 5 Experimental Study of Flow Characteristics in Electroflotation Reactor

A version of this chapter has been submitted to the Water Quality Research Journal, IWA Publishing in 2018.

The contributions of the co-authors are:

Mohtashami, R.: conducted the experimental study, performed the data analysis and wrote the draft and final version of the paper.

Shang, J. Q.: revised the paper.

Acknowledgements

I would like to thank my supervisor Dr. Julie Shang for her ongoing support, help, criticism and humour throughout my study. I have been lucky to have her as my mentor, and finishing my research was not possible without her guidance and encouragement.

I am grateful to Ms. Caitlin Marshall and Mr. Nael Yasri for their assistance during the laboratory experiments. I would like to thank my friends Jack Gu and Raquibul Alam for their support and help. I would also like to thank Profs Imtiaz Shah, Clare Robinson, Ernest Yanful, Konstantin Kreyman and Zhifeng Ding from whom I have learned a lot, attending their classes during my PhD study. Thank you to the Faculty and Staff of the Department of Civil and Environmental Engineering, especially Ms. Kristen Edwards, Ms. Cynthia Quintus, Ms. Stephanie Lawrence and Ms. Whitney Barrett.

I have been blessed with friendships during my studies from outside the department, in particular, during my time with the PSAC Local 610.

Finally, and most importantly, all my love and gratitude to my family, especially my mother.

Dedications

To My Family

Tables of Contents

ABSTRACT.....	I
CO-AUTHORSHIP	III
ACKNOWLEDGEMENTS	V
DEDICATIONS.....	VI
TABLES OF CONTENTS	VII
LIST OF TABLES	XII
LIST OF FIGURES	XVI
LIST OF SYMBOLS	XXV
CHAPTER 1 INTRODUCTION	1
1.1 Background.....	1
1.2 Research Objectives.....	3
1.3 Thesis Outline	4
1.4 Original Contributions	6
References.....	7
CHAPTER 2 ELECTROFLOTATION FOR TREATMENT OF INDUSTRIAL WASTEWATERS: A REVIEW.....	9
2.1 Introduction.....	9
2.2 Fundamentals	10
2.3 Electrodes.....	12
2.3.1 Electrode Material.....	12
2.3.2 Electrode Arrangement	13

2.4 Reactor Design.....	15
2.5 Process Variables	22
2.5.1 Current Density	22
2.5.2 Retention Time.....	23
2.5.3 Pollutant Concentration and Electrical Conductivity	23
2.5.4 Wastewater pH.....	24
2.6 Application for Industrial Effluents	26
2.6.1 Textile Industry	26
2.6.2 Dairy Industry	27
2.6.3 Tannery Industry	28
2.6.4 Semiconductor Industry	29
2.6.5 Pulp and Paper Industry	30
2.6.6 Oil Industry	31
2.6.7 Maritime Transportation	32
2.6.8 Food Industry	32
2.6.9 Laundry	33
2.6.10 Oily Industrial Effluents	34
2.6.11 Metal Finishing	35
2.6.12 Synthetic Effluents Containing Heavy Metals.....	35
2.6.13 Other Industries.....	36
2.7 Full-scale Electroflotation Units	48
2.8 Conclusions.....	50
Acknowledgements.....	51
References.....	52
CHAPTER 3 ELECTROFLOTATION: KINETIC STUDY AND DATA ANALYSIS. 68	
3.1 Kinetic Models.....	68
3.1.1 Theory of Mass Balance	68
3.1.2 Theory of Kinetic Rate.....	71
3.2 Kinetics of Electroflotation of Auto Paint Wastewater	75
3.2.1 First-Order Rate Constant	82
3.2.2 Second-Order Rate Constant.....	84
3.2.3 Discussion	90
3.3 Statistical Analysis: Multivariate and Modelling	94

3.3.1 Analysis of All Wastewater Samples.....	94
3.3.1.1 Influencing Factors: Multivariate Analysis	94
3.3.1.2 Regression Equation	97
3.3.2 Analysis of Individual Wastewater Samples	101
3.3.2.1 ClearCoat_TS1992.....	102
3.3.2.2 ClearCoat_TS4669.....	104
3.3.2.3 Primer_TS1432.....	107
3.3.2.4 Primer_TS2374.....	108
3.3.2.5 MixedPaint_TS2789.....	110
3.3.3 Discussion.....	112
3.4 Conclusions.....	115
Acknowledgments.....	117
References.....	118
CHAPTER 4 CONTINUOUS-FLOW ELECTROFLOTATION OF AUTOMOTIVE PAINT WASTEWATER.....	121
4.1 Introduction.....	121
4.2 Treatment of Automotive Paint Wastewater Using Electroflotation.....	124
4.3 Materials and Methods.....	127
4.3.1 Electroflotation Reactor	127
4.3.2 Electrodes.....	131
4.3.3 Automotive Paint Wastewater	132
4.3.4 Instrumentation	134
4.4 Experimental Results and Discussion.....	136
4.4.1 Effect of Influent Concentration	138
4.4.2 Effect of Applied Current Density.....	143
4.4.3 Effect of Hydraulic Retention Time (HRT).....	148
4.4.4 Automotive Paint Turbidity Removal by Electroflotation.....	151
4.4.5 Electrochemistry and pH Change	153
4.4.6 Power Consumption.....	156
4.5 Statistical Analysis and Empirical Correlation.....	164
4.5.1 Response Surface Methodology (RSM)	164
4.5.2 Multiple Linear Regression.....	166
4.6 Conclusions.....	170

Acknowledgements.....	172
References.....	173
CHAPTER 5 EXPERIMENTAL STUDY OF FLOW CHARACTERISTICS IN ELECTROFLOTATION REACTOR	179
5.1 Introduction.....	179
5.2 Residence Time Distribution (RTD).....	181
5.2.1 Pulse Method	182
5.2.2 Step Method.....	183
5.3 Materials and Methods.....	188
5.3.1 The Reactor	188
5.3.2 Electrodes.....	188
5.3.3 Tracer Fluid.....	189
5.3.4 Measurement methods	190
5.4 Operating Condition.....	191
5.5 Results and Discussion	192
5.5.1 Effect of Hydraulic Retention Time	199
5.5.2 Effect of Gas Bubbles	207
5.5.3 Electroflotation Process Modelling.....	209
5.5.4 Discussion	215
5.6 Conclusions.....	218
Acknowledgements.....	220
References.....	221
CHAPTER 6 SUMMARY, CONCLUSIONS AND RECOMMENDATIONS	223
6.1 Summary.....	223
6.2 Conclusions.....	224
6.2.1 Literature Review.....	224
6.2.2 Kinetic Study	225
6.2.3 Continuous-Flow Treatment Study.....	225
6.2.4 Hydrodynamic Study	226

6.3 Recommendations.....	228
APPENDIX A.....	229
APPENDIX B.....	276
APPENDIX C.....	284
CURRICULUM VITAE.....	296

List of Tables

Table 2.1: Applications of Electroflotation in Treatment of Industrial Effluents.....	38
Table 3.1: ClearCoat_TS4669 Wastewater: TSS (mg/L) concentration change over time under different current densities (Shang, 2004).....	77
Table 3.2: ClearCoat_TS1992 Wastewater: TSS (mg/L) concentration change over time under different current densities (Shang, 2004).....	78
Table 3.3: Primer_TS1432 Wastewater: TSS (mg/L) concentration change over time under different current densities (Shang, 2004).....	79
Table 3.4: Primer_TS2374 Wastewater: TSS (mg/L) concentration change over time under different current densities (Shang, 2004).....	80
Table 3.5: MixedPaint_TS2789 Wastewater: TSS (mg/L) concentration change over time under different current densities (Shang, 2004).....	81
Table 3.6: First-order kinetics, Rate Constant and R-sq values for different wastewaters under different current densities	83
Table 3.7: Second-order kinetics, Rate Constant and R-sq values for different wastewaters under different current densities.....	85
Table 3.8: Treatment efficiency (%Removal of TSS) for different wastewater samples under different current densities (Shang, 2004).....	90
Table 3.9: Best Subsets Regression: k (second-order rate constant) versus Initial TSS, Current-Density, pH, Zeta Potential and Conductivity.....	95
Table 3.10: Stepwise Regression, Backward Elimination Method. Candidate terms: Initial-TSS, Current-Density, pH, Zeta-Potential and Conductivity.....	97
Table 3.11: Analysis of Variance (ANOVA) with response of second-order rate constant, k.....	99

Table 4.1: Wastewater parameters measured in this study	124
Table 4.2: Composition/information on ingredients of PERFECT MATCH Premium Automotive Paint Black (Dupli-Color, 2017).....	133
Table 4.3: Physical and chemical properties of PERFECT MATCH Premium Automotive Paint Black (Dupli-Color, 2017).....	134
Table 4.4: Process variables studied in treatment of auto paint wastewater.....	136
Table 4.5: Experimental plan of treatment of auto paint wastewater using continuous-flow electroflotation system.....	137
Table 4.6: TSS_{inf} and TSS_{eff} for different TS, current densities and retention times in electroflotation reactor	141
Table 4.7: Removal efficiency of electroflotation process in treatment of total suspended solids under different current densities	146
Table 4.8: Values of Turbidity (NTU) the influent and effluent of the electroflotation reactor under different experimental conditions	152
Table 4.9: Values of pH in the influent and effluent of the electroflotation reactor under different experimental conditions	154
Table 4.10: Specific energy consumption, E, of treatment of auto paint wastewater using electroflotation process under different experimental conditions.....	157
Table 4.11: Electric conductivity change in the electroflotation reactor, treating auto paint wastewater.....	161
Table 4.12: Specific energy consumption of electroflotation process treating various types of wastewater.....	163
Table 4.13: Report of Analysis of Variance for RSM analysis with the response of %removal of TSS	165

Table 4.14: Report of Analysis of Variance for linear regression analysis with the response of %removal of TSS.....	167
Table 5.1: Process variables studied in Residence Time Distribution experiments	191
Table 5.2: Theoretical and calculated mean residence time of the reactor under different conditions	198
Table 5.3: Percent dead volume of the electroflotation reactor under different conditions	198
Table 5.4: Parameters and results of the process model	214
Table A.1: Summary of operating parameters (Shang, 2004)	229
Table B.1: TSS values in different conditions	276
Table B.2: Conductivity values in different conditions	278
Table B.3: pH values in different conditions	280
Table B.4: Turbidity values in different conditions.....	282
Table C.1: RTD experiment results for HRT=7.4 min and Electroflotation=ON: EC, concentration, F(t) and E(t) values at different times	284
Table C.2: RTD experiment results for HRT=7.4 min and Electroflotation=OFF: EC, concentration, F(t) and E(t) values at different times	286
Table C.3: RTD experiment results for HRT=8.5 min and Electroflotation=ON: EC, concentration, F(t) and E(t) values at different times	288
Table C.4: RTD experiment results for HRT=8.5 min and Electroflotation=OFF: EC, concentration, F(t) and E(t) values at different times	290
Table C.5: RTD experiment results for HRT=15.3 min and Electroflotation=ON: EC, concentration, F(t) and E(t) values at different times	292

Table C.6: RTD experiment results for HRT=15.3 min and Electroflotation=OFF: EC, concentration, F(t) and E(t) values at different times 294

List of Figures

Figure 2.1: Schematics of electrodes connection modes: (a) Bipolar, (b) Monopolar series, (c) Monopolar parallel	14
Figure 2.2: Schematics of a simple batch electroflotation system with vertical monopolar electrodes	15
Figure 2.3: Batch cylindrical reactor with rotating cathode electrode (Un et al., 2013) ..	16
Figure 2.4: Batch acrylic cylindrical cell with iron cylinder electrodes (Nunez et al., 2011)	17
Figure 2.5: Batch reactor with cylindrical stainless steel cathodes and rod-shaped iron anodes (Lakshmanan et al., 2010).....	18
Figure 2.6: Schematic of 3-stage electrochemical reactor. Electrocoagulation Unit, Electroflotation Unit, Precipitation Tank (Hassani et al., 2016).....	19
Figure 2.7: Bipolar up-flow reactor with separate flotation unit (Ge et al., 2004)	19
Figure 2.8: U-shaped reactor/cathode with screw-type anode (Un et al., 2014)	20
Figure 2.9: Enclosed electrochemical cell with sheet electrodes (Lacasa et al., 2011)	21
Figure 2.10: Schematic of E-Flo Dr. Baer electroflotation package.....	48
Figure 2.11: Schematic of electroflotation unit manufactured by Mendeleev University Science Park.....	49
Figure 3.1: Schematic of a complete-mix reactor with inflow and outflow	68
Figure 3.2: Schematic of the electroflotation batch experimental system (Shang, 2004)	75
Figure 3.3: ClearCoat_TS4669 Wastewater, Treatment Efficiency (%Removal) and Second-order Rate Constant ($k \times 10^4$) vs. Current Density (A/m^2).....	87

Figure 3.4: ClearCoat_TS1992 Wastewater, Treatment Efficiency (%Removal) and Second-order Rate Constant ($k \times 10^4$) vs. Current Density (A/m^2).....	87
Figure 3.5: Primer_TS1432 Wastewater, Treatment Efficiency (%Removal) and Second-order Rate Constant ($k \times 10^4$) vs. Current Density (A/m^2).....	88
Figure 3.6: Primer_TS2374 Wastewater, Treatment Efficiency (%Removal) and Second-order Rate Constant ($k \times 10^4$) vs. Current Density (A/m^2).....	88
Figure 3.7: MixedPaint_TS2789 Wastewater, Treatment Efficiency (%Removal) and Second-order Rate Constant ($k \times 10^4$) vs. Current Density (A/m^2).....	89
Figure 3.8: Initial phase and long-term behavior of flotation process (Matis, 1994)	91
Figure 3.9: First-order behavior of electroflotation process in short-term experiments...	92
Figure 3.10: Contour plot of second-order rate constant, k , vs Current Density (J) and Initial TSS concentration	100
Figure 3.11: Surface plot of second-order rate constant, k , vs Current Density (J) and Initial TSS concentration	101
Figure 3.12: Contour plot of %removal of TSS for ClearCoat_TS1992 wastewater vs Current Density and Time.....	103
Figure 3.13: Surface plot of %removal of TSS for ClearCoat_TS1992 wastewater vs Current Density and Time.....	104
Figure 3.14: Contour plot of %removal of TSS for ClearCoat_TS4669 wastewater vs Current Density and Time.....	106
Figure 3.15: Surface plot of %removal of TSS for ClearCoat_TS4669 wastewater vs Current Density and Time.....	107
Figure 3.16: Contour plot of %removal of TSS for Primer_TS2374 wastewater vs Current Density and Time	109

Figure 3.17: Surface plot of %removal of TSS for Primer_TS2374 wastewater vs Current Density and Time	110
Figure 3.18: Contour plot of %removal of TSS for MixedPaint_TS2789 wastewater vs Current Density and Time.....	111
Figure 3.19: Surface plot of %removal of TSS for MixedPaint_TS2789 wastewater vs Current Density and Time.....	112
Figure 4.1: Schematic of the experimental setup and electroflotation reactor	127
Figure 4.2: Electroflotation tank used for the treatment experiments	128
Figure 4.3: Details of weir installed in electroflotation reactor	129
Figure 4.4: Continuous-horizontal-flow electroflotation reactors used by other researchers (a: Mollah et al. 2004; b: Zhou et al. 2016; c: Hassani et al. 2016).....	130
Figure 4.5: Internal baffled installed in electroflotation reactor	131
Figure 4.6: Details of electrodes module	132
Figure 4.7: Photo of electrodes used in treatment experiments	132
Figure 4.8: %Removal of TSS at different current densities and influent TS with HRT 4 minutes.....	139
Figure 4.9: %Removal of TSS at different current densities and influent TS with HRT 6 minutes.....	139
Figure 4.10: %Removal of TSS at different current densities and influent TS with HRT 8 minutes.....	140
Figure 4.11: %Removal of TSS at different current densities and HRT with influent TS of 500 mg/L.....	143

Figure 4.12: %Removal of TSS at different current densities and HRT with influent TS of 1500 mg/L.....	144
Figure 4.13: %Removal of TSS at different current densities and HRT with influent TS of 3000 mg/L.....	144
Figure 4.14: %Removal of TSS at different Hydraulic Retention Times and influent TS with applied current density of 50 A/m ²	149
Figure 4.15: %Removal of TSS at different Hydraulic Retention Times and influent TS with applied current density of 75 A/m ²	149
Figure 4.16: %Removal of TSS at different Hydraulic Retention Times and influent TS with applied current density of 100 A/m ²	150
Figure 4.17: Specific Energy Consumption at different current densities and influent TS with HRT 4 minutes.....	158
Figure 4.18: Specific Energy Consumption at different current densities and influent TS with HRT 6 minutes.....	159
Figure 4.19: Specific Energy Consumption at different current densities and influent TS with HRT 8 minutes.....	159
Figure 4.20: Contour plot of removal efficiency of TSS, Y (C: Influent TSS mg/L; J: Current Density, A/m ² and t: HRT, min).....	168
Figure 4.21: Surface plot of removal efficiency of TSS, Y (C: Influent TSS mg/L; J: Current Density, A/m ² and t: HRT, min).....	169
Figure 5.1: Schematic of Residence Time Distribution (RTD) test.....	181
Figure 5.2: (a) Injection and (b) response curve in pulse method	182
Figure 5.3: (a) Injection and (b) response curve in step method	184
Figure 5.4: Relationship between E(t) and F(t) (Levenspiel, 1999)	186

Figure 5.5: Relationship between the NaCl concentration and electrical conductivity..	189
Figure 5.6: F(t) curve of the RTD experiments of the electroflotation reactor HRT=7.4 min	192
Figure 5.7: F(t) curve of the RTD experiments of the electroflotation reactor HRT=8.5 min	193
Figure 5.8: F(t) curve of the RTD experiments of the electroflotation reactor HRT=15.3 min	193
Figure 5.9: E(t) curve of the RTD experiments of the electroflotation reactor HRT=7.4 min	194
Figure 5.10: E(t) curve of the RTD experiments of the electroflotation reactor HRT=8.5 min	195
Figure 5.11: E(t) curve of the RTD experiments of the electroflotation reactor HRT=15.3 min	195
Figure 5.12: Possible regions of the flow recirculation in the EF reactor	197
Figure 5.13: F(t) curve of the RTD experiments of the electroflotation reactor EF:ON	199
Figure 5.14: F(t) curve of the RTD experiments of the electroflotation reactor EF:OFF	200
Figure 5.15: E(t) curve of the RTD experiments of the electroflotation reactor EF:ON	200
Figure 5.16: E(t) curve of the RTD experiments of the electroflotation reactor EF:OFF	201
Figure 5.17: F(t) curve of the RTD experiments vs θ , EF: ON	202
Figure 5.18: F(t) curve of the RTD experiments vs θ , EF: OFF	202
Figure 5.19: E(t) curve of the RTD experiments vs θ , EF: ON	203

Figure 5.20: E(t) curve of the RTD experiments vs θ , EF: OFF.....	204
Figure 5.21: Dead volume of the EF reactor in different conditions	205
Figure 5.22: Mean residence time of the EF reactor in different conditions	205
Figure 5.23: RTD spread parameter, σ^2 , in different conditions.....	206
Figure 5.24: RTD skewness parameter, s^3 , in different conditions	207
Figure 5.25: Variables for a closed plug-flow reactor with reaction and dispersion (Levenspiel, 1999)	210
Figure 5.26: Graphical solution of axial dispersion model for second-order reactions (Levenspiel, 1999)	212
Figure 5.27: (a) Ideal plug-flow E curve; (b) Actual plug-flow E curve.....	215
Figure A.1: ClearCoat_TS4669 Wastewater, Current Density 11 (A/m ²): First-order Rate Constant (k = slope).....	236
Figure A.2: ClearCoat_TS4669 Wastewater, Current Density 22 (A/m ²): First-order Rate Constant (k = slope).....	237
Figure A.3: ClearCoat_TS4669 Wastewater, Current Density 33 (A/m ²): First-order Rate Constant (k = slope).....	238
Figure A.4: ClearCoat_TS4669 Wastewater, Current Density 44 (A/m ²): First-order Rate Constant (k = slope).....	239
Figure A.5: ClearCoat_TS1992 Wastewater, Current Density 11 (A/m ²): First-order Rate Constant (k = slope).....	240
Figure A.6: ClearCoat_TS1992 Wastewater, Current Density 22 (A/m ²): First-order Rate Constant (k = slope).....	241

Figure A.7: ClearCoat_TS1992 Wastewater, Current Density 33 (A/m ²): First-order Rate Constant (k = slope).....	242
Figure A.8: ClearCoat_TS1992 Wastewater, Current Density 44 (A/m ²): First-order Rate Constant (k = slope).....	243
Figure A.9: Primer_TS1432 Wastewater, Current Density 11 (A/m ²): First-order Rate Constant (k = slope).....	244
Figure A.10: Primer_TS1432 Wastewater, Current Density 22 (A/m ²): First-order Rate Constant (k = slope).....	245
Figure A.11: Primer_TS1432 Wastewater, Current Density 33 (A/m ²): First-order Rate Constant (k = slope).....	246
Figure A.12: Primer_TS1432 Wastewater, Current Density 44 (A/m ²): First-order Rate Constant (k = slope).....	247
Figure A.13: Primer_TS2374 Wastewater, Current Density 11 (A/m ²): First-order Rate Constant (k = slope).....	248
Figure A.14: Primer_TS2374 Wastewater, Current Density 22 (A/m ²): First-order Rate Constant (k = slope).....	249
Figure A.15: Primer_TS2374 Wastewater, Current Density 33 (A/m ²): First-order Rate Constant (k = slope).....	250
Figure A.16: Primer_TS2374 Wastewater, Current Density 44 (A/m ²): First-order Rate Constant (k = slope).....	251
Figure A.17: MixedPaint_TS2789 Wastewater, Current Density 11 (A/m ²): First-order Rate Constant (k = slope).....	252
Figure A.18: MixedPaint_TS2789 Wastewater, Current Density 22 (A/m ²): First-order Rate Constant (k = slope).....	253

Figure A.19: MixedPaint_TS2789 Wastewater, Current Density 33 (A/m ²): First-order Rate Constant (k = slope).....	254
Figure A.20: MixedPaint_TS2789 Wastewater, Current Density 44 (A/m ²): First-order Rate Constant (k = slope).....	255
Figure A.21: ClearCoat_TS4669 Wastewater, Current Density 11 (A/m ²): Second-order Rate Constant (k = slope).....	256
Figure A.22: ClearCoat_TS4669 Wastewater, Current Density 22 (A/m ²): Second-order Rate Constant (k = slope).....	257
Figure A.23: ClearCoat_TS4669 Wastewater, Current Density 33 (A/m ²): Second-order Rate Constant (k = slope).....	258
Figure A.24: ClearCoat_TS4669 Wastewater, Current Density 44 (A/m ²): Second-order Rate Constant (k = slope).....	259
Figure A.25: ClearCoat_TS1992 Wastewater, Current Density 11 (A/m ²): Second-order Rate Constant (k = slope).....	260
Figure A.26: ClearCoat_TS1992 Wastewater, Current Density 22 (A/m ²): Second-order Rate Constant (k = slope).....	261
Figure A.27: ClearCoat_TS1992 Wastewater, Current Density 33 (A/m ²): Second-order Rate Constant (k = slope).....	262
Figure A.28: ClearCoat_TS1992 Wastewater, Current Density 44 (A/m ²): Second-order Rate Constant (k = slope).....	263
Figure A.29: Primer_TS1432 Wastewater, Current Density 11 (A/m ²): Second-order Rate Constant (k = slope).....	264
Figure A.30: Primer_TS1432 Wastewater, Current Density 22 (A/m ²): Second-order Rate Constant (k = slope).....	265

Figure A.31: Primer_TS1432 Wastewater, Current Density 33 (A/m ²): Second-order Rate Constant (k = slope).....	266
Figure A.32: Primer_TS1432 Wastewater, Current Density 44 (A/m ²): Second-order Rate Constant (k = slope).....	267
Figure A.33: Primer_TS2374 Wastewater, Current Density 11 (A/m ²): Second-order Rate Constant (k = slope).....	268
Figure A.34: Primer_TS2374 Wastewater, Current Density 22 (A/m ²): Second-order Rate Constant (k = slope).....	269
Figure A.35: Primer_TS2374 Wastewater, Current Density 33 (A/m ²): Second-order Rate Constant (k = slope).....	270
Figure A.36: Primer_TS2374 Wastewater, Current Density 44 (A/m ²): Second-order Rate Constant (k = slope).....	271
Figure A.37: MixedPaint_TS2789 Wastewater, Current Density 11 (A/m ²): Second-order Rate Constant (k = slope).....	272
Figure A.38: MixedPaint_TS2789 Wastewater, Current Density 22 (A/m ²): Second-order Rate Constant (k = slope).....	273
Figure A.39: MixedPaint_TS2789 Wastewater, Current Density 33 (A/m ²): Second-order Rate Constant (k = slope).....	274
Figure A.40: MixedPaint_TS2789 Wastewater, Current Density 44 (A/m ²): Second-order Rate Constant (k = slope).....	275

List of Symbols

$\%V_D$: dead volume percentage, %

Δt_i : time increment, min

\dot{m} : influent flowrate of tracer, mg/min

R_j^2 : coefficient of determination from the regression of X_j

s^3 : skewness parameter in tracer test, $\text{min}^{1.5}$

\bar{t} : actual mean retention time, min

V_A : active volume, L

V_D : dead volume, L

σ^2 : variance parameter in tracer test, min^2

BOD: biochemical oxygen demand, mg/L

C : substance concentration, g/m^3 or mg/L

C_{eff} : effluent concentration, g/m^3 or mg/L

C_{in} : concentration of inflow, g/m^3 or mg/L

C_{inf} : influent concentration, g/m^3 or mg/L

C_{max} : influent concentration of tracer in step method, mg/L

COD: chemical oxygen demand, mg/L

C_{out} : concentration of outflow, g/m^3 or mg/L

C_{pulse} : concentration of tracer in pulse method, mg/L

C_{step} : effluent concentration of tracer in step method, mg/L

DF: Degree of freedom, number of observations in the sample, -

E_{ox} : standard oxidation potential, V

E_{red} : standard reduction potential, V

$E(t)$: exit age distribution, 1/min

E: specific energy consumption, W.h/m³

EC: electrical conductivity, μ S/cm

EF: electroflotation

EF-OFF: electroflotation DC power OFF

EF-ON: electroflotation DC power ON

$F(t)$: dimensionless effluent concentration curve against time, -

F: Faraday's constant, 96486 C/mol

HRT: hydraulic retention time, min or hr

I: electrical current, A

J: current density, A/m²

k: rate constant, unit depends on the reaction order

m: mass of material, g

MM: molar mass, g/mol

\emptyset : diameter, mm

P-value: Probability value, -

Q: volumetric flowrate, m³/hr or L/min

r: reaction rate, $\text{g/m}^3\cdot\text{s}$ or $\text{mg/L}\cdot\text{s}$

R^2 : coefficient of determination, -

R-sq(adj): adjusted coefficient of determination, -

R-sq: coefficient of determination, -

Seq SS: Sequential sums of squares, measure of variation for different components of the model, -

t: time, s or min or hr

T: time, s or min or hr

TDS: total dissolved solids, mg/L

TS: total solids, mg/L

TSS: total suspended solids, mg/L

TSS_{eff} : effluent total suspended solids concentration, mg/L

TSS_{inf} : influent total suspended solids concentration, mg/L

$\text{Turbidity}_{\text{eff}}$: effluent turbidity, NTU

$\text{Turbidity}_{\text{inf}}$: influent turbidity, NTU

U: electric potential, V

V: volume, m^3 or L

VIF_j : variance inflation factor, -

X_i : independent variable

X_j : independent variable

Y: %Removal of pollutant, %

Z: number of transferred electrons, -

β_0 : regression coefficients for intercept, -

β_i : regression coefficients for linear term, -

β_{ii} : regression coefficients for quadratic term, -

β_{ij} : regression coefficients for 2-way interaction term, -

θ : dimensionless time parameter, -

CHAPTER 1 Introduction

1.1 Background

With the worldwide water scarcity, growing water demand and environmental concerns of industrialization, it is essential for industries to find alternative sources of water supplies. Treatment of industrial wastewaters is performed in order to meet wastewater discharge standards, recycle and reuse the treated water as well as recover valuable constituents. The treatment methods that can fulfill these objectives are becoming progressively attractive. This dissertation focuses on the fundamentals and applications of electroflotation (EF) in the treatment of industrial wastewaters and in particular, treatment of automotive paint wastewater. The auto industry is a major economic sector in Ontario, Canada and worldwide. Globally, 97.3 million vehicles were manufactured in 2017, growing from 58.4 million units in 2000 (OICA, 2017). According to the published studies (Geffen and Rothenberg, 2000; Papasavva et al. 2001; Zorpas and Inglezakis, 2012) painting and coating operations are the origin of 60 to 80% of environmental concerns in automotive industry. Automotive paint wastewater is produced in car factories and in auto body paint spray booths and contains auto paint, detackifier, pH booster and biocides. Chemical methods, e.g., coagulation and flocculation, are usually employed for treatment of this wastewater and involve addition of chemicals and create considerable volume of waste sludge that usually ends up in landfills. Hence, alternative treatment methods are needed to improve the water quality, reduce the chemical usage and reduce and recycle the sludge.

Electroflotation is the utilization of gas bubbles generated during the water electrolysis to effectively separate suspended particles by flotation. It was first used in mineral processing (Bhaskar Raju and Khangaonkar, 1984) and later adopted in the wastewater treatment. Scientific researches and full-scale installations have proposed electroflotation as an effective and efficient method for treatment of various industrial wastewaters, e.g., tannery effluents (Feng et al., 2007), electroplating wastewater (Mendelev University Science Park., 2008), oil-field wastewater (Bande et al., 2008), pulp and paper industry effluents (Bellebia et al., 2012), textile industry effluents (Amour et al., 2016),

semiconductor wastewater (Aoudj et al., 2017) and dairy effluent (Bassala et al., 2017). Electroflotation is a suitable treatment process for wastewaters with high electrical conductivity (EC), as high EC reduces the power consumption and operating costs of the system. However, electrodes replacement should be considered in the operating costs as well. Studying the literature and commercial systems shows that, by generating a high density of fine bubbles, electroflotation is a good method for small to medium-scale operations of treatment of hydrophobic fine suspended particles, where other treatment methods are not effective or are expensive. Also, by choosing effective and proper electrode materials, electroflotation can be implemented for treatment of other types of wastewater, e.g., wastewaters containing heavy metals. There are several process variables, e.g., current density, water pH, electrical conductivity and retention time, that affect the electroflotation efficiency. In addition, the hydrodynamics and particularly flow regime in the reactor, that plays a significant role in the treatment performance, need to be considered as well.

The lab-scale batch experiments previously performed by Dr. Julie Shang and her research group at Western University showed promising results on the electroflotation treatment of auto paint wastewater. This study is the continuation of the previous project, focusing on the analysis of experimental data from the previous study, and design and implementation of a continuous-flow electroflotation reactor for treatment of the auto paint wastewater.

1.2 Research Objectives

The objectives of this research are to study the fundamentals and application of electroflotation process in treatment of industrial effluents, with the focus on automotive paint wastewater.

The specific goals of the study are as follows:

- I. To present the fundamentals of electroflotation (EF) process, critically review the applications of EF in treatment of industrial wastewaters, and provide a guideline on design aspects, limitations and prospects of EF.
- II. To study the kinetics of EF process in treatment of auto paint wastewater and determine the kinetic order of process, decide the most important process variables, and produce mathematical models of the treatment system.
- III. To study the treatment of automotive paint wastewater in a continuous-flow EF reactor, find the optimal operating conditions, assess the flotation performance as influenced by operating parameters (paint concentration, current density and retention time), investigate the chemistry of the process, and determine the energy consumption of the system.
- IV. To experimentally investigate the hydrodynamics of electroflotation reactor and evaluate the effects of retention time and EF gas bubbles on residence time distribution (RTD) curves and parameters, e.g., dead volume, variance and skewness.

1.3 Thesis Outline

The thesis is prepared in manuscript style and comprises 6 chapters outlined as follows:

- **Chapter 1 Introduction, presents the background of the study**, introduces the research objectives and thesis outlines, and states the original contributions of the study.
- **Chapter 2 Electroflotation for Treatment of Industrial Wastewaters: A Review**, presents fundamentals of electroflotation process, electrodes materials and arrangements, reactor design, process variables, applications of electroflotation in treatment of industrial effluents and full-scale installations of the system.
- **Chapter 3 Electroflotation: Kinetic Study and Data Analysis**, introduces the theory of kinetics, investigates the rate order of electroflotation process, statistically examines the influencing process variables and presents empirical modeling of the process
- **Chapter 4 Continuous-Flow Electroflotation of Automotive Paint Wastewater**, presents the design of a continuous-flow electroflotation system and electrodes modules for treatment of auto paint wastewater, describes the experimental plan and methods, discusses the results and investigates the effects of operational parameters, electrochemistry of the process and energy consumption, and proposes empirical modeling of the treatment system.
- **Chapter 5 Experimental Study of Flow Characteristics in Electroflotation Reactor**, presents the theory of residence time distribution and an experimental plan and methods for conducting the tracer tests on the electroflotation reactor, evaluates the effects of hydraulic retention time and EF gas bubbles on the residence time distribution, presents and examines the related parameters, provides practical recommendations on hydraulic design of the reactor.

- **Chapter 6 Summary, Conclusions and Recommendations**, presents a summary of the research, draws conclusion, and provides recommendations for future studies

1.4 Original Contributions

The original contributions of the present study are as follows:

- I. The study provides a focused review on fundamentals and applications of electroflotation in treatment of industrial wastewaters that serves as a guideline for researchers and engineers.
- II. An extensive kinetic study of electroflotation process was conducted. With calculation of the first and second-order reaction rate constants it was revealed that the second-order kinetics was a better fit to the process. The statistical analysis was performed and the applied current density and the initial TSS concentration were identified as the most critical factors in the EF process. The empirical modeling was conducted using Response Surface Methodology (RSM) and Stepwise Regression methods.
- III. A continuous-flow pilot-scale electroflotation reactor along with the electrodes modules were designed and constructed. The experimental plan was developed, and the treatment study of auto paint wastewater was conducted. The effects of operational parameters on the treatment efficiency were determined and the specific energy consumption of the system and the empirical equation of the process were established and presented.
- IV. The experimental plan and methods for the residence time distribution (RTD) studies were introduced. The tracer tests were conducted on the electroflotation reactor under different hydraulic retention times and electroflotation modes (EF: ON/OFF). The effects of parameters were evaluated, and the hands-on design recommendations were presented.

References

- Amour, A., Merzouk, B., Leclerc, J. P., & Lapicque, F. (2016). Removal of reactive textile dye from aqueous solutions by electrocoagulation in a continuous cell. *Desalination and Water Treatment*, 57(48-49), 22764-22773.
- Aoudj, S., Khelifa, A., & Drouiche, N. (2017). Removal of fluoride, SDS, ammonia and turbidity from semiconductor wastewater by combined electrocoagulation–electroflotation. *Chemosphere*, 180, 379-387.
- Bande, R. M., Prasad, B., Mishra, I. M., & Wasewar, K. L. (2008). Oil field effluent water treatment for safe disposal by electroflotation. *Chemical Engineering Journal*, 137(3), 503-509.
- Bassala, H. D., Dedzo, G. K., Bememba, C. B. N., Seumo, P. M. T., Dazie, J. D., Nanseu-Njiki, C. P., & Ngameni, E. (2017). Investigation of the efficiency of a designed electrocoagulation reactor: Application for dairy effluent treatment. *Process Safety and Environmental Protection*, 111, 122-127.
- Bellebia, S., Kacha, S., Bouyakoub, A. Z., & Derriche, Z. (2012). Experimental investigation of chemical oxygen demand and turbidity removal from cardboard paper mill effluents using combined electrocoagulation and adsorption processes. *Environmental Progress & Sustainable Energy*, 31(3), 361-370.
- Bhaskar Raju, G., & Khangaonkar, P. R. (1984). Electroflotation-A critical review. *Transactions of the Indian Institute of Metals*, 37(1), 59-66.
- Feng, J. W., Sun, Y. B., Zheng, Z., Zhang, J. B., Shu, L. I., & Tian, Y. C. (2007). Treatment of tannery wastewater by electrocoagulation. *Journal of Environmental Sciences*, 19(12), 1409-1415.
- Geffen, C. A., & Rothenberg, S. (2000). Suppliers and environmental innovation: the automotive paint process. *International Journal of Operations & Production Management*, 20(2), 166-186

Mendeleev University Science Park. (2008) *Table.1. Electroflotation system capability*. Retrieved from <http://enviropark.ru/course/category.php?id=10> (Accessed 11 January 2018).

OICA. (2017). *Production Statistics. International Organization of Motor Vehicle Manufacturers*. Retrieved from <http://www.oica.net/production-statistics>. (Accessed 9 April 2018).

Papasavva, S., Kia, S., Claya, J., & Gunther, R. (2001). Characterization of automotive paints: an environmental impact analysis. *Progress in Organic Coatings*, 43(1-3), 193-206.

Shang, J. Q. (2004). *Electrokinetic Flotation of Paint Sludge Water*, Western University, London, Canada.

Zorpas, A. A., & Inglezakis, V. J. (2012). Automotive industry challenges in meeting EU 2015 environmental standard. *Technology in Society*, 34(1), 55-83.

CHAPTER 2 Electroflotation for Treatment of Industrial Wastewaters: A Review

2.1 Introduction

The world population will exceed 8 billion in 2025, double the number it was in 1975 (United Nations, 2018). This will lead to rapid increase of water consumption in different sectors, i.e., domestic, agriculture and industry. While water scarcity is already a key concern in several countries, with the future water demand, industries need to search for alternative sources of water supplies other than surface and ground water. Industries use large quantities of water that mostly ends up as wastewater. Thus, recovered industrial wastewater is an important water resource. Industrial effluents are treated for meeting wastewater discharge standards, recovery of valuable constituents, and reuse. Treatment methods that can satisfy these objectives are becoming progressively attractive. This study aims on applications of electroflotation in treatment of industrial wastewaters, with detailed discussions on fundamentals of electroflotation process, electrode materials and arrangements, design aspects of electroflotation reactor and influential process variables. In this chapter, a comprehensive review on related subjects is presented.

2.2 Fundamentals

Electroflotation is separation of suspended particles from water by means of gas bubble generated at electrodes during electrolysis of water. The process was first employed in the mineral industry and later was implemented in water and wastewater treatment (Bhaskar Raju and Khangaonkar, 1984). Throughout the process, fine bubbles nucleate at electrodes, detach and while rising to the water surface, collide with solid or liquid particles suspended in water. Some of these collisions lead to attachment of particles and bubbles and formation of bubble-particle aggregates. Then, the aggregates ascend to the water surface and are collected by mechanical skimming. In electrolysis of pure water using inert electrodes, the following redox reactions occur:

at cathode electrode:



at anode electrode:



overall redox reaction:



If there are impurities present in water, other reactions may take place, e.g., in presence of chloride (Cl^-), chlorine gas bubbles (Cl_2) release at anode electrode. Also, when anodes are made of active metals, e.g., aluminium or iron, metal ions liberate into solution according to following reactions (Daneshvar et al., 2007).



Then, the produced metal ions at “sacrificial anode” undergo hydrolysis, produce hydroxide ions that act as coagulants and enhance the removal efficiency of electroflotation process.

Electroflotation has been receiving increasing attention by researchers for treatment of different effluents including industrial wastewaters in recent years. By generating fine bubbles, e.g., 1-30 μm compared to 50-100 μm in pressurized air flotation (Il'in and Sedashova, 1999) the process efficiency is higher than conventional flotation methods because of larger number and surface area of bubbles. The greater density of bubbles increases the chance of bubble-particle collision, aggregation and removal. Furthermore, fine bubbles have greater surface to volume ratio, and therefore, greater overall surface interactions between bubbles and particles occur. Electroflotation systems do not usually include mechanically-moving parts, making the installation, retrofit and maintenance simpler and more convenient. Also, process adjustments can be readily accomplished by changing applied electric potential/current.

Electroflotation can be an alternative to chemical treatment methods. The chemical methods involve addition of coagulant and flocculant chemicals to wastewater, which can be expensive and also produce large quantities of non-recoverable sludge. In comparison electroflotation can be implemented without adding chemicals.

2.3 Electrodes

2.3.1 Electrode Material

Electrodes are the heart of electroflotation reactors and therefore, their material and design are crucial for the performance of the system. Electrode materials are divided into two categories, i.e., inert and active. This is the case especially for anode electrodes.

Since the cathode does not corrode in electroflotation, stainless steel and aluminium are the most common and inexpensive materials used for the cathodes in the treatment of industrial wastewaters (Mostefa and Tir, 2004; Mansour and Chalbi, 2006; Kobya et al., 2006; Ezechi et al., 2014; Aoudj et al., 2017).

Inert anodes are used for production of oxygen gas bubbles in electroflotation. Graphite is used as an anode in electrochemical processes and electroflotation treatment of wastewater (Muruganathan et al., 2004; Yang, 2007; Zaidi et al., 2016). It has a relatively stable condition; however, studies show that graphite deteriorated rather quickly (e.g., Hernlem and Tsai, 2000), and lost its smooth surface resulting in the production of coarse-sized bubbles and reduction of separation efficiency.

Dimensionally stable anodes (DSA) are made of coated metals such as titanium. They were first patented in the US in 1966 in form of $\text{TiO}_2\text{-RuO}_2$ -coated titanium for chlorine evolution. Oxides of other metals, e.g., Pb, Sb, Zr and Sn, have been used as coating as well (Chen and Chen, 2005). Ho and Chan (1986) employed $\text{PbO}_2\text{-Ti}$ anode for electroflotation treatment of palm oil mill effluents. Also, treatment of radioactive wastewater using titanium anode with coating of isomorphous titanium and ruthenium oxides was reported by Il'in and Kolesnikov (2001). These electrodes are expensive and have short service life. In recent years, studies have been performed on production of cheaper DSA electrodes with longer service lives. $\text{Ti/IrO}_2\text{-Ta}_2\text{O}_5$ anodes were used for treatment of synthetic wastewater containing oil and peptides (Mraz and Krýsa, 1994). More complex electrodes made of $\text{Ti/IrO}_x\text{-Sb}_2\text{O}_5\text{-SnO}_2$ and $\text{Ti/RuO}_2\text{-Sb}_2\text{O}_5\text{-SnO}_2$ have demonstrated significantly longer service lives (Chen et al., 2002; Chen and Chen, 2005).

Active anodes made of metals such as Al and Fe have also been employed for treatment of industrial wastewaters, e.g., urban wastewater (Pouet and Grasmick, 1995), slaughterhouse wastewater (Bayramoglu et al., 2007), textile wastewater (Aouni et al., 2009), leachate of oil-drilling (Ighilahriz et al., 2014) and dairy effluents (Bassala et al., 2017). During the process, metal ions are released from the 'sacrificial anodes' and react with hydroxide ions, forming metal hydroxides such as $\text{Al}(\text{OH})_3$, $\text{Al}(\text{OH})_4^-$, $\text{Fe}(\text{OH})_3$ and polymeric species such as $\text{Al}_2(\text{OH})_2^{4+}$, $\text{Al}_6(\text{OH})_{15}^{3+}$, $\text{Fe}(\text{H}_2\text{O})_6^{3+}$ and $\text{Fe}(\text{H}_2\text{O})_5\text{OH}^{2+}$ (Aouni et al., 2009; Kim et al., 2002). These metal hydroxides act as coagulant and adsorb colloidal particles, form bonds and create aggregates, rise to surface and remove the particles from water.

2.3.2 Electrode Arrangement

Simple electroflotation systems comprise a reactor and electrodes (anode and cathode) connected to a DC power supply. The connection mode of electrodes to DC power supply can be monopolar (parallel or series) or bipolar. While in monopolar-connection mode all electrodes are connected to each other or to DC power supply, only outmost electrodes connect to power supply in bipolar connection mode. Schematic of different electrode connection modes are depicted in Figure 2.1.

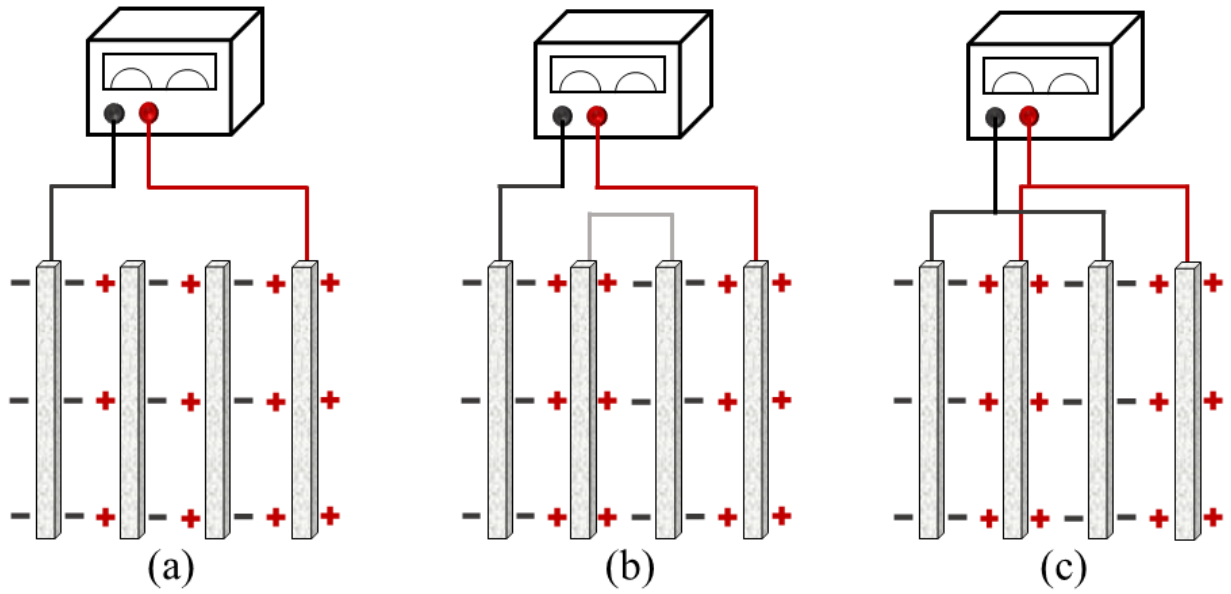


Figure 2.1: Schematics of electrodes connection modes: (a) Bipolar, (b) Monopolar series, (c) Monopolar parallel

Comparative studies of electrodes connection modes have been conducted by different researchers. The monopolar connection mode is considered more advantageous than the bipolar mode, in terms of separation efficiency and power consumption (Daneshvar et al., 2004; Golder et al., 2007; Modirshahla et al., 2007; Kobya et al., 2007; Ghosh et al., 2008; Solak et al., 2009).

2.4 Reactor Design

A design of electroflotation reactor includes the electrodes arrangement, reactor shape and flow regime inside the reactor. Most lab/bench-scale electroflotation experiments have been performed in batch-flow processing regime. They usually consist of a small cell as the reactor and a few electrodes. Figure 2.2 presents a basic and simple design of a batch electroflotation reactor with vertically-oriented monopolar electrodes. Other batch reactors have been presented by researchers as well.

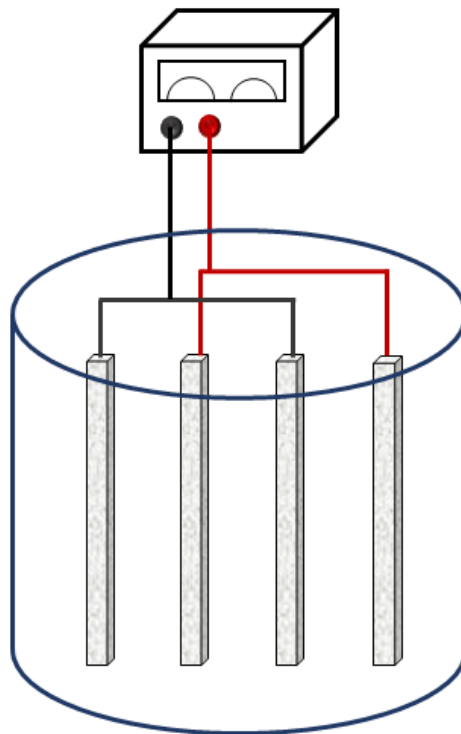


Figure 2.2: Schematics of a simple batch electroflotation system with vertical monopolar electrodes

Figure 2.3 shows a cylindrical aluminum reactor which works as the anode, and an aluminium impeller cathode, used for defluoridation (Un et al. 2013).

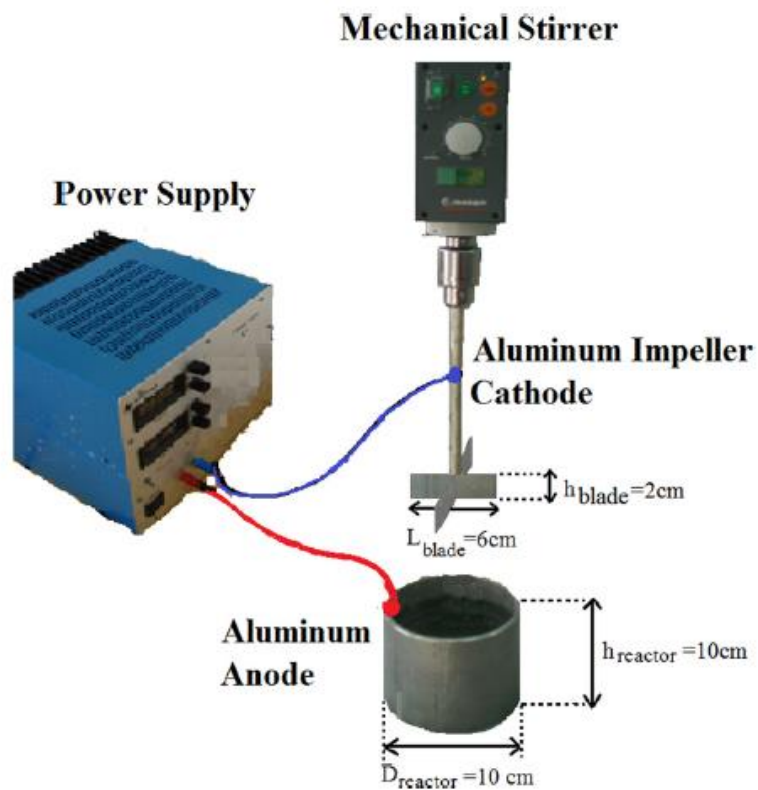


Figure 2.3: Batch cylindrical reactor with rotating cathode electrode (Un et al., 2013)

In another study, Nunez et al. (2011) used iron cylinders with different diameters as anode and cathode in a cylindrical acrylic cell, Figure 2.4, for arsenic removal from wastewater.

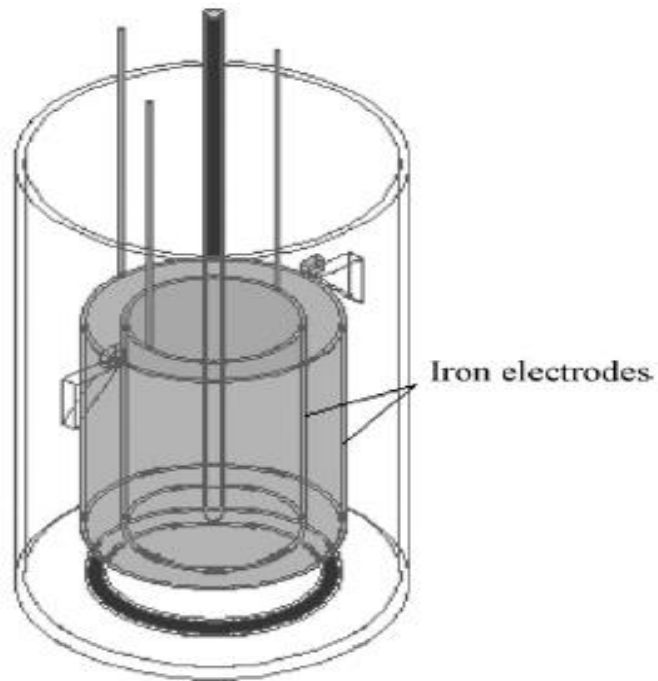


Figure 2.4: Batch acrylic cylindrical cell with iron cylinder electrodes (Nunez et al., 2011)

A bench-scale batch reactor with about 0.5 L volume and equipped with porous cylindrical stainless steel cathodes and rod-shaped iron anodes, Figure 2.5, was designed and examined for arsenic removal, by Lakshmanan et al. (2010).

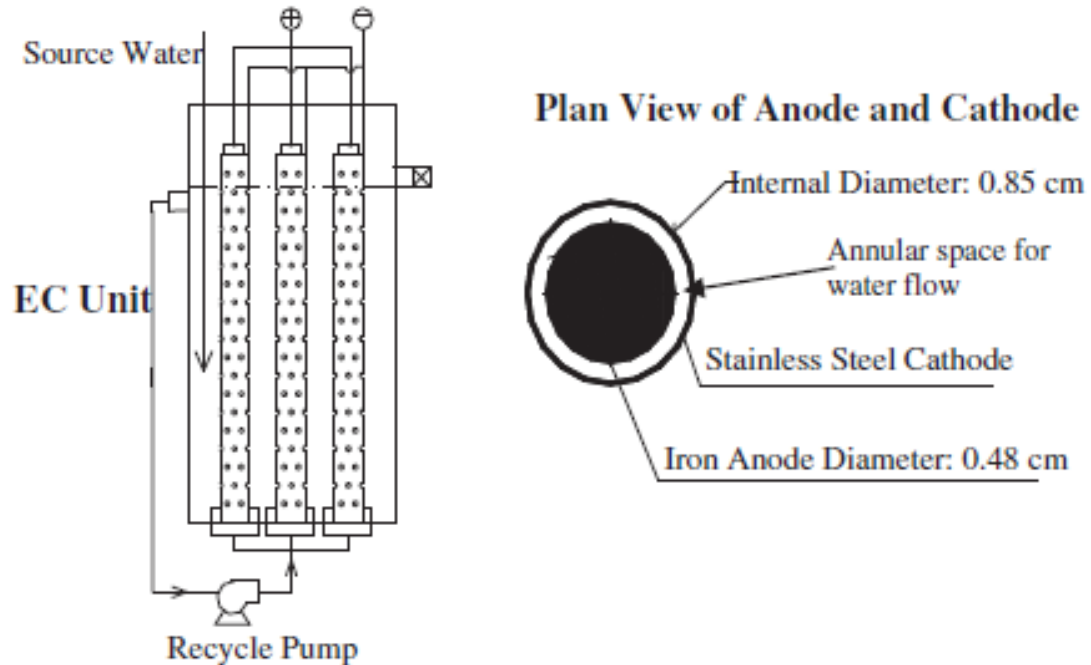


Figure 2.5: Batch reactor with cylindrical stainless steel cathodes and rod-shaped iron anodes (Lakshmanan et al., 2010)

Studies of continuous-flow reactors often involve larger reactors and are the next step before the full-scale design of the process. Hassani et al. (2016) designed a 3-stage continuous-flow reactor including electrocoagulation (release of metal ions from sacrificial anode) unit with Al and Fe electrode plates, and electroflotation unit with stainless steel cathodes and Ti/RuO₂ anodes followed by precipitation unit to capture the remaining solids from landfill leachate, Figure 2.6.

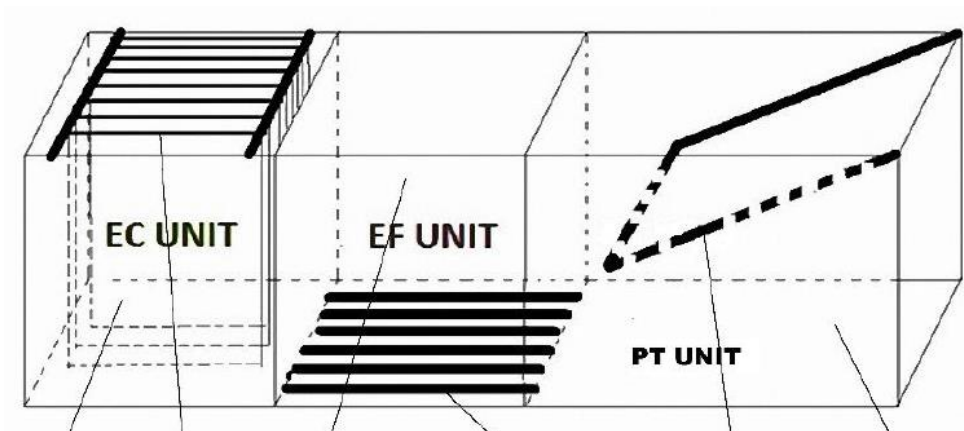


Figure 2.6: Schematic of 3-stage electrochemical reactor. Electrocoagulation Unit, Electroflotation Unit, Precipitation Tank (Hassani et al., 2016)

An up-flow electrochemical reactor with 4 sets of bipolar Ti and Al electrodes and a subsequent separator were studied for treatment of laundry wastewater (Ge et al., 2004). Schematic of the system is illustrated in Figure 2.7.

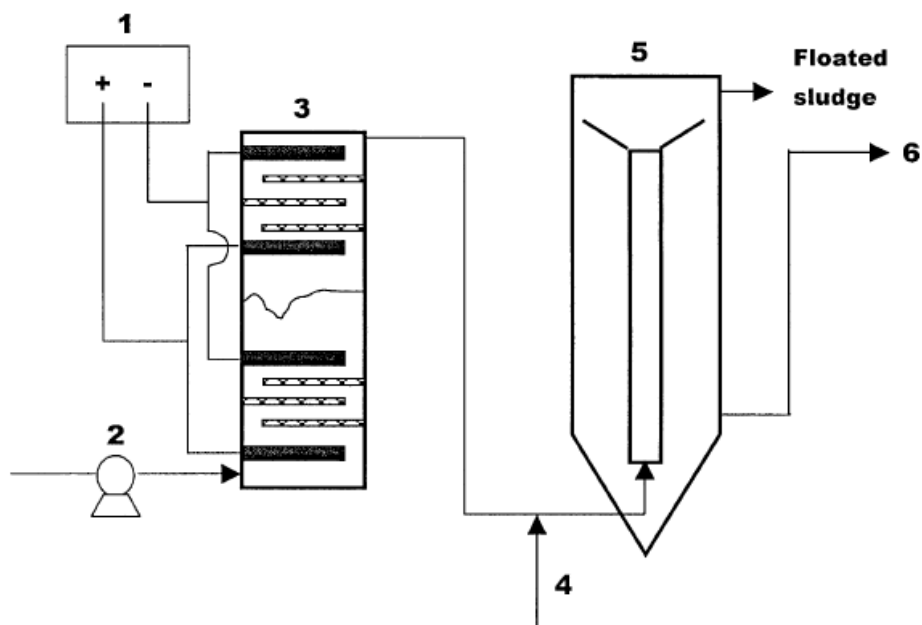


Figure 2.7: Bipolar up-flow reactor with separate flotation unit (Ge et al., 2004)

In an unconventional design of electroflotation reactor, Un et al. (2014) proposed a continuous-flow U-shaped iron reactor (also working as cathode) with screw-type iron anode, as shown in Figure 2.8.

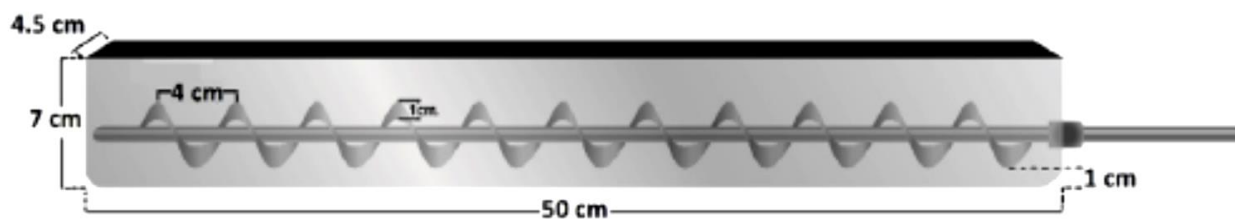


Figure 2.8: U-shaped reactor/cathode with screw-type anode (Un et al., 2014)

Figure 2.9 presents an enclosed electrochemical reactor equipped with Al and Fe sheet electrodes used for removal of phosphate from a synthesized wastewater (Lacasa et al., 2011).

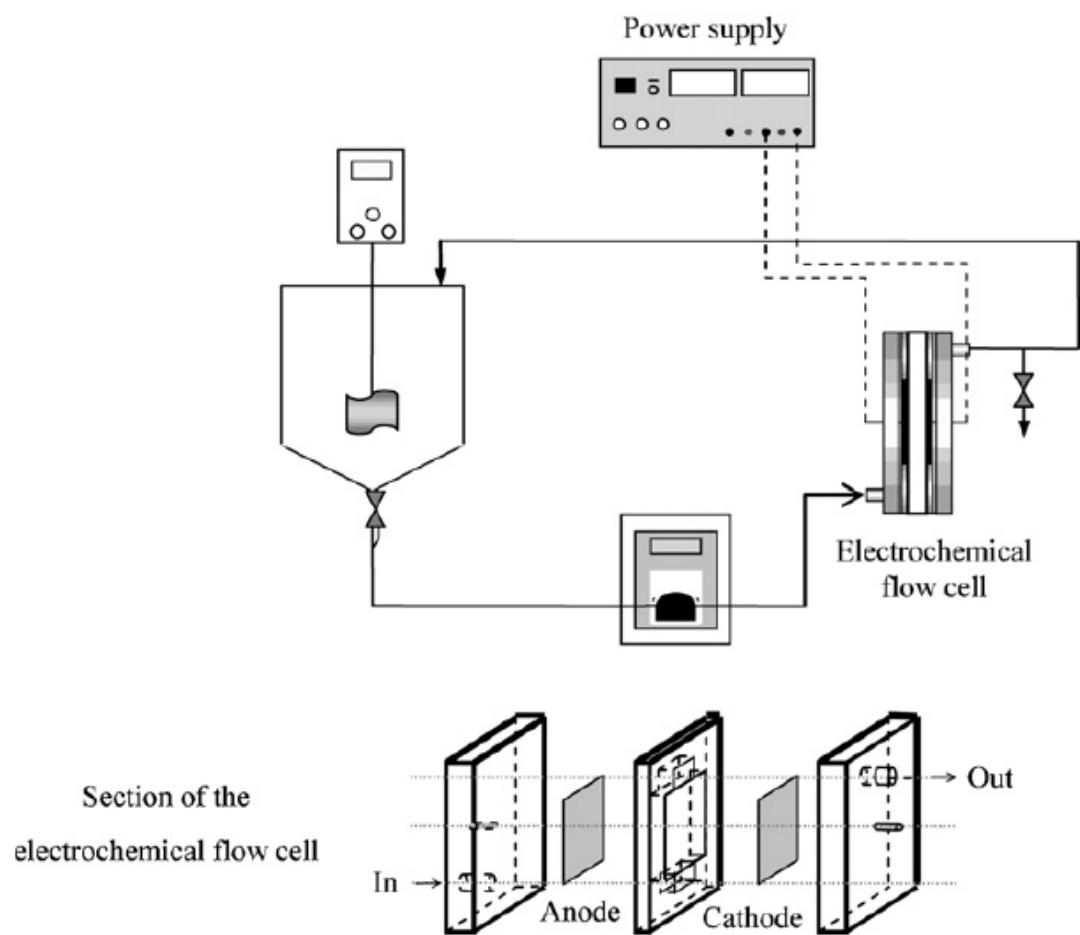


Figure 2.9: Enclosed electrochemical cell with sheet electrodes (Lacasa et al., 2011)

2.5 Process Variables

2.5.1 Current Density

Current density, described as ratio of applied electric current to the active surface area of electrodes, is considered as the most important process variable in the electroflotation process. According to Faraday's law of electrolysis, Eq. 2.6, mass of released gas (H₂ and O₂) or metal ions (e.g., Al and Fe ions) at electrodes, m (g), is proportional to applied electrical current, I (A), to system. In this equation, t is reaction duration (s), MM is molar mass of released element (g/mol), Z is number of transferred electrons and F is Faraday's constant (96486 C/mol).

$$m = \frac{(I \times t \times MM)}{Z \times F} \quad (2.6)$$

From Eq. (2.6), it can be seen that the increase of electrical current and current density results in the increase of released bubbles density and/or metal ion coagulants.

Consequently, probability of bubble-particle and/or coagulant-particle collisions and attachments increases and separation efficiency rises. This fact has been established in several studies (Meas et al., 2010; da Mota et al., 2015; Hakizimana et al., 2017; Alam and Shang, 2017).

However, current density affects the generated bubble size and consequently the treatment efficiency of electroflotation system as well. While some authors (Landolt et al. 1970; Sides, 1986) reported increase of electroflotation bubble size with increasing current density, there are studies suggesting the opposite effects, i.e., bubble size reduction with the increase of current density (Khosla et al. 1991; da Cruz et al. 2016). Also, neutral influence of applied current density on bubble size is observed in some experimental studies (Burns et al. 1997; Sarkar et al. 2010). In articles presented by Jiménez et al. (2010) and Alam et al. (2017), it was stated that the bubble size decreased with the increase of current density; but when applied current density surpassed a threshold, the nucleated small bubbles coalesced and created coarse bubbles and reduced the treatment efficiency. Therefore, it seems that there is an optimum current density,

producing the finest bubbles considering the electrode material and other experimental conditions.

The applied current density affects energy consumption of the treatment system as well. Besides, the electrical current as the main process variable, is a parameter that can be readily adjusted during the operating phase of treatment system.

2.5.2 Retention Time

In wastewater treatment, the hydraulic retention time, HRT (Eq. 2.7), plays a significant role. In electroflotation process, generation of bubbles, bubble-particle collisions and attachments, aggregates formation, aggregates ascending, and skimming are all time-dependent. Therefore, it is important to have adequate retention time (Poon, 1997; Perfil'eva et al., 2016; Kolesnikov et al., 2017).

$$\text{HRT} = \frac{V}{Q} \quad (2.7)$$

where, HRT is hydraulic retention time, hr, V is volume of reactor, m^3 , and Q is flowrate entering reactor, m^3/hr .

The retention time in electroflotation reactor is directly related to the size of treatment facility (capital cost) and electricity consumption (operating cost); hence, the design of reactors should be performed so that while providing sufficient retention time for treatment process, economy of projects be taken into consideration as well.

2.5.3 Pollutant Concentration and Electrical Conductivity

The removal efficiency of electroflotation system declines with increasing initial pollutant concentration in wastewater, which has been reported in studies of electroflotation treatment of metal finishing effluents (Khelifa et al., 2005), removal of

silica gel particles from synthetic textile wastewater (Merzouk et al., 2010), treatment of semiconductor industry effluent (Aoudj et al., 2015) and other researches (Mahvi et al., 2011; Bennajah et al., 2010).

The electrical conductivity, EC, of wastewater is another influencing parameter in electroflotation process. EC is related to the ionic strength of wastewater (Bagotskii, 2006). It has a great impact on energy consumption of electroflotation process.

Based on Eq. (2.8), the specific energy consumption is defined as the product of applied electric potential, current and time divided by unit volume of treated wastewater.

$$E = \frac{(U \times I \times t)}{V} \quad (2.8)$$

where, E is specific energy consumption, W.h/m^3 , U is electric potential, V , I is applied electrical current, A , t is reactor retention time, hr , and V is reactor volume, m^3 .

With the increase of electrical conductivity of wastewater, the electric current decreases under the same electric potential, i.e., the higher electrical conductivity of wastewater leads to less energy consumption and operating cost of electroflotation. This has been confirmed in the literature (Bayramoglu et al., 2004; Belkacem, et al., 2008). Some authors added salt to wastewater to increase the EC and reduce the energy consumption (Kobyia et al., 2006; Daneshvar, et al., 2006).

2.5.4 Wastewater pH

Wastewater pH is a critical process variable and influences the electroflotation process in two ways, i.e., impacting bubble formation and size, and controlling metal hydroxide species when sacrificial anodes are used. These effects have been studied in the literature. An experimental study, (Bhaskar Raju and Khangaonkar, 1984), revealed that, independent of the cathode material, electroflotation H_2 bubbles were smaller in alkaline and neutral environment compared to acidic conditions. In this study, the minimum

bubble diameters were produced in neutral solutions. On the other hand, using Ti anodes, the O₂ bubbles size decreased in acidic condition and increased with increasing pH.

In an electroflotation study using stainless steel cathode and platinum anode, Jiménez et al. (2010) reported that smaller O₂ and H₂ bubbles were nucleated at neutral pH condition, and concurrently greater number of bubbles were generated. The opposite condition took place in strongly acidic wastewater. Alam et al. (2017) conducted electroflotation studies on effect of pH on bubbles size using Iridium dioxide-coated titanium anode, and SS 316 cathode and concluded that the neutral pH condition was in favour of smaller hydrogen bubbles whereas smaller oxygen bubbles were produced in acidic solution. Therefore, it can be stated that for H₂ generation, the neutral condition is favourable concerning the bubble size and optimal treatment condition, while no general rule for optimal pH for O₂ bubble size can be defined. It should be mentioned that H₂ is the defining gas in the EF process in the most cases.

The effect of pH on metal hydroxide species is investigated by Kim et al. (2002). They used Al sacrificial anodes and observed that in strong acidic condition (pH 2-3), Al³⁺ and Al(OH)₂⁺ were dominant species; Al₁₃O₄(OH)₂₄⁷⁺ was produced at pH range of 4 to 9 and at pH higher than 10, Al(OH)₄⁻ concentration increased. Presence of different ionic species under different pH conditions immensely affected the removal efficiency of the system. Matis and Peleka (2010) reported the high treatment efficiency of electroflotation reactor employing stainless steel electrodes happened only inside a narrow pH range (too alkaline condition), whereas it drastically decreased outside of that range.

2.6 Application for Industrial Effluents

2.6.1 Textile Industry

The textile industry consumes large amounts of water and generates high volume of effluents that contain dyes, acids, surfactants, hydrogen peroxide and alkalis (Paul et al., 2012). It was reported that textile dyeing and the related operations, produce up to 20 percent of industrial wastewater (Kant, 2012).

The electroflotation process has been investigated in several studies for treatment of textile industry effluents. Zaroual et al. (2006) used iron electrodes in a batch reactor to treat industrial textile effluent taken from a commercial textile-dyeing unit in Morocco. At optimum condition, viz., 3 min operation time and 600 mV electrolysis potential, and after filtering the sample solution, 100% color removal and 84% COD removal were achieved. Daneshvar et al. (2007) implemented electrocoagulation-electroflotation method to remove color from dye solution containing C.I. Acid Yellow 23. About 98% color and 69% COD removal were attained for a solution of 50 mg/L dye and under current density 112.5 A/m^2 and 5 min reaction time. Steel 304 was used as cathode and Iron (ST 37-2) and aluminum plates were used as anode. The iron anodes showed significantly better performance in color removal.

A 20L electrocoagulation-electroflotation external loop airlift reactor was used by Essadki et al. (2008) to decolorize a synthetic textile wastewater containing a mixture of 2-naphthoic acid and 2-naphthol red dyes with aluminium electrodes as anode and cathode. It was concluded that at 80% COD and color removal, the external-loop airlift reactor behaved as a conventional electrocoagulation reactor. Effluent of Algerian velvet manufacturer was treated in a 1-L batch electroflotation reactor with aluminium electrodes as anode and cathode (Belkacem et al., 2008). Under 20 min residence time and 20 V electric potential, the following removal rates were obtained: BOD₅: 93.5%, COD: 90.3%, turbidity: 78.7%, SS: 93.3% and color: >93%. In addition, an average removal rate of 93% was achieved for treatment of a solution with initial concentration of 100 mg/L of different heavy metals.

In a more recent work by Amour et al. (2016), synthetic dye wastewater was prepared by dissolving Red nylosan dye N-2RBL into deionized water to reach initial concentrations of 50 to 300 mg/L. In a continuous-flow 3.1-L electroflotation reactor with aluminium cathodes and anodes, about 97% color and 90% turbidity removals were observed under 35 min residence time and 300 A/m² current density when initial dye concentration was less than 300 mg/L (Amour et al., 2016).

Kim et al. (2016) employed a bipolar electrochemical pilot-scale reactor with aluminium anodes and titanium cathodes to treat raw textile dyeing wastewater from a plant in Gyeonggi-do, Korea. With 30 min residence time, maximum removal rates of TSS, COD and color were 88, 84 and 99 percent, respectively. Also, more than 70% toxicity reductions were achieved after coagulant addition under residence time of 20 min and current density of 150 to 300 A/m² (Kim et al., 2016).

2.6.2 Dairy Industry

Dairy industry effluents contain large amount of organic pollutants and consequently have high chemical oxygen demand (COD). Sengil and Ozacar (2006) investigated COD and oil-grease removal from a dairy factory wastewater in Turkey using electroflotation. The treatment system included a 650-mL batch container and four iron electrodes as anode and cathode. When initial COD concentration was 18300 mg/L, the overall COD and oil-grease removals of 98% and 99%, respectively, were achieved under current density 0.6 mA/cm² and retention time of 6 min. Using a 2-L batch reactor and 6 aluminium electrodes, Bazrafshan et al. (2012) studied treatability of real dairy wastewater samples taken from a factory in Iran. It was shown that the electroflotation was capable of 98.84% COD removal, 97.95% BOD removal and 97.75% TSS removal at 60 V and 60 min retention time. The concentrations of COD, BOD and TSS in the beginning of the tests were approximately 6100, 2900 and 730 mg/L, respectively. Melchioris et al. (2016) used electroflotation method for treatment of synthetic and real dairy wastewater and recovery of solid whey in a 0.6 L cell with aluminium or iron electrodes. Both electrodes showed promising results in removal of organic matter. With

potential intensity of 5 V and in 60 min retention time, COD and turbidity removals of 97.0% and 99.6% were obtained using aluminium electrodes. The efficiencies of iron electrodes in treatment of COD and turbidity were 97.4% and 99.1%, respectively, in similar operational condition. The white solid whey flocs produced during using aluminium electrodes could be recovered and reused in different products.

Bassala et al. (2017) proposed a continuous up-flow 25.8-L electroflotation reactor incorporating 20 inclined aluminium electrodes for removal of organics from synthetic dairy wastewater. In the optimum condition of current density 0.65 A/m^2 and treatment time 20 min, the removal efficiencies of COD, phosphate, TSS and turbidity were 80%, 98%, 100% and 100%, respectively.

Evdokimov et al. (2017) used electroflotation in conjunction with ultrafiltration for concentrating and extraction of whey proteins from dairy crude. It was suggested that thanks to the improved properties of floated whey due to electroflotation, filtration rate of whey almost doubled compared to the initial base rate.

2.6.3 Tannery Industry

Effluents of leather-making industry contain both organic and inorganic pollutants originated from the raw material and added chemicals (Muruganathan et al., 2004). Muruganathan et al. (2004) conducted treatment experiments of real tannery wastewater in a 3-L EF cell using different electrode materials. In this study, with aluminium electrodes, at current density 46 mA/cm^2 , 900 s retention time, TSS removal efficiency of 95.3% was achieved while the initial TSS concentration was 1372 mg/L. The system was observed to be successful in removal of COD, BOD, sulfide and chromium as well.

Similar results have been reported by Feng et al. (2007). A parallel-plate EF reactor was implemented for treatment of sample collected from a sedimentation tank of a tannery unit in China. After two stage treatment, under 1 A electrical current and 20 min retention time, total removal rates of TOC, $\text{NH}_3\text{-N}$, BOD_5 , COD and sulfide were 55.1, 43.1, 61.8, 68.0 and 96.7 percent, respectively.

In addition, batch experiments have been conducted for removal of chromium from tannery wastewater by other researchers (Espinoza-Quiñones et al., 2009; Golder et al., 2011). In a new design, Selvaraj et al. (2018) presented a membrane electroflotation reactor with dimensionally stable electrodes for recovery of chromium(III) from tannery spent liquor effluent. The separation efficiencies were 98%, 91% and 95% for chromium, lipid and protein, respectively.

2.6.4 Semiconductor Industry

Semiconductor industry generates effluents containing fine suspended solids of metal compounds such as aluminium and silicon. Den and Huang (2006) studied the treatability of effluent of a semiconductor manufacturing plant in Taiwan in lab and pilot-scale continuous-flow electroflotation reactors with iron anodes and stainless steel cathodes. More than 90% turbidity removals were reached at hydraulic retention times more than 60 min and current densities greater than 5.7 A/m^2 (Den and Huang, 2006).

Adouj et al. (2016) implemented a combination of coagulation and electroflotation methods in a 1.5-L cell with stainless steel cathode and Ti/RuO₂ anode and batch flow regime for turbidity and fluoride removal from a synthetic solution containing sodium fluoride and calcium hydroxide. Aluminium salts were used as chemical coagulant and effects of different parameters were studied. The results revealed that under optimal condition, the overall efficiencies of the system were 97% turbidity removal and 73% fluoride removal (Adouj et al., 2016).

Ouslimane et al. (2017) studied removal of fluoride and copper from a synthetic semiconductor industry effluent in 1.5L beaker cell with stainless steel cathode and iron/aluminium anode. The optimum condition was presented as 400 mA current, 80 min retention time and initial pH of 3, corresponding to 99% removals of copper and fluoride. Also, removal of ammonia and sodium dodecyl sulfate (SDS) from semiconductor industry effluent using electroflotation technique was conducted by Adouj et al. (2017). Oxidation of ammonia and treatment of SDS was reported by the authors.

2.6.5 Pulp and Paper Industry

Pulp and paper industry produces a large amount of wastewater containing organics and suspended particles. Mansour et al. (2007) proposed a coagulation-electroflotation continuous-flow system for treatment of paper company wastewater in Tunisia. The system consisted of a coagulation tank followed by a two-compartment electroflotation cell equipped with stainless steel cathodes and titanium coated with ruthenium oxide anodes. More than 95% suspended solids removal was reported in 15-17 min retention time. Mansour and Kesentini (2008) used the same experimental setup for treatment of machine-washing effluent of cardboard industry and, in optimal condition, achieved 96%, 91% and 96.5% removals of COD, BOD₅ and suspended solids, respectively.

Electroflotation was implemented for color and COD removal from a pulp and paper industry wastewater using in 250mL batch cell with stainless steel cathode and aluminium/mild steel anode (Kalyani et al., 2009). Maximum color removal of 92% and COD removal of 95% was achieved using mild steel anode. The reaction time was 40 min and current density was 10 mA/cm².

Black liquor containing lignin (hardly biodegradable mixture of polyphenolic compounds) from a pulp and paper firm in South Tunisia was treated in a small batch electrochemical cell using aluminium/iron electrodes by Zaied and Bellakhal (2009). Under current density 14 mA/cm², reaction time 50 min and pH 7, the removal efficiencies of the system were 98%, 92% and 99% for removal of COD, polyphenols and color, respectively.

Bleaching process generates industrial wastewater in pulp and paper industry as well. Treatment study, i.e., COD, BOD and color removal, of this wastewater in batch electrocoagulation cell with aluminium anode was conducted by Sridhar et al. (2012). Also, electroflotation was employed in Jordan, for treatment of effluent of primary sedimentation tank of a paper and cardboard factory (Al-Shannag et al., 2012). The treatment technique removed up to 80% of TSS and COD with iron anodes and under current density 60 A/m², reaction time 30 min and 78% internal recirculation rate.

COD and turbidity removal from cardboard paper mill wastewater using aluminium/iron electrodes in a 250mL cell was experimentally investigated by Bellebia et al. (2012). The optimum operating condition was 10 min reaction time and 4.41 mA/cm² current density. Under this condition and with iron anodes 78.76% COD removal and 99.92% turbidity removal were reported by the authors.

2.6.6 Oil Industry

Since extraction of crude oil consumes large quantity of water, it produces effluents containing different contaminants, e.g., crude oil, suspended solids and dissolved solids. Electroflotation was presented as a treatment technique for removal of these contaminants. Bande et al. (2008) used a 2L rectangular batch cell with perforated aluminium plates at top and bottom of the cell as anode and cathode. Optimum electrical current was 0.4 A and optimum retention time was 20 min. Under these conditions, initial oil concentration of 100 mg/L dropped to less than 10 mg/L.

Leachate of oil-drilling mud was treated in a batch electrochemical cell with aluminium electrodes (Ighilahriz et al., 2014). 95% COD removal in 1 hr reaction time and under current density 0.0496A A/cm² was reported. In another study conducted by Hassan et al. (2015), a synthetic wastewater containing 500 mg/L crude oil and 15% surfactant and NaCl was prepared to simulate the oil industry effluent and a 2.42-L electroflotation batch cell with aluminium plate cathode and aluminium cylinders as anode was designed for treatment of the effluent. The treatment efficiencies after 5 and 35 min were 85 and 99%, respectively (Hassan et al., 2015).

Oil sands deposit is another source of crude oil; and tailings, containing bitumen, are environmental concerns associated with this industry. Alam and Shang (2017) studied treatability of synthetic oil sand tailing in a batch cell electroflotation reactor with stainless steel mesh cathode and Ti-IrO₂ mesh anode. 90% oil flotation efficiency was achieved at current density of 150 A/m².

2.6.7 Maritime Transportation

Maritime transportation produces wastewater mostly from washing operations that contains oil, fuel, etc. Treatment of oily bilge water from a stock reservoir in Canada was studied in a 1.71-L batch cell with iron and aluminium electrodes (Asselin et al., 2008). At a 1.5 A electrical current and 60-90 min reaction time, 95.6% oil and grease, 99.8% turbidity and 78.1% COD were separated.

Ulucan and Kurt (2015) examined treatment of bilge water from a waste-receiving facility in Turkey by electrochemical methods including electroflotation. Using aluminium electrodes in a 0.5-L reactor, 64.8% COD and 57% oil and grease removals were obtained in their study.

Treatability study of bilge water of ships, implementing electrochemical methods was conducted in Chile as well (Carlesi et al., 2015). The researchers run the experiments in a continuous-flow electroflotation reactor equipped with stainless steel cathode and oxidized titanium anode plates. After 2 hrs reaction time, percent removals of color, turbidity, COD and Pb-Zn were 80%, 70%, 50% and 40%, respectively.

2.6.8 Food Industry

Food industry has several subcategories and contaminating constituents of their wastewaters, depend on each industry's process and product. Poultry chiller water from a poultry processing plant in California, USA, was treated in a 2.2L column electroflotation reactor with nonconsumable electrodes (Tsai et al., 2002). Electroflotation separated 82% of TSS and was efficient in disinfection of the effluent. In a study, Drogui et al. (2008) performed the treatment studies of four types of food industry effluents, i.e., meat processing, fruit beverage production, cereal production and slaughterhouse wastewaters. The experiments were conducted in a 1.71L batch cell with aluminium or mild steel electrodes and reaction time was 90 min. Initial COD concentrations ranged between 366 and 3210 mg/L and current density was 5×10^{-3} A/cm². Maximum COD removals for meat processing, fruit beverage production, cereal production and slaughterhouse

wastewaters were 33.5% (Al electrodes), 40.2% (Fe electrodes), 23.3% (Fe electrodes) and 86.3% (Al electrodes), respectively. Wastewater from a prawn farm in China was treated by electrochemical method (Yunqing and Jianwei, 2011). Electroflotation reactor had a volume of 0.6 L, with Ti/IrO₂-SnO₂-Sb₂O₅ anodes and titanium cathodes, followed by a 1.2-L floated-sludge separator. COD, nitrogen and TSS were effectively removed from the wastewater while optimum condition was determined as 40 min retention time and 25 A/m² current density.

Davila et al. (2011) evaluated performance of a 0.5L electroflotation reactor in treatment of vinasse (liquid residue of alcohol distillation). Results revealed that percent removals of COD, turbidity, TS and TOC were 61, 89, 50 and 25, respectively. Effluent of a pistachio processing plant in Turkey was treated in a 1L batch cell using aluminium electrodes (Bayar et al., 2014). Under optimum current density of 6 mA/cm² and retention time of 180 min, COD removal was 60.1% and phenol removal was 77.3%. Esfandiyari et al. (2015) studied electrochemical treatment (with Al anode and RuO₂/Ti cathode electrodes) of an olive oil factory effluent in Iran. While H₂O₂ was added to improve the removal efficiency, under optimal condition, more than 90% removals of COD, TSS, color and oil and grease were reached. Orssatto et al. (2017) optimized performance of a batch electrochemical cell with Al electrodes in treatment of slaughterhouse and meat-packing unit. Optimum condition was presented as current density of 21.6 mA/cm² and retention time of 25 min. Removal rates were 81%, 99% and 99% for COD, turbidity and color, respectively.

2.6.9 Laundry

Laundry wastewater was treated in a 2.8-L electrochemical cell with Ti and Al electrodes followed by a 11.2-L separator (Ge et al., 2004). More than 70% COD removal and 90% turbidity, phosphate and surfactants removals were reported by the authors.

Wang et al. (2009) employed a 1-L electroflotation cell with Al anodes and cathodes to remove COD from simulated laundry wastewater. Highest COD removal rate was 62% while optimum electric potential was 5 V.

A 1.5-L electroflotation cell equipped with aluminium electrodes was used for treatment of actual laundry wastewater in Iran (Janpoor et al., 2011). The authors examined effects of different parameters and with initial COD concentration of 4155 mg/L, removal percentages of 93.2, 96.7, 95.9 and 93.5 were reported for COD, phosphorus, turbidity and detergent.

2.6.10 Oily Industrial Effluents

Oily effluents are produced in different industries, e.g., metal cutting and machining, rolling mill operation, food processing, etc. Yang (2007) studied treatment of synthetic wastewater containing motor oil and surfactants in a bench-scale electrochemical cell with iron anodes. Under continuous-flow condition and 2 A electrical current, effluent turbidity was less than 14 FAU (Formazin Attenuation Units). In another research, Chen et al. (2008) conducted treatment study of oil-bearing effluent from aluminum alloy machining process in USA. An 88-cm³ electrochemical reactor with Al anode and graphite cathode were implemented to reduce turbidity from 3261 to 60 FAU in 3 min retention time. Canizares et al. (2008) made synthetic oil-water emulsion with lubricant, soluble oils, supporting electrolyte and water, with total oil concentration of 1500 to 6000 mg/L. Using aluminium electrodes, the system was successful in removal of COD from the wastewater.

Hot-rolling mills generate oily wastewater that can be treated by electroflotation technique. Maksimov and Ostsemin (2015) employed a 6-L electroflotation cell with graphite anode and steel-mesh cathode for secondary treatment of rolled-product manufacturing effluent. When initial petroleum concentration was 100 mg/L, up to 95% removal efficiency was achieved. Optimal condition was reported as HRT of 10 min and current density of 0.8 A/cm². Oily effluent of part-washing operation in train industry

was treated with aluminium and iron electrodes of a batch electrochemical cell under different operational conditions (Ozyonar, 2016). Under 5 min retention time, maximum removal rates of turbidity, COD and TOC were 98.5%, 94.5% and 79.5%, respectively. Optimum current density of 75 A/m^2 was reported.

2.6.11 Metal Finishing

Electroflotation treatment of synthetic metal finishing industry effluent containing copper sulfate, nickel sulfate and sodium sulfate was examined by Khelifa et al. (2005). They used ruthenium oxide-coated titanium plate anode and stainless steel mesh cathode in a batch reactor with effective volume of 4 L. The system removal rate of heavy metals increased to 98 to 99% in optimum condition.

Heidmann and Calmano (2010) presented results of electrochemical treatment of actual industrial galvanic wastewater in Germany. Experiments were conducted in a 2-L beaker with iron and aluminium electrodes. Removal rates of Ni, Cu and Cr and effects of operating conditions were studied. While the initial concentration of Cu was as high as 2500 mg/L, under 180 min reaction time and initial pH of 5.0, the Cu concentration was reduced to 6.5 mg/L. It was concluded that for galvanic wastewater with high concentration of metals, electroflotation can be an effective secondary treatment method.

Effluent of a metal-coating plant in Turkey was treated in a 1-L electrochemical cell and removal rates of manganese, phosphate and iron, using aluminium electrodes were assessed (Ince, 2013). Under optimized condition (current density: 20 A/m^2 , retention time: 35 min), more than 97% removal of iron, manganese and phosphate was reported.

2.6.12 Synthetic Effluents Containing Heavy Metals

There are several studies working on removal of heavy metals from industrial effluents. Gao et al. (2005) studied removal of Chromium(VI) through electrochemical reactor with

iron electrodes. In 1.2 hr reaction time, effluent suspended solids concentration was below 3 mg/L and total Chromium concentration was 0.5 mg/L.

Escobar et al. (2006) performed experimental studies on treatability of synthetic wastewater containing copper, lead and cadmium. Under current density of 31-54 A/m² and using steel electrodes, 80% copper removal was reported in 6 min retention time. Successful separation of zinc (96%) from synthetic wastewater under current density of 8 mA/cm² with platinum anode and steel cathode was observed in another study (Casqueira et al., 2006). There are also other researches on treatment of simulated wastewaters and removal of Cr³⁺ (Golder and Samanta, 2007), heavy metal ions, e.g., Zn²⁺, Cu²⁺, Ni²⁺, Ag⁺ and Cr₂O₇²⁻ (Heidmann and Calmano, 2008; Kolesnikov et al., 2015), mercury(II) (Nanseu-Njiki et al., 2009) and cerium(III,IV) (Gaydukova et al., 2017) in laboratory.

Electroflotation technique was evaluated for removal of heavy metals from simulated wastewater from washing soil contaminated by drilling fluids from oil wells (da Mota et al., 2015). Under 20 min reaction time, 350 A/m² current density, initial metals concentrations of 15 mg/L and using stainless steel electrodes, 97% removal of heavy metals, i.e., lead, barium and zinc was achieved. Copper removal rate of 100% in 5 min reaction time with addition of 30 mg/L *Opuntia ficus indica* mucilage as natural coagulant in electrochemical cell with Al electrodes is stated in a recent study by Adjeroud et al. (2018).

2.6.13 Other Industries

Electroflotation was employed for treatment of radioactive wastewater by Il'in and Kolesnikov (2001). A continuous-flow reactor with stainless steel cathode and active-surface coating titanium anode electrodes showed promising separation efficiency compared to settlers, leading to shorter treatment time and smaller footprint.

Shen et al. (2003) studied electrochemical treatment of synthetic wastewater containing fluoride. In 20 min retention time, influent and effluent fluoride concentration values were 15 and 2 mg/L, respectively. Sawmills produce effluents composing of tannins,

carbohydrates, phenolic compounds, etc. Drogui et al. (2009) conducted experimental studies on treatment of sawmill effluents in Canada using electroflotation. In 9 min reaction time and under electrical current of 2 A, only 12% COD removal was reported. In another work, Khelifa et al. (2009) performed electroflotation tests to remove EDTA (a common chelating agent used in different industries) in a 3-L cell with Ti/RuO₂ anodes. Under current of 0.8 A, 2 hr reaction time and with 10 g/L NaCl concentration, electroflotation completely removed 400 mg/L of initial EDTA concentration. Skender et al. (2010) studied removal of non-ionic surfactants (widely used in detergents, fire deterrents, food industry, etc.) using steel electrodes and found that under optimal conditions, i.e., 8.42 mA/cm² current density and 7 g/L salt concentration, 74.79% removal rate was obtained. Electroflotation has been examined by other researchers for treatment of carwash wastewater (Panizza and Cerisola, 2010), recycling of fluorescent penetrant oil in aircraft industry (Meas et al., 2010), contaminants removal from landfill leachate (Bouhezila et al., 2011; Hassani et al., 2016) and nitrogen removal from industrial effluent of bone glue industry (El-Shazly, 2011) as well.

Optimum conditions of electroflotation treatment of effluent of a biodiesel refinery in Brazil were established by Palomino Romero et al. (2013). In a 2-L reactor equipped with aluminium electrodes with retention time of 60 min and current density of 8.0 mA/cm², removal rates of COD, TS (total solids), turbidity and oil and grease were 57%, 98%, 92% and 100%, respectively.

Mansoorian et al. (2014) evaluated performance of electroflotation in removal of lead and zinc from a battery manufacturer in Iran. With iron electrodes and under 6.0 mA/cm² current density, 97.2% lead and 95.5% zinc removals were achieved. Ceramic manufacturing units generate effluents containing clay particles and glazes of heavy metals. Kolesnikov et al. (2015) studied enhancement of electroflotation system with ruthenium-titanium oxide anode and stainless steel cathode plates for treatment of ceramic manufacturing wastewater. In another study, more than 90% removal rate of doxycycline hyclate (DCH) from a synthetic pharmaceutical effluent in a 1.5-L electrochemical reactor with Al electrodes in 80 min reaction time was reported by Zaidi et al. (2016).

Table 2.1 presents a summary of works of authors on applications of electroflotation in treatment of different industrial wastewaters, including the type of industrial wastewater, the used reactor and electrodes, treatment efficiency and operating conditions, e.g., retention time and applied electrical power.

Table 2.1: Applications of Electroflotation in Treatment of Industrial Effluents

Industrial Wastewater	Reactor	Electrodes	Retention Time	Applied Electricity	System Performance	Reference
Textile Industry						
Taken from a commercial textile-dyeing operation in Morocco	100 mL - batch	Iron Cathode, Iron Anode	2 to 8 min	600 mV	100% color and 84% COD removal at 3 min HRT and 600 mV potential	Zaroual et al. (2006)
Synthetic solution, C.I. Acid Yellow 23 dye and tap water	250 mL - batch	Steel Cathode, Iron and Aluminium Anode	2-6 min	25-400 A/m ²	98% color and 69% COD removal at 5 min HRT, 112.5 A/m ² C.D., 50 mg/L initial concentration	Daneshvar et al. (2007)
Synthetic solution, mixture of 2-naphthoic acid and 2-naphtol red dyes and tap water	20 L- external loop	Aluminium anode and cathode	0-50 min	5.5-34.3 mA/cm ²	80% COD and color removal	Essadki et al. (2008)
Effluent of Algerian velvet manufacturer	1 L, batch	Aluminium anode and cathode	5-25 min	10-25 V	BOD ₅ : 93.5%, COD: 90.3%, turbidity: 78.7%, SS: 93.3% and color: >93%. at HRT 20 min, 20 V – 93% heavy metals	Belkacem et al., (2008)
Synthetic dye wastewater	3.1 L, continuous	Al anode and cathode	35 min	300 A/m ²	90% for turbidity and 97% for color	Amour et al. (2016)
raw textile dyeing wastewater from a plant in Korea.	7 m ³ continuous	Aluminium anodes and titanium cathodes	0-30 min	0–300 A/m ²	92% TSS 94% COD, 98% color, 70% toxicity removals	Kim et al. (2016)
Synthetic dye wastewater	0.25 L batch	aluminum electrodes	5 and 15 min	1-4 mA/cm ²	99% of color removal from acid dye solutions	Bellebia et al. (2009)

Industrial Wastewater	Reactor	Electrodes	Retention Time	Applied Electricity	System Performance	Reference
Synthetic wastewater containing silica gel	1.5 L batch	aluminum electrodes	0-25 min	11.5-91.5 mA/cm ²	86.5% TSS, 81.56% turbidity, 83% BOD ₅ , 68% COD, 92.5% color	Merzouk et al. (2009)
Synthetic textile wastewater	8.6 L continuous	aluminum electrodes	0-32 min	20.8- 62.5 mA/cm ²	85% color, 80 COD	Merzouk et al. (2009)
Effluent of textile industry in Algeria.	1.5 L batch	aluminum electrodes	0-25 min	11.5-91.5 mA/cm ²	BOD ₅ 88.9%, COD 79.7%, SS 85.5%, turbidity 76.2%, and color 93%.	Merzouk et al. (2010)
Acid Blue 113 Dye Solution	250 mL batch	iron anode and stainless-steel cathode	60 min	1-5 A/dm ²	91% COD, 95% color	Saravanan et al. (2010)
Synthetic dye wastewater	1.0 l batch	cast iron electrodes	1-45 min	0.25 – 1 A	72.7 percent COD and 99.8 percent color	Altin (2011)
Solutions containing the dye yellow	1.0 L batch	aluminum electrodes	0-120 min	0.5 – 12 V	95% decolourization	Gonçalves et al. (2016)
Batik staining wastewater	5 L batch	316L stainless steel	2- 12 min	10 – 20 V	More than 93% color, turbidity and TSS removal	Warjito and Nurrohman. (2016)
Dairy Industry						
Dairy factory wastewater	650 mL batch	iron electrodes	0-600 min	0.3-0.8 mA/cm ²	98% COD and 99% oil and grease	Sengil and Ozacar (2006)
Real dairy wastewater	2 L batch	aluminium electrodes	15-60 min	10-60 V	98.84% COD, 97.95% BOD and 97.75% TSS removal	Bazrafshan et al. (2012)
Synthetic and real dairy wastewater	0.6 L batch	aluminium or iron electrodes	20-60 min	5-7 V	97.4% COD and 99.1% turbidity with iron	Melchioris et al. (2016)
Synthesized dairy wastewater	25.8 L continuous up-flow	aluminium electrodes	20 min	0.3-0.7 A/m ²	80% COD, 98% phosphate, 100% TSS and 100% turbidity	Bassala et al. (2017)

Industrial Wastewater	Reactor	Electrodes	Retention Time	Applied Electricity	System Performance	Reference
Tannery Industry						
Real tannery wastewater	3 L continuous	Al, Fe, Ti with Ir/Ta/Ru oxides and graphite anode;	60-300 s	31-62 mA/cm ²	95.3% TSS removal	Muruganathan et al. (2004)
Synthetic tannins effluent	3 L continuous	Iron rods TaO ₂ /RuO ₂ /IrO ₂ coated titanium rods electrodes	0-700 s	47 mA/cm ²	75–99% COD	Muruganathan et al. (2005)
Effluent of sedimentation tank of a tannery unit	2 L batch	mild steel or aluminum electrodes	0-60 min	0.4 – 1.0 A	55.1% TOC, 43.1% NH ₃ -N, 61.8% BOD, 68.0% COD and 96.7% sulfide	Feng et al. (2007)
Wastewater of leather finishing processing factory	5 L batch	Iron electrodes	0-120 min	43–68 mA/cm ²	90–99% turbidity; 30–60% TSS; 40–80% calcium removal	Espinoza-Quiñones et al. (2009)
Industrial chrome tanning effluents	1 L batch	Mild steel or Al electrodes	0-90 min	65-98 mA/cm ²	More than 90% Cr(III) removal	Golder et al. (2011)
Chromium contaminated tannery spent liquor effluent	Membrane-EF batch	Ti/TiO ₂ -RuO ₂ anode and Ti expanded mesh cathode	0-120 min	100 mA/cm ²	98% chromium(III), 91% lipid and 95% protein removal	Selvaraj et al. (2018)
Semiconductor Industry						
Effluent of a semiconductor manufacturing plant	180 L pilot-scale continuous-flow	iron anodes and stainless steel cathodes	30-100 min	4.4-7.3 A/m ²	More than 90% turbidity removal in 60 min HRT	Den and Huang (2006)
Simulated semiconductor wastewater	2.5 L batch	aluminium anode and stainless steel cathode	0-120 min	320-800 mA	90% fluoride, 85% turbidity	Adouj et al. (2015)
Simulated semiconductor wastewater	batch	Al-Fe and Ti/RuO ₂ anode and stainless steel cathode	0-90 min	300-600 mA	complete Cr(VI) removal	Adouj et al. (2015)
Synthetic solution of sodium fluoride and calcium hydroxide	1.5 L batch	stainless steel cathode and Ti/RuO ₂ anode	0-60 min	100 to 250 mA	97% turbidity and 73% fluoride removal	Adouj et al. (2016)

Industrial Wastewater	Reactor	Electrodes	Retention Time	Applied Electricity	System Performance	Reference
Synthetic silicon etching rinse baths	1000 mL batch	aluminum electrodes	0-120 min	100-800 mA	99% fluoride and copper removal	Ouslimane et al. (2017)
Simulated semiconductor wastewater	7 L total, batch	Al-Fe and Ti/RuO ₂ anode and stainless steel cathode	Up to 350 min	400-600 mA	Effluent concentrations of sodium dodecyl sulfate, fluoride, ammonia and turbidity below discharge limit	Adouj et al. (2017)
Pulp and Paper Industry						
Paper company wastewater in Tunisia	4.2 L continuous	stainless steel cathodes, Ti/RuO ₂ anode	10-22 min	200 A/m ²	95% suspended solids removal	Mansour et al. (2007)
Machine-washing effluent of cardboard industry	4.2 L continuous	stainless steel cathodes, Ti/RuO ₂ anode	28 min optimized	148.7 A/m ² optimized	96% COD, 91% BOD and 96.5% TSS removals	Mansour and Kesentini (2008)
Pulp and paper industry wastewater	250 mL batch	stainless steel cathode and aluminium/mild steel anode	0-40 min	5-10 mA/cm ²	92% color and 95% COD removal with mild steel anode	Kalyani et al. (2009)
Black liquor containing lignin from factory	0.3 L batch	aluminium/iron electrodes	0-100 min	1.7-16.7 mA/cm ²	98% COD, 92% polyphenol and 99% color removal	Zaied and Bellakhal (2009)
Bleaching effluent from pulp and paper mill	0.3 L batch	aluminium electrodes	10-30 min	5-25 mA/cm ²	More than 90% COD and BOD removal	Sridhar et al. (2012)
Paper and Cardboard effluent in Jordan	6 L batch	Iron electrodes	Up to 90 min	20-80 A/m ²	80% TSS and COD removal	Al-Shannag et al. (2012)
Cardboard paper mill wastewater	250 mL batch	aluminium/iron electrodes	2-25 min	1.47-13.23 mA/cm ²	78.76% COD and 99.92% turbidity removal with Fe electrodes	Bellebia et al. (2012)
Oil Industry						
Produced water from oil platform in North Sea	Continuous-flow reactor	Al anode, Stainless steel cathode	0.5 to 1.5 m ³ /hr flowrate	50 and 150 A	91.2% Zinc, 94% Iron, >90% oil removal	Saur et al. (1996)
Synthetic oil-field effluent	Batch and continuous	stainless steel screens	0-50 min	5-20 mA/cm ²	90% oil removal in 30 min and 20 mA/cm ²	Ibrahim et al. (2001)

Industrial Wastewater	Reactor	Electrodes	Retention Time	Applied Electricity	System Performance	Reference
Marine Mediterranean crude oil suspension	0.35 L batch	Stainless steel cathode, Titanium anode	0-60 min	30-180 A/m ²	70% oil removal at optimum condition	Mansour and Chalbi (2006)
Synthetic crude oil solution	2 L batch	perforated aluminium plates	10-50 min	2.5-7.5 V	More than 90% oil removal	Bande et al. (2008)
Leachate of oil-drilling mud	200 mL batch	Aluminum electrodes, stainless steel anode and ruthenium cathode	10-90 min	0.015-0.06 A/cm ²	95% COD removal	Ighilahriz et al. (2014)
Synthetic crude oil solution	2.42 L batch	aluminium plate cathode, aluminium cylinders anode	0-35 min	0.002-0.01 A/cm ²	99% oil removal in 35 min	Hassan et al. (2015)
Samples from mature fine tailings pond in Canada	4.5 L batch	stainless steel mesh cathode and Ti-IrO ₂ mesh anode	0-90 min	50-300 A/m ²	90% oil removal at 150 A/m ²	Alam and Shang (2017)
Maritime Transportation						
Actual oily bilge water	1.71 L batch	iron and aluminium electrodes	0-90 min	0.3-1.5 A	95.6% oil and grease, 99.8% turbidity and 78.1% COD removal	Asselin et al. (2008)
Actual bilge water	0.5 L batch	aluminium electrodes	5-120 min	2.5-25 mA/cm ²	64.8% COD and 57% oil and grease removal	Ulucan and Kurt (2015)
Actual bilge water	4 L continuous	stainless steel cathode and oxidized titanium anode	Up to 120 min	2-6 A	80% color, 70% turbidity, 50% COD and 40% Pb-Zn removal in 120 min	Carlesi et al. (2015)
Food Industry						
Actual poultry chiller water	2.2 L continuous	nonconsumable electrodes	29.3 min	280-1200 coulomb/L charge	82% TSS removal, successful disinfection	Tsai et al. (2002)
Poultry slaughterhouse effluent	250 mL batch	Al or Fe electrodes	5-40 min	20-200 A/m ²	93% COD, 98% oil and grease removal	Bayramoglu et al. (2006)

Industrial Wastewater	Reactor	Electrodes	Retention Time	Applied Electricity	System Performance	Reference
Meat processing, beverage and cereal production and slaughterhouse effluents	1.71 L batch	aluminium or mild steel electrodes	10-90 min	0.002-0.096 A/cm ²	86.3% COD for slaughterhouse with Al electrodes	Drogui et al. (2008)
Prawn farm wastewater	0.6 L batch	Ti/IrO ₂ -SnO ₂ -Sb ₂ O ₅ anodes and titanium cathodes	10-90 min	10-50 A/m ²	79% COD, 91% TSS, 91% TAN, 92% NO ₂ -N removal	Yunqing and Jianwei (2011)
Vinasse from alcohol distillation unit	0.5 L batch	Al, Fe, galvanized steel	n/a	20-60 mA/cm ²	50% TSS, 89% turbidity, 25% TOC, 61% COD removal	Davila et al. (2011)
Wastewater of pistachio processing plant	1 L batch	aluminium electrodes	Up to 180 min	1-6 mA/cm ²	60.1% COD, 77.3% phenol removal	Bayar et al., 2014
Olive oil factory effluent	7.5 L continuous	Al anode and RuO ₂ /Ti cathode	5-30 min	5-40 mA/cm ²	> 90% COD, TSS, color and oil and grease removal	Esfandyari et al. (2015)
Slaughterhouse and meat packing unit effluents	1 L batch	Al electrodes	25 min optimal	21.6 mA/cm ² optimal	81% COD, 99% turbidity, 99% color removal	Orssatto et al. (2017)
Olive pomace oil refinery wastewater	300 mL batch, 4.2 L continuous	Ti/RuO ₂ anode, stainless steel cathode	25 min optimized	205 A/m ² optimized	> 92% COD and TSS removal	Hmidi et al. (2017)
Effluent of vegetable oil refining industry	1 L batch	Ti/RuO ₂ anode, stainless steel cathode	30 min	40-260 A/m ²	Successful removal of turbidity	Issaoui et al. (2017)
Laundry						
Actual laundry wastewater	14 L total, continuous	Al and Titanium electrodes	5-28 min	0.8-2 A	70% COD, 90% turbidity, phosphate and surfactant removal	Ge et al. (2004)
Simulated laundry wastewater	1 L batch	Al or Fe electrodes	Up to 40 min	0.2-7.0 V	62% COD removal with Al electrodes	Wang et al. (2009)

Industrial Wastewater	Reactor	Electrodes	Retention Time	Applied Electricity	System Performance	Reference
Actual laundry wastewater ¹	.5 L batch	Aluminium electrodes	Up to 90 min	0.15-1.32 A	93.2% COD, 96.7% phosphorus, 95.9% turbidity and 93.5% detergent removal	Janpoor et al. (2011)
Oily Industrial Effluents						
Synthetic oily wastewater	5.5 L batch	Stainless steel cathode, steel anode	30-120 min	6-14 mA/cm ²	99% oil removal	Mostefa and Tir (2004)
Synthetic wastewater containing motor oil and surfactants	616 cm ³ continuous	Cast iron electrodes	0-30 min	1-2 A	effluent turbidity less than 14 FAU	Yang (2007)
Oily effluent from aluminum alloy machining process	88 cm ³ batch	Al anode and graphite cathode	0-14 min	5 and 10 V	turbidity reduced to 60 from 3261 FAU in 3 min	Chen et al. (2008)
Synthetic oil-water emulsion	1.5 L continuous	Al electrodes	Up to 25 min	10.1 mA/cm ²	Successful COD removal	Canizares et al. (2008)
Rolled-product manufacturing effluent	6 L continuous	Graphite anode, steel mesh cathode	0-30 min	1-3.6 A/cm ²	95% petroleum removal	Maksimov and Ostsemin (2015)
Oily effluent of part washing operation in train industry	1000 mL batch	Al and Fe electrodes	0-45 min	25-150 A/m ²	98.5% turbidity, 94.5% COD and 79.5% TOC removal in 5 min	Ozyonar (2016)
Metal Finishing Industry						
Synthetic metal finishing effluent	4 L batch	Ti/RuO ₂ anode, stainless steel cathode	Up to 5 hr	0.2-1.0 A	98-99% nickel and copper removal in optimum condition	Khelifa et al. (2005)
Actual industrial galvanic wastewater	2 L batch	iron and aluminium electrodes	0-180 min	0.05 to 1.5 A	> 90% Ni, Cu and Cr removal	Heidmann and Calmano (2010)
Effluent of a metal-coating plant	1 L batch	aluminium electrodes	0-60 min	2.5-30 A/m ²	> 97% removal of iron, manganese and phosphate	Ince (2013)

Industrial Wastewater	Reactor	Electrodes	Retention Time	Applied Electricity	System Performance	Reference
Synthetic Effluents Containing Heavy Metals						
Synthetic wastewater	0.46 L continuous	iron electrodes	9.23-24 min	30 A/m ²	effluent TSS < 3 mg/L and total Chromium: 0.5 mg/L	Gao et al. (2005)
Synthetic wastewater	0.02 L continuous	steel electrodes	6-17 mL/min flowrate	30-110 A/m ²	Close to 100% copper, lead and cadmium removal	Escobar et al. (2006)
Synthetic wastewater	Continuous-flow reactor	platinum anode and steel cathode	30 and 60 min	2-12 mA/cm ²	96% zinc removal	Casqueira et al. (2006)
Synthetic wastewater	800 mL batch	Mild steel electrodes	5-60 min	10.84 and 32.52 mA/cm ²	99.9% Cr ³⁺ removal	Golder and Samanta (2007)
Synthetic wastewater	2000 mL batch	aluminium electrodes	0-30 min	3.3-98 A/m ²	Zn, Cu, Ni, Ag, Cr removal mechanism studied	Heidmann and Calmano (2008)
Synthetic wastewater	0.5 dm ³ . batch	Ti/RuO ₂ anode, stainless steel cathode	30 min	0.2 A/L	> 95% copper, nickel, and zinc hydroxides removal	Kolesnikov et al. (2015)
Synthetic wastewater	100 mL batch	aluminium and iron electrodes.	15 and 25 min	0.625-3.125 Adm ⁻²	99% mercury(II) removal	Nanseau-Njiki et al. (2009)
Synthetic wastewater	1 dm ³	stainless steel electrodes	5-30 min	75-350 A/m ²	97% removal of lead, barium and zinc	da Mota et al. (2015)
Synthetic wastewater	2 L batch	aluminum electrodes	0-60 min	11.55 mA/cm ²	100% copper removal with addition of natural coagulant	Adjeroud et al. (2018).
Synthetic wastewater	2000 mL batch	iron electrodes	0-120 min	0.05-3.0 A	Cr(VI) removal process studied	Heidmann and Calmano (2008)

Industrial Wastewater	Reactor	Electrodes	Retention Time	Applied Electricity	System Performance	Reference
Other Industries						
Radioactive wastewater	Continuous-flow	stainless steel cathode, Ti/TiO ₂ -RuO ₂ anode	10 m ³ /h flowrate	0.2–0.4 kW·h/m ³ energy consumption	Successful separation of the solid and liquid phases.	Il'in and Kolesnikov (2001)
Synthetic wastewater containing fluoride	Continuous-flow	aluminum electrodes	20 min	0-6 Faradays/m ³ Charge Loading	Effluent fluoride less than 2 mg/L	Shen et al. (2003)
Sawmill effluents in Canada	1.7 L batch	mild steel or aluminium electrodes	90 min	2.0 A	12.5% to 13.6% COD removal	Droguet et al. (2009)
Synthetic wastewater containing EDTA	3 L batch	Ti/RuO ₂ anodes, steel cathode	0-300 min	200-800 mA	400 mg/L of initial EDTA removed in 2 hr	Khelifa et al. (2009)
Synthetic wastewater containing non-ionic surfactants	batch	Stainless steel electrodes	0-30 min	2-13 mA/cm ²	74.79% removal at 8.42 mA/cm ² current density	Skender et al. (2010)
Carwash wastewater	0.300 dm ³ batch	Iron anode, stainless steel cathode	0-10 min	1 and 10 mA/cm ²	75% COD removal in optimum condition	Panizza and Cerisola (2010)
Solution of fluorescent penetrant oil in aircraft industry	3.75 L continuous	Al electrodes	0-20 min	00–1000 A/m ²	95% COD, 99% color and 99% turbidity removal	Meas et al. (2010)
Landfill leachate	500 cm ³ batch	Al and Fe electrodes	0-30 min	125 and 500 A/m ² ,	70% COD, 60% turbidity, 56% color, and 24% nitrogen removal	Bouhezila et al. (2011)
Landfill leachate	Continuous-flow	Al and Ti/RuO ₂ anode, stainless steel cathode	0-120 min	10-40 V	86.9% COD, 88.7% TSS, 90.2% oil and grease, and 93.7% turbidity removal	Hassani et al. (2016)
Effluent of bone glue industry	1000 mL batch	Al electrode	25-125 min	1-4 mA/cm ²	60–80% Nitrogen, 68% BOD, 61% COD, 85% TSS removal	El-Shazly (2011)
Effluent of a biodiesel refinery	2 L batch	Al electrode	0-60 min	2-8 mA/cm ²	57% COD, 98% TS, 92% turbidity and 100% oil and grease removal	Palomino Romero et al. (2013)

Industrial Wastewater	Reactor	Electrodes	Retention Time	Applied Electricity	System Performance	Reference
Battery manufacturing wastewater	1 L batch	iron and stainless steel electrodes	10-40 min	2-10 mA/cm ²	97.2% lead and 95.5% zinc removal with Fe electrode	Mansoorian et al. (2014)
Ceramic manufacturing wastewater	Continuous-flow	Ti/TiO ₂ -RuO ₂ anode, stainless steel cathode	5-10 min	n/a	Optimized reactor design	Kolesnikov et al. (2015)
Synthetic pharmaceutical effluent	1.5 L batch	Al electrodes	0-120 min	3.59-14.39 mA/cm ²	> 90% doxycycline hyclate (DCH) removal	Zaidi et al. (2016)

2.7 Full-scale Electroflotation Units

Full-scale commercial electroflotation systems are mostly available in package units constructed by private companies for industrial applications. E-Flo Dr. Baer electroflotation unit (Envirochemie, 2014) developed by Envirochemie company in Germany is stated to be for treatment of small to medium quantities of wastewater, process water and rinsing water, managing influents in temperature range of 5 to 70 C. It is equipped with patented inert coated electrodes for production of H₂ and O₂ bubbles. Energy consumption of electroflotation unit is reported as 0.1 kWh/m³ treated wastewater. The unit is comprised of two compartments with electrode units installed in the bottom of first compartment, Figure 2.10.

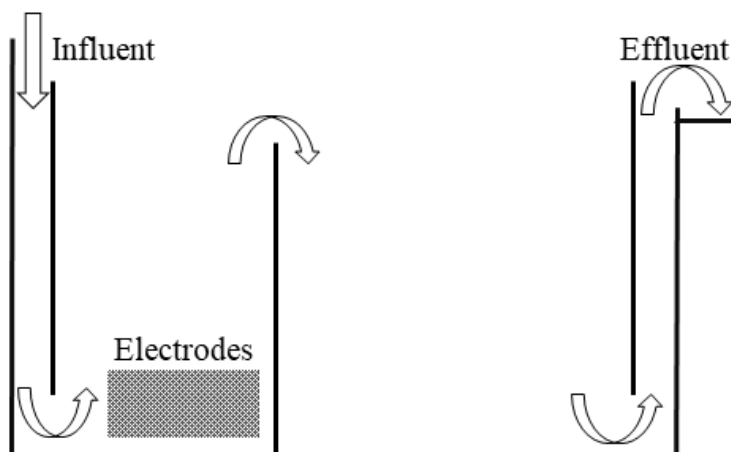


Figure 2.10: Schematic of E-Flo Dr. Baer electroflotation package

Electroflotation unit designed and constructed by Mendeleev University Science Park (2008) is shown in Figure 2.11.

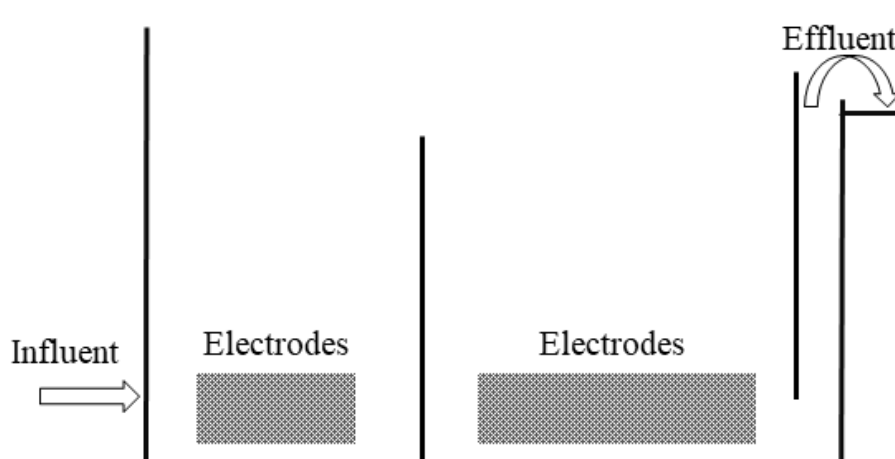


Figure 2.11: Schematic of electroflotation unit manufactured by Mendeleev University Science Park

The unit has two compartments and uses insoluble anodes, with up to 10 years lifetime, in both compartments. It includes DC power supply of 100-150 A with voltage of 15-20 V and sludge collecting system. The electroflotation unit was employed for removal of heavy metals from wastewater of electroplating and printed circuit board production. With power consumption of less than 0.5 kWh/m³ treated wastewater, while initial concentrations of different heavy metals, e.g., Cu²⁺, Ni²⁺, Zn²⁺, Cd²⁺, Cr³⁺, Fe²⁺, Fe³⁺, Al³⁺, ranged from 5 to 30 mg/L, effluent concentrations of electroflotation unit were 0.2-2 mg/L. The unit was capable of removing suspended solid and oil and grease as well (Mendeleev University Science Park, 2008).

2.8 Conclusions

With the global water demand and environmental concerns of industrialization, more effective and efficient wastewater treatment techniques are needed. In this chapter, the electroflotation treatment of a wide range of industrial effluents was reviewed, e.g., oily wastewater, food industry effluents, textile industry effluents, etc. Modern long-life and less expensive electrode materials have been developed and manufactured, making the process increasingly attractive in terms of capital and operating costs. In addition, sacrificial metals, e.g., Al and Fe, have been used as anodes when in situ coagulations were needed to reach the desired effluent concentrations. Commercialized full-scale electroflotation units, especially pre-constructed package units, have been established and operated in different industries and countries, promising more installations of electroflotation plants in the future.

Up to date, there is no published design handbook of electroflotation plants, thus it was the objective of this research to explore the fundamentals, design aspects and applications of electroflotation process, to serve scientists and engineers working in this field.

Acknowledgements

This study has been supported by University of Western Ontario and The Natural Sciences and Engineering Research Council of Canada, NSERC.

References

- Adjeroud, N., Elabbas, S., Merzouk, B., Hammoui, Y., Felkai-Haddache, L., Remini, H., ... & Madani, K. (2018). Effect of *Opuntia ficus indica* mucilage on copper removal from water by electrocoagulation-electroflotation technique. *Journal of Electroanalytical Chemistry*, *811*, 26-36.
- Alam, R., & Shang, J. Q. (2017). Removal of bitumen from mature oil sands tailings slurries by electro-flotation. *Journal of Water Process Engineering*, *15*, 116-123.
- Alam, R., Shang, J. Q., & Khan, A. H. (2017). Bubble size distribution in a laboratory-scale electroflotation study. *Environmental monitoring and assessment*, *189*(4), 193.
- Al-Shannag, M., Lafi, W., Bani-Melhem, K., Gharagheer, F., & Dhaimat, O. (2012). Reduction of COD and TSS from paper industries wastewater using electro-coagulation and chemical coagulation. *Separation Science and Technology*, *47*(5), 700-708.
- Altin, S. (2011). Removal of Remazol Turquoise Blue (G-133) and Polyvinyl Alcohol (PVA) by Electrocoagulation using Monopolar and Bipolar Electrodes. *International Journal of Chemical Reactor Engineering*, *9*(1).
- Amour, A., Merzouk, B., Leclerc, J. P., & Lopicque, F. (2016). Removal of reactive textile dye from aqueous solutions by electrocoagulation in a continuous cell. *Desalination and Water Treatment*, *57*(48-49), 22764-22773.
- Aoudj, S., Khelifa, A., & Drouiche, N. (2017). Removal of fluoride, SDS, ammonia and turbidity from semiconductor wastewater by combined electrocoagulation–electroflotation. *Chemosphere*, *180*, 379-387.
- Aoudj, S., Khelifa, A., Drouiche, N., & Hecini, M. (2015). Development of an integrated electro-coagulation–flotation for semiconductor wastewater treatment. *Desalination and Water Treatment*, *55*(6), 1422-1432.

Aoudj, S., Khelifa, A., Drouiche, N., & Hecini, M. (2016). Removal of fluoride and turbidity from semiconductor industry wastewater by combined coagulation and electroflotation. *Desalination and Water Treatment*, 57(39), 18398-18405.

Aoudj, S., Khelifa, A., Drouiche, N., Belkada, R., & Miroud, D. (2015). Simultaneous removal of chromium (VI) and fluoride by electrocoagulation–electroflotation: application of a hybrid Fe-Al anode. *Chemical Engineering Journal*, 267, 153-162.

Aouni, A., Fersi, C., Ali, M. B. S., & Dhahbi, M. (2009). Treatment of textile wastewater by a hybrid electrocoagulation/nanofiltration process. *Journal of hazardous materials*, 168(2-3), 868-874.

Asselin, M., Drogui, P., Brar, S. K., Benmoussa, H., & Blais, J. F. (2008). Organics removal in oily bilgewater by electrocoagulation process. *Journal of Hazardous Materials*, 151(2-3), 446-455.

Bagotskii, V. S. (2006). *Fundamentals of electrochemistry*. Wiley-Interscience. Hoboken, NJ, USA.

Bande, R. M., Prasad, B., Mishra, I. M., & Wasewar, K. L. (2008). Oil field effluent water treatment for safe disposal by electroflotation. *Chemical Engineering Journal*, 137(3), 503-509.

Bassala, H. D., Dedzo, G. K., Bememba, C. B. N., Seumo, P. M. T., Dazie, J. D., Nansu-Njiki, C. P., & Ngameni, E. (2017). Investigation of the efficiency of a designed electrocoagulation reactor: Application for dairy effluent treatment. *Process Safety and Environmental Protection*, 111, 122-127.

Bayar, S., Boncukcuoğlu, R., Yilmaz, A. E., & Fil, B. A. (2014). Pre-treatment of pistachio processing industry wastewaters (PPIW) by electrocoagulation using Al plate electrode. *Separation Science and Technology*, 49(7), 1008-1018.

Bayramoglu, M., Kobya, M., Can, O. T., & Sozbir, M. (2004). Operating cost analysis of electrocoagulation of textile dye wastewater. *Separation and Purification Technology*, 37(2), 117-125.

- Bayramoglu, M., Kobya, M., Eyvaz, M., & Senturk, E. (2006). Technical and economic analysis of electrocoagulation for the treatment of poultry slaughterhouse wastewater. *Separation and Purification Technology*, 51(3), 404-408.
- Bazrafshan, E., Moein, H., Kord Mostafapour, F., & Nakhaie, S. (2012). Application of electrocoagulation process for dairy wastewater treatment. *Journal of Chemistry*, 2013.
- Belkacem, M., Khodir, M., & Abdelkrim, S. (2008). Treatment characteristics of textile wastewater and removal of heavy metals using the electroflotation technique. *Desalination*, 228(1-3), 245-254.
- Bellebia, S., Kacha, S., Bouberka, Z., Bouyakoub, A. Z., & Derriche, Z. (2009). Color removal from acid and reactive dye solutions by electrocoagulation and electrocoagulation/adsorption processes. *Water Environment Research*, 81(4), 382-393.
- Bellebia, S., Kacha, S., Bouyakoub, A. Z., & Derriche, Z. (2012). Experimental investigation of chemical oxygen demand and turbidity removal from cardboard paper mill effluents using combined electrocoagulation and adsorption processes. *Environmental Progress & Sustainable Energy*, 31(3), 361-370.
- Bennajah, M., Maalmi, M., Darmane, Y., & Touhami, M. E. (2010). Defluoridation of drinking water by electrocoagulation/electroflotation: kinetic study. *Journal of Urban and Environmental Engineering*, 4(1), 37-45.
- Bhaskar Raju, G., & Khangaonkar, P. R. (1984). Electroflotation-A critical review. *Transactions of the Indian Institute of Metals*, 37(1), 59-66.
- Bouhezila, F., Hariti, M., Lounici, H., & Mameri, N. (2011). Treatment of the OUED SMAR town landfill leachate by an electrochemical reactor. *Desalination*, 280(1-3), 347-353.
- Burns, S. E., Yiacoumi, S., & Tsouris, C. (1997). Microbubble generation for environmental and industrial separations. *Separation and Purification Technology*, 11(3), 221-232.

- Canizares, P., Martínez, F., Jiménez, C., Sáez, C., & Rodrigo, M. A. (2008). Coagulation and electrocoagulation of oil-in-water emulsions. *Journal of Hazardous Materials*, *151*(1), 44-51.
- Carlesi, C., Guajardo Ramírez, N., Carvajal, D., Cataldo Hernández, M., & Fino, D. (2015). Electrochemical treatment of bilge wastewater. *Desalination and Water Treatment*, *54*(6), 1556-1562.
- Casqueira, R. G., Torem, M. L., & Kohler, H. M. (2006). The removal of zinc from liquid streams by electroflotation. *Minerals engineering*, *19*(13), 1388-1392.
- Chen, L., Hsieh, C. C., Wetherbee, J., & Yang, C. L. (2008). Characteristics and treatability of oil-bearing wastes from aluminum alloy machining operations. *Journal of hazardous materials*, *152*(3), 1220-1228.
- Chen, X., & Chen, G. (2005). Stable Ti/RuO₂-Sb₂O₅-SnO₂ electrodes for O₂ evolution. *Electrochimica Acta*, *50*(20), 4155-4159.
- Chen, X., Chen, G., & Yue, P. L. (2002). Novel electrode system for electroflotation of wastewater. *Environmental science & technology*, *36*(4), 778-783.
- da Cruz, S. G., Dutra, A. J., & Monte, M. B. (2016). The influence of some parameters on bubble average diameter in an electroflotation cell by laser diffraction method. *Journal of Environmental Chemical Engineering*, *4*(3), 3681-3687.
- da Mota, I. D. O., de Castro, J. A., de Góes Casqueira, R., & de Oliveira Junior, A. G. (2015). Study of electroflotation method for treatment of wastewater from washing soil contaminated by heavy metals. *Journal of Materials Research and Technology*, *4*(2), 109-113.
- Daneshvar, N., Khataee, A. R., Ghadim, A. A., & Rasoulifard, M. H. (2007). Decolorization of CI Acid Yellow 23 solution by electrocoagulation process: Investigation of operational parameters and evaluation of specific electrical energy consumption (SEEC). *Journal of hazardous materials*, *148*(3), 566-572.

Daneshvar, N., Oladegaragoze, A., & Djafarzadeh, N. (2006). Decolorization of basic dye solutions by electrocoagulation: an investigation of the effect of operational parameters. *Journal of hazardous materials*, 129(1-3), 116-122.

Daneshvar, N., Sorkhabi, H. A., & Kasiri, M. B. (2004). Decolorization of dye solution containing Acid Red 14 by electrocoagulation with a comparative investigation of different electrode connections. *Journal of hazardous materials*, 112(1-2), 55-62.

Davila, J. A., Machuca, F., & Marrianga, N. (2011). Treatment of vinasses by electrocoagulation–electroflotation using the Taguchi method. *Electrochimica Acta*, 56(22), 7433-7436.

Den, W., & Huang, C. (2006). Electrocoagulation of silica nanoparticles in wafer polishing wastewater by a multichannel flow reactor: A kinetic study. *Journal of Environmental Engineering*, 132(12), 1651-1658.

Drogui, P., Asselin, M., Brar, S. K., Benmoussa, H., & Blais, J. F. (2008). Electrochemical removal of pollutants from agro-industry wastewaters. *Separation and Purification Technology*, 61(3), 301-310.

Drogui, P., Asselin, M., Brar, S. K., Benmoussa, H., & Blais, J. F. (2009). Electrochemical removal of organics and oil from sawmill and ship effluents. *Canadian Journal of Civil Engineering*, 36(3), 529-539.

El-Shazly, A. H. (2011). Investigation for the possibility of nitrogen removal from industrial effluent of bone glue industry using a batch electrocoagulation unit with monopolar horizontal electrodes. *Desalination and Water Treatment*, 25(1-3), 31-38.

EnviroChemie. (2014). *Product information: Compact electroflotation - an energy-saving and resource-saving alternative for water treatment*. Retrieved from https://envirochemie.com/cms/upload/news/20140616gb/Compact_electroflotation.pdf (Accessed 11 January 2018).

Escobar, C., Soto-Salazar, C., & Toral, M. I. (2006). Optimization of the electrocoagulation process for the removal of copper, lead and cadmium in natural waters and simulated wastewater. *Journal of environmental management*, 81(4), 384-391.

Esfandyari, Y., Mahdavi, Y., Seyedsalehi, M., Hoseini, M., Safari, G. H., Ghozikali, M. G., ... & Jaafari, J. (2015). Degradation and biodegradability improvement of the olive mill wastewater by peroxi-electrocoagulation/electrooxidation-electroflotation process with bipolar aluminum electrodes. *Environmental Science and Pollution Research*, 22(8), 6288-6297.

Espinoza-Quiñones, F. R., Fornari, M. M., Módenes, A. N., Palácio, S. M., da Silva Jr, F. G., Szymanski, N., ... & Trigueros, D. E. (2009). Pollutant removal from tannery effluent by electrocoagulation. *Chemical engineering journal*, 151(1-3), 59-65.

Essadki, A. H., Bennajah, M., Gourich, B., Vial, C., Azzi, M., & Delmas, H. (2008). Electrocoagulation/electroflotation in an external-loop airlift reactor—application to the decolorization of textile dye wastewater: a case study. *Chemical engineering and processing: Process intensification*, 47(8), 1211-1223.

Evdokimov, I. A., Titov, S. A., Polyansky, K. K., & Saiko, D. S. (2017). Ultrafiltration concentrating of curd whey after electroflotation treatment. *Foods and Raw materials*, 5(1).

Ezechi, E. H., Isa, M. H., Kutty, S. R. M., & Yaqub, A. (2014). Boron removal from produced water using electrocoagulation. *Process safety and environmental protection*, 92(6), 509-514.

Feng, J. W., Sun, Y. B., Zheng, Z., Zhang, J. B., Shu, L. I., & Tian, Y. C. (2007). Treatment of tannery wastewater by electrocoagulation. *Journal of Environmental Sciences*, 19(12), 1409-1415.

Gao, P., Chen, X., Shen, F., & Chen, G. (2005). Removal of chromium (VI) from wastewater by combined electrocoagulation–electroflotation without a filter. *Separation and purification technology*, 43(2), 117-123.

- Gaydukova, A. M., Brodskiy, V. A., Volkova, V. V., & Kolesnikov, V. A. (2017). Selective separation and extraction of copper (II), iron (II, III), and Cerium (III, IV) ions from aqueous solutions by electroflotation method. *Russian Journal of Applied Chemistry*, 90(8), 1252-1257.
- Ge, J., Qu, J., Lei, P., & Liu, H. (2004). New bipolar electrocoagulation–electroflotation process for the treatment of laundry wastewater. *Separation and Purification Technology*, 36(1), 33-39.
- Ghosh, D., Medhi, C. R., & Purkait, M. K. (2008). Treatment of fluoride containing drinking water by electrocoagulation using monopolar and bipolar electrode connections. *Chemosphere*, 73(9), 1393-1400.
- Golder, A. K., Samanta, A. N., & Ray, S. (2007). Removal of Cr³⁺ by electrocoagulation with multiple electrodes: Bipolar and monopolar configurations. *Journal of Hazardous Materials*, 141(3), 653-661.
- Golder, A. K., Samanta, A. N., & Ray, S. (2011). Removal of chromium and organic pollutants from industrial chrome tanning effluents by electrocoagulation. *Chemical Engineering & Technology*, 34(5), 775-783.
- Gonçalves, M. V., De Oliveira, S. C., Abreu, B. M., Guerra, E. M., & Cestarolli, D. T. (2016). Electrocoagulation/electroflotation Process Applied to Decolourization of a Solution Containing the Dye Yellow Sirius. *Int. J. Electrochem. Sci*, 11, 7576-7583.
- Hakizimana, J. N., Najid, N., Gourich, B., Vial, C., Stiriba, Y., & Naja, J. (2017). Hybrid electrocoagulation/electroflotation/electrodisinfection process as a pretreatment for seawater desalination. *Chemical Engineering Science*, 170, 530-541.
- Hassan, I., Nirdosh, I., & Sedahmed, G. H. (2015). Separation of oil from oil–water emulsions by electrocoagulation in an electrochemical reactor with a fixed-bed anode. *Water, Air, & Soil Pollution*, 226(8), 271.
- Hassani, G., Alinejad, A., Sadat, A., Esmaeili, A., Ziaei, M., Bazrafshan, A. A., & Sadat, T. (2016). Optimization of landfill leachate treatment process by electrocoagulation,

- electroflotation and sedimentation sequential method. *International Journal of Electrochemical Science*, 11, 6705-6718.
- Heidmann, I., & Calmano, W. (2008). Removal of Cr (VI) from model wastewaters by electrocoagulation with Fe electrodes. *Separation and Purification Technology*, 61(1), 15-21.
- Heidmann, I., & Calmano, W. (2008). Removal of Zn (II), Cu (II), Ni (II), Ag (I) and Cr (VI) present in aqueous solutions by aluminium electrocoagulation. *Journal of Hazardous Materials*, 152(3), 934-941.
- Heidmann, I., & Calmano, W. (2010). Removal of Ni, Cu and Cr from a galvanic wastewater in an electrocoagulation system with Fe-and Al-electrodes. *Separation and Purification Technology*, 71(3), 308-314.
- Hernlem, B. J., & Tsai, L. S. (2000). Chlorine generation and disinfection by electroflotation. *Journal of food science*, 65(5), 834-837.
- Hmidi, K., Ksentini, I., & Mansour, L. B. (2017). Treatment of olive-pomace oil refinery wastewater using combined coagulation-electroflotation process. *Journal of Water Chemistry and Technology*, 39(5), 275-280.
- Ho, C. C., & Chan, C. Y. (1986). The application of lead dioxide-coated titanium anode in the electroflotation of palm oil mill effluent. *Water Research*, 20(12), 1523-1527.
- Ibrahim, M. Y., Mostafa, S. R., Fahmy, M. F. M., & Hafez, A. I. (2001). Utilization of electroflotation in remediation of oily wastewater. *Separation science and technology*, 36(16), 3749-3762.
- Ighilahriz, K., Ahmed, M. T., Djelal, H., & Maachi, R. (2014). Electrocoagulation and electro-oxidation treatment for the leachate of oil-drilling mud. *Desalination and Water Treatment*, 52(31-33), 5833-5839.
- Il'in, V. I., & Kolesnikov, V. A. (2001). Electroflotation purification of radioactive waste waters. *Atomic Energy*, 91(1), 551-554.

- Il'in, V. I., & Sedashova, O. N. (1999). An electroflotation method and plant for removing oil products from effluents. *Chemical and petroleum engineering*, 35(8), 480-481.
- Ince, M. (2013). Treatment of manganese-phosphate coating wastewater by electrocoagulation. *Separation Science and Technology*, 48(3), 515-522.
- Issaoui, R., Ksentini, I., Kotti, M., & Mansour, L. B. (2017). Effect of current density and oil concentration on hydrodynamic aspects in electroflotation column during oil/water emulsion treatment. *Journal of Water Chemistry and Technology*, 39(3), 166-170.
- Janpoor, F., Torabian, A., & Khatibikamal, V. (2011). Treatment of laundry waste-water by electrocoagulation. *Journal of Chemical Technology & Biotechnology*, 86(8), 1113-1120.
- Jiménez, C., Talavera, B., Saez, C., Cañizares, P., & Rodrigo, M. A. (2010). Study of the production of hydrogen bubbles at low current densities for electroflotation processes. *Journal of Chemical Technology & Biotechnology*, 85(10), 1368-1373.
- Kalyani, K. P., Balasubramanian, N., & Srinivasakannan, C. (2009). Decolorization and COD reduction of paper industrial effluent using electro-coagulation. *Chemical Engineering Journal*, 151(1-3), 97-104.
- Kant, R. (2012). Textile dyeing industry an environmental hazard. *Natural science*, 4(1), 22-26.
- Khelifa, A., Aoudj, S., Moulay, S., Hecini, M., & De Petris-Wery, M. (2009). Degradation of EDTA by in-situ electrogenerated active chlorine in an electroflotation cell. *Desalination and Water Treatment*, 7(1-3), 119-123.
- Khelifa, A., Moulay, S., & Naceur, A. W. (2005). Treatment of metal finishing effluents by the electroflotation technique. *Desalination*, 181(1-3), 27-33.
- Khosla, N. K., Venkatachalam, S., & Somasundaran, P. (1991). Pulsed electrogeneration of bubbles for electroflotation. *Journal of Applied Electrochemistry*, 21(11), 986-990.

- Kim, H. L., Cho, J. B., Park, Y. J., & Cho, I. H. (2016). Treatment and toxicity reduction of textile dyeing wastewater using the electrocoagulation-electroflotation process. *Journal of Environmental Science and Health, Part A*, 51(8), 661-668.
- Kim, T. H., Park, C., Shin, E. B., & Kim, S. (2002). Decolorization of disperse and reactive dyes by continuous electrocoagulation process. *Desalination*, 150(2), 165-175.
- Kobyas, M., Bayramoglu, M., & Eyvaz, M. (2007). Techno-economical evaluation of electrocoagulation for the textile wastewater using different electrode connections. *Journal of hazardous materials*, 148(1-2), 311-318.
- Kobyas, M., Senturk, E., & Bayramoglu, M. (2006). Treatment of poultry slaughterhouse wastewaters by electrocoagulation. *Journal of hazardous materials*, 133(1-3), 172-176.
- Kolesnikov, A. V., Kuznetsov, V. V., Kolesnikov, V. A., & Kapustin, Y. I. (2015). The role of surfactants in the electroflotation extraction of copper, nickel, and zinc hydroxides and phosphates. *Theoretical Foundations of Chemical Engineering*, 49(1), 1-9.
- Kolesnikov, V. A., Il'in, V. I., Brodskii, V. A., Guseva, T. V., & Vartanyan, M. A. (2015). Improvement of electroflotation treatment of waste waters from ceramic enterprises. *Glass and Ceramics*, 71(11-12), 421-424.
- Kolesnikov, V. A., Il'in, V. I., Brodskiy, V. A., & Kolesnikov, A. V. (2017). Electroflotation during wastewater treatment and extraction of valuable compounds from liquid technogenic waste: A review. *Theoretical Foundations of Chemical Engineering*, 51(4), 369-383.
- Lacasa, E., Canizares, P., Saez, C., Fernandez, F. J., & Rodrigo, M. A. (2011). Electrochemical phosphates removal using iron and aluminium electrodes. *Chemical Engineering Journal*, 172(1), 137-143.
- Lakshmanan, D., Clifford, D. A., & Samanta, G. (2010). Comparative study of arsenic removal by iron using electrocoagulation and chemical coagulation. *Water research*, 44(19), 5641-5652.

Landolt, D., Acosta, R., Muller, R. H., & Tobias, C. W. (1970). An Optical Study of Cathodic Hydrogen Evolution in High-Rate Electrolysis. *Journal of the Electrochemical Society*, 117(6), 839-845.

Mahvi, A. H., Ebrahimi, S. J. A. D., Mesdaghinia, A., Gharibi, H., & Sowlat, M. H. (2011). Performance evaluation of a continuous bipolar electrocoagulation/electrooxidation–electroflotation (ECEO–EF) reactor designed for simultaneous removal of ammonia and phosphate from wastewater effluent. *Journal of hazardous materials*, 192(3), 1267-1274.

Maksimov, E. A., & Ostsemin, A. A. (2015). Intensifying the cleaning of emulsion-and oil-bearing waste water from rolled-product manufacturing by electroflotation. *Metallurgist*, 58(11-12), 945-949.

Mansoorian, H. J., Mahvi, A. H., & Jafari, A. J. (2014). Removal of lead and zinc from battery industry wastewater using electrocoagulation process: influence of direct and alternating current by using iron and stainless steel rod electrodes. *Separation and Purification Technology*, 135, 165-175.

Mansour, L. B., & Chalbi, S. (2006). Removal of oil from oil/water emulsions using electroflotation process. *Journal of Applied Electrochemistry*, 36(5), 577-581.

Mansour, L. B., & Kesentini, I. (2008). Treatment of effluents from cardboard industry by coagulation–electroflotation. *Journal of hazardous materials*, 153(3), 1067-1070.

Mansour, L. B., Ksentini, I., & Elleuch, B. (2007). Treatment of wastewaters of paper industry by coagulation–electroflotation. *Desalination*, 208(1-3), 34-41.

Matis, K. A., & Peleka, E. N. (2010). Alternative flotation techniques for wastewater treatment: focus on electroflotation. *Separation Science and Technology*, 45(16), 2465-2474.

Meas, Y., Ramirez, J. A., Villalon, M. A., & Chapman, T. W. (2010). Industrial wastewaters treated by electrocoagulation. *Electrochimica Acta*, 55(27), 8165-8171.

Melchioris, M. S., Piovesan, M., Becegato, V. R., Becegato, V. A., Tambourgi, E. B., & Paulino, A. T. (2016). Treatment of wastewater from the dairy industry using electroflocculation and solid whey recovery. *Journal of environmental management*, 182, 574-580.

Mendeleev University Science Park. (2008) *Table.1. Electroflotation system capability*. Retrieved from <http://enviropark.ru/course/category.php?id=10> (Accessed 11 January 2018).

Merzouk, B., Gourich, B., Sekki, A., Madani, K., & Chibane, M. (2009). Removal turbidity and separation of heavy metals using electrocoagulation–electroflotation technique: A case study. *Journal of hazardous materials*, 164(1), 215-222.

Merzouk, B., Gourich, B., Sekki, A., Madani, K., Vial, C., & Barkaoui, M. (2009). Studies on the decolorization of textile dye wastewater by continuous electrocoagulation process. *Chemical Engineering Journal*, 149(1-3), 207-214.

Merzouk, B., Madani, K., & Sekki, A. (2010). Using electrocoagulation–electroflotation technology to treat synthetic solution and textile wastewater, two case studies. *Desalination*, 250(2), 573-577.

Modirshahla, N., Behnajady, M. A., & Kooshaiian, S. (2007). Investigation of the effect of different electrode connections on the removal efficiency of Tartrazine from aqueous solutions by electrocoagulation. *Dyes and pigments*, 74(2), 249-257.

Mostefa, N. M., & Tir, M. (2004). Coupling flocculation with electroflotation for waste oil/water emulsion treatment. Optimization of the operating conditions. *Desalination*, 161(2), 115-121.

Mraz, R., & Krýsa, J. (1994). Long service life IrO₂/Ta₂O₅ electrodes for electroflotation. *Journal of Applied Electrochemistry*, 24(12), 1262-1266.

Murugananthan, M., Bhaskar Raju, G., & Prabhakar, S. (2005). Removal of tannins and polyhydroxy phenols by electro-chemical techniques. *Journal of Chemical Technology &*

Biotechnology: International Research in Process, Environmental & Clean Technology, 80(10), 1188-1197.

Murugananthan, M., Raju, G. B., & Prabhakar, S. (2004). Removal of sulfide, sulfate and sulfite ions by electro coagulation. *Journal of Hazardous Materials*, 109(1-3), 37-44.

Murugananthan, M., Raju, G. B., & Prabhakar, S. (2004). Separation of pollutants from tannery effluents by electro flotation. *Separation and Purification Technology*, 40(1), 69-75.

Nanseu-Njiki, C. P., Tchamango, S. R., Ngom, P. C., Darchen, A., & Ngameni, E. (2009). Mercury (II) removal from water by electrocoagulation using aluminium and iron electrodes. *Journal of Hazardous Materials*, 168(2-3), 1430-1436.

Nunez, P., Hansen, H. K., Aguirre, S., & Maureira, C. (2011). Electrocoagulation of arsenic using iron nanoparticles to treat copper mineral processing wastewater. *Separation and purification technology*, 79(2), 285-290.

Orssatto, F., Ferreira Tavares, M. H., Manente da Silva, F., Eyng, E., Farias Biassi, B., & Fleck, L. (2017). Optimization of the pretreatment of wastewater from a slaughterhouse and packing plant through electrocoagulation in a batch reactor. *Environmental technology*, 38(19), 2465-2475.

Ouslimane, T., Aoudj, S., Amara, M., & Drouiche, N. (2017). Removal of Copper and Fluoride from Mixed Cu-CMP and Fluoride-Bearing Wastewaters by Electrocoagulation. *International Journal of Environmental Research*, 11(5-6), 677-684.

Ozyonar, F. (2016). Treatment of Train Industry Oily Wastewater by Electrocoagulation with Hybrid Electrode Pairs and Different Electrode Connection Modes. *International Journal of Electrochemical Science*, 11, 1456-1471.

Palomino Romero, J. A., Cardoso Junior, F. S. S., Figueiredo, R. T., Silva, D. P., & Cavalcanti, E. B. (2013). Treatment of biodiesel wastewater by combined electroflotation and electrooxidation processes. *Separation Science and Technology*, 48(13), 2073-2079.

Panizza, M., & Cerisola, G. (2010). Applicability of electrochemical methods to carwash wastewaters for reuse. Part 2: Electrocoagulation and anodic oxidation integrated process. *Journal of Electroanalytical Chemistry*, 638(2), 236-240.

Paul, S. A., Chavan, S. K., & Khambe, S. D. (2012). Studies on characterization of textile industrial waste water in Solapur city. *International Journal of Chemical Sciences*, 10(2), 635-642.

Perfil'eva, A. V., Brodskii, V. A., Il'in, V. I., & Kolesnikov, V. A. (2016). Effect of the composition of the medium and electroflotation processing parameters on extraction efficiency of chromium (III) dispersed phase from aqueous solutions. *Russian Journal of Applied Chemistry*, 89(3), 388-393.

Poon, C. P. (1997). Electroflotation for groundwater decontamination. *Journal of hazardous materials*, 55(1-3), 159-170.

Pouet, M. F., & Grasmick, A. (1995). Urban wastewater treatment by electrocoagulation and flotation. *Water science and technology*, 31(3-4), 275.

Saravanan, M., Sambhamurthy, N. P., & Sivarajan, M. (2010). Treatment of acid blue 113 dye solution using iron electrocoagulation. *CLEAN–Soil, Air, Water*, 38(5-6), 565-571.

Sarkar, M. S. K. A., Evans, G. M., & Donne, S. W. (2010). Bubble size measurement in electroflotation. *Minerals engineering*, 23(11-13), 1058-1065.

Saur, I. F., Rubach, S., Forde, J. S., Kjaerheim, G., & Syversen, U. (1996). Electroflocculation: removal of oil, heavy metals and organic compounds from oil-in-water emulsions. *Filtration and Separation*, 4(33), 295+-297+.

Selvaraj, R., Santhanam, M., Selvamani, V., Sundaramoorthy, S., & Sundaram, M. (2018). A membrane electroflotation process for recovery of recyclable chromium (III) from tannery spent liquor effluent. *Journal of hazardous materials*, 346, 133-139.

Sengil, I. A., & Ozacar, M. (2006). Treatment of dairy wastewaters by electrocoagulation using mild steel electrodes. *Journal of hazardous materials*, 137(2), 1197-1205.

Shen, F., Chen, X., Gao, P., & Chen, G. (2003). Electrochemical removal of fluoride ions from industrial wastewater. *Chemical Engineering Science*, 58(3-6), 987-993.

Sides, P. J. (1986). Phenomena and effects of electrolytic gas evolution. In *Modern aspects of electrochemistry* (pp. 303-354). Springer, Boston, MA.

Skender, A., Moulai-Mostefa, N., & Tir, M. (2010). Effects of operational parameters on the removal efficiency of non-ionic surfactant by electroflotation. *Desalination and Water Treatment*, 13(1-3), 213-216.

Solak, M., Kılıç, M., & Şencan, A. (2009). Removal of suspended solids and turbidity from marble processing wastewaters by electrocoagulation: Comparison of electrode materials and electrode connection systems. *Journal of hazardous materials*, 172(1), 345-352.

Sridhar, R., Sivakumar, V., Immanuel, V. P., & Maran, J. P. (2012). Development of model for treatment of pulp and paper industry bleaching effluent using response surface methodology. *Environmental Progress & Sustainable Energy*, 31(4), 558-565.

Tsai, L. S., Hernlem, B., & Huxsoll, C. C. (2002). Disinfection and solids removal of poultry chiller water by electroflotation. *Journal of food science*, 67(6), 2160-2164.

Ulucan, K., & Kurt, U. (2015). Comparative study of electrochemical wastewater treatment processes for bilge water as oily wastewater: a kinetic approach. *Journal of Electroanalytical Chemistry*, 747, 104-111.

Un, U. T., Kandemir, A., Erginel, N., & Ocal, S. E. (2014). Continuous electrocoagulation of cheese whey wastewater: an application of response surface methodology. *Journal of environmental management*, 146, 245-250.

Un, U. T., Koparal, A. S., & Ogutveren, U. B. (2013). Fluoride removal from water and wastewater with a batch cylindrical electrode using electrocoagulation. *Chemical engineering journal*, 223, 110-115.

United Nations, Department of Economic and Social Affairs, Population Division (2017). *World Population Prospects: The 2017 Revision, custom data acquired via website*. Retrieved from <https://esa.un.org/unpd/wpp/DataQuery/> (Accessed 26 July 2018).

Wang, C. T., Chou, W. L., & Kuo, Y. M. (2009). Removal of COD from laundry wastewater by electrocoagulation/electroflotation. *Journal of hazardous materials*, 164(1), 81-86.

Warjito, & Nurrohman. (2016). Bubble Dynamics of Batik Dyeing Waste Separation using Flotation. *International Journal of Technology*, 7(5), 898-909.

Yang, C. L. (2007). Electrochemical coagulation for oily water demulsification. *Separation and Purification Technology*, 54(3), 388-395

Yunqing, X., & Jianwei, L. (2011). Application of electrochemical treatment for the effluent from marine recirculating aquaculture systems. *Procedia Environmental Sciences*, 10, 2329-2335.

Zaidi, S., Chaabane, T., Sivasankar, V., Darchen, A., Maachi, R., Msagati, T. A. M., & Prabhakaran, M. (2016). Performance efficiency of electro-coagulation coupled electro-flotation process (EC-EF) versus adsorption process in doxycycline removal from aqueous solutions. *Process Safety and Environmental Protection*, 102, 450-461.

Zaied, M., & Bellakhal, N. (2009). Electrocoagulation treatment of black liquor from paper industry. *Journal of hazardous materials*, 163(2-3), 995-1000.

Zaroual, Z., Azzi, M., Saib, N., & Chaînet, E. (2006). Contribution to the study of electrocoagulation mechanism in basic textile effluent. *Journal of Hazardous materials*, 131(1-3), 73-78.

CHAPTER 3 Electroflotation: Kinetic Study and Data Analysis

In this chapter, the kinetics of electroflotation process will be discussed, followed by kinetic study and statistical analysis of the available data from the batch tests of electroflotation treatment carried on several types of auto paint wastewater.

3.1 Kinetic Models

3.1.1 Theory of Mass Balance

The theory of mass balance is based on the concept of conservation of mass: mass is neither created nor destroyed; although, the form of it can be changed. This theory is widely used in discussion of efficiency of water and wastewater treatment systems. In order to investigate this basic concept, consider the complete-mix reactor depicted in Figure 3.1.

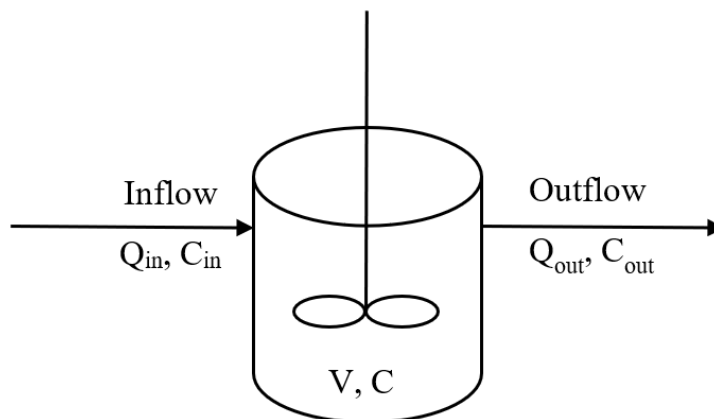


Figure 3.1: Schematic of a complete-mix reactor with inflow and outflow

The inflow is Q_{in} (L^3/T), with reactant mass concentration of C_{in} (M/L^3) and the outflow discharge and concentration are Q_{out} and C_{out} , respectively. While, the mixer is shown to

represent the complete-mix characteristic of the reactor with volume V and concentration C (Metcalf and Eddy, 2003).

For the above system, the mass-balance theory can be represented as:

$$\begin{array}{ccccccc} \text{Rate of} & & \text{Rate of reactant} & & \text{Rate of reactant} & & \text{Rate of change of} \\ \text{accumulation of} & = & \text{flow entering the} & - & \text{flow out of the} & + & \text{reactant within} \\ \text{reactant in the} & & \text{system} & & \text{system} & & \text{the system} \\ \text{system} & & & & & & \\ & & & & & & \end{array} \quad (3.1)$$

or in summary:

$$\text{Accumulation} = \text{Inflow} - \text{Outflow} + \text{Change} \quad (3.2)$$

The equation is comprised of four terms and based on the nature of the process and the reactor characteristics, one or more of the terms could be zero. The change represents the generation or decaying of the mass resulting from the activities or reactions occurring within the system, which is the reactor in here.

To explain and quantify Eq. (3.2), some variables and quantities need to be defined. The first term is Mass (M). Mass can have units of g, Kg, etc. and be defined as the product of Concentration (C) and Volume (V).

$$\text{Mass} = \text{Concentration} \times \text{Volume}; \text{ or } M = C \times V \quad (3.3)$$

where,

M : Mass, g or mg

C : Concentration, g/m^3 or mg/L

Volume: V , m^3 or L

Also, since the parameters change in the system, another parameter, i.e., the flowrate, should be considered:

Q: Volumetric flowrate, L/s, L/min or m³/min

Subsequently, the mass flow rate ($\frac{dM}{dt}$) can be defined as follows:

$$\frac{dM}{dt} = \frac{d(C.V)}{dt} \quad (3.4)$$

In this study, it is assumed that the volume of fluid in the system remains constant.

Therefore, Eq. (3.4) can be written as:

$$\frac{dM}{dt} = \frac{dC}{dt} V \quad (3.5)$$

For the terms of inflow and outflow of mass in Eq. (3.2), the mass rate can be defined as the product of flowrate and concentration.

$$\frac{dM}{dt} = \frac{dV}{dt} C = Q \times C \quad (3.6)$$

So far, all the terms in Eq. (3.2) have been defined, except the Change or Generation. If r is considered as the change rate (or reaction rate) per unit volume, $r \times V$ will be the last term in Eq. (3.2). Substituting the above-defined terms, the mass balance Eq. (3.2) can be rewritten as Eq. (3.7) (Metcalf and Eddy, 2003).

$$V \frac{dC}{dt} = QC_{in} - QC_{out} + rV \quad (3.7)$$

where,

r: reaction rate, g/m³.s or mg/L.s

Eq. (3.7) is the mass balance equation in a closed system defined with the parameters of volume, flowrate, concentration and reaction rate.

3.1.2 Theory of Kinetic Rate

The term r (reaction rate) in Eq. (3.7) is related to a subject called kinetics, which is the study of rates of chemical processes. Assuming the following chemical reaction between substances A and B result in some products, i.e.



With [A] and [B] defined as the concentrations of reactants A and B, respectively, the rate of reaction is given by Eq. (3.9) (Levenspiel, 1999):

$$\text{Rate of Reaction} = r = k [A]^x [B]^y \quad (3.9)$$

where,

k : rate constant at a given temperature

[A]: concentration of reactant A

[B]: concentration of reactant B

x and y : order for each reactant determined experimentally

It should be mentioned that the orders of reactants (exponents x and y) have no relationship with the stoichiometric reaction coefficients, e.g., a and b in Eq. (3.8) and can only be found by experiments.

The order of reaction shows how the reaction rate is influenced by the concentration of reactants. For example, if x is equal to zero, the reaction is independent of reactant A and is called *zero order* with respect to A. Or if y is equal to 2, the reaction is the *second*

order with respect to B. The summation of x and y determines the total order of reaction (Levenspiel, 1999).

Now, assume the reaction $C \rightarrow \text{products}$ is zero order with respect to C.

$$r = -\frac{\Delta[C]}{\Delta t} = k [C]^0 = k \quad (3.10)$$

The negative sign in Eq. (3.10) shows that the concentration C, as a reactant, decreases as the reaction proceeds. Rewriting the Eq. (3.10) as a differential equation and integrating:

$$r = -\frac{dC}{dt} = k \quad (3.11)$$

$$dC = -k \cdot dt \rightarrow \int_{C_0}^{C_t} dC = \int_0^t -k \cdot dt$$

$$[C]_t - [C]_0 = -kt \quad (3.12)$$

or

$$[C]_0 - [C]_t = kt$$

where,

$[C]_t$: concentration at time t, mg/L

$[C]_0$: initial concentration, mg/L

k : rate constant, (1/min for first order, L/mg.min for second order)

t : time passed, min

Eq. (3.12) can be utilized to analyze experimental data including the concentration at different times and find the rate constant of a zero-order process.

Assuming the reaction $C \rightarrow \text{products}$ is first order with respect to C, the mathematical equations can be derived as follows:

$$r = -\frac{\Delta[C]}{\Delta t} = k [C] = k \cdot C$$

$$r = -\frac{dC}{dt} = k \cdot C \quad (3.13)$$

$$\frac{dC}{C} = -k \cdot dt \rightarrow \int_{C_0}^{C_t} \frac{dC}{C} = \int_0^t -k \cdot dt$$

$$\ln \frac{[C]_t}{[C]_0} = -kt \text{ or } \ln[C]_t - \ln[C]_0 = -kt \quad (3.14)$$

or

$$[C]_t = [C]_0 e^{-kt}$$

Therefore, in a first order process, having experimental data of concentration at different times, one can find the rate constant of the process.

Assuming the reaction $C \rightarrow \text{products}$ is second order with respect to C, the equation relating the concentration, time and rate constant can be derived as follows:

$$r = -\frac{\Delta[C]}{\Delta t} = k [C]^2 = k \cdot C^2$$

$$r = -\frac{dC}{dt} = k \cdot C^2 \quad (3.15)$$

$$\frac{dC}{C^2} = -k \cdot dt \rightarrow \int_{C_0}^{C_t} \frac{dC}{C^2} = \int_0^t -k \cdot dt$$

$$\frac{1}{[C]_t} - \frac{1}{[C]_0} = kt \quad (3.16)$$

or

$$\frac{1}{[C]_t} = kt + \frac{1}{[C]_0}$$

As a result, in a second order process, having experimental data of concentration at different times, one can find that a plot of $1/[C]_t$ vs time will be linear with the slope of k and *y-intercept* of $1/[C]_0$ (Levenspiel, 1999).

3.2 Kinetics of Electroflotation of Auto Paint Wastewater

The use of the bubbles formed during the water electrolysis to remove suspended particles/liquids by flotation is called electroflotation. The technique was originally employed in mineral processing and then adopted in the field of wastewater treatment (Bhaskar Raju and Khangaonkar, 1984). With the improvement of technology, electricity cost reduction and higher standards of effluent characteristics, electroflotation is being increasingly considered as a reliable option, particularly for industrial wastewater treatment. (Kyzas and Matis, 2016).

A comprehensive laboratory experimental study was conducted on the application of electroflotation (EF) method in the removal of paint from auto paint wastewater in a batch system (Shang, 2004). In this section, a kinetic study of treatment of auto paint wastewater is conducted based on the experimental data.

The experimental system consisted of a DC power supply, electrode assembly, a multi-meter and a testing column. Figure 3.2 presents a schematic of the experimental system (Shang, 2004).

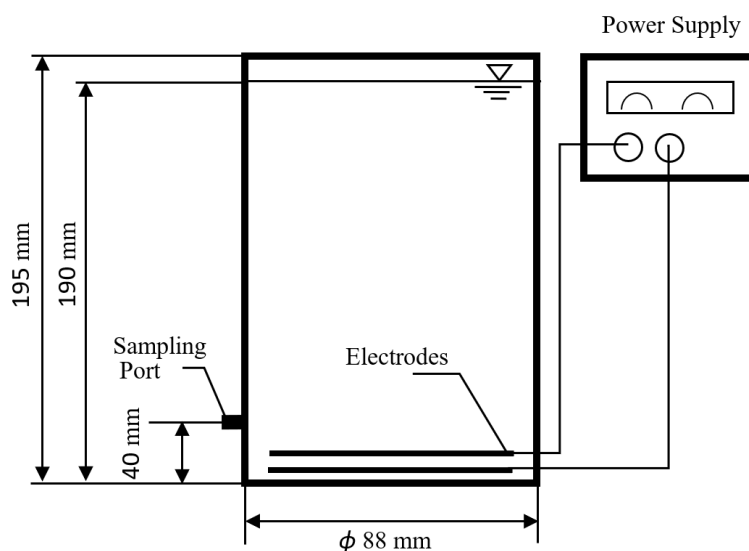


Figure 3.2: Schematic of the electroflotation batch experimental system (Shang, 2004)

The electric current density was controlled by the applied voltage. The testing column was made of Plexiglas pipe with 5 mm wall thickness, 19.0 cm in effective height and 60.79 cm² in sectional area, with an effective volume of 1.1 L. The sampling port of the column was on the wall, 4.0 cm above the bottom. Two circular-shaped parallel electrodes with 13 mm spacing were placed on the bottom of the column, the bottom anode was made of 1 mm thick graphite and the top cathode was made of stainless steel mesh (Shang, 2004).

Two types of solvent-based auto paint, i.e., Clear Coat and Primer, as well as their mixtures were used to prepare the wastewater samples using tap water. Detackifier and sodium hydroxide solution were added to simulate operation of paint booth in automotive assembly plant. The detackifier is a chemical used to reduce the stickiness of the paint wastewater and sodium hydroxide was added to adjust the pH of the solution.

The batch tests were performed on 5 wastewater samples under current densities (defined as the ratio of applied current to surface area of electrodes) of 11 to 44 A/m². The total testing time was 40 minutes, and water samples were taken at five-minute intervals during the first 20 minutes and ten-minute intervals during the second 20 minutes of testing (Shang, 2004). Five types of the tested wastewater samples are as follows:

1. ClearCoat_TS4669
2. ClearCoat_TS1992
3. Primer_TS1432
4. Primer_TS2374
5. MixedPaint_TS2789

Results of the electroflotation treatment of these wastewaters are summarized in Tables 3.1 to 3.5 (Shang, 2004).

Table 3.1: ClearCoat_TS4669 Wastewater: TSS (mg/L) concentration change over time under different current densities (Shang, 2004)

Time, min	Current Density = 11 A/m ²	Current Density = 22 A/m ²	Current Density = 33 A/m ²	Current Density = 44 A/m ²
0	759	759	759	759
5	-	560	102	78
10	432	215	63	66
15	188	105	57	66
20	60	75	57	60
30	51	54	51	48
40	51	51	48	42

Table 3.2: ClearCoat_TS1992 Wastewater: TSS (mg/L) concentration change over time under different current densities (Shang, 2004)

Time, min	Current Density = 11 A/m ²	Current Density = 22 A/m ²	Current Density = 33 A/m ²	Current Density = 44 A/m ²
0	563	563	563	563
5	325	316	265	251
10	233	185	75	66
15	185	63	45	48
20	117	54	42	39
30	48	45	36	36
40	48	36	22	22

Table 3.3: Primer_TS1432 Wastewater: TSS (mg/L) concentration change over time under different current densities (Shang, 2004)

Time, min	Current Density = 11 A/m ²	Current Density = 22 A/m ²	Current Density = 33 A/m ²	Current Density = 44 A/m ²
0	156	156	156	156
5	60	37	28	25
10	44	31	31	25
15	28	21	28	21
20	31	18	21	18
30	25	15	15	21
40	25	18	15	15

Table 3.4: Primer_TS2374 Wastewater: TSS (mg/L) concentration change over time under different current densities (Shang, 2004)

Time, min	Current Density = 11 A/m ²	Current Density = 22 A/m ²	Current Density = 33 A/m ²	Current Density = 44 A/m ²
0	383	383	383	383
5	843	411	220	121
10	479	172	76	47
15	197	25	25	18
20	108	21	21	21
30	34	25	21	21
40	34	21	15	15

Table 3.5: MixedPaint_TS2789 Wastewater: TSS (mg/L) concentration change over time under different current densities (Shang, 2004)

Time, min	Current Density = 11 A/m ²	Current Density = 22 A/m ²	Current Density = 33 A/m ²	Current Density = 44 A/m ²
0	562	562	562	562
5	408	174	99	64
10	92	64	47	38
15	87	61	47	38
20	82	61	45	29
30	80	45	22	19
40	68	22	19	15

In this study, the performance of the system is evaluated based on the concentrations of total suspended solids (TSS) in real time as well as after 40 mins treatment.

For the wastewater prepared with ClearCoat_TS4669 paint, the initial concentration of TSS in all experiments was 759 mg/L. As it can be seen in Table 3.1, with the increase of current density, the treatment efficiency increased, resulting in the final TSS of 51, 51, 48 and 42 mg/L for current densities of 11, 22, 33 and 44 A/m², respectively.

On the other hand, the ClearCoat_TS1992 wastewater samples, had an initial TSS of 563 mg/L in all runs. Similar to the previous runs, the current density had a direct effect on the removal rate of paint, leading to the final TSS of 48, 36, 22 and 22 mg/L with applied current densities of 11, 22, 33 and 44 A/m², respectively, after 40 min treatment.

There were two types of wastewater prepared with Primer paint, i.e., Primer_TS1432 and Primer_TS2374. The initial TSS for Primer_TS1432 was 156 mg/L and that of Primer_TS2374 was 383 mg/L. Four current densities, i.e., 11, 22, 33 and 44 A/m², were applied during the 40-mins treatment time, leading to the final TSS of 25, 18, 15 and 15 mg/L, respectively, for the wastewater sample Primer_TS1432. The wastewater sample Primer_TS2374 had the final TSS concentrations 34, 21, 15 and 15 mg/L under applied current densities of 11, 22, 33 and 44 A/m², respectively.

In the next section, these data will be used to study the kinetic of electroflotation treatment and produce first-order and second-order rate constants for the wastewater samples prepared by different paints.

3.2.1 First-Order Rate Constant

First-order and second-order kinetic rate constants were developed for the samples of wastewater treated under applied current densities of 11, 22, 33 and 44 A/m². A linear trend between $\ln(C_0/C_t)$ and time would indicate a first order rate constant, i.e., the slope of the trend line defines the rate constant k , based on Eq. (3.14). The Plots are presented in Figure A.1 to Figure A.20 in Appendix A.

Results of the first-order rate constants and their corresponding R-sq (R^2) values (coefficient of determination) are summarized in Table 3.6.

Table 3.6: First-order kinetics, Rate Constant and R-sq values for different wastewaters under different current densities

Sample ID	Current Density 11 A/m ²	Current Density 22 A/m ²	Current Density 33 A/m ²	Current Density 44 A/m ²	Average R-sq	Parameter
ClearCoat_TS4669	0.0825	0.0853	0.9740	0.9890		Rate Constant, k, 1/min
	0.81	0.78	-0.32	-0.31	0.24	R-sq Coefficient
ClearCoat_TS1992	0.0716	0.0858	0.1004	0.1010		Rate Constant, k, 1/min
	0.93	0.74	0.63	0.59	0.72	R-sq Coefficient
Primer_TS1432	0.0630	0.0776	0.0782	0.0781		Rate Constant, k, 1/min
	0.25	0.03	0.06	-0.04	0.08	R-sq Coefficient
Primer_TS2374	0.0654	0.0945	0.1028	0.1066		Rate Constant, k, 1/min
	0.92	0.56	0.67	0.39	0.64	R-sq Coefficient
MixedPaint_TS2789	0.0705	0.0959	0.1090	0.1187		Rate Constant, k, 1/min
	0.42	0.53	0.34	0.18	0.37	R-sq Coefficient

By definition, the closer the R-sq value to 1, the curve is a better fit to the data. A fitted horizontal line (slope = 0) will have R-sq equal to zero and a negative-value R-sq means the fitted line does not follow the trend of data and hence it fits worse than a horizontal line (Brown, 2002). The R-sq value is a function of sum-of-squares of model and total sum-of-squares ($1 - \frac{SS_{model}}{SS_{total}}$). If the fit of model is worse than a horizontal line, the sum-of-squares of model is larger than total sum-of-squares and therefore, the equation calculates a negative R-sq.

As shown in Table 3.6, the R-sq values for ClearCoat_TS4669 were 0.81, 0.78, -0.32 and -0.31 (average 0.24) at current densities of 11, 22, 33 and 44 A/m², respectively. While the former two values can be considered as a good fit, the latter two were negative,

showing the linear model was not valid. Nevertheless, it was noted that the first-order rate constants increased with the applied current density.

On the other hand, the R-sq values for ClearCoat_TS1992 were all positive, i.e., 0.93, 0.74, 0.63 and 0.59 (average 0.72) at current densities of 11, 22, 33 and 44 A/m², respectively. The first-order rate constants increased consistently with the increase of the current density.

For the wastewater sample Primer_TS1432, the coefficients of determination were in the range of -0.04 to 0.25 (average 0.08) and did not show an obvious fit of the model. The coefficients of determination for Primer_TS2374 presented a better agreement with the model, being 0.92, 0.56, 0.67 and 0.39 (average 0.64) at applied current densities of 11, 22, 33 and 44 A/m², respectively. The first-order rate constants for this wastewater sample were 0.0654, 0.0945, 0.1028 and 0.1066 at applied current densities of 11, 22, 33 and 44 A/m², respectively, indicating the increase of k values with the increase of current density.

Although the R-sq values were all positive in the test runs of MixedPaint_TS2789, the values were low, ranging from 0.18 to 0.53 (average 0.37). However, the consistent trend of direct effect of current density on rate constant could be noticed again.

Overall, considering the coefficients of determination, R-sq, the experimental data did not appear to follow a first-order kinetic model. In the next section, the same set of experimental results will be used to develop and evaluate the second-order rate constants. The agreement of the model will be compared with the first-order constants, subsequently.

3.2.2 Second-Order Rate Constant

The second-order rate constants were developed for each type of wastewater based on the applied current densities of 11, 22, 33 and 44 A/m². According to Eq. (3.16), in the plot of $[(1/C_t) - (1/C_0)]$ versus time, the slope of linear trend line represents the second-order

rate constant, k . The plots of second-order kinetics are presented in Figure A.21 to Figure A.40 in Appendix A.

Results of the second-order rate constants and their corresponding R-sq (R^2) values (coefficient of determination) are summarized in Table 3.7.

Table 3.7: Second-order kinetics, Rate Constant and R-sq values for different wastewaters under different current densities

Sample ID	Current Density 11 A/m ²	Current Density 22 A/m ²	Current Density 33 A/m ²	Current Density 44 A/m ²	Average R-sq	Parameter
ClearCoat_TS4669	5	5	6	7		Rate Constant, $k \times 10^4$ L/mg.min
	0.82	0.94	0.33	0.48	0.64	R-sq Coefficient
ClearCoat_TS1992	5	7	11	11		Rate Constant, $k \times 10^4$ L/mg.min
	0.88	0.93	0.95	0.95	0.93	R-sq Coefficient
Primer_TS1432	11	18	18	18		Rate Constant, $k \times 10^4$ L/mg.min
	0.67	0.57	0.74	0.25	0.56	R-sq Coefficient
Primer_TS2374	7	14	17	18		Rate Constant, $k \times 10^4$ L/mg.min
	0.79	0.61	0.89	0.76	0.76	R-sq Coefficient
MixedPaint_TS2789	4	9	13	17		Rate Constant, $k \times 10^4$ L/mg.min
	0.63	0.88	0.94	0.97	0.86	R-sq Coefficient

For the wastewater sample ClearCoat_TS4669, R-sq values were 0.82, 0.94, 0.33 and 0.48 (average 0.64) at current densities of 11, 22, 33 and 44 A/m², respectively. The values were all positive. The second-order rate constants ($k \times 10^4$) generally showed an overall increase with the increase of applied current density, having the values of 5, 5, 6 and 7 at current densities of 11, 22, 33 and 44 A/m², respectively.

The R-sq value of 0.88, 0.93, 0.95 and 0.95 (average 0.93), for TSS removal of sample ClearCoat_TS1992 indicated a good fit between the model and the experimental data.

Referring back to Table 3.1 and Table 3.2, it can be seen that the initial TSS concentrations for ClearCoat_TS4669 and ClearCoat_TS1992 were 759 and 563 mg/L, respectively. Higher initial TSS concentration of ClearCoat_TS4669, resulted in lower rate constants, specially at higher current densities. For instance, at current density = 44 A/m², the rate constant of ClearCoat_TS4669 was 7×10^{-4} L/mg.min which was smaller than the rate constant of ClearCoat_TS1992, 117×10^{-4} L/mg.min.

The calculated R-sq values of second-order kinetics for sample Primer_TS1432 were 0.67, 0.57, 0.74 and 0.25 (average 0.56) at current densities of 11, 22, 33 and 44 A/m², respectively. Again, these values were all positive. The second-order rate constants ($k \times 10^4$) had an upward trend with the increase of applied current density, having the values of 11, 18, 18 and 18 at current densities of 11, 22, 33 and 44 A/m², respectively.

On the other hand, in Primer_TS2374 sample, the second-order rate constant values ($k \times 10^4$) were 7, 14, 17 and 18 at current densities of 11, 22, 33 and 44 A/m², respectively, slightly lower than the rate constant values of Primer_TS1432 sample. This was because of the higher concentration of initial TSS of Primer_TS2374 sample, 383 mg/L, compared to 156 mg/L for Primer_TS1432 sample. The coefficients of determination for the second-order model were 0.79, 0.61, 0.89 and 0.76 (average 0.76) at applied current densities of 11, 22, 33 and 44 A/m², respectively.

For the MixedPaint_TS2789 sample, the R-sq values were 0.63, 0.88, 0.94 and 0.97 (average 0.86) at current densities of 11, 22, 33 and 44 A/m², respectively. The values were all positive. The corresponding $k \times 10^4$ values were 47×10^{-4} , 97×10^{-4} , 137×10^{-4} and 177×10^{-4} L/mg.min, respectively.

The removal rates of TSS and rate constant values under various applied current densities for tested wastewater samples are depicted in Figure 3.3 through 3.7.

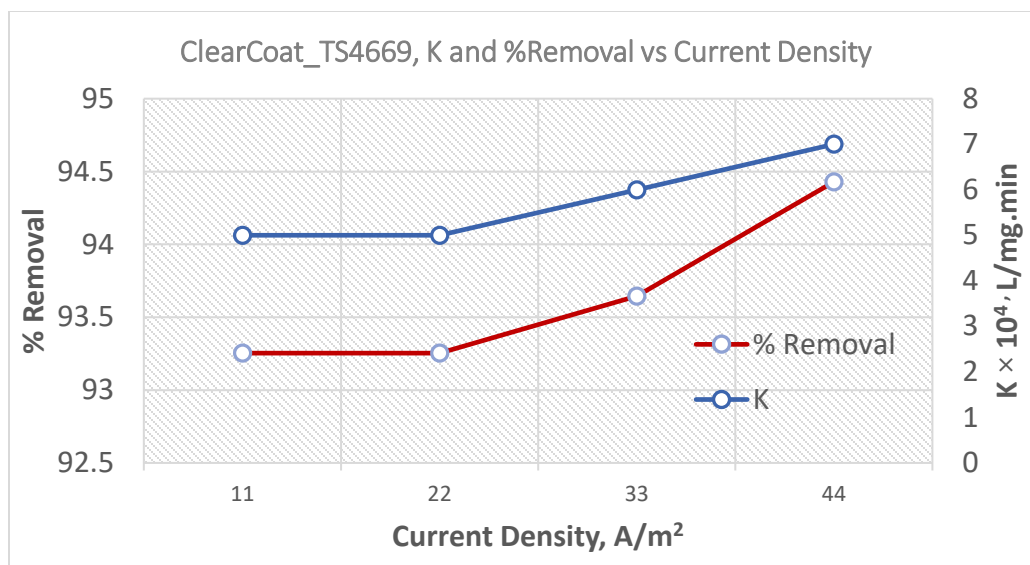


Figure 3.3: ClearCoat_TS4669 Wastewater, Treatment Efficiency (%Removal) and Second-order Rate Constant ($k \times 10^4$) vs. Current Density (A/m^2)

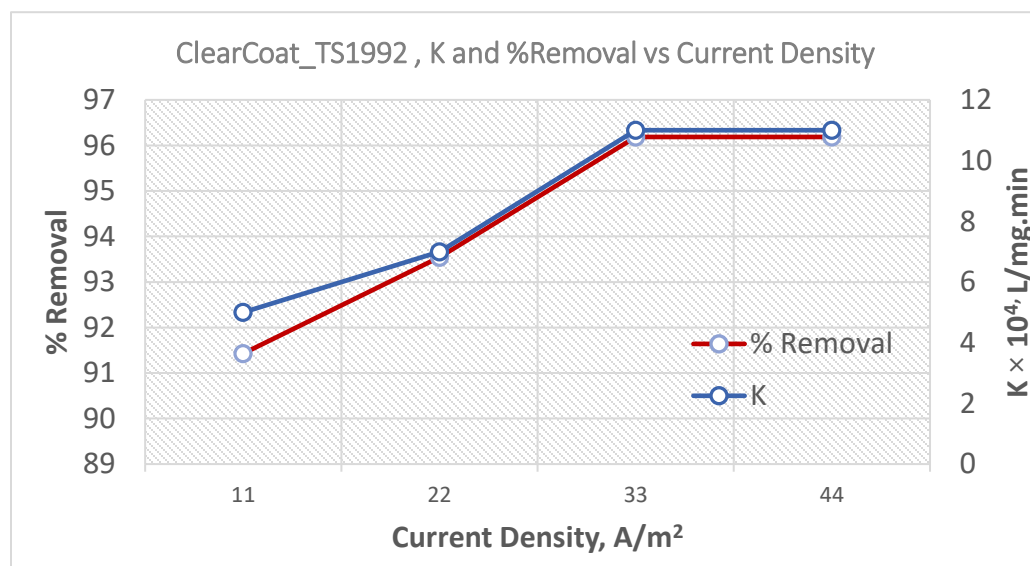


Figure 3.4: ClearCoat_TS1992 Wastewater, Treatment Efficiency (%Removal) and Second-order Rate Constant ($k \times 10^4$) vs. Current Density (A/m^2)

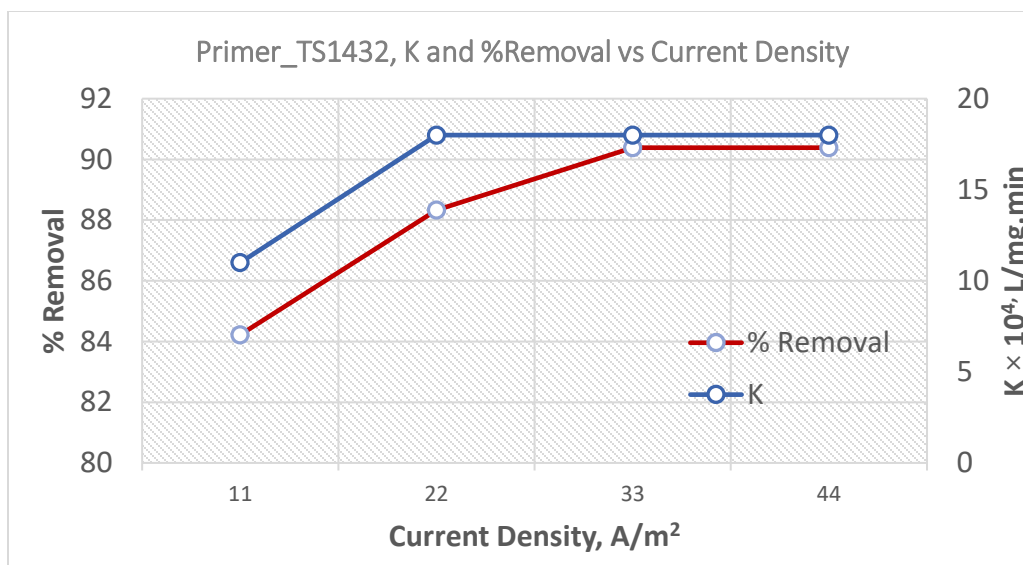


Figure 3.5: Primer_TS1432 Wastewater, Treatment Efficiency (%Removal) and Second-order Rate Constant ($k \times 10^4$) vs. Current Density (A/m^2)

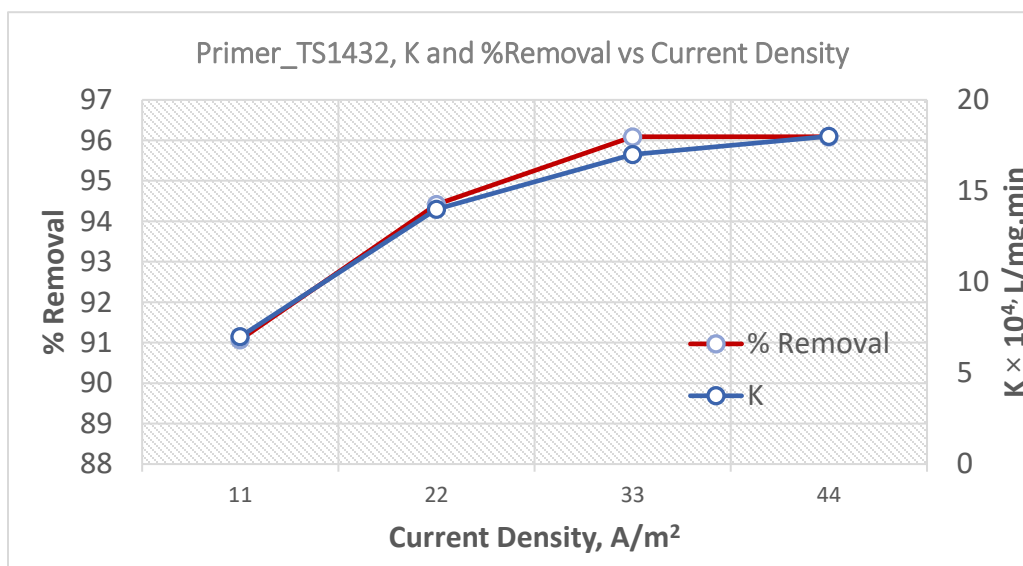


Figure 3.6: Primer_TS2374 Wastewater, Treatment Efficiency (%Removal) and Second-order Rate Constant ($k \times 10^4$) vs. Current Density (A/m^2)

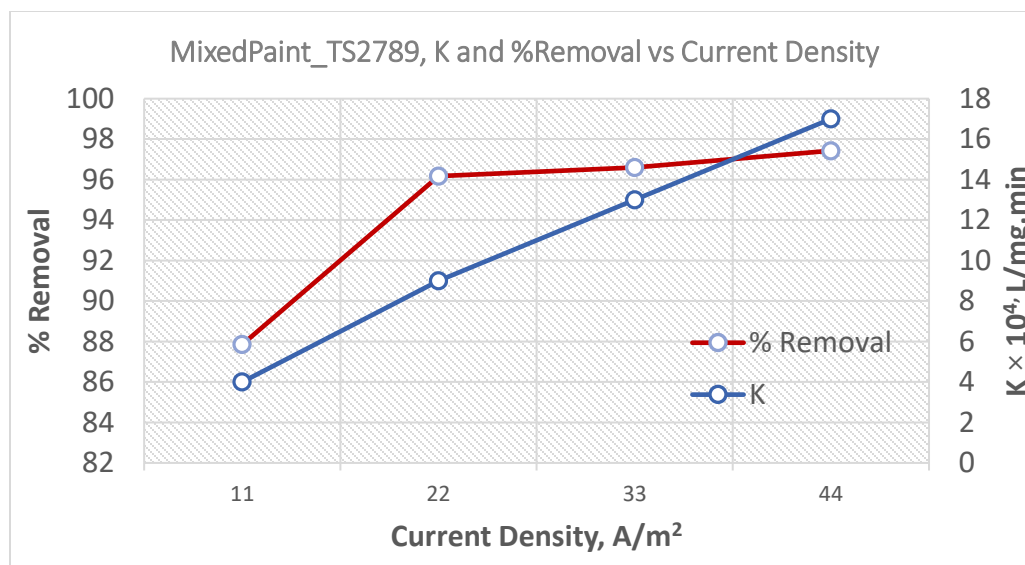


Figure 3.7: MixedPaint_TS2789 Wastewater, Treatment Efficiency (%Removal) and Second-order Rate Constant ($k \times 10^4$) vs. Current Density (A/m^2)

It was observed that, the k and removal efficiencies nearly followed a similar trend. The increase in the applied current density had a direct influence on the second-order rate constants and consequently the treatment efficiency.

As previously mentioned, the closer the R-sq value to 1, the curve is a better fit to the data. Comparing the results of the second-order model with the first-order model, it was noted that the second-order model described the TSS removal of auto paint, more accurately. For instance, the average R-sq of second-order model of ClearCoat_TS1992 sample was 0.93, while it was 0.72 for the first-order model. Similarly, for MixedPaint_TS2789 sample, the average R-sq of second-order model was 0.86 and it was 0.37 for the first-order model.

Furthermore, it was noticed that for a similar type of paint sample, the wastewater with lower initial concentration, had generally, greater k values, showing the effect of the initial concentration on the treatment rate. Another observation was the overall increase in the reaction rate constants with the increase of applied current density.

The treatment efficiencies (%Removal of TSS) of the electroflotation setup under different applied current densities are summarized in Table 3.8.

Table 3.8: Treatment efficiency (%Removal of TSS) for different wastewater samples under different current densities (Shang, 2004)

Sample ID	Current Density = 11 A/m ²	Current Density = 22 A/m ²	Current Density = 33 A/m ²	Current Density = 44 A/m ²
ClearCoat_TS4669	93	93	94	94
ClearCoat_TS1992	91	94	96	96
Primer_TS1432	84	88	90	90
Primer_TS2374	91	94	96	96
MixedPaint_TS2789	88	96	97	97

The values are after 40 minutes treatment time. The results of electroflotation were promising for treatment of auto paint wastewaters. The efficiencies were 94%, 96% 90%, 96% and 97% after 40 mins treatment under 44 A/m² current density for ClearCoat_TS4669, ClearCoat_TS1992, Primer_TS1432, Primer_TS2374 and MixedPaint_TS2789 auto paint wastewaters, respectively.

3.2.3 Discussion

The first-order and second-order kinetic studies were performed on the data from the batch experiments of the electroflotation treatment of auto paint wastewater. The results showed that the second-order kinetic was a better model to describe the treatment process. The kinetic study of the electroflotation process has been conducted by other researchers as well.

The COD removal from pulp and paper wastewater using electrocoagulation was studied by Kalyani et al. (2009), including the influence of treatment time and applied charge density. They used a first-order kinetic to find the COD removal reaction rates. The wastewater from a slaughterhouse was treated by electrocoagulation using Fe electrodes (Ahmadian et al., 2012). BOD₅, COD, TSS and TN removal were measured under different operating conditions such as the current density and time. The removal efficiency increased with increasing current density and operating time. The results showed that the removal rates of BOD₅, COD, TSS and TN followed the first-order kinetics with R-sq values of 0.93 to 0.99.

Kyzas and Matis (2016) stated that the electroflotation, generally, follows a first-order kinetics in long-term experiments, excluding the early stage of the process. In Figure 3.8 (Matis, 1994), it is evident that the first-order behavior in the electroflotation experiments conducted under current density of 100 A/m², began only after 30 min flotation time.

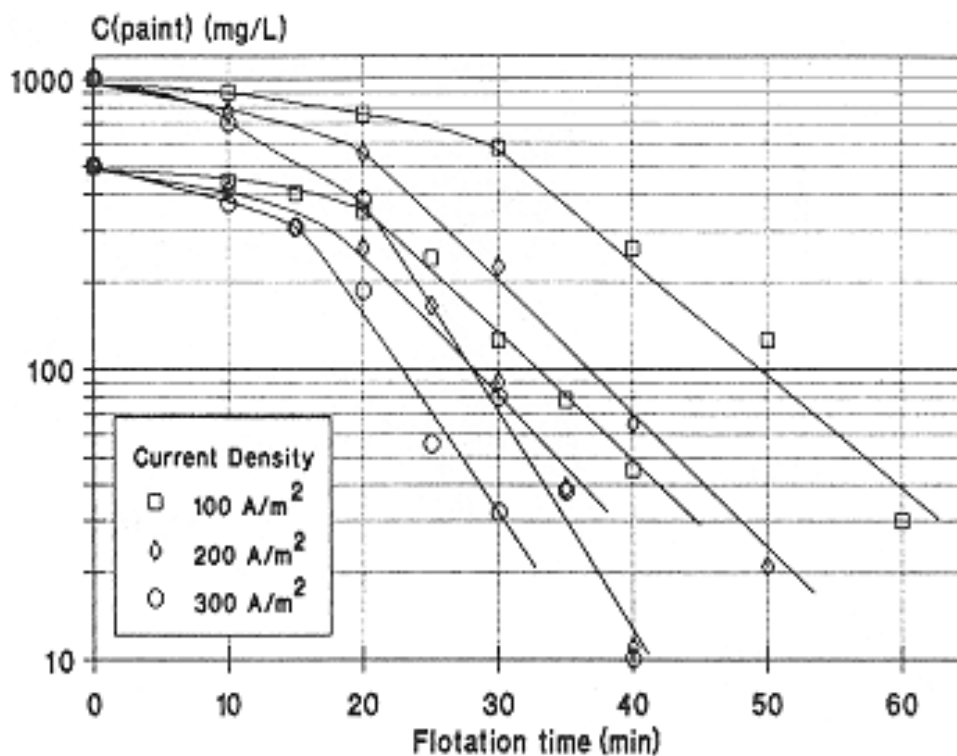


Figure 3.8: Initial phase and long-term behavior of flotation process (Matis, 1994)

This can explain the second-order kinetics of the treatment of auto paint wastewater in this study; as the experiments were conducted in 40 minutes, which is, relatively, considered as the early stage of the process.

Another reason for the first-order kinetics in some studies can be the short testing time of the electroflotation experiments. In mathematics, it is known that a segment of a curve can be approximated as a straight line, if the ΔX is not large (Figure 3.9).

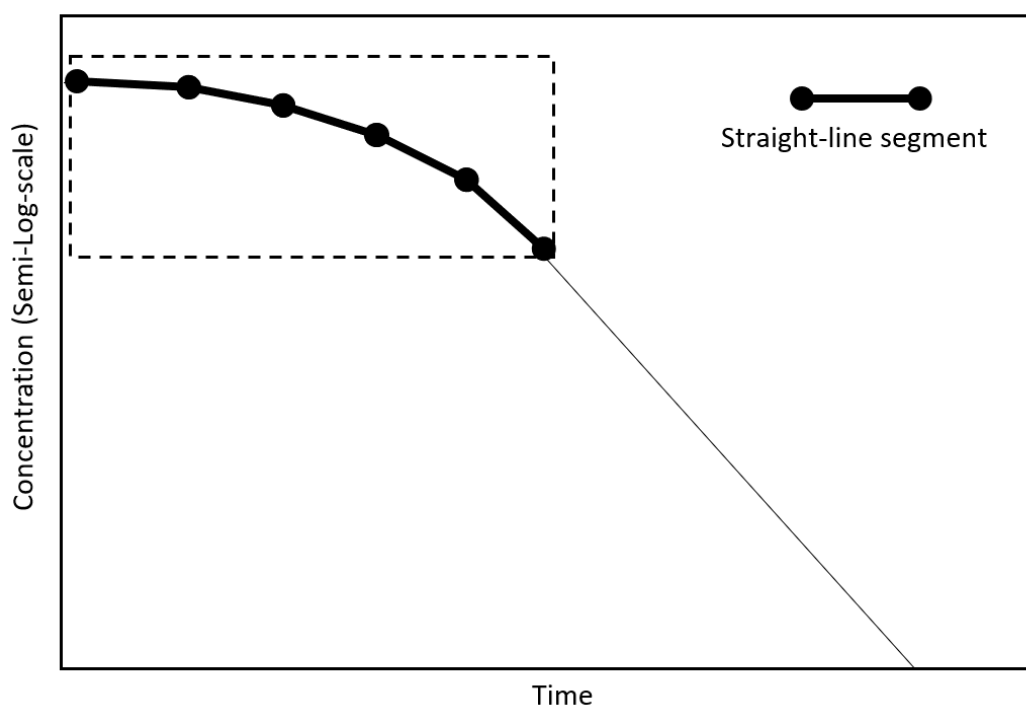


Figure 3.9: First-order behavior of electroflotation process in short-term experiments

This can describe the first-order model in the study conducted by Muruganathan et al. (2004). They investigated the treatment of tannery wastewater by electroflotation in a 300 sec (5 min) testing time. The effects of current density and electrode material on

treatment efficiency of TSS, COD and other pollutants were studied. Comparing the curves of different kinetic models with the experimental data, the kinetic study found that the short-term TSS removal followed the first-order kinetics model (Muruganathan et al., 2004).

In addition, there are studies reporting the second-order flotation kinetics as a better fit (with R-sq of 0.97 to 0.99) to the experimental data, in some cases (Zhang et al., 2013; Ni et al., 2016). This indicates that the type and the nature of the suspended particles can affect the rate constant order as well.

Overall, according to the results of this study, the second-order rate constants were selected as the best fit to the data, and used in the next section, the statistical analysis.

3.3 Statistical Analysis: Multivariate and Modelling

3.3.1 Analysis of All Wastewater Samples

In this section, experimental data (Shang, 2004) will be statistically analyzed. System parameters, including the initial TSS concentration, current density (J), water pH, zeta potential and electrical conductivity are studied as the influencing factors. The data used in this process are summarized in Table A.1 in Appendix A. Also, the second-order rate constants, k , calculated in the previous section, are used as the dependent variable (the model response). It should be mentioned that in the current section 3.3.1 (including: 3.3.1.1 Influencing Factors and 3.3.1.2 Regression Equation), the analysis is performed on all wastewater samples together. Statistical analysis of the individual wastewater samples is conducted in the section 3.3.2.

3.3.1.1 Influencing Factors: Multivariate Analysis

Electroflotation is a complex process and multiple influencing factors affect the performance of treatment. In order to further investigate the process, the significance of these factors needs to be quantified.

The first statistical method employed to find the most influencing factors is called the “Best Subsets Regression”, which is a statistical tool to identify sufficiently fit models with as few influencing factors as possible. This method presents models with different number of predictors along with a summary of their statistical parameters, e.g. R-sq(adj), and it is up to the researcher to decide the best model. A Statistical Analysis software Minitab 18.1 was implemented to perform the calculations. To find the influencing factors, the data from all wastewater samples were entered in the software. The response was the second-order rate constant, k , and the predictors were the initial TSS, current density, pH, zeta potential and electrical conductivity. The Results of analysis are shown in Table 3.9.

Table 3.9: Best Subsets Regression: k (second-order rate constant) versus Initial TSS, Current-Density, pH, Zeta Potential and Conductivity

Run ID	Vars	R-Sq, %	R-Sq (adj), %	Initial TSS (mg/L)	Current Density, J (A/m ²)	pH	Zeta-potential (mV)	Conductivity (μS/Cm)
R1	1	51.3	48.6	X				
R2	1	36.2	32.7			X		
R3	2	83.6	81.7	X	X			
R4	2	68.5	64.8		X	X		
R5	3	84.8	81.9	X	X			X
R6	3	83.9	80.9	X	X		X	
R7	4	86.9	83.4	X	X		X	X
R8	4	86.3	82.6	X	X	X		X
R9	5	87	82.4	X	X	X	X	X

The “best” model is the one that adequately describes data with the fewest parameters (Brown, 2002). The model with two predictors, i.e., the Initial TSS and Current Density was selected as the best choice (Run ID: R3 in Table 3.9). The R-sq value was 83.6% for this run. Other models (R5, R6, R7, R8 and R9) had slightly higher R-sq values, but they incorporated higher numbers of the independent variables (predictors). Overall, R3 had the highest R-sq value among the models with 1 and 2 predictors (R1, R2, R3 and R4).

When comparing the models with different number of predictors, adjusted R-sq, R-sq(adj), values should be considered as well. While the R-sq value increases as the predictors are added to the model (even when the model does not improve), the R-sq(adj) incorporates the number of predictors in the model and tends to stabilize around an upper limit (Rawlings et al., 2001). The selected model, R3, had R-sq (adj) of 81.7% which was acceptably close to the R-sq (83.6%). The larger differences between the R-sq and R-sq(adj) could be noticed in the models with the higher number of the predictors, e.g., R9.

Considering these factors, the selected model, R3, with two influencing factors, i.e., the Initial TSS and Current Density, was selected as the best model with enough predictors and good fit and backing statistical parameters.

The second method implemented to find the most significant influencing factors in electroflotation treatment of auto paint wastewater was the Stepwise Regression Analysis. The Stepwise Regression Analysis requires decisions on which predictors to be included in the model, the form of predictors (e.g., X, X², 1/X, etc.), and the functional form of the model. The Backward Elimination method was applied by Minitab 18.1 software. This method starts with the full model and then eliminates at each step one predictor, whose deletion will cause the residual sum of squares (RSS) to increase the least. The RSS represents deviations from the actual data and is a measure of the discrepancy between the data and the estimated model (Rawlings et al., 2001).

The response was the second-order rate constant, k , and continuous predictors were the initial TSS, current density, pH, zeta potential and electrical conductivity. The model stopped when all the remaining predictors (independent variables) had p-values (probability values) that were less than the Alpha value ($\alpha=0.1$ was selected). The elimination comprised of 4 steps. It started with 5 predictors and 1 predictor was removed in each step. As shown in Table 3.10, the eliminated predictors were the water pH, Zeta Potential and Electrical Conductivity, respectively; and the remaining predictors, the Initial TSS and Current Density had the p-value of 0.000 (i.e., < 0.001).

Table 3.10: Stepwise Regression, Backward Elimination Method. Candidate terms: Initial-TSS, Current-Density, pH, Zeta-Potential and Conductivity

	-----Step 1-----		-----Step 2-----		-----Step 3-----	
	Coef	p-value	Coef	p-value	Coef	p-value
Constant	-11.1		8.23		11.39	
Initial-TSS (mg/L)	-0.0178	0.112	-0.02092	0.000	-0.01871	0.000
Current-Density (A/m ²)	0.2345	0.000	0.2345	0.000	0.2345	0.000
pH	2.02	0.758				
Zeta-Potential (mV)	-0.681	0.379	-0.467	0.137		
Conductivity (μS/Cm)	0.00317	0.089	0.00308	0.083	0.00156	0.283
R-sq		87.02%		86.93%		84.78%
R-sq(adj)		82.38%		83.44%		81.92%
			-----Step 4-----			
			Coef	p-value		
Constant			13.27			
Initial-TSS (mg/L)			-0.01789	0.000		
Current-Density (A/m ²)			0.2345	0.000		
pH						
Zeta-Potential (mV)						
Conductivity (μS/Cm)						

- p-value 0.000 means < 0.001

Thus, similar to the Best Subset Regression method, the most influencing factors in the second-order reaction rate and subsequently, the auto paint electroflotation treatment performance, were found to be the Initial TSS and Current Density.

3.3.1.2 Regression Equation

Based on the findings of the previous section, multiple linear regression analysis was performed, and the following regression equation was established:

$$k = 13.27 - 0.01789 C_0 + 0.2345 J \quad (3.17)$$

(valid for C_0 : 157 to 759 mg/L, J : 11-44 A/m²)

where

C_0 : Initial TSS, mg/L

J : Current Density, A/m²

k : Second-order rate constant, L/mg.min

This equation relates the second-order rate constant to the initial TSS and current density for all auto paint wastewater samples. The results of the Analysis of Variance (ANOVA) are presented in Table 3.11.

Table 3.11: Analysis of Variance (ANOVA) with response of second-order rate constant, k

Source	DF	Seq SS	Contribution	p-value
Regression	2	430.53	83.61%	0.000
Current-Density	1	166.41	32.32%	0.000
Initial-TSS	1	264.12	51.29%	0.000
Error	17	84.42	16.39%	
Total	19	514.95	100.00%	

- DF (Degree of freedom): number of observations in the sample
- Seq SS (Sequential sums of squares): measure of variation for different components of the model
- Contributions: the percentage that each source in the ANOVA table contributes to the total Seq SS
- p-value (Probability value): is compared to significance level (alpha value) to assess the null hypothesis. P-value 0.000 means it is less than 0.001

In Table 3.11, DF (Degree of Freedom) was determined by the number of observations in the sample. The DF for each parameter represents how much information that parameter utilizes. Seq SS or Sequential Sums of Squares are measures of variation for different components of the model. This value was used to determine the p-Value. The Contribution represents the percentage that each component in the ANOVA table contributes to the total sequential sums of squares (Seq SS) (Rawlings et al., 2001).

P-value as the most significant term, shows the probability of null hypothesis against the model. It measures how compatible the data are with the null hypothesis. The P-value is compared to alpha-value. Alpha-value (α -value: significance level) is the probability of rejecting the null hypothesis given that is true. If the p-value is less than or equal to the

alpha-value, the null hypothesis is rejected, and the regression results are statistically significant (Minitab Express Support, 2017).

The alpha-value of 0.05 was selected. As shown in Table 3.11, in the Analysis of Variance (ANOVA), the Current Density and Initial SS were identified as the most important factors since their p-values were 0.000 (less than alpha-value =0.05) meaning that the null hypothesis was rejected, and the results were statistically significant. The contribution percentages of the Initial TSS and Current Density were 51.29% and 32.32%, respectively.

The contour plot and surface plot of the second-order rate constant, k , versus Current Density, J , and Initial TSS are depicted in Figures 3.10 and 3.11. A contour plot is a graphical representation of three variables in two dimensions and a surface plot is a three-dimensional diagram of a data of dependent variables.

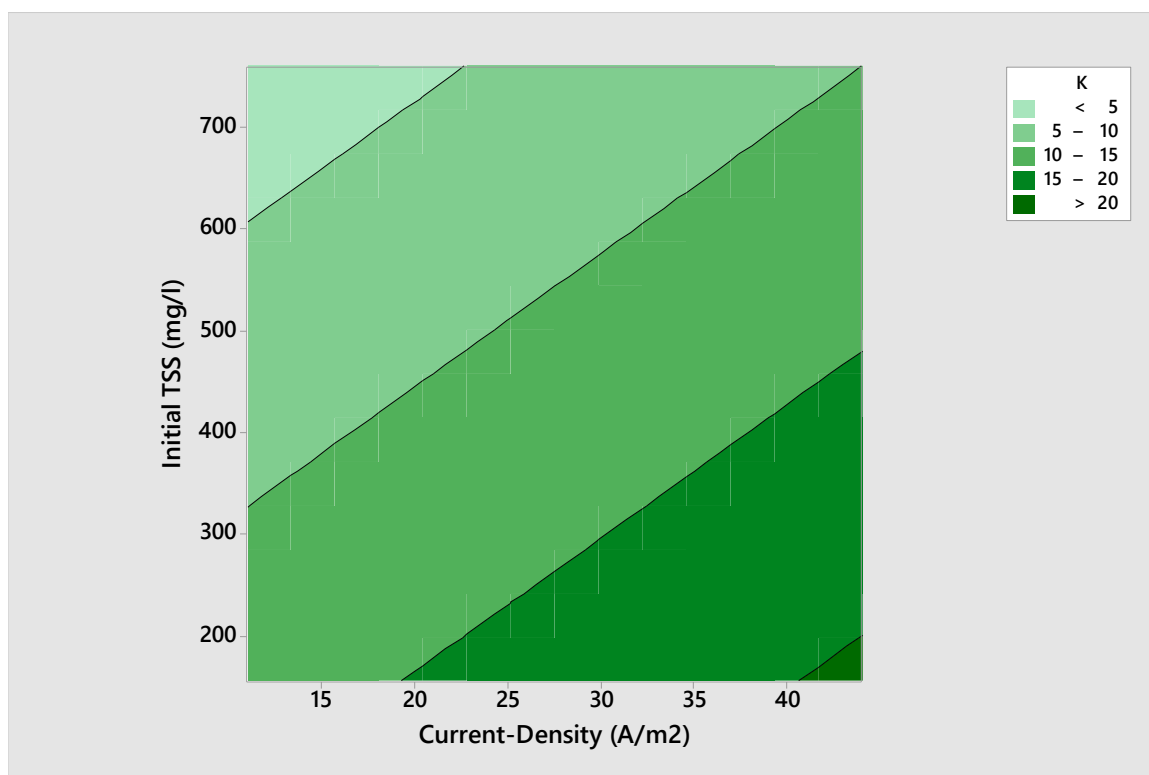


Figure 3.10: Contour plot of second-order rate constant, k , vs Current Density (J) and Initial TSS concentration

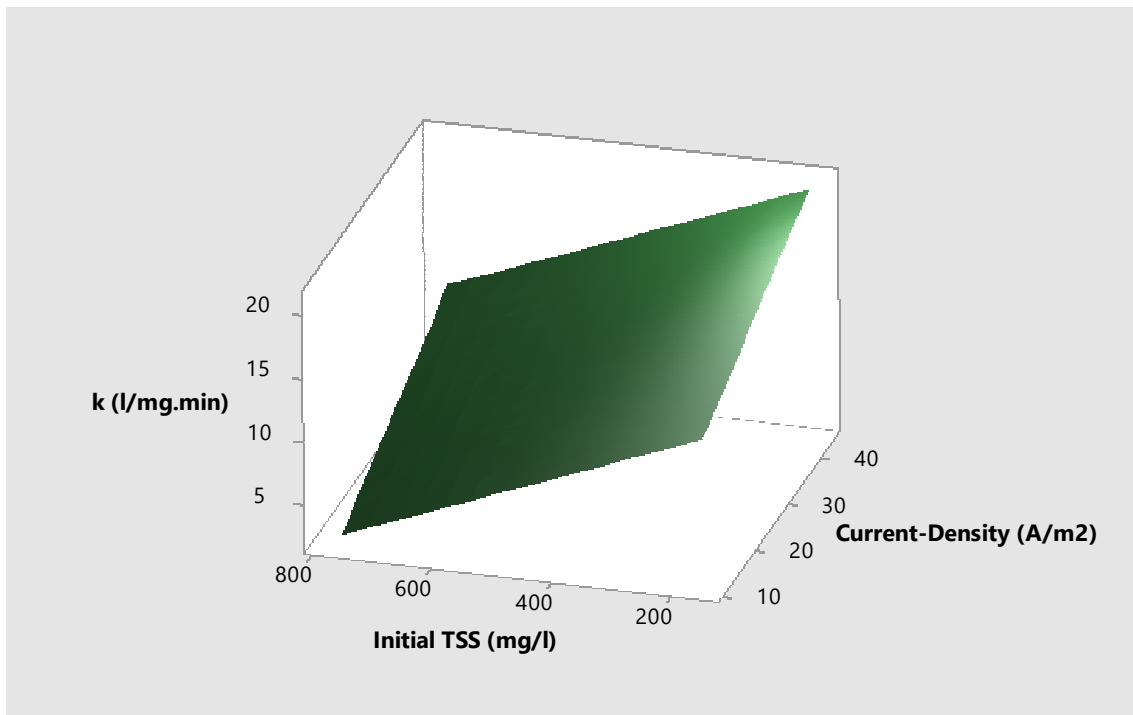


Figure 3.11: Surface plot of second-order rate constant, k , vs Current Density (J) and Initial TSS concentration

3.3.2 Analysis of Individual Wastewater Samples

In this section, Response Surface Methodology, ANOVA and Regression Analysis are used to analyze the data from each auto paint wastewater sample, separately.

Response surface methodology (RSM) is a group of statistical and mathematical methods used to advance and optimize a process. It is particularly beneficial where various variables (independent variables or predictors) have potential effects on a dependent variable (response) (Myers et al., 2009).

Response surface regression was performed on the experimental data of each wastewater sample. The predictors were treatment time, T , and applied current density, J , and the response was %Removal of TSS. Therefore, the treatment efficiency for each wastewater sample was defined based on the reaction time and current density. Two methods were considered. In the first method, the response surface analysis, RSA, the model incorporated all terms (X_1 , X_2 , X_1^2 , X_2^2 , X_1X_2). In the second method, the stepwise

regression, through the stepwise selection of the independent variables (predictors), the model only included the most significant factors.

3.3.2.1 ClearCoat_TS1992

Response Surface Analysis, RSA, was performed on ClearCoat_TS1992 wastewater data and the following equation was resulted:

$$Y = -10.4 + 6.656 T + 1.180 J - 0.1134 T^2 - 0.0122 J^2 - 0.0070 T*J \quad (3.18)$$

(valid for J: 11-44 A/m², T: 0-40 min)

where,

T: Time, min

J: Current Density, A/m²

Y: %Removal

R-sq= 91.33%, R-sq (adj)= 89.36%

The Stepwise Selection of Terms (α to enter = 0.15, α to remove = 0.15) was performed in order to identify the most significant terms and the following equation was established:

$$Y = 0.27 + 6.464 T + 0.391 J - 0.1134 T^2 \quad (3.19)$$

(valid for J: 11-44 A/m², T: 0-40 min)

R-sq= 91.01%, R-sq (adj)= 89.89%

Contour plot and surface plot of %removal of TSS for ClearCoat_TS1992 wastewater vs Current Density and Time are presented in Figure 3.12 and 3.13.

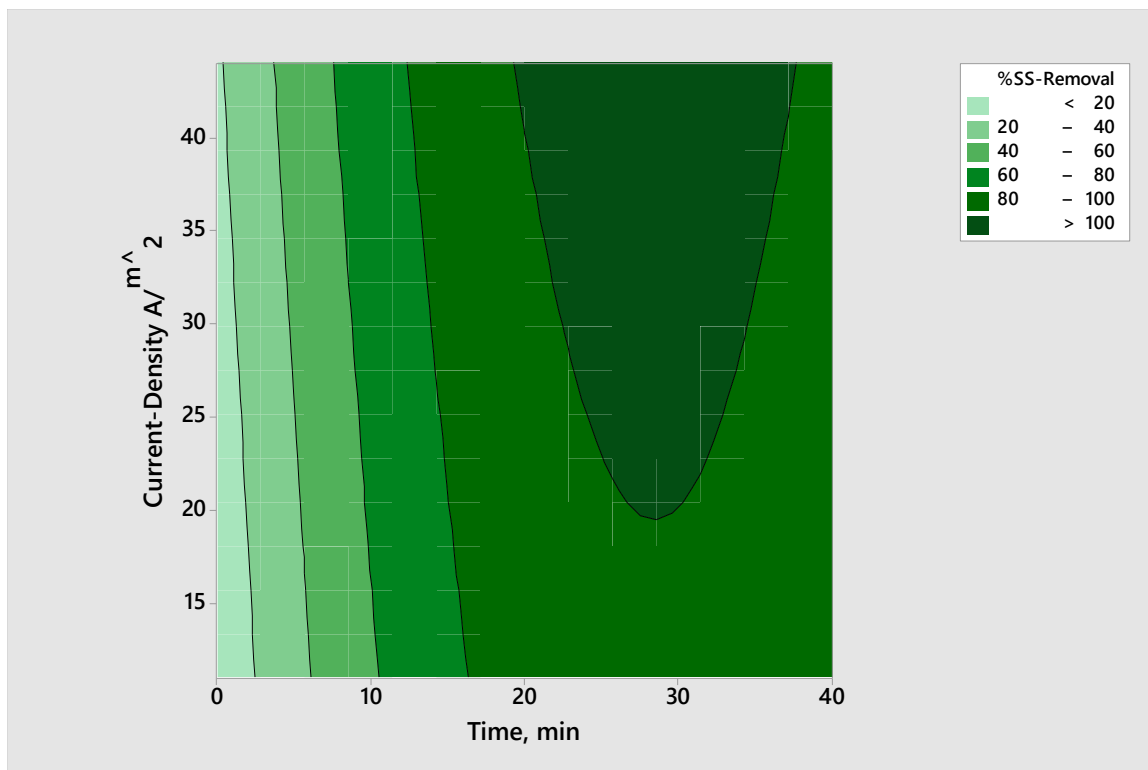


Figure 3.12: Contour plot of %removal of TSS for ClearCoat_TS1992 wastewater vs Current Density and Time

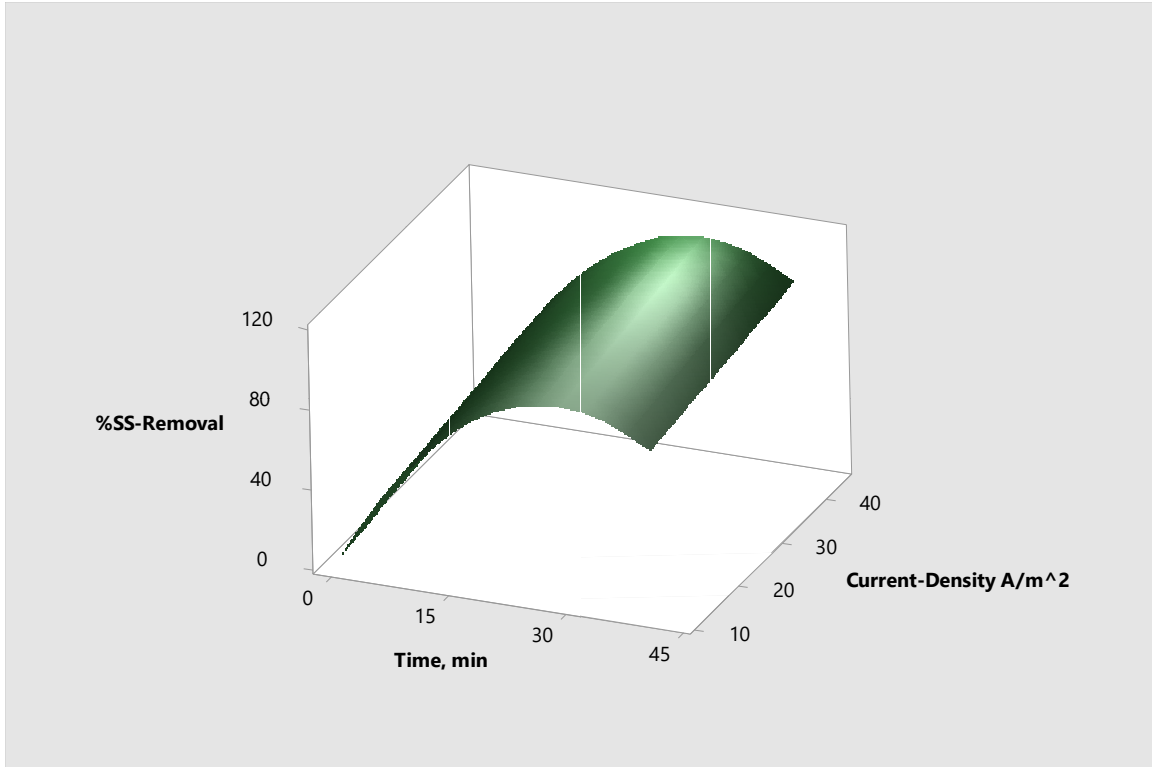


Figure 3.13: Surface plot of %removal of TSS for ClearCoat_TS1992 wastewater vs Current Density and Time

Comparing Eq. (3.18) and (3.19) showed that the only significant quadratic interaction was Time² and the R-sq values in Stepwise regression and RSA were 91.01% and 91.33%, respectively.

3.3.2.2 ClearCoat_TS4669

Response Surface Analysis, RSA, was applied to ClearCoat_TS4669 wastewater data and following was the resulted equation:

$$Y = -25.5 + 7.40 T + 1.77 J - 0.1164 T^2 - 0.0107 J^2 - 0.0325 T*J \quad (3.20)$$

(valid for J: 11-44 A/m², T: 0-40 min)

where,

T: Time, min

J: Current Density, A/m²

Y: %Removal

R-sq= 81.86%, R-sq (adj)= 77.54%

The Stepwise Selection of Terms (α to enter = 0.15, α to remove = 0.15) was performed in order to identify the most significant terms and the following equation was established:

$$Y = -18.5 + 7.376 T + 1.169 J - 0.1163 T^2 - 0.0321 T*J \quad (3.21)$$

(valid for J: 11-44 A/m², T: 0-40 min)

R-sq= 81.72%, R-sq (adj)= 78.39%

Also, Eq. (3.21) showed that the significant quadratic interactions were Time² and Time×Current Density. The R-sq values in Stepwise regression and RSA were 81.72% and 81.86%, respectively. Contour plot and surface plot of %removal of TSS for ClearCoat_TS4669 wastewater vs Current Density and Time are presented in Figure 3.14 and 3.15.

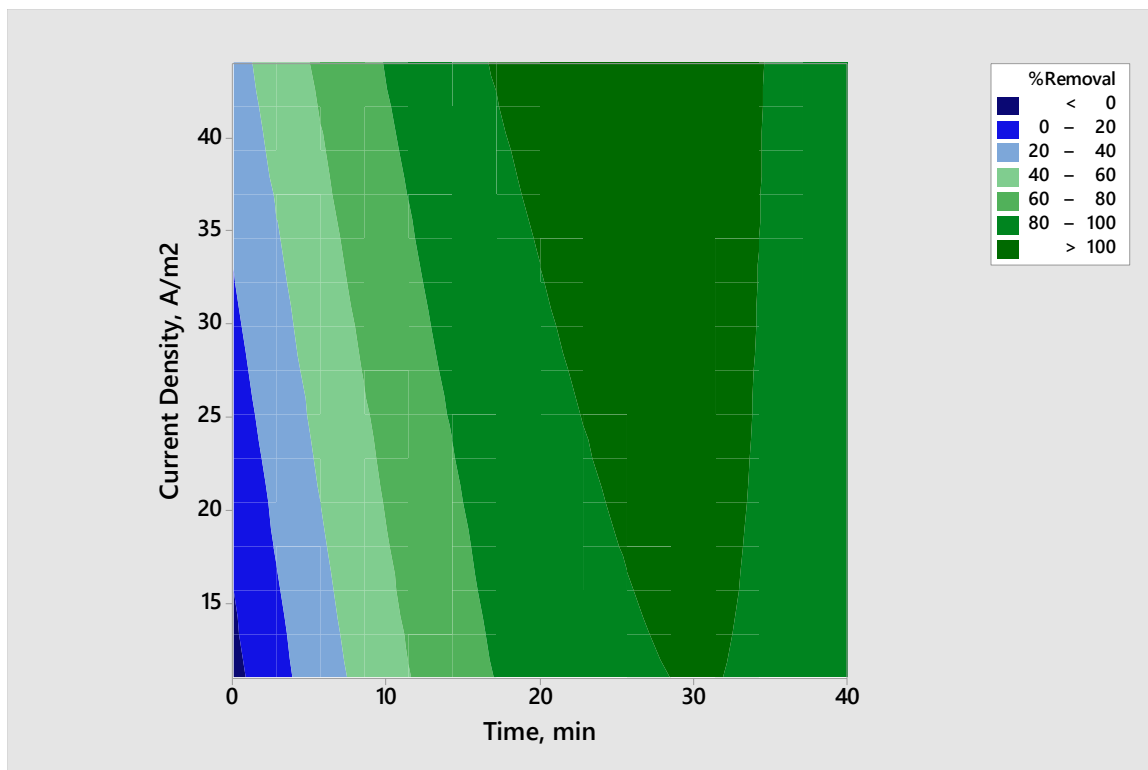


Figure 3.14: Contour plot of %removal of TSS for ClearCoat_TS4669 wastewater vs Current Density and Time

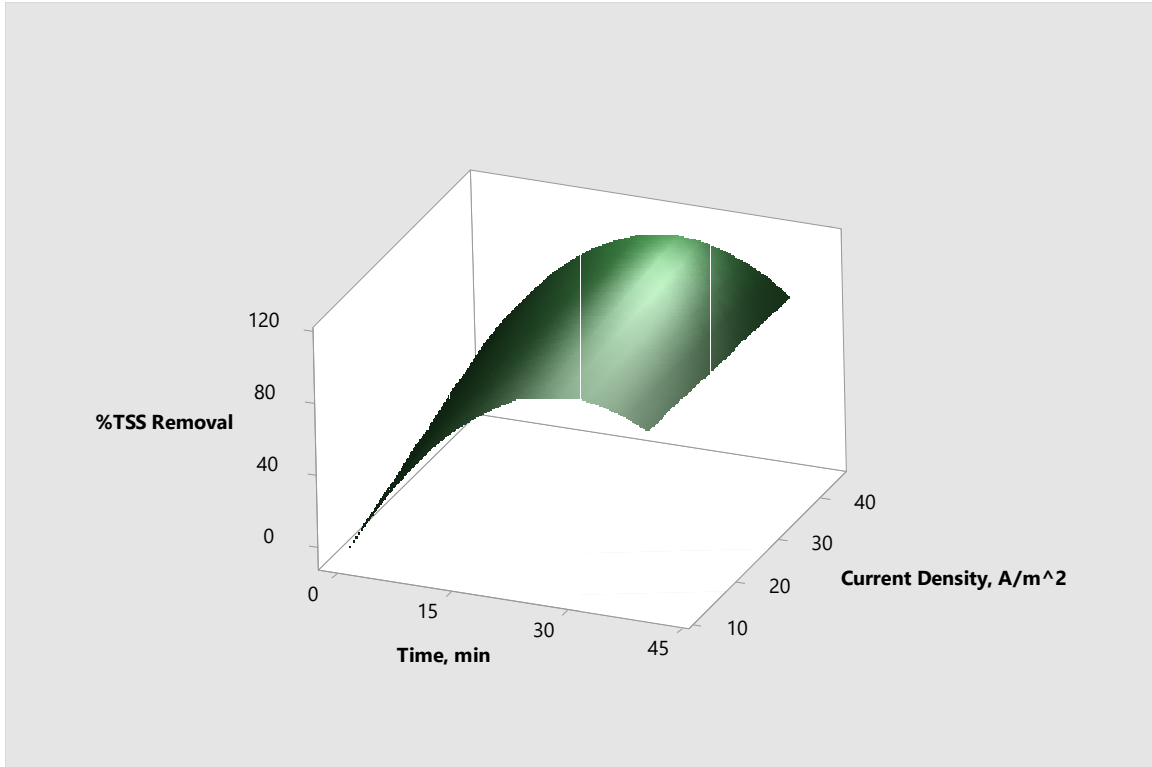


Figure 3.15: Surface plot of %removal of TSS for ClearCoat_TS4669 wastewater vs Current Density and Time

3.3.2.3 Primer_TS1432

Response Surface Analysis was performed on Primer_TS1432 wastewater data and following was the produced equation:

$$Y = 7.8 + 5.95 T + 0.89 J - 0.1094 T^2 - 0.0109 J^2 - 0.0043 T*J \quad (3.22)$$

(valid for J: 11-44 A/m², T: 0-40 min)

where,

T: Time, min

J: Current Density, A/m²

Y: %Removal

R-sq= 73.34%, R-sq (adj)= 67.28%

The Stepwise Selection of Terms (α to enter = 0.15, α to remove = 0.15) was performed in order to identify the most significant terms and the following equation was generated:

$$Y = 22.49 + 5.828 T - 0.1094 T^2 \quad (3.23)$$

(valid for J: 11-44 A/m², T: 0-40 min)

R-sq= 72.27%, R-sq (adj)= 70.06%

It could be noticed from Eq. (3.22) and (3.23) that the only significant quadratic interaction was Time². The R-sq values in Stepwise regression and RSA were 72.27% and 73.34%, respectively.

3.3.2.4 Primer_TS2374

Response Surface Analysis, RSA, was applied to Primer_TS2374 wastewater data and following was the produced equation:

$$Y = -34.0 + 7.028 T + 2.11 J - 0.1100 T^2 - 0.0191 J^2 - 0.0202 T*J \quad (3.24)$$

(valid for J: 11-44 A/m², T: 0-40 min)

where,

T: Time, min

J: Current Density, A/m²

Y: %Removal

R-sq= 90.32%, R-sq (adj)= 87.78%

The Stepwise Selection of Terms (α to enter = 0.15, α to remove = 0.15) was performed in order to identify the most significant terms and the following equation was established:

$$Y = -10.32 + 6.449 T + 0.660 J - 0.1102 T^2 \quad (3.25)$$

(valid for J: 11-44 A/m², T: 0-40 min)

R-sq= 89.10%, R-sq (adj)= 87.55%

Also, it could be realized from Eq. (3.25) that the significant quadratic interaction was Time². The R-sq values in Stepwise regression and RSA were 89.10% and 90.32%, respectively. Contour plot and surface plot of %removal of TSS for Primer_TS2374 wastewater vs Current Density and Time are presented in Figure 3.16 and 3.17.

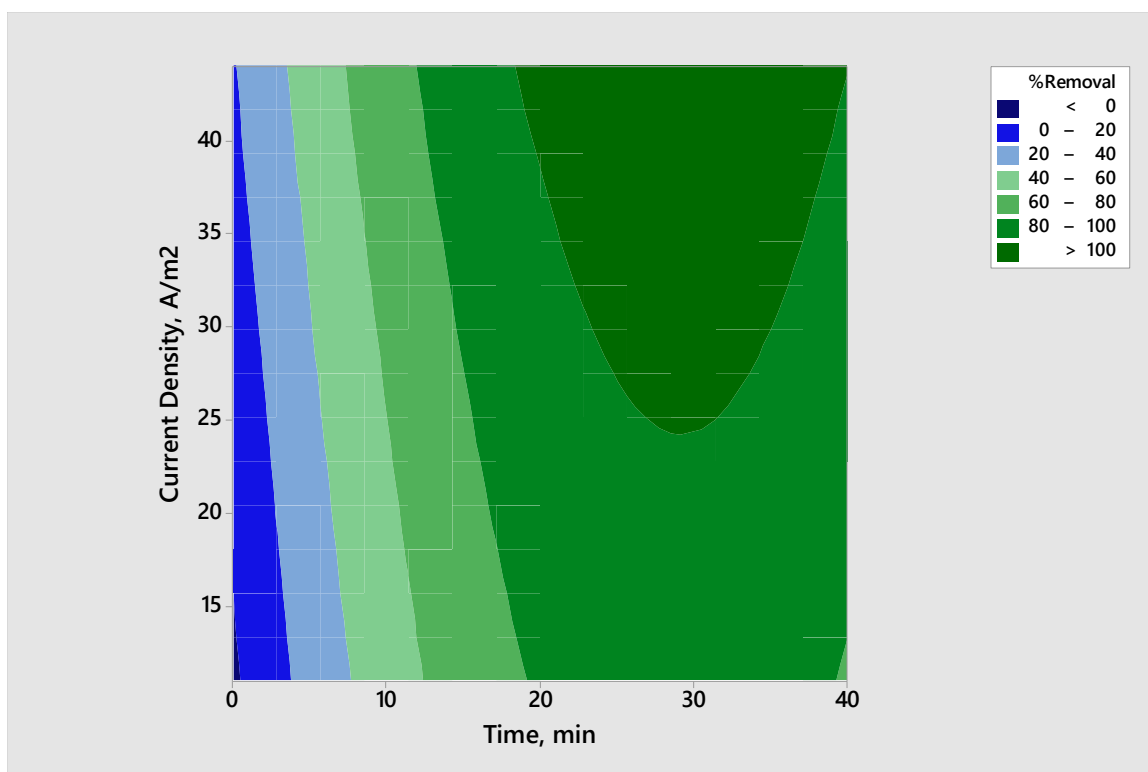


Figure 3.16: Contour plot of %removal of TSS for Primer_TS2374 wastewater vs Current Density and Time

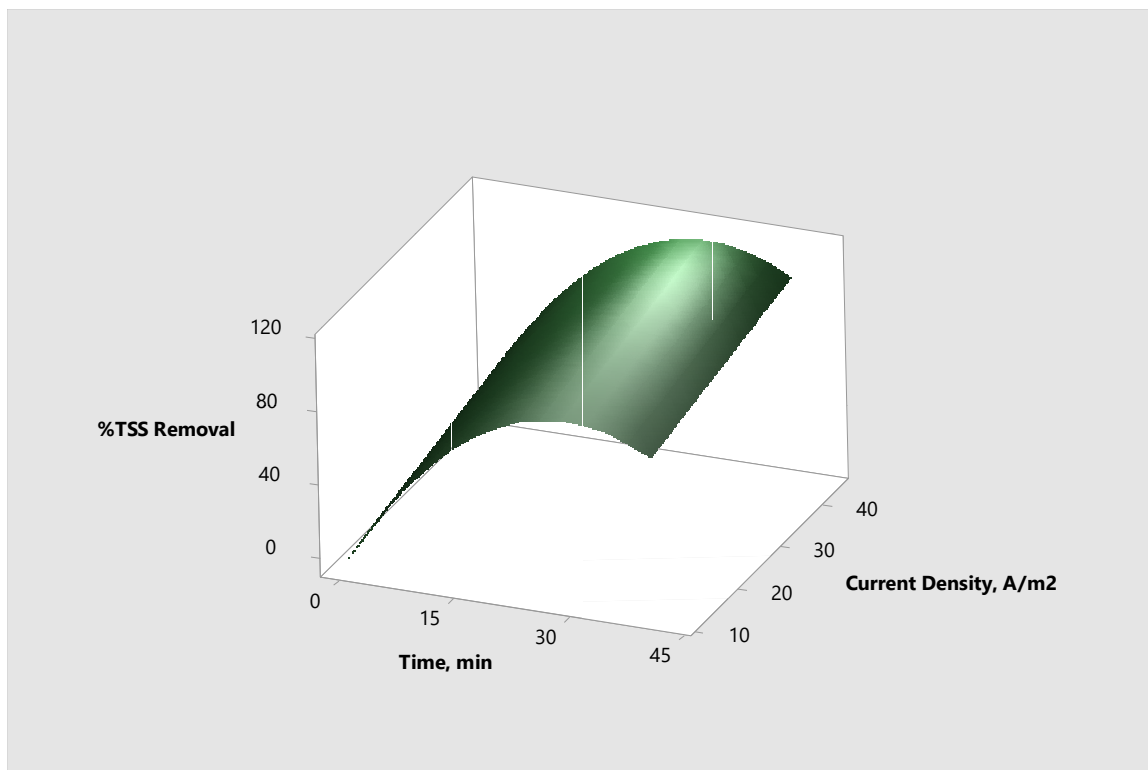


Figure 3.17: Surface plot of %removal of TSS for Primer_TS2374 wastewater vs Current Density and Time

3.3.2.5 MixedPaint_TS2789

Response Surface Analysis performed on MixedPaint_TS2789 wastewater data and following equation was generated:

$$Y = -8.2 + 6.79 T + 1.56 J - 0.1207 T^2 - 0.0165 J^2 - 0.0111 T*J \quad (3.26)$$

(valid for J: 11-44 A/m², T: 0-40 min)

where,

T: Time, min

J: Current Density, A/m²

Y: %Removal

R-sq= 77.71%, R-sq (adj)= 72.64%

The Stepwise Selection of Terms (α to enter = 0.15, α to remove = 0.15) was performed in order to identify the most significant terms and the following equation was established:

$$Y = 7.0 + 6.483 T + 0.461 J - 0.1207 T^2 \quad (3.27)$$

(valid for J: 11-44 A/m², T: 0-40 min)

R-sq= 77.06%, R-sq (adj)= 74.19%

Contour plot and surface plot of %removal of TSS for MixedPaint_TS2789 wastewater vs Current Density and Time are presented in Figure 3.18 and 3.19.

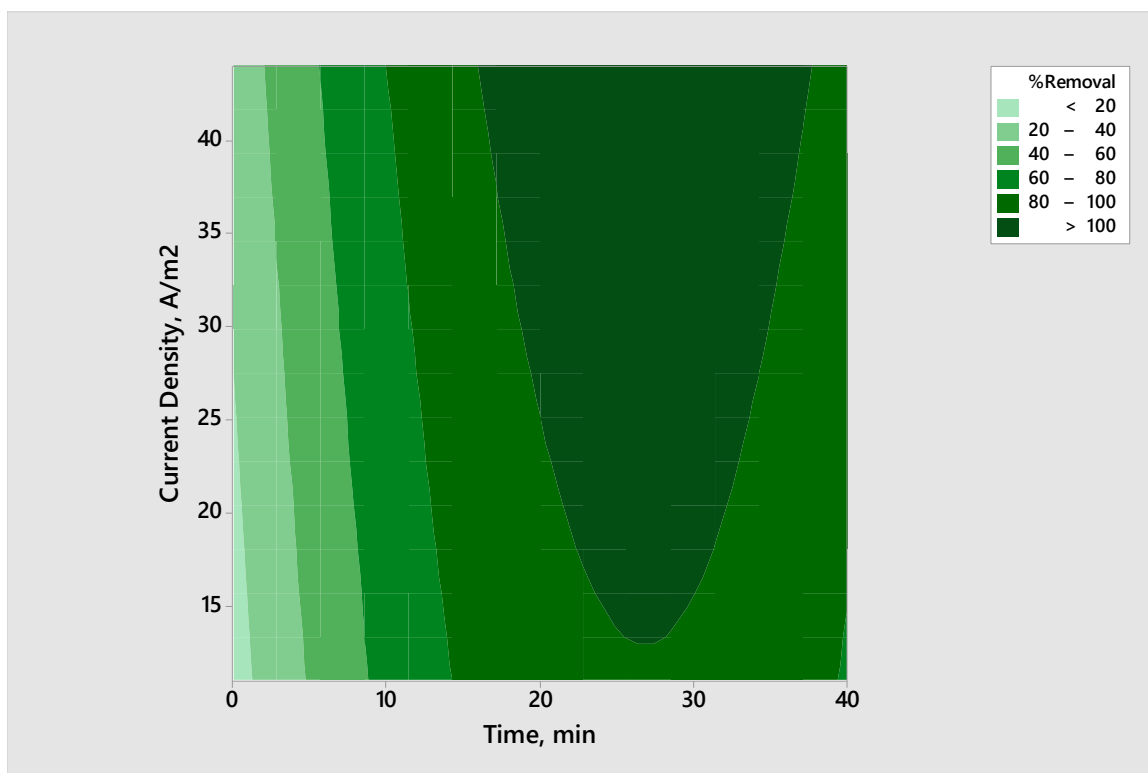


Figure 3.18: Contour plot of %removal of TSS for MixedPaint_TS2789 wastewater vs Current Density and Time

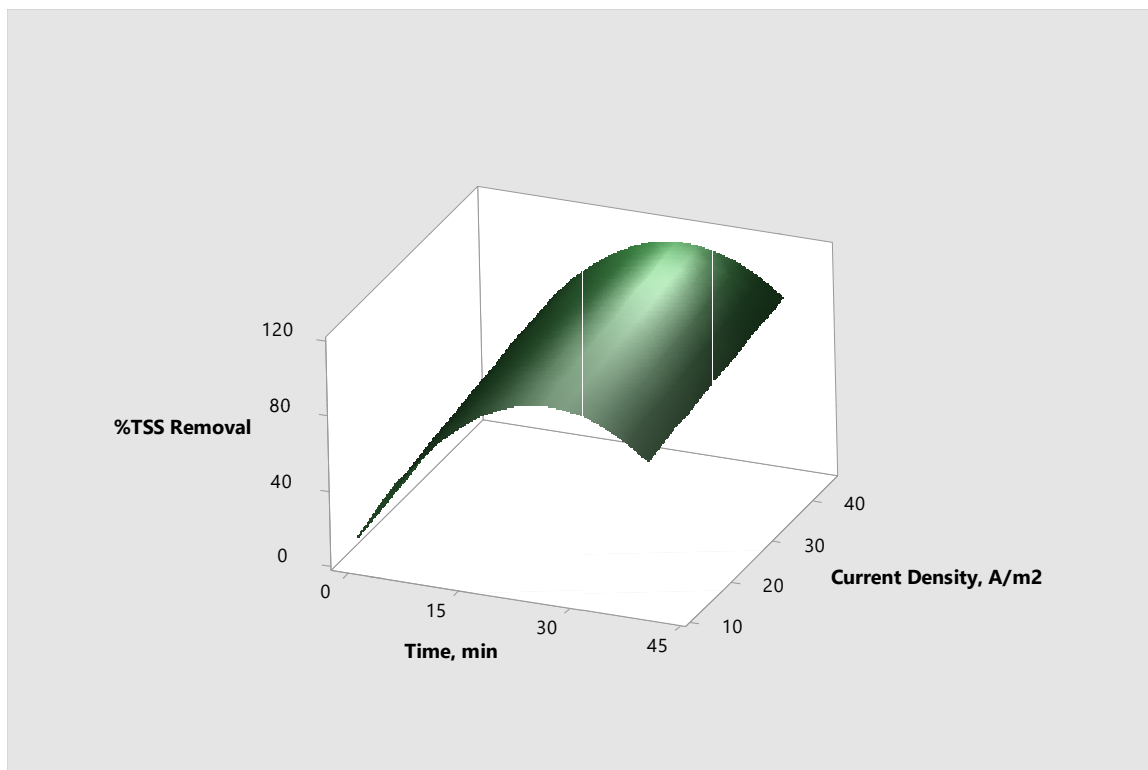


Figure 3.19: Surface plot of %removal of TSS for MixedPaint_TS2789 wastewater vs Current Density and Time

Based on the Eq. (3.27), the only significant quadratic interaction was Time^2 and no interactions between Time and Current Density were considered significant in terms of their effect on %Removal of TSS. The R-sq values in Stepwise regression and RSA were 77.06% and 77.71%, respectively.

3.3.3 Discussion

Using the statistical methods (best subset regression and stepwise regression), the initial TSS and current density were recognized as the most influencing factors in the electroflotation of the auto paint wastewater. This result can be compared with the literature. The study of hardness, COD and turbidity removal from produced water and prior to reverse osmosis using electrocoagulation was performed by Zhao et al. (2014).

Effects of current density, pH and treatment time were studied and through the ANOVA, it was found that current density was the most significant influencing factor (Zhao et al., 2014). These results are in agreement with the current study, except that the effect of initial pollutant concentration was not investigated in their research.

Response surface methodology, RSM, proved to be a robust tool to analyze and model the data from the batch tests of electroflotation of auto paint wastewater, in this study. Other authors implemented the RSM as well. Adjeroud et al. (2015) used the RSM method to improve and optimize electrocoagulation-electroflotation water treatment. In another study, Kobya et al. (2011) investigated and optimized the electrocoagulation treatment of metal cutting wastewater, using the RSM. Quadratic models of COD, TOC and turbidity removal with respect to different factor were established. According to this study, RSM was found to be a suitable tool to study and optimize this treatment method (Kobya et al., 2011).

Removal of COD, BOD and color, from the effluent of pulp and paper factory using electrocoagulation method was investigated by Sridhar et al. (2012). The RSM was implemented to study the effect of current density, initial pH and other parameters. As a result, a second-order polynomial model found to be good fit with the experimental results (Sridhar et al., 2012). Jimenez et al. (2016) also used RSM method to analyze the results of electroflotation treatment of kaolin suspension, oily wastewater and coloured organic solution. Current density, residence time and pollutant concentrations were considered as the influencing factors of the performance of treatment system (Jimenez et al., 2016).

Removal of colour caused by organic matters from groundwater using an electroflotation-filtration continuous-flow reactor was investigated and effective parameters like current and electrode material were studied using response surface methodology to optimize the treatment efficiency of the system (Zhou et al., 2016). In another research, effects of input rate and current density on treatment of oil extraction wastewater using electroflotation and filtration processes were statistically studied through the Analysis of Variance (Nonato et al., 2018). Qin et al. (2012) also used the RSM and ANOVA

methods to optimize the electrocoagulation-electroflotation treatment of restaurant wastewater.

In the current section of this study, the response surface analysis, RSA, and the stepwise regression methods were used to find the regression equations of %removal of TSS (as the response) for each wastewater sample. Comparing the equations and the corresponding coefficient of determinations (R^2), it was noted that although the equations produced by the stepwise regression method had fewer number of terms, their corresponding R^2 values were comparable to the results of the RSA method. For example, the R^2 values of the regression equations of ClearCoat_TS1992 sample were 91.33% and 91.01% for the RSA and stepwise methods, respectively. This was favorable because the simpler equations were obtained without compromising the accuracy of the model.

In addition, in stepwise regression method, T^2 was found to be the most repeated quadratic term (Eq. 3.19, 3.21, 3.23, 3.25 and 3.27), showing the significance of the treatment time in the performance of the process and the TSS removal from the auto paint wastewater.

3.4 Conclusions

Electroflotation (EF) is the use of the bubbles formed during the water electrolysis to remove suspended particles/liquids by flotation. The experimental data from batch treatment of auto paint wastewater using EF were used to investigate the kinetics of the treatment and perform the statistical analysis. Five types of wastewater samples, synthesized by addition of three types of solvent-based auto paint, were used in the experiments.

The first and second-order kinetic study were performed on the experimental data. The results indicated that the second-order model, having higher R-sq values, was a better fit to the experimental data. Also, it was noticed that the reaction rate constants increased with the increase of applied current density, and for the wastewater samples prepared by the same type of auto paint, the lower initial concentrations led to the higher rate constant values.

Afterwards, the initial TSS concentration, Current Density (J), pH, Zeta Potential and Conductivity of all wastewater samples, as the affecting parameters were statistically analyzed, and it was found that the current density and the initial TSS concentration were the most significant factors, influencing the second-order rate constant. The Best Subsets Regression, Backward Elimination and Analysis of Variance (ANOVA) were the methods implemented using Minitab 18.1 software. The regression equation with the response of the second-order k and the predictors of the current density and the initial TSS was established.

Further, using the Response Surface Methodology (RSM), the equations of the removal rate of TSS (as the response) for each wastewater sample were established, with the reaction time and the applied current density as the predictors of the equations. The equations were created using the response surface analysis and the stepwise regression methods. The stepwise regression method created better regression equations, with the fewer number of the variables and acceptable accuracy. The time, T, was confirmed to be a significant influencing factor in the TSS removal, as the T^2 was the most repeated quadratic term in the equations of the stepwise method. For each wastewater sample, the

contour plot and surface plot of %removal of TSS vs Current Density and Time were prepared and illustrated.

Acknowledgments

This study was supported by the University of Western Ontario and the National Science and Engineering Research Council of Canada (NSERC). The experimental program was partially funded by Daimler Chrysler Co.

References

- Adjeroud, N., Dahmoune, F., Merzouk, B., Leclerc, J. P., & Madani, K. (2015). Improvement of electrocoagulation–electroflotation treatment of effluent by addition of *Opuntia ficus indica* pad juice. *Separation and Purification Technology*, *144*, 168-176.
- Ahmadian, M., Yousefi, N., Van Ginkel, S. W., Zare, M. R., Rahimi, S., & Fatehizadeh, A. (2012). Kinetic study of slaughterhouse wastewater treatment by electrocoagulation using Fe electrodes. *Water Science and Technology*, *66*(4), 754-760.
- Bhaskar Raju, G., & Khangaonkar, P. R. (1984). Electroflotation-A critical review. *Transactions of the Indian Institute of Metals*, *37*(1), 59-66.
- Brown, P. M. B. L. C., & Hambley, D. F. (2002). Statistics for environmental engineers.
- Jiménez, C., Sáez, C., Cañizares, P., & Rodrigo, M. A. (2016). Optimization of a combined electrocoagulation-electroflotation reactor. *Environmental Science and Pollution Research*, *23*(10), 9700-9711.
- Kalyani, K. P., Balasubramanian, N., & Srinivasakannan, C. (2009). Decolorization and COD reduction of paper industrial effluent using electro-coagulation. *Chemical Engineering Journal*, *151*(1-3), 97-104.
- Kobyas, M., Demirbas, E., Bayramoglu, M., & Sensoy, M. T. (2011). Optimization of electrocoagulation process for the treatment of metal cutting wastewaters with response surface methodology. *Water, Air, & Soil Pollution*, *215*(1-4), 399-410.
- Kyzas, G. Z., & Matis, K. A. (2016). Electroflotation process: A review. *Journal of Molecular Liquids*, *220*, 657-664.
- Levenspiel, O. (1999). *Chemical reaction engineering*. Wiley.
- Matis, K. A. (Ed.). (1994). *Flotation science and engineering*. CRC Press.
- Metcalf & Eddy, Burton, F. L., Stensel, H. D., & Tchobanoglous, G. (2003). *Wastewater engineering: treatment and reuse*. McGraw Hill.

- Minitab Express Support. (2017). *Interpret all statistics and graphs for One-Way ANOVA*. Retrieved from: <http://support.minitab.com/en-us/minitab-express/1/help-and-how-to/modeling-statistics/anova/how-to/one-way-anova/interpret-the-results/all-statistics-and-graphs/> (accessed 13 December 2017)
- Murugananthan, M., Raju, G. B., & Prabhakar, S. (2004). Separation of pollutants from tannery effluents by electro flotation. *Separation and Purification Technology*, 40(1), 69-75.
- Myers, R. H., Montgomery, D. C., & Anderson-Cook, C. M. (2009). *Response surface methodology: Process and product optimization using designed experiments*.
- Ni, C., Xie, G., Jin, M., Peng, Y., & Xia, W. (2016). The difference in flotation kinetics of various size fractions of bituminous coal between rougher and cleaner flotation processes. *Powder Technology*, 292, 210-216.
- Nonato, T. C. M., Schöntag, J. M., Burgardt, T., Alves, A. A. D. A., Broock, W. F., Dalsasso, R. L., & Sens, M. L. (2018). Combination of electroflotation process and down-flow granular filtration to treat wastewater contaminated with oil. *Environmental technology*, 39(6), 717-724.
- Qin, X., Yang, B., Gao, F., & Chen, G. (2012). Treatment of restaurant wastewater by pilot-scale electrocoagulation-electroflotation: Optimization of operating conditions. *Journal of environmental engineering*, 139(7), 1004-1016.
- Rawlings, J. O., Pantula, S. G., & Dickey, D. A. (2001). *Applied regression analysis: a research tool*. Springer Science & Business Media.
- Shang, J. Q. (2004). *Electrokinetic Flotation of Paint Sludge Water*, Western University, London, Canada.
- Sridhar, R., Sivakumar, V., Immanuel, V. P., & Maran, J. P. (2012). Development of model for treatment of pulp and paper industry bleaching effluent using response surface methodology. *Environmental Progress & Sustainable Energy*, 31(4), 558-565.

Zhang, H., Liu, J., Cao, Y., & Wang, Y. (2013). Effects of particle size on lignite reverse flotation kinetics in the presence of sodium chloride. *Powder Technology*, 246, 658-663.

Zhao, S., Huang, G., Cheng, G., Wang, Y., & Fu, H. (2014). Hardness, COD and turbidity removals from produced water by electrocoagulation pretreatment prior to reverse osmosis membranes. *Desalination*, 344, 454-462.

Zhou, J., Chen, D., Jiang, Y., Yang, K., Wang, H., & Zhou, J. (2016). Removal of color caused by dissolved organic matter from groundwater by electroflotation-filtration continuous flow reactor and optimization by response surface methodology. *Desalination and Water Treatment*, 57(2), 754-764.

CHAPTER 4 Continuous-Flow Electroflotation of Automotive Paint Wastewater

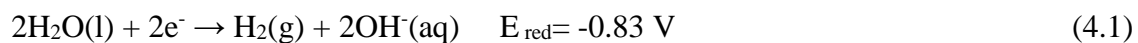
This chapter begins with an introduction to electroflotation and applications of this method in treatment of automotive paint wastewater. Afterwards, the experimental study of continuous-flow treatment of auto paint wastewater is presented, including: materials and methods, and results of the experiments. The results are discussed, and the effects of different influencing factors are investigated.

4.1 Introduction

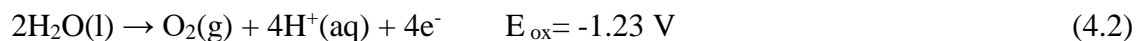
Flotation is an effective unit operation implemented in different industries. It has been first used as a separation method in mineral processing, with applications extended to new fields such as wastewater treatment for separation of fats, rubber, clays, sugar, etc. (Matis, 1994). In the flotation process, solid or liquid particles are separated from a liquid phase: particles attach to bubbles and the buoyancy, forces them to rise to the surface, and consequently, removed by skimming process. Gas bubbles can be introduced by different methods, such as dissolved-air flotation (DAF), dispersed-air flotation and electroflotation (EF). Dissolved-air flotation is mostly used in municipal wastewater treatment, in which air is dissolved in water under high pressure and then released in wastewater, creating fine bubbles. Dispersed-air or induced-air flotation is frequently used in industries to remove suspended solids or liquid such as oils from a suspension. In this process, a spinning impeller submerged in the suspension, forces air into the liquid through the induced vacuum (Metcalf and Eddy, 2003).

In electroflotation, bubbles are created through electrolysis (Kyzas and Matis, 2016). The process consists of a treatment tank, two electrodes (cathode and anode) placed at the bottom of the tank creating small bubbles of gases (hydrogen and oxygen) through the applied direct electric current (Matis, 1994). In the electrolysis of neutral water, redox reactions occur at the inert anode and cathode (Bagotsky, 2006):

at the cathode:



and at the anode:



The overall reaction can be obtained by doubling the reduction reaction, Eq. (4.1), at the cathode and adding it to the oxidation reaction at the anode:



Therefore, in reaction of 2 molecules of water, 4 electrons are involved. The theoretical minimum required voltage of the electrolysis of pure water is 2.06 V (Bagotsky, 2006). It should be mentioned that in practice, since water is not pure and also, the electrodes might not be inert, other reactions might occur, resulting in different gases, e.g., production of Cl_2 in salt water.

The electroflotation process has several advantages over other flotation methods: the bubbles produced are smaller, creating more surface area and therefore, higher removal efficiency, particularly for removal of finer particles. Also, having no moving parts, the control and operation is simpler. (Kyzas and Matis, 2016). The electrodes can be designed based on the size and dimensions of the tank and can retrofit in the existing tank as well.

According to the experimental results of treatment of automotive paint wastewater using electroflotation (EF) in a batch system (Shang, 2004), this technique can be a promising method for treatment of this type of industrial wastewater. However, those experiments were carried out in a small scale and batch system. Therefore, in order to further investigate the suitability of electroflotation method and obtain more realistic results, applicable to full-scale environments, more research is required.

In this chapter, a series of continuous-flow pilot-scale experiments on the electroflotation treatment of the automotive paint wastewater is conducted and effects of different process variables on the system performance are investigated. The energy consumption of the process is calculated and evaluated and through the statistical methods, empirical equations are produced, and the experimental results are analyzed.

4.2 Treatment of Automotive Paint Wastewater Using Electroflotation

The performance of electroflotation system in treatment of auto paint wastewater was studied by examining the parameters presented in Table 4.1.

Table 4.1: Wastewater parameters measured in this study

Parameter	Unit
Total Solids, TS	mg/L
Total Suspended Solids, TSS	mg/L
Turbidity	NTU
pH	-
Electrical Conductivity	$\mu\text{S/cm}$

The removal rate, R , and efficiency of the process was defined in Eq. 4.4.

$$R (\%) = \left(1 - \frac{C_{eff}}{C_{inf}}\right) \times 100 \quad (4.4)$$

where, C_{inf} and C_{eff} are concentrations of the measured parameters in the influent and effluent of the reactor, respectively.

Also, the specific energy consumption E (W h m^{-3}) of the electroflotation process for the removal of auto paint was calculated using Eq. 4.5.

$$E = \frac{(U \times I \times t)}{V} \quad (4.5)$$

where, U represents the applied voltage (Volts), I is the current (Amp), t is the retention time (Hour) and V is the reactor volume (m^3).

In the electroflotation process, electrolysis occurs, and gas is produced. Amount of mass generated at electrode can be calculated by Faraday's law of electrolysis (Holt et al., 2002):

$$m = \frac{(I \times t \times MM)}{Z \times F} \quad (4.6)$$

where,

m : amount of mass generated at electrode, g

I : electrical current, A

t : electrolysis time, seconds

MM : molar mass, gram per mol

Z : number of electrons transferred

F : Faraday's constant, 96486 C per mol

Several factors affect the removal rate in an electroflotation process. Among them, the following were studied in this research:

- Concentration of Total Solids (TS) in the influent, mg/L; which is a measure of total suspended solids and total dissolved solids (TSS = TSS+TDS)
- Applied current density, A/m^2 ; which is applied DC current, I , divided by electrodes active surface area, A ($J = I/A$)

- Hydraulic retention time (HRT) of the system, minutes; which is reactors volume, V , divided by flowrate, Q , ($HRT = V/Q$)

4.3 Materials and Methods

The treatment system consisted of a feed tank and mixer, feeding pump, electroflotation tank, electrodes module and DC power supply. The schematic of the reactor is presented in Figure 4.1.

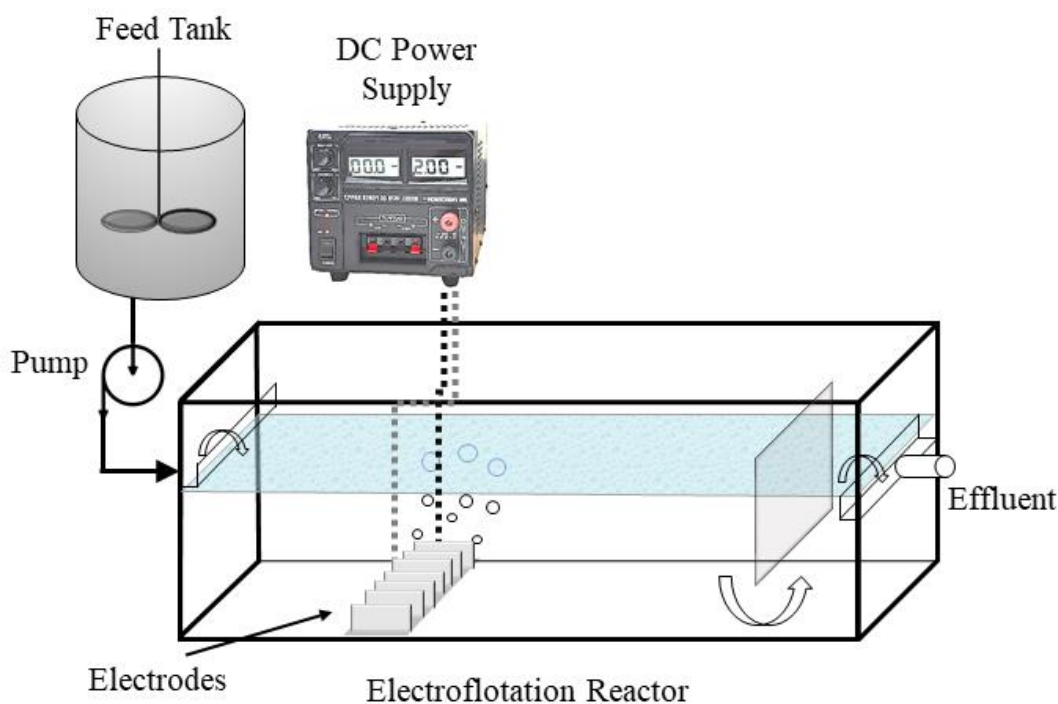


Figure 4.1: Schematic of the experimental setup and electroflotation reactor

4.3.1 Electroflotation Reactor

The electroflotation reactor was made of 12-mm-thick Plexiglass® material with the inner dimensions of 80×32×25 cm and the effective operational volume of 38.4 L. Figure 4.2 shows a picture of the electroflotation tank with the electrodes module placed at the bottom.

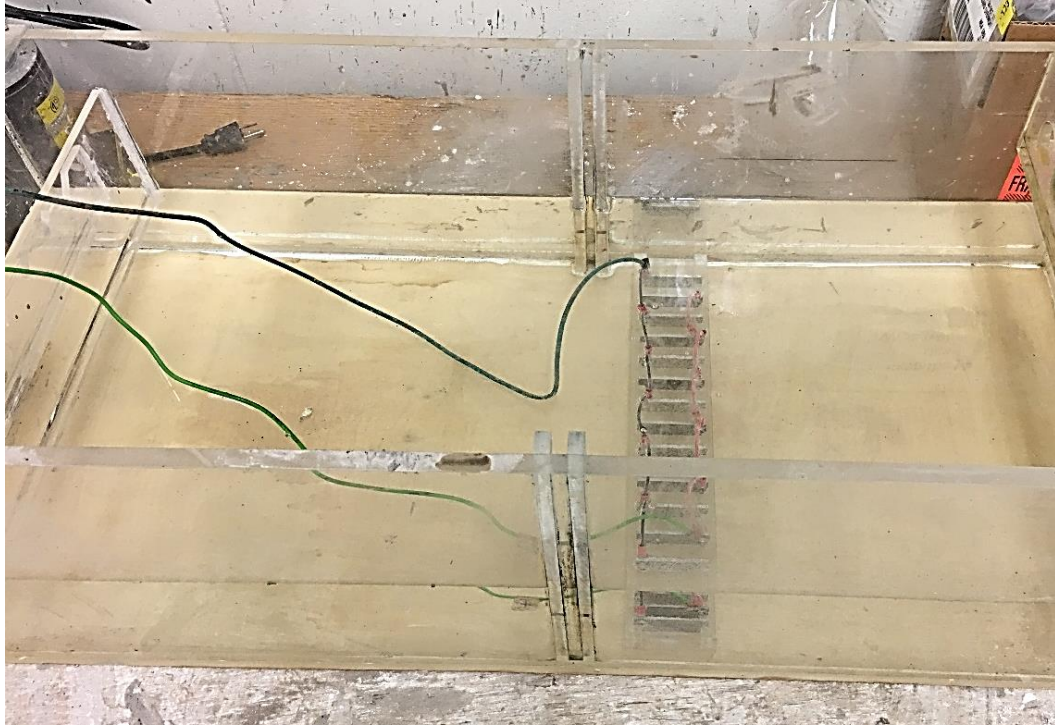


Figure 4.2: Electroflotation tank used for the treatment experiments

In the literature, researchers usually focus on the process aspect of the electroflotation system, while, reactor geometry, inlet and outlet, flow regime and hydrodynamics of the reactor influences the overall treatment efficiency, significantly (section 2.4, Chapter 2). Therefore, the reactor used in this study involved a new design and modifications, considering these important aspects. In order to have a uniform flow entering and exiting the reactor, inlet and outlet weirs were designed and installed. Details of the weir are presented in Figure 4.3.

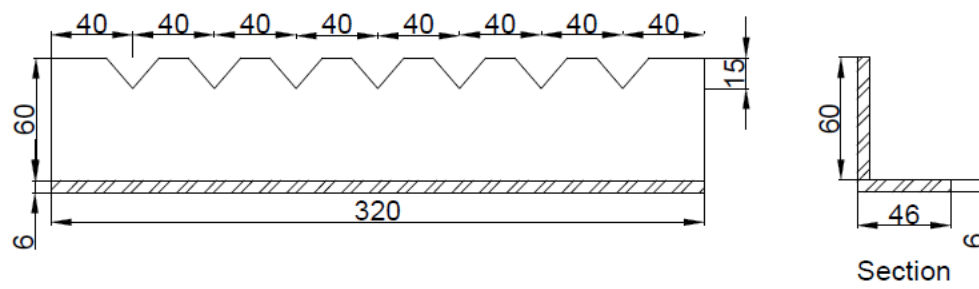


Figure 4.3: Details of weir installed in electroflotation reactor

By providing an even distribution of flow entering and exiting the reactor, the weirs significantly reduce the unfavorable hydrodynamic effects, e.g., channeling and short-circuiting, and decrease the stagnant regions of the reactor. This design can be compared with the horizontal-flow reactors used by Mollah et al. (2004), Figure 4.4(a), Zhou et al. (2016), Figure 4.4(b), and Hassani et al. (2016), Figure 4.4(c), where the even distribution of flow was ignored in their reactors.

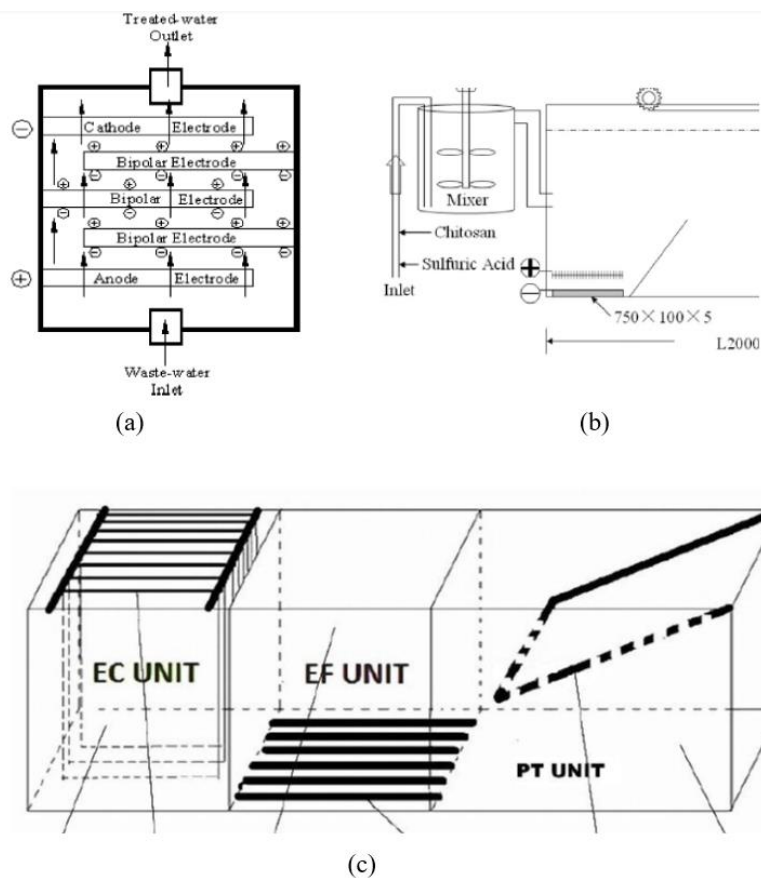


Figure 4.4: Continuous-horizontal-flow electroflotation reactors used by other researchers (a: Mollah et al. 2004; b: Zhou et al. 2016; c: Hassani et al. 2016)

In the electroflotation reactor, the bubble-particle aggregates ascend to the water surface to be skimmed off. The horizontal momentum of flow tends to push the floated paint particles towards the outlet weir and out of the reactor. Therefore, in order to inhibit this effect and prevent the floated paint particles being washed out of the reactor, an internal baffle was installed close to the exit end of the electroflotation reactor, as presented in Figure 4.2. This modification can also be compared with the reactors in Figure 4.4. Figure 4.5 presents the details of internal baffle.

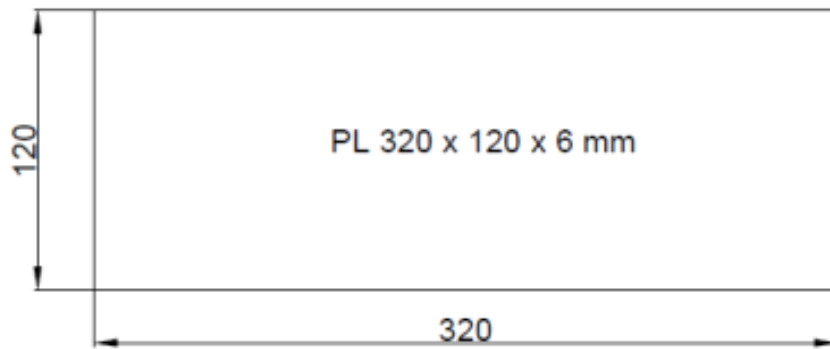


Figure 4.5: Internal baffled installed in electroflotation reactor

Overall, considering the hydraulic and hydrodynamic aspects, along with the process variables, the objective was to improve and maximize the treatment performance of the electroflotation system. Experimental study of the flow characteristics inside the reactor are presented in Chapter 5.

4.3.2 Electrodes

The cathodes and anodes were made of 3-mm-thick Stainless Steel (SS316) plates, which was suitable for electrochemical treatment (Symes et al., 2013). There were 13 electrodes with the dimensions of 50x20 mm with 17 mm spacing. Figures 4.6 and 4.7 show the details and photo of the electrodes module, respectively.

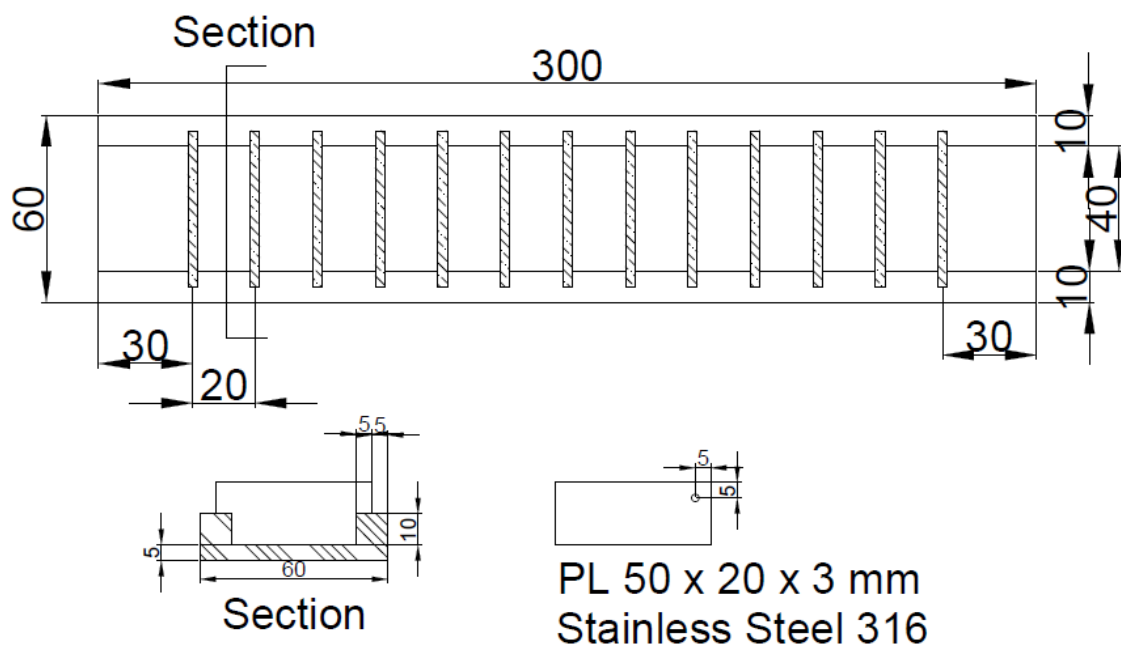


Figure 4.6: Details of electrodes module

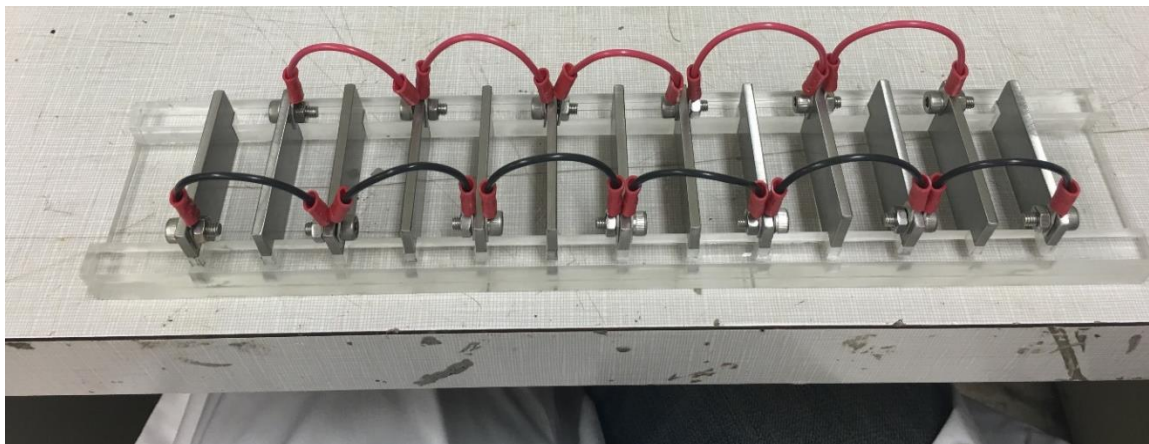


Figure 4.7: Photo of electrodes used in treatment experiments

4.3.3 Automotive Paint Wastewater

The automotive paint wastewater was synthetically prepared in the laboratory.

Preparation of the wastewater was according to the paint spray process in the paint booth

of auto factories, and was a mixture of black paint, detackifier and tap water. A mixer was used in the feed tank to keep the raw wastewater, uniform and solids, suspended. Also, an Iwaki pump model # MD-15RT-115NL and a peristaltic pump model Cole Parmer Masterflex were used to feed the wastewater into the tank at the desired flowrate.

An acrylic lacquer aerosol paint, named “PERFECT MATCH Premium Automotive Paint Black”, the product of Dupli-Color Products Company (Cleveland, OH), was used in this study. Ingredients and physical and chemical properties of the paint are summarized in Table 4.2 and Table 4.3, respectively.

Table 4.2: Composition/information on ingredients of PERFECT MATCH Premium Automotive Paint Black (Dupli-Color, 2017)

Ingredient name	% by weight	CAS number
Methyl Acetate	44	79-20-9
Propane	10.2	74-98-6
Butane	9.8	106-97-8
Toluene	8.35	108-88-3
1-Methoxy-2-Propanol Acetate	5.97	108-65-6
Methyl Ethyl Ketone	5.53	78-93-3
Ethyl Acetate	3.86	141-78-6
Ethanol	1.54	64-17-5
Ethyl 3-Ethoxypropionate	1.14	763-69-9
Cellulose Nitrate	1.06	9004-70-0
Carbon Black	0.45	1333-86-4

Table 4.3: Physical and chemical properties of PERFECT MATCH Premium Automotive Paint Black (Dupli-Color, 2017)

Property	Value
Flash point	Closed cup: -29°C (-20.2°F) [Pensky-Martens Closed Cup]
Evaporation rate	5.6 (butyl acetate = 1)
Lower and upper explosive (flammable) limits	Lower: 1%, Upper: 19%
Vapor pressure	101.3 kPa (760 mm Hg) [at 20°C]
Vapor density	1.5 [Air = 1]
Relative density	0.8
Viscosity	Kinematic (40°C (104°F)): <0.205 cm ² /s (<20.5 cSt)
Type of aerosol	Spray
Heat of combustion	36.176 kJ/g

The feed was prepared by spraying the paint into the water to obtain the desired concentration. In addition, paint detackifier was added to the mixture. Paint detackifier is a chemical used for the disruption of paint drops by altering the qualities of the paint into non-adhering moving particles (Salihoglu and Salihoglu, 2016). The detackifier used in the study was “GARDOFLOC 2000” (Chemetall Canada Limited).

4.3.4 Instrumentation

The Turbidity of the wastewater was measured using a turbidity meter model HI98703 (HANNA instruments) with the accuracy of $\pm 2\%$ of reading plus 0.02 NTU, which met and exceeded the requirements of EPA Method 180.1 and Standard Methods for the Examination of Water and Wastewater 2130 B for turbidity measurements (HANNA instruments, 2014).

An EC Meter HI8733 (HANNA instruments) was used to measure the electrical conductivity of the wastewater samples. With four-ring probe, the conductivity readings were adjusted with Automatic Temperature Compensation (ATC). A VWR SYMPHONY SP90M5 was used to measure pH of the wastewater samples. The Total Solids (TS) and

Total Suspended Solids (TSS) were measured according to Standard Methods for the Examination of Water and Wastewater (WEF and APHA, 2005). The tests were performed in three replicates.

4.4 Experimental Results and Discussion

Experimental studies were performed to investigate the performance of the continuous-flow electroflotation system in treatment of the auto paint wastewater. The analysis of batch experiments (Chapter 3) showed that the applied current density and concentration (or loading) of the auto paint in the influent were the most significant factors influencing the treatment efficiency. Also, it was certain that the treatment time had essential effect on the removal rate of pollutants in wastewater treatment systems. Therefore, these three factors, i.e., the applied current density, influent total solids (TS) concentration and Hydraulic Retention Time (HRT) of the treatment reactor, were chosen as the main parameters in the study to assess the system performance.

The system was studied under three influent Total Solids (TS) concentrations, i.e., 500, 1500 and 3000 mg/L. These concentrations were selected based on the normal and extreme operating conditions of actual wastewater in auto paint booths in car factories. Based on the batch experimental data and by adjusting the flowrate, retention times of 4, 6 and 8 minutes were applied to the system. Finally, the applied current densities were set as 50, 75 and 100 A/m². Summary of these data is presented in Table 4.4.

Table 4.4: Process variables studied in treatment of auto paint wastewater

Parameters	Unit	Values
Influent Total Solids (TS)	mg/L	500, 1500, 3000
Applied Current Density	A/m ²	50, 75, 100
Hydraulic Retention Time (HRT)	min	4, 6, 8

The performance of the treatment system was evaluated based on the percent removal of total suspended solids (TSS) from the auto paint wastewater samples, which is the common parameter in the auto industry. The experimental plan was prepared to evaluate the significance of the process variables and to optimize the system performance. The experimental plan is presented in Table 4.5.

Table 4.5: Experimental plan of treatment of auto paint wastewater using continuous-flow electroflotation system

Run No.	Influent TS (mg/L)	Current Density (A/m ²)	Hydraulic Retention Time (min)
1	500	50	4
2	500	75	4
3	500	100	4
4	500	50	6
5	500	75	6
6	500	100	6
7	500	50	8
8	500	75	8
9	500	100	8
10	1500	50	4
11	1500	75	4
12	1500	100	4
13	1500	50	6
14	1500	75	6
15	1500	100	6
16	1500	50	8

Run No.	Influent TS (mg/L)	Current Density (A/m ²)	Hydraulic Retention Time (min)
17	1500	75	8
18	1500	100	8
19	3000	50	4
20	3000	75	4
21	3000	100	4
22	3000	50	6
23	3000	75	6
24	3000	100	6
25	3000	50	8
26	3000	75	8
27	3000	100	8

4.4.1 Effect of Influent Concentration

Treatment of auto paint wastewater using electroflotation process with the influent total solids (TS) concentrations of 500, 1500 and 3000 mg/L was examined. The total suspended solids (TSS) concentration is one of the key parameters for performance assessment, and %Removal was used to evaluate the efficiency of the system in separation and removal of TSS. Results of %removal of TSS as functions of influent TS and applied current density, and retention time are presented in Figures 4.8, 4.9 and 4.10.

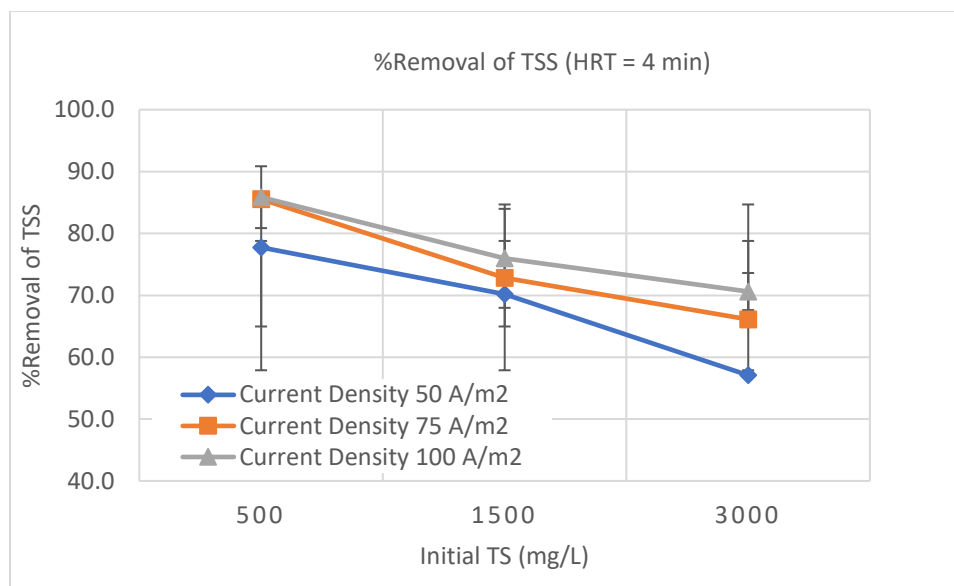


Figure 4.8: %Removal of TSS at different current densities and influent TS with HRT 4 minutes

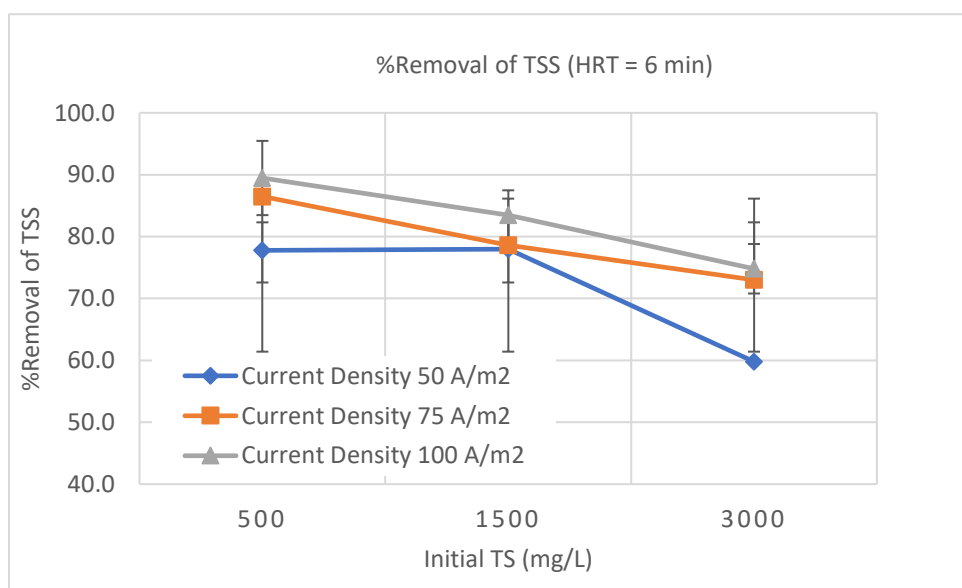


Figure 4.9: %Removal of TSS at different current densities and influent TS with HRT 6 minutes

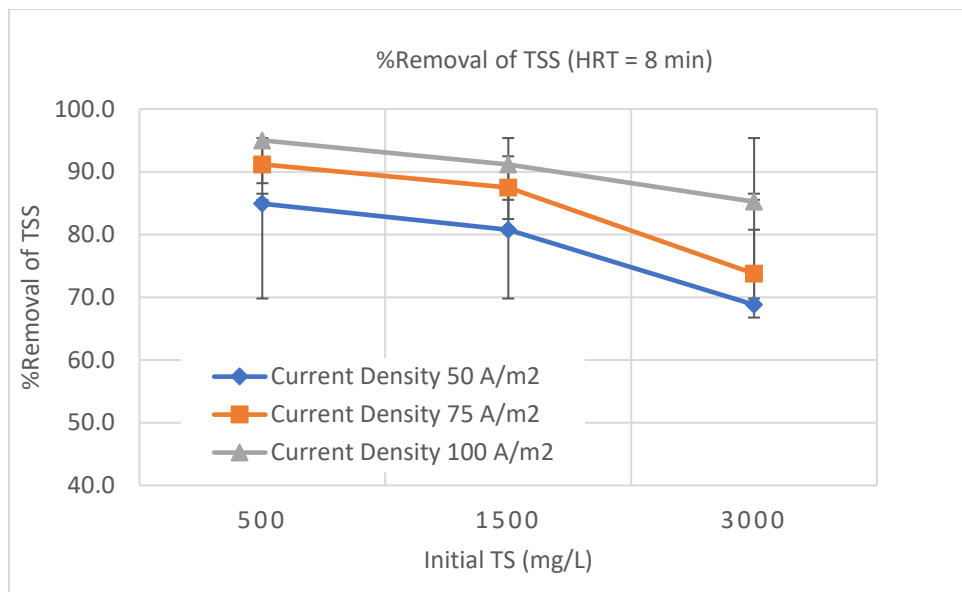


Figure 4.10: %Removal of TSS at different current densities and influent TS with HRT 8 minutes

The removal rates in the text are the average values. The results showed that the highest TSS removal rate, 95% was achieved with the influent TS of 500 mg/L, at HRT= 8 min and current density = 100 A/m². The removal efficiencies were 86, 76 and 71 percent for influent TS of 500, 1500 and 3000 mg/L, respectively, at HRT = 4 min and current density =100 A/m². At HRT= 8 min and current density= 100 A/m², the process performance increased and TSS removal efficiencies were 95, 91 and 85 percent for influent TS of 500, 1500 and 3000 mg/L, respectively. In general, the removal rates reduced with the increase of the influent TS. Table 4.6 shows the values of the suspended solids in the influent (TSS_{inf}) and effluent (TSS_{eff}) under different TS concentration, current densities and retention times. The replicated experimental results are presented in Table B.1, Appendix B.

Table 4.6: TSS_{inf} and TSS_{eff} for different TS, current densities and retention times in electroflotation reactor

Run No.	Influent TS (mg/L)	Applied Current Density(A/m ²)	Hydraulic Retention Time (min)	TSS _{inf} (mg/L)	TSS _{eff} (mg/L)
1	500	50	4	175±3	39±2
2	500	75	4	175±3	25±2
3	500	100	4	175±3	25±1
4	500	50	6	175±3	39±2
5	500	75	6	175±3	24±1
6	500	100	6	175±3	18±1
7	500	50	8	175±3	26±1
8	500	75	8	175±3	15±1
9	500	100	8	175±3	9±1
10	1500	50	4	531±1	158±3
11	1500	75	4	531±1	144±2
12	1500	100	4	531±1	128±1
13	1500	50	6	531±1	117±2
14	1500	75	6	531±1	114±1
15	1500	100	6	531±1	88±1
16	1500	50	8	531±1	102±2
17	1500	75	8	531±1	67±2
18	1500	100	8	531±1	47±1
19	3000	50	4	1108±4	476±3
20	3000	75	4	1108±4	375±3
21	3000	100	4	1108±4	326±4
22	3000	50	6	1108±4	445±4
23	3000	75	6	1108±4	299±4
24	3000	100	6	1108±4	279±1
25	3000	50	8	1108±4	346±2
26	3000	75	8	1108±4	291±5
27	3000	100	8	1108±4	164±4

The concentrations of suspended solids in the influent (TSS_{inf}) were 175, 531 and 1108 mg/L, whereas the lowest value of suspended solids in the effluent (TSS_{eff}) was 9 mg/L, achieved under the condition of influent TS = 500 mg/L, HRT = 8 min and applied current density: 100 A/m².

Based on the results of this study, it was concluded that the removal rate and efficiency of electroflotation process was inversely related to the influent solid concentration. This was in agreement with the batch experiments' results reported in Chapter 3.

Similar trends have been reported by other authors as well. Khelifa et al. (2005) studied the effect of initial copper concentration in removal efficiency of electroflotation of metal finishing effluents. They reported that the increase of initial concentration resulted in a decline in removal efficiency. For example, 99% removal rate of the 50 mg/L copper concentration was achieved, versus 71% for 500 mg/L initial concentration under the same 1-hour HRT (Khelifa et al., 2005). Comparable results were observed in treatment of synthetic textile wastewater by Merzouk et al. (2010). They reported that using aluminium as anode, removal efficiency, as judged by turbidity, declined at higher initial concentrations of silica gel particles. (Merzouk et al., 2010). Aoudj et al. (2015) also reported that in treatment of synthetic semiconductor industry wastewater, removal of Cr(V) and fluoride improved by decreasing the initial concentrations (Aoudj et al., 2015).

Performance of a continuous electrocoagulation/electrooxidation–electroflotation system for removal of ammonia and phosphate was investigated by Mahvi et al. (2011). It was revealed that the removal rate of phosphate and ammonia were higher at lower initial concentrations (Mahvi et al., 2011). Also, in defluoridation of drinking water by electrocoagulation/electroflotation process, Bennajah et al. (2010) observed that higher initial concentrations of fluoride, required more retention time in order to reach the acceptable effluent concentration (Bennajah et al., 2010).

The optimum operating conditions of the electroflotation system for the different influent TSS values can be determined from the Table 4.6 data. The TSS concentrations in the text are the average values. A TSS_{eff} concentration ≤ 100 mg/L was selected as the criterion for the recirculation water in the auto paint booths (Xu et al., 2009). Therefore, for the influent TS 500 mg/L, the optimum condition of the applied current density 50 A/m² and retention time 4 min, resulted in the TSS_{eff} 39 mg/L (less than 100 mg/L). When the influent TS was 1500 mg/L, at the current density 100 A/m² and retention time 6 min, the TSS_{eff} was 88 mg/L. Also, at the current density 75 A/m² and retention time 8

min, the TSS_{eff} was 67 mg/L, below the criterion level as well. For the highest tested influent TS, 3000 mg/L, the TSS_{eff} concentration ≤ 100 mg/L was not achieved under the current densities and retention times experimented in this study.

4.4.2 Effect of Applied Current Density

The applied current density, defined as the ratio of applied DC current to the active surface area of electrodes, is one of the key design parameters in an electroflotation process. In this study, the applied current densities were 50, 75 and 100 A/m². The removal efficiencies of electroflotation treatment of TSS as affected by the current density are presented in Figures 4.11, 4.12 and 4.13.

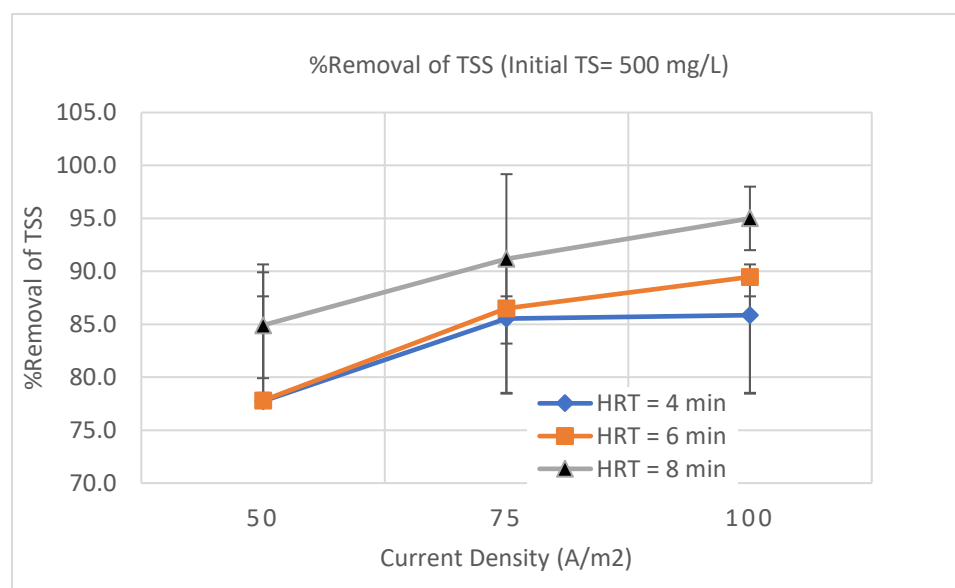


Figure 4.11: %Removal of TSS at different current densities and HRT with influent TS of 500 mg/L

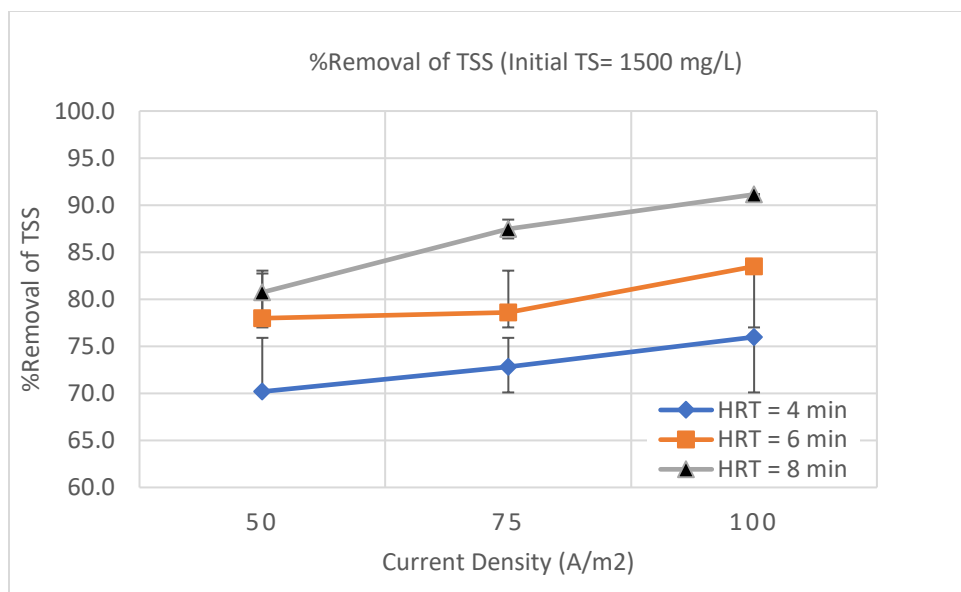


Figure 4.12: %Removal of TSS at different current densities and HRT with influent TS of 1500 mg/L

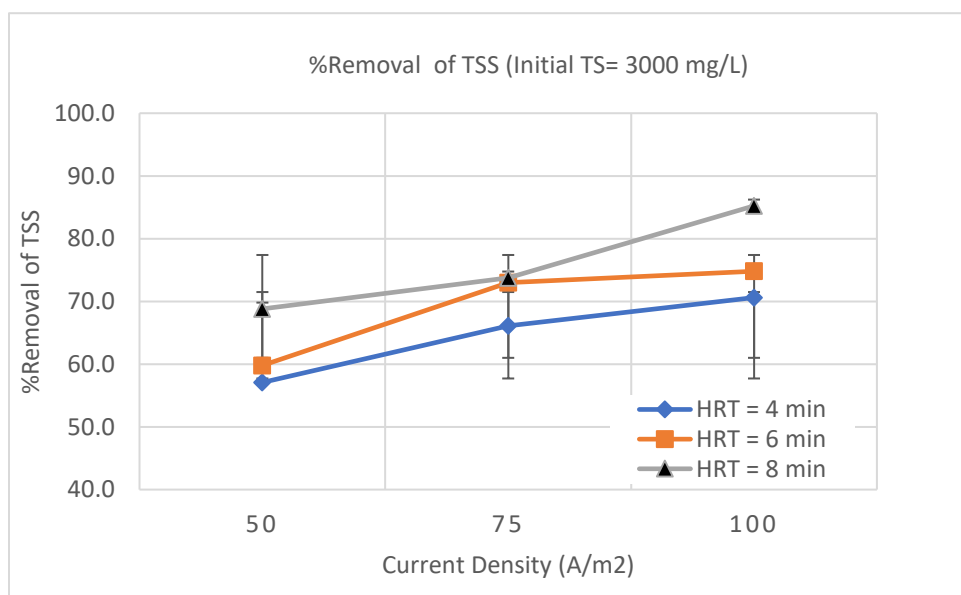


Figure 4.13: %Removal of TSS at different current densities and HRT with influent TS of 3000 mg/L

With influent TS=500 mg/L, the removal rates of TSS in HRT=4 min were 78, 88 and 86 percent under current densities of 50, 75 and 100 A/m², respectively. Similarly, at HRT=8 min, the removal efficiencies increased with the current density, i.e., the %removal of TSS were 85, 92 and 95 percent under current densities of 50, 75 and 100 A/m², respectively.

Similar trends were observed in experiments with other influent TS concentrations. For example, with the influent TS = 1500 mg/L, %removal of TSS in HRT = 8 min were 81, 87 and 91 percent under current densities of 50, 75 and 100 A/m², respectively. The removal efficiencies under current densities of 50, 75 and 100 A/m², with influent TS = 3000 mg/L and HRT = 8 min, were 69, 74 and 85 percent, respectively. A summary of experimental results is presented in Table 4.7.

Table 4.7: Removal efficiency of electroflotation process in treatment of total suspended solids under different current densities

Influent TS (mg/L)	Hydraulic Retention Time (min)	Applied Current Density, J (A/m ²)	Solids to Current Density Ratio TS/J (mg.m ² /L.A)	% Removal of TSS
500	4	50	10	78±5
500	4	75	7	86±8
500	4	100	5	86±3
500	6	50	10	78±6
500	6	75	7	86±4
500	6	100	5	90±4
500	8	50	10	85±3
500	8	75	7	92±5
500	8	100	5	95±7
1500	4	50	30	70±2
1500	4	75	20	73±1
1500	4	100	15	76±0
1500	6	50	30	78±1
1500	6	75	20	79±1
1500	6	100	15	83±1
1500	8	50	30	81±2
1500	8	75	20	87±3
1500	8	100	15	91±1
3000	4	50	60	57±1
3000	4	75	40	66±1
3000	4	100	30	71±1
3000	6	50	60	60±1
3000	6	75	40	73±1
3000	6	100	30	75±0
3000	8	50	60	69±1
3000	8	75	40	74±1
3000	8	100	30	85±2

The experimental results showed that, in general, the process performance, as indicated in the %removal of TSS, improved with the increase of applied current density. This has been reported in other studies. Hakizimana et al. (2017) studied pre-treatment of seawater (prior to desalination) using electrocoagulation/electroflotation process with aluminium

electrodes and under applied current densities of 2 to 20 mA/cm². In removal of dissolved organic carbon (DOC) efficiencies of 29.0% and 63.1% was achieved at current densities of 2 mA/cm² and 20 mA/cm², respectively, at the lowest flow rate of 0.25 L/min, while at the highest flow rate of 1.2 L/min, the treatment efficiency improved from 13.4% to 33.9% at current densities of 2 mA/cm² and 20 mA/cm², respectively (Hakizimana et al., 2017).

Alam and Shang (2017) reported the effects of current density (50 to 300 A/m²) in removal of bitumen from mature oil sands tailings in a batch electroflotation system. It was found that the removal percent of bitumen increased with the increase of applied current density up to an optimum value of 150 A/m² (Alam and Shang, 2017). Similar effects were observed in removal of COD from contaminated rinse water in aircraft industry (Meas et al., 2010) and treatment of wastewater from washing soil contaminated by heavy metals (da Mota et al., 2015).

Efficiency improvements and increased removal rates of electroflotation systems with increase of applied current densities can be explained by Faraday's law. According to Faraday's law of electrolysis, Eq. 4.6, there is a direct relationship between current and generation of mass at electrodes. This relationship is confirmed by Jiménez et al. (2010). In an electroflotation study, they investigated generation of hydrogen bubbles and it was concluded that higher current densities, resulted in higher hydrogen production (Jiménez et al., 2010). In the electroflotation process, while the active surface area of electrodes is constant, applied electrical current and applied current density are interchangeable, i.e., increase of electrical current is equivalent to increase of applied current density. And according to Faraday's law of electrolysis, increase of electrical current results in the increase of gas bubbles generation at electrodes. The higher number of gas bubbles enhances the collision and attachment of bubbles and suspended particles of pollutant (paint particles in this study) and consequently, intensifies the separation and removal of suspended solids from the wastewater.

Another parameter that can be considered in evaluation of performance of electroflotation system is "Solids-to-Current Density Ratio", defined as the ratio of initial TS to the

applied current density, TS/J . The values of this ratio are presented in Table 4.7 and range between 5 and 60 $\text{mg.m}^2/\text{L.A}$. Overall, it was noticed that with the increase of this ratio, the treatment efficiency of electroflotation process decreased. For instance, under a Solids-to-Current Density Ratio of 5 $\text{mg.m}^2/\text{L.A}$, the removal efficiencies were 86, 90 and 95 percent, under Solids-to-Current Density Ratio of 20 $\text{mg.m}^2/\text{L.A}$, the removal efficiencies were 73, 79 and 87 percent, and under the highest Solids-to-Current Density Ratio, i.e., 60 $\text{mg.m}^2/\text{L.A}$, the removal efficiencies were 57, 60 and 69 percent.

4.4.3 Effect of Hydraulic Retention Time (HRT)

Treatment of auto paint wastewater by continuous-flow electroflotation was studied under the hydraulic retention times of 4, 6 and 8 minutes. The hydraulic retention time is a significant design factor in treatment systems, which directly affects the dimensions of facility and power consumption. It is defined as the time between the flow entering and exiting a reactor for a conservative impulse, with the theoretical value of the volume of reactor over the flowrate, (Vesilind et al., 2010).

$$\bar{t} = \frac{V}{Q} \quad (4.7)$$

where,

\bar{t} : hydraulic retention time, min

V: volume of reactor, L

Q: flowrate entering reactor, L/min

In this study, the intended HRTs were achieved by adjusting the flowrate in the electroflotation reactor. Results of these experiments are presented in Figures 4.14, 4.15 and 4.16. Each graph depicts the %removal of TSS against the retention time for different influent TS concentrations and under a specific current density.

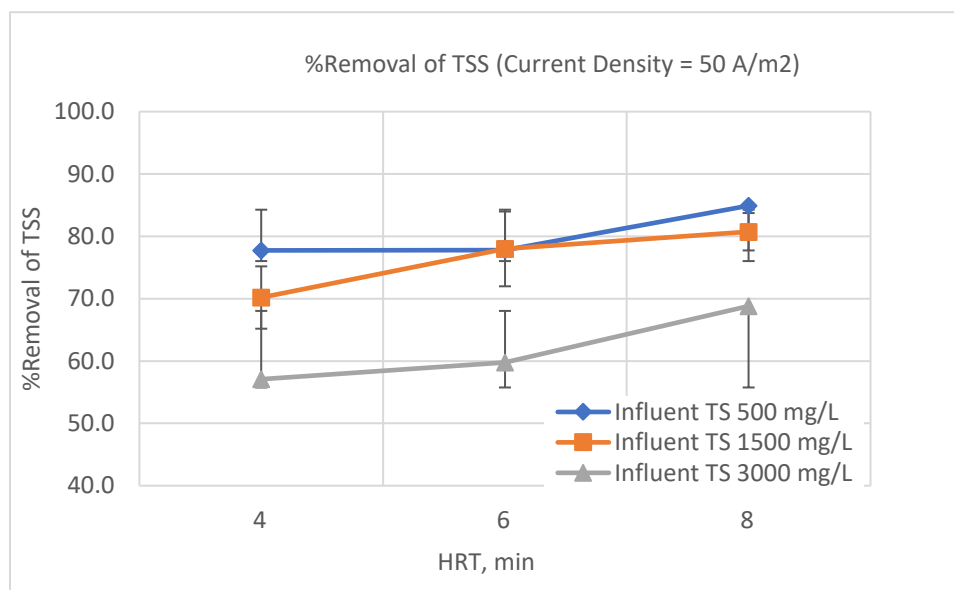


Figure 4.14: %Removal of TSS at different Hydraulic Retention Times and influent TS with applied current density of 50 A/m²

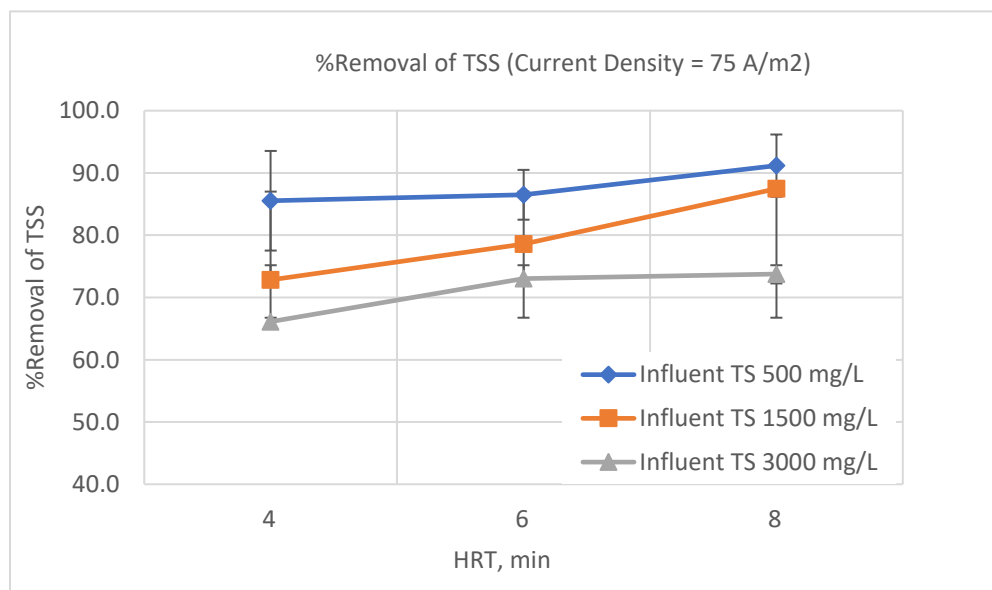


Figure 4.15: %Removal of TSS at different Hydraulic Retention Times and influent TS with applied current density of 75 A/m²

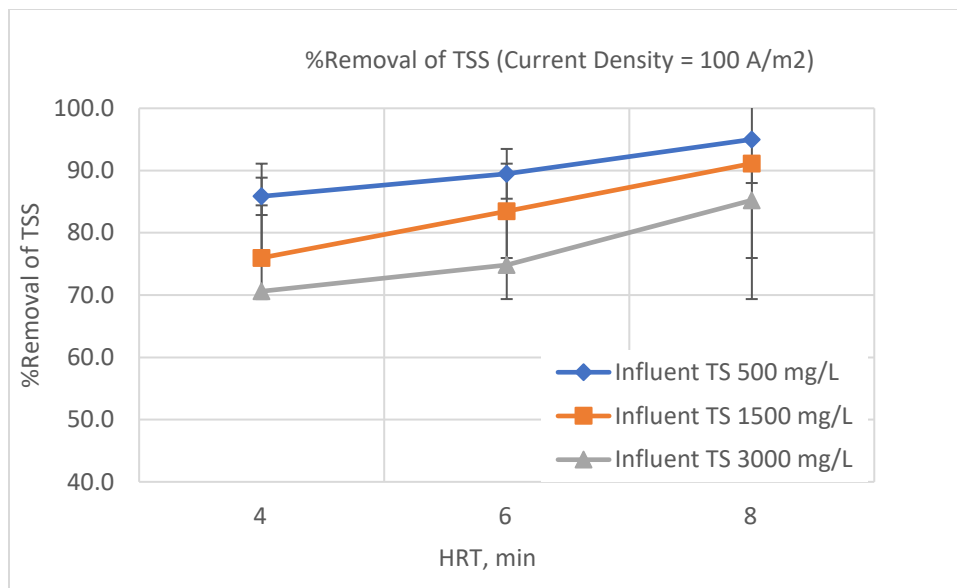


Figure 4.16: %Removal of TSS at different Hydraulic Retention Times and influent TS with applied current density of 100 A/m²

The treatment efficiencies and TSS removals were observed through the experiments. For instance, for influent TS = 500 mg/L and applied current density = 75 A/m², the %removal of TSS were 86, 86 and 92 percent for HRT 4, 6 and 8 min, respectively. These values corresponded to the effluent TSS concentrations of 25, 24 and 15 mg/L, respectively. Under higher influent TS concentration of 3000 mg/L and with the applied current density of 100 A/m², the removal efficiencies of 71, 75 and 85 percent were achieved for HRT of 4, 6 and 8 min, respectively. On the other hand, with the influent TS 500 mg/L and current density 100 A/m², the TSS removal of 86 percent was obtained in 4 min retention time. The corresponding TSS_{inf} and TSS_{eff} concentrations were 175 and 25 mg/L, respectively. For the same values of influent TS and current density, the %removal was 90% (TSS_{eff}: 18 mg/L) at HRT 6 min and 95% (TSS_{eff}: 9 mg/L) at HRT 8 min.

It was noted that the treatment efficiencies increased with the increase of hydraulic retention time in electroflotation process. This conclusion can be explained as follows: in electroflotation, suspended particles collide with gas bubbles, attachment occurs, and they slowly rise to the surface to be skimmed off. Each phase of this process is time-dependent, i.e., an adequate time allows the process to reach completion. Therefore, it is

important to provide adequate retention time for the collision, attachment and ascent of bubble-particle aggregates in separation process.

It is reported in the literature (Vu et al., 2014) that a combined electrocoagulation-electroflotation process was used to remove powdered activated carbon from urban wastewater effluent. Different retention times were applied, and it was found that increasing the retention time leads to the improvement of removal efficiency (Vu et al., 2014). Baierle et al. (2015) studied and optimized the removal of biomass of microalgae using electroflotation and aluminum and iron spiral electrodes, under retention times of 10, 15 and 20 min. They concluded that the increase in the flotation time had a positive effect on the yield of microalgal biomass (Baierle et al., 2015).

Also, the electroflotation method was used for thickening activated sludge under different operating times (5-20 min), by Rahmani et al. (2013). Sludge volume reduction (SVR) and sludge solid concentration (SSC) were improved with the increase of operating time, and the 20 min optimal time was reported for the system (Rahmani et al., 2013).

Comparable outcomes were obtained in another study on removal of valuable compounds from liquid technogenic waste (Kolesnikov et al., 2017), extraction of chromium(III) dispersed phase from aqueous solution (Perfil'eva et al., 2016) and decontamination of groundwater (Poon, 1997).

4.4.4 Automotive Paint Turbidity Removal by Electroflotation

Turbidity is another parameter used to quantify the residual suspended matters in wastewater and is an indicator of light-transmitting properties of a solution (Metcalf and Eddy, 2003). In this study, the turbidity values in influent and effluent of the electroflotation reactor were measured, as reported in Table 4.8. The replicated experimental results are presented in Table B.4, Appendix B.

Table 4.8: Values of Turbidity (NTU) the influent and effluent of the electroflotation reactor under different experimental conditions

Influent TS (mg/L)	Hydraulic Retention Time (min)	Applied Current Density(A/m ²)	Turbidity _{inf} (NTU)	Turbidity _{eff} (NTU)
500	4	50	199±2	93±2
500	4	75	199±2	48±5
500	4	100	199±2	47±3
500	6	50	199±2	93±2
500	6	75	199±2	44±4
500	6	100	199±2	31±2
500	8	50	199±2	51±5
500	8	75	199±2	24±2
500	8	100	199±2	11±1
1500	4	50	754±4	426±4
1500	4	75	754±4	367±7
1500	4	100	754±4	302±2
1500	6	50	754±4	263±4
1500	6	75	754±4	252±6
1500	6	100	754±4	170±1
1500	8	50	754±4	214±1
1500	8	75	754±4	114±4
1500	8	100	754±4	71±2
3000	4	50	1850±7	1517±6
3000	4	75	1850±7	1025±6
3000	4	100	1850±7	814±4
3000	6	50	1850±7	1360±5
3000	6	75	1850±7	711±6
3000	6	100	1850±7	638±1
3000	8	50	1850±7	896±4
3000	8	75	1850±7	680±10
3000	8	100	1850±7	287±4

The turbidity values in the text are the average values. As presented in Table 4.8, while the values of turbidity ranged between 199 and 1850 NTU in the influent of the reactor, the effluent turbidity values were significantly decreased in the effluent, demonstrating that electroflotation was effective in reducing turbidity of auto paint wastewater. For

example, with the influent TS of 500 mg/L, HRT 8 min and current density 100 A/m², the turbidity reduced to 11 NTU from its initial value of 199 NTU, corresponding to the removal efficiency of 94%. In a higher influent TS concentration of 3000 mg/L with turbidity 1850 NTU, after 8 min treatment under a current density of 100 A/m², the removal efficiency was 84% with the final turbidity 287 NTU.

In the literature, successful implementations of the electroflotation process for turbidity removal have been reported as well, e.g., 100% turbidity removal from dairy wastewater effluent (Bassala et al., 2017), effective performance of turbidity removal from slaughterhouse and packing plant effluent (Orssatto et al., 2017), and 98.5% turbidity reduction in treatment of train industry oily wastewater (Ozyonar et al., 2016).

4.4.5 Electrochemistry and pH Change

There are several factors affecting the pH of wastewater and how it changes during the electroflotation process, including the electrode material, electrolyte type and composition, applied voltage and current and treatment time (Ciblak et al., 2012). The values of pH in the influent and effluent of the reactor under different experimental conditions are presented in Table 4.9. The replicated experimental results are presented in Table B.3, Appendix B.

Table 4.9: Values of pH in the influent and effluent of the electroflotation reactor under different experimental conditions

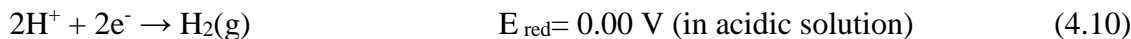
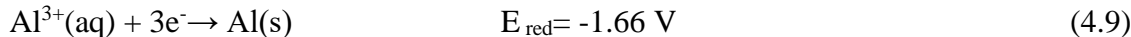
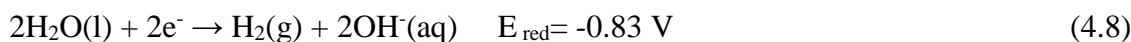
Influent TS (mg/L)	Hydraulic Retention Time (min)	Applied Current Density(A/m ²)	pH _{inf}	pH _{eff}
500	4	50	6.89±0.02	6.91±0.02
500	4	75	6.89±0.02	6.99±0.01
500	4	100	6.89±0.02	7.14±0.03
500	6	50	6.89±0.02	6.93±0.02
500	6	75	6.89±0.02	7.08±0.01
500	6	100	6.89±0.02	7.34±0.03
500	8	50	6.89±0.02	6.96±0.02
500	8	75	6.89±0.02	7.22±0.01
500	8	100	6.89±0.02	7.75±0.02
1500	4	50	6.66±0.02	6.67±0.02
1500	4	75	6.66±0.02	6.74±0.01
1500	4	100	6.66±0.02	6.88±0.02
1500	6	50	6.66±0.02	6.70±0.02
1500	6	75	6.66±0.02	6.81±0.04
1500	6	100	6.66±0.02	7.06±0.04
1500	8	50	6.66±0.02	6.74±0.03
1500	8	75	6.66±0.02	6.94±0.01
1500	8	100	6.66±0.02	7.41±0.03
3000	4	50	6.61±0.02	6.62±0.01
3000	4	75	6.61±0.02	6.68±0.02
3000	4	100	6.61±0.02	6.81±0.02
3000	6	50	6.61±0.02	6.63±0.02
3000	6	75	6.61±0.02	6.75±0.02
3000	6	100	6.61±0.02	7.01±0.01
3000	8	50	6.61±0.02	6.65±0.02
3000	8	75	6.61±0.02	6.91±0.05
3000	8	100	6.61±0.02	7.38±0.03

It can be noticed that the pH increased during the electroflotation process, which is in agreement with other studies. In electrochemical treatment of nitrite solution using stainless steel electrodes, increase of pH was observed, specially under higher electrical currents (Abuzaid et al., 1999). In treatment of laundry wastewater using

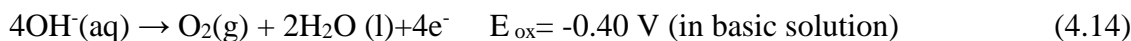
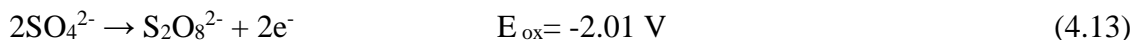
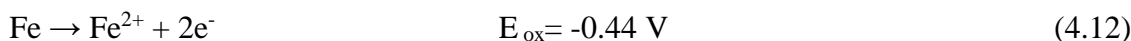
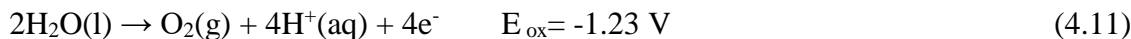
electrocoagulation-electroflotation process, at HRT 10 min and electrical current 1.0 A, the pH of the solution increased compared to the influent pH (Ge et al., 2014). Similar results were observed in other studies as well (da Mota et al., 2015; Poon, 1997; Baierle et al., 2015).

The pH increase in this study can be explained by half-reactions occurring at the cathode and anode:

Possible reduction reactions at the cathode:



Possible oxidation reactions at the anode:



The automotive paint solution is slightly acidic in the beginning because of presence of the detackifier, containing aluminium sulphate. The available H^+ ions are reduced shortly after the beginning of the electrolysis at the cathode, Eq. 4.10, at high current densities such as 55 A/m^2 and voltage 25 V. Comparing the reduction potentials, Eq. 4.8 is the reduction half-reaction that occurs afterwards at the cathode, producing OH^- ions and increasing pH of the solution.

At the anode, oxygen bubbles and H^+ ions are generated, as well as iron ions according to Eq. 4.11 and 4.12. The aluminium ions (Al^{3+} , from aluminium sulphate) undergo hydrolysis, form aluminium hydroxide flocs, then being removed from the solution. Overall, hydroxides (OH^-) overcome the H^+ ions, leading to the increase of pH in the effluent.

4.4.6 Power Consumption

In electroflotation, the energy requirements and power consumption are the major factors in terms of operating costs. Hence engineers and decision-makers must consider these factors carefully, when evaluating any proposed treatment method.

In this study, the electroflotation reactor received the electrical energy from a DC power supply. The energy consumption is determined by the applied current and voltage per unit volume of water treated. In water and wastewater treatment, another term is defined as the Specific Energy Consumption; which takes the treatment time (HRT) and volume of treatment reactor into consideration. This term is defined in Eq. 4.5. Using this equation, the specific energy consumption of auto paint wastewater treatment using electroflotation process was calculated. The results are presented in Table 4.10.

Table 4.10: Specific energy consumption, E, of treatment of auto paint wastewater using electroflotation process under different experimental conditions

Influent TS (mg/L)	Hydraulic Retention Time (min)	Applied Current Density(A/m ²)	Specific Energy Consumption (W.h/m ³)
500	4	50	26
500	4	75	60
500	4	100	101
500	6	50	40
500	6	75	86
500	6	100	149
500	8	50	52
500	8	75	119
500	8	100	197
1500	4	50	22
1500	4	75	49
1500	4	100	89
1500	6	50	31
1500	6	75	70
1500	6	100	137
1500	8	50	40
1500	8	75	96
1500	8	100	178
3000	4	50	17
3000	4	75	39
3000	4	100	72
3000	6	50	25
3000	6	75	57
3000	6	100	108
3000	8	50	33
3000	8	75	75
3000	8	100	145

As it can be noticed, the specific energy consumption varied drastically with experimental conditions, ranging from 17 to 197 W.h.m⁻³. For example, with HRT 4 min and applied current density 50 A/m², the specific energy consumption was 26, 22 and 17 W.h.m⁻³ for influent TS concentrations of 500, 1500 and 3000 mg/L, respectively. The

same trend was observed when retention time was, for instance, 8 min, and applied current density was 75 A/m^2 . The specific energy consumptions corresponding to influent TS concentration of 500, 1500 and 3000 mg/L were 119, 96 and 75 W.h.m^{-3} , respectively, indicating that for the constant values of HRT and current density, energy consumption decreased with the increase of TS concentration. The specific energy consumptions at different influent TS and under different applied current densities are presented in Figure 4.17, 4.18 and 4.19.

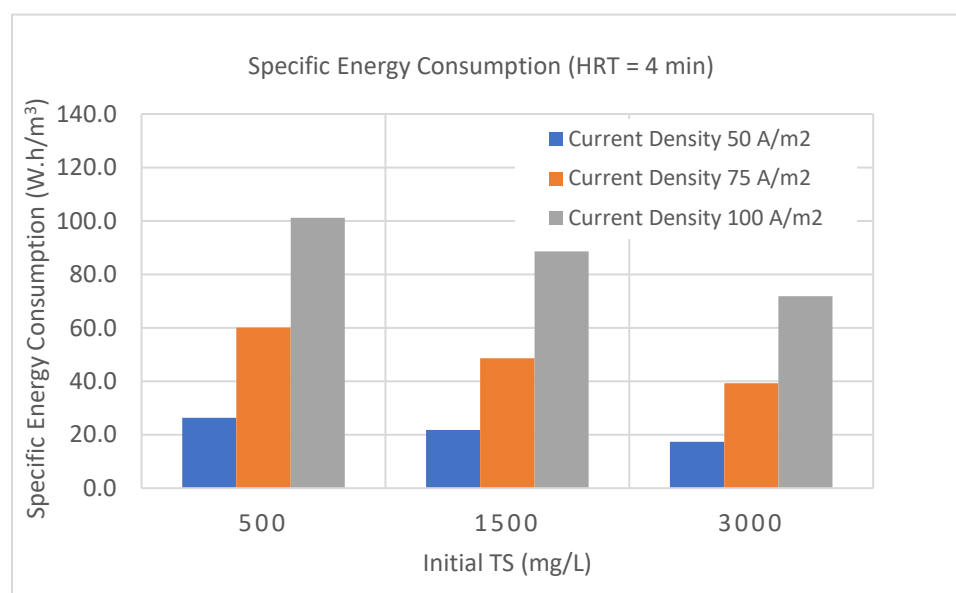


Figure 4.17: Specific Energy Consumption at different current densities and influent TS with HRT 4 minutes

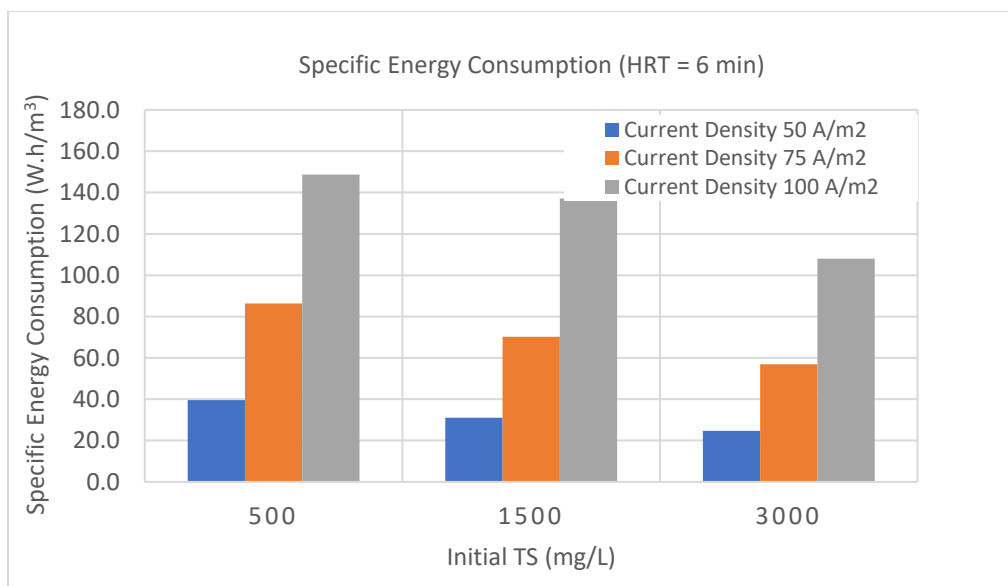


Figure 4.18: Specific Energy Consumption at different current densities and influent TS with HRT 6 minutes

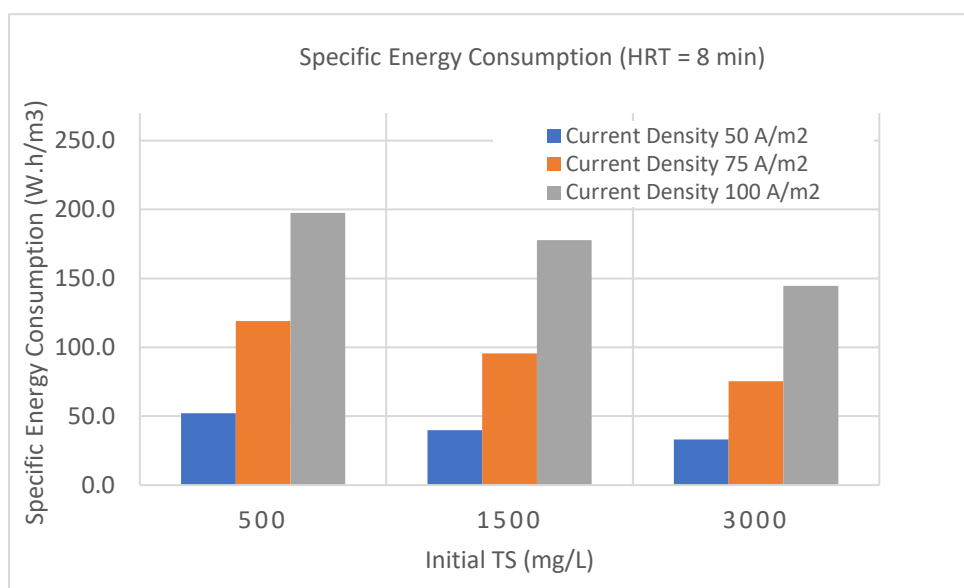


Figure 4.19: Specific Energy Consumption at different current densities and influent TS with HRT 8 minutes

Referring to Eq. 4.5, the specific energy consumption is the product of voltage, current and time over the volume of water under treatment. Therefore, while the volume of the

reactor was constant, for a constant set of HRT (time) and current density (current over active surface area of electrodes), a higher TS concentration (higher electrolyte strength) led to a lower applied voltage. In other words, all parameters kept constant, the specific power consumption decreased with the increase of solids concentration in the solution. This can be explained by the electrical conductivity of the solution. The Electrical conductivity (EC) characterizes quantitatively the ability of a material to conduct electric current and has a direct relationship with the ions concentration in electrolyte solutions (Bagotsky, 2006). Table 4.11 presents the values of electrical conductivity of auto paint wastewater treated with the electroflotation process, in the influent and effluent. The replicated experimental results are presented in Table B.2, Appendix B.

Table 4.11: Electric conductivity change in the electroflotation reactor, treating auto paint wastewater

Influent TS (mg/L)	Hydraulic Retention Time (min)	Applied Current Density(A/m ²)	Conductivity _{inf} (μS/cm)	Conductivity _{eff} (μS/cm)
500	4	50	313±3	344±2
500	4	75	313±3	345±2
500	4	100	313±3	346±6
500	6	50	313±3	344±4
500	6	75	313±3	345±3
500	6	100	313±3	348±8
500	8	50	313±3	344±2
500	8	75	313±3	347±1
500	8	100	313±3	350±4
1500	4	50	989±4	1088±5
1500	4	75	989±4	1089±1
1500	4	100	989±4	1092±2
1500	6	50	989±4	1088±9
1500	6	75	989±4	1091±5
1500	6	100	989±4	1096±6
1500	8	50	989±4	1089±9
1500	8	75	989±4	1094±8
1500	8	100	989±4	1102±10
3000	4	50	2126±10	2337±8
3000	4	75	2126±10	2340±12
3000	4	100	2126±10	2346±12
3000	6	50	2126±10	2339±2
3000	6	75	2126±10	2344±13
3000	6	100	2126±10	2353±3
3000	8	50	2126±10	2340±5
3000	8	75	2126±10	2352±4
3000	8	100	2126±10	2367±17

The electrical conductivity values in the text are the average values. The electrical conductivity of 313, 989 and 2126 μS/cm, corresponded to the influent TS 500, 1500 and 3000 mg/L, respectively. It was observed that the higher influent TS concentrations corresponded to the higher electrical conductivity values. It was because the conductivity

was directly related to the ionic strength in the wastewater and the sources of ions were auto paint solids and the detackifier (aluminium sulphate).

Similar results have been reported in the literature. In the analysis of the operating costs of electrocoagulation of textile dye wastewater by aluminum and iron electrodes, it was found that operating cost decreases with increasing the water conductivity (Bayramoglu et al., 2004). The positive effect of electrical conductivity on turbidity removal by electroflotation is reported by Belkacem, et al., (2008). Some researchers added table salt to the solution to improve the electrical conductivity and found the improvement of the system performance and reduction of energy consumption (Daneshvar et al., 2006; Kobya et al., 2006). From the analysis of the electrical conductivity of influent and effluent, a slight increase was observed after an electroflotation process. This was attributed to the release of cations (e.g., iron) from the anode into the solution (Zhou et al., 2016).

In order to acquire a better understanding of the values of specific energy consumption presented in Table 4.10, Table 4.12 shows the specific energy consumption of the electroflotation process reported in the literature.

Table 4.12: Specific energy consumption of electroflotation process treating various types of wastewater

Application	Specific Energy Consumption W.h /m ³	Test Scale	Reference
Oil/water wastewater	400-1600	Lab	Mansour and Chalbi, 2006
Restaurant wastewater	500	Lab	Chen et al., 2000
Emulsified Oil wastewater	480-4500	Lab	Nahui et al., 2008
Rolling-mill, glass fibre wastewater	100	Commercial Full-scale	EnviroChemie Company
Algae removal	1840	Lab	Tumsri and Chavalparit, 2011
Electroplating and printed circuit wastewater	200-500	Commercial Full-scale	Mendeleev University Science Park

It was noted from comparison of the Tables 4.10 and 4.12 that the energy consumption of the electroflotation system for treatment of automotive paint wastewater, as conducted in this study, was among the lowest and was comparable with the commercial systems, making the electroflotation an attractive choice for the automotive paint wastewater treatment.

4.5 Statistical Analysis and Empirical Correlation

4.5.1 Response Surface Methodology (RSM)

Response Surface Methodology and Multiple Linear Regression methods are used in this section to analyze the experimental data of the electroflotation of auto paint wastewater and the process variables. Response Surface Methodology (RSM) is a set of mathematical and statistical procedures suitable for creating, advancing and optimizing processes. In the industry, the RSM is mostly implemented where several variables potentially affect the system performance or the quality of products (Myers et al., 2009).

A custom response surface design was defined with the %removal of TSS as the response and the applied current density (J , A/m²), HRT (t , min) and influent TSS concentration (C , mg/L) as the predictors of the model. A full quadratic model with regression coefficients was designated to fit the experimental data using a statistical software Minitab 18. The Linear, quadratic, 2-way interaction and intercept can be specified by this model (Zhao et al., 2014), which is expressed as

$$Y = \beta_0 + \sum_{i=1}^k \beta_i X_i + \sum_{i=1}^k \beta_{ii} X_i^2 + \sum_{i=1}^k \sum_{j=1}^k \beta_{ij} X_i X_j + \varepsilon \quad (4.15)$$

where

Y : %removal TSS;

β_0 , β_i , β_{ii} and β_{ij} : regression coefficients for intercept, linear, quadratic and 2-way interaction terms, respectively;

X_i and X_j : independent variables; including the applied current density (J , A/m²), HRT (t , min) and influent TSS concentration (C , mg/L)

The established full quadratic model is presented in Eq. (4.16).

$$Y = 70.0 + 0.356 J - 1.92 t - 0.03205 C - 0.00207 J*J + 0.240 t*t + 0.000000 C*C + 0.0158 J*t + 0.000123 J*C + 0.000884 t*C \quad (4.16)$$

R-sq value 95.96%, R-sq(adj)= 93.83%

It should be mentioned that this equation is only valid for the data-range in this study, i.e., (HRT: 4-8 min, Current Density: 50-100 Am/m² and influent TSS: 175-1108 mg/L).

Also, using Analysis of Variance (ANOVA) method, the interaction between the process predictors and the responses was established. The coefficient of determination (R-sq) evaluates the quality of the fit and the statistical significance is assessed by the p-value with 95% confidence level. Results of ANOVA are presented in Table 4.13.

Table 4.13: Report of Analysis of Variance for RSM analysis with the response of %removal of TSS

Source	DF	Seq SS	Contribution	Adj SS	p-Value	Remark
Model	9	2274.69	95.96%	2274.69	0.000	Significant
Linear	3	2218.08	93.58%	2222.31	0.000	Significant
J: Current Density, A/m ²	1	517.82	21.85%	535.05	0.000	Significant
t: HRT, min	1	515.14	21.73%	522.96	0.000	Significant
C, Influent TSS, mg/L	1	1185.11	50.00%	1164.3	0.000	Significant
Square	3	15.59	0.66%	15.59	0.451	
J*J	1	10.06	0.42%	10.06	0.199	
t*t	1	5.52	0.23%	5.52	0.336	
C*C	1	0.01	0.00%	0.01	0.966	
2-Way Interaction	3	41.03	1.73%	41.03	0.101	
J*t	1	7.46	0.31%	7.46	0.265	
J*C	1	25.25	1.07%	25.25	0.049	
t*C	1	8.31	0.35%	8.31	0.241	
Error	17	95.68	4.04%	95.68		
Total	26	2370.38	100.00%			
p-value 0.000 means < 0.001						

Although the R-sq value was 95.96%, as shown in Table 4.13, the contribution of linear section was 93.58% with the p-value of 0.000 (less than 0.05) for linear terms of J , t and C . In contrast, the p-value for Square was 0.451 and for 2-way interaction was 0.101, indicating the insignificance of these terms. Therefore, a Multiple Linear Regression appeared to be a better model to describe the electroflotation response and predictors in this study. It should be mentioned that the significance of current density, HRT and influent TSS values as the predictors, and their effects on the removal efficiency of TSS, were demonstrated again, which was in agreement with the results of the statistical analysis of batch electroflotation experiments, presented in Chapter 3.

4.5.2 Multiple Linear Regression

Empirical models are extensively implemented in engineering and the regression analysis provides the tools for selecting and fitting a good model and examining its inadequacies (Berthouex and Brown, 2002).

An empirical model, based on multiple linear regression, Eq. (4.17), was developed. The %removal of TSS was the response, and the applied current density (J , A/m²), HRT (t , min) and influent TSS concentration (C , mg/L) were the predictors of the model. ANOVA was used to assess the statistical significance of the predictors, to find the coefficient of determination and to examine multicollinearity of the predictors.

$$Y = \beta_0 + \beta_1 X_1 + \beta_2 X_2 + \dots + \beta_i X_i + \varepsilon \quad (4.17)$$

where

Y : %removal TSS;

β_0 and β_i : regression coefficients;

X_i : independent variables; including applied current density (J , A/m²), HRT (t , min) and influent TSS concentration (C , mg/L).

Eq. (4.18) shows the empirical model, describing the relationship between the %removal of TSS, and the predictors: influent TSS, HRT and current density,

$$Y = 56.86 + 0.2145 J + 2.675 t - 0.01723 C \quad (4.18)$$

The values of R-sq and R-sq(adj) were 93.58% and 92.74%, respectively. It should be mentioned that this equation is only valid for the data-range in this study; i.e., (HRT: 4-8 min, Current Density: 50-100 Am/m² and influent TSS: 175-1108 mg/L).

Results of ANOVA are summarized in Table 4.14.

Table 4.14: Report of Analysis of Variance for linear regression analysis with the response of %removal of TSS

Source	DF	Seq SS	VIF	p-Value	Remark
Regression	3	2218.1		0.000	Significant
J: Current Density, A/m ²	1	517.8	1.00	0.000	Significant, No Multicollinearity
t: HRT, min	1	515.1	1.00	0.000	Significant, No Multicollinearity
C, Influent TSS, mg/L	1	1185.1	1.00	0.000	Significant, No Multicollinearity
Error	23	152.3			
Total	26	2370.4			
p-value 0.000 means < 0.001					

The p-values for current density, HRT and influent TSS were 0.000 (i.e., < 0.001), indicating the significance of these process variables and their effect on the efficiency of the electroflotation system. VIF, the variance inflation factor, shows how much the variance of a coefficient is inflated due to the correlations among the predictors in the model. The relationship between VIF_j and collinearity is through the following equation:

$$VIF_j = \frac{1}{1 - R_j^2} \quad (4.19)$$

where R_j^2 is the coefficient of determination from the regression of X_j on other independent variables. As a guideline, $VIF=1$ is considered as no multicollinearity in the regression analysis and VIF values more than 5, mean the predictors are highly correlated (Rawlings et al., 2001). From Table 4.14, it was observed that VIF values were all 1.00, meaning the multicollinearity did not exist between the predictors.

Figures 4.20 and 4.21 depict the contour plot and surface plot of removal efficiency of TSS, respectively.

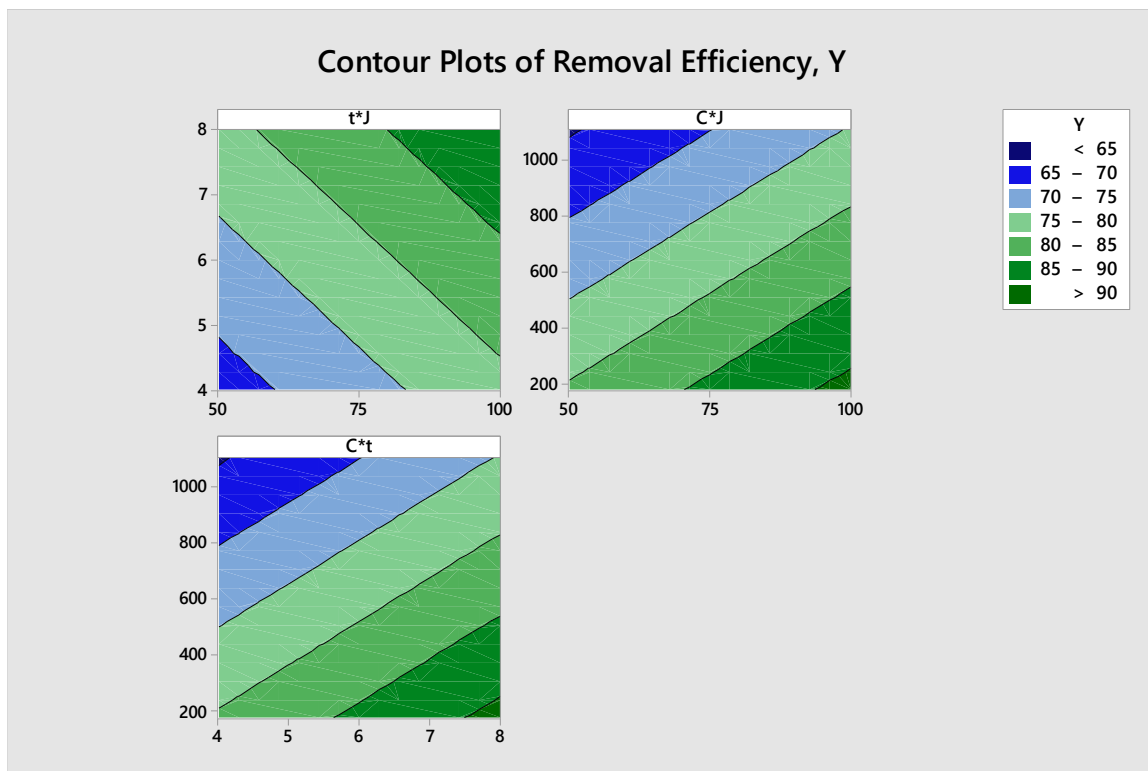


Figure 4.20: Contour plot of removal efficiency of TSS, Y (C: Influent TSS mg/L; J: Current Density, A/m² and t: HRT, min)

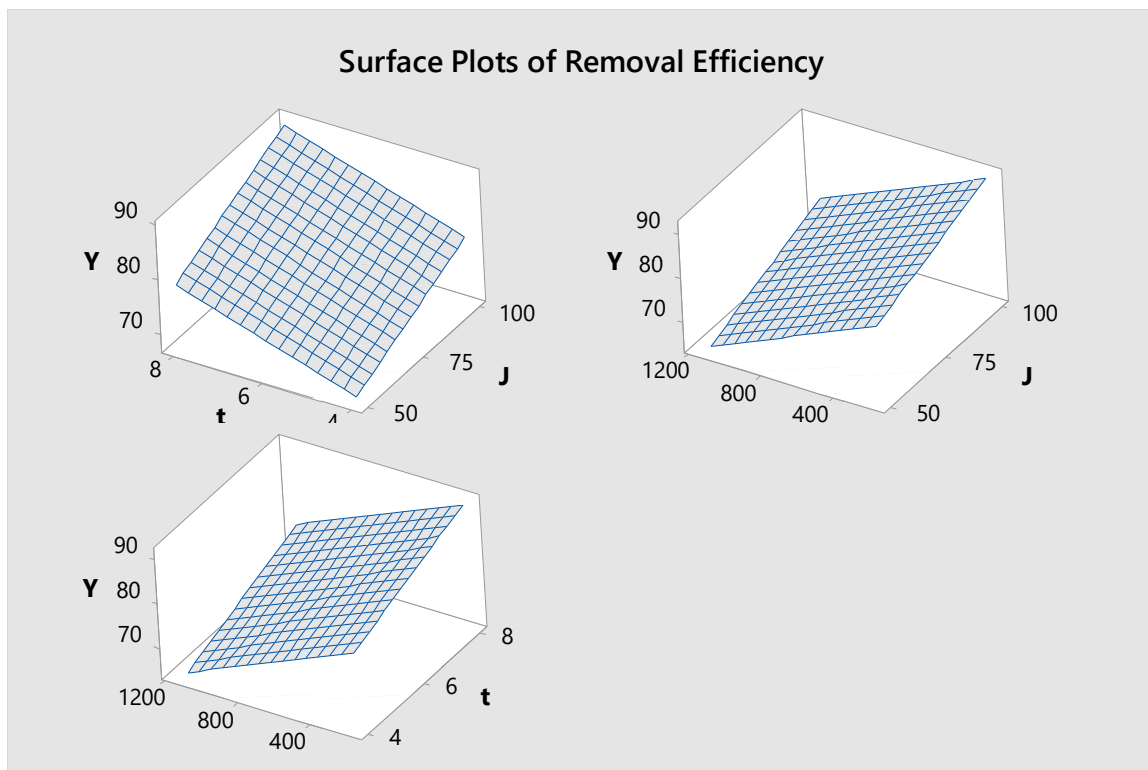


Figure 4.21: Surface plot of removal efficiency of TSS, Y (C: Influent TSS mg/L; J: Current Density, A/m² and t: HRT, min)

4.6 Conclusions

The continuous-flow treatment of auto paint wastewater was successfully conducted using the electroflotation process in a experimental lab program.

The performance of electroflotation system in treatment of auto paint wastewater, synthetically prepared in the lab, was studied by examining the influencing parameters including the TS, TSS, electrical conductivity, turbidity and pH in a pilot-scale reactor with the effective volume of 38.4 L and using Stainless Steel electrodes.

Effects of the influent concentration of TS, applied current density, and hydraulic retention time on the system performance were investigated under three influent total solids (TS) concentrations of 500, 1500 and 3000 mg/L. Also, retention times of 4, 6 and 8 minutes were applied to the system and the treatment efficiency was studied under current densities of 50, 75 and 100 A/m².

The auto paint wastewater was successfully treated in the electroflotation reactor with the maximum removal rate of 95% at the influent TS 500 mg/L, HRT 8 min, and applied current density 100 A/m². The optimum operating conditions for the different influent TS values were also determined.

Based on the findings of this study, with the increase of influent concentration of auto paint in the wastewater, the removal rate of electroflotation process decreased. For instance, at HRT 8 min and current density 100 A/m², the removal rates for influent TS of 500, 1500 and 3000 mg/L were 95, 91 and 85 percent, respectively.

The removal rate was directly related to the applied current density. The removal rates under current densities of 50, 75 and 100 A/m², with influent TS: 3000 mg/L and HRT: 8 min, were 69, 74 and 85 percent, respectively. Efficiency improvements and increased removal rates of electroflotation systems with increase of applied current densities were explained by Faraday's law of electrolysis.

The removal rate increased with increasing the hydraulic retention time. At a current density of 100 A/m² and influent TSS concentration of 175 mg/L, the %removal of TSS was 90% (TSS_{eff}: 18 mg/L) at HRT of 6 min, and 95% (TSS_{eff}: 9 mg/L) at HRT of 8 min.

The water pH increased slightly during the electroflotation process. The electrochemistry of this phenomenon was explained. The energy consumption of the electroflotation system for treatment of auto paint wastewater was found among the lowest compared with the commercial systems, making the electroflotation an attractive choice for the treatment of auto paint wastewater.

The statistical analysis was carried out on the experimental results of this study. A full quadratic model with regression coefficients was selected to fit the experimental data. Through the ANOVA, it was found that the contribution of linear section was 93.58% with the p-value of 0.000; whereas the p-value for the Square term was 0.451 and for the 2-way interaction term was 0.101, indicating that these terms were insignificant.

Thereafter, an empirical model was established, which could predict the TSS removal rate as affected by three variables, i.e., the HRT, influent TSS and applied current density. The model was based on the multiple linear regression and the values of R-sq and R-sq(Adj) were 93.58% and 92.74%, respectively.

Acknowledgements

This study was supported by the University of Western Ontario and the National Science and Engineering Research Council of Canada (NSERC). Also, Chemetall Canada, Ltd. is acknowledged for providing the detackifier.

References

- Abuzaid, N. S., Al-Hamouz, Z., Bukhari, A. A., & Essa, M. H. (1999). Electrochemical treatment of nitrite using stainless steel electrodes. *Water, Air, and Soil Pollution*, 109(1-4), 429-442.
- Alam, R., & Shang, J. Q. (2017). Removal of bitumen from mature oil sands tailings slurries by electro-flotation. *Journal of Water Process Engineering*, 15, 116-123.
- Aoudj, S., Khelifa, A., Drouiche, N., Belkada, R., & Miroud, D. (2015). Simultaneous removal of chromium (VI) and fluoride by electrocoagulation–electroflotation: application of a hybrid Fe-Al anode. *Chemical Engineering Journal*, 267, 153-162.
- Bagotsky, V. S. (2006). *Fundamentals of electrochemistry* (Vol. 44). John Wiley & Sons, New Jersey.
- Baierle, F., John, D. K., Souza, M. P., Bjerk, T. R., Moraes, M. S., Hoeltz, M., Rohlfes, A. L., Camargo, M. E., Corbellini, V. A. & Schneider, R. C. (2015). Biomass from microalgae separation by electroflotation with iron and aluminum spiral electrodes. *Chemical Engineering Journal*, 267, 274-281.
- Bassala, H. D., Dedzo, G. K., Bememba, C. B. N., Seumo, P. M. T., Dazie, J. D., Nanseu-Njiki, C. P., & Ngameni, E. (2017). Investigation of the efficiency of a designed electrocoagulation reactor: Application for dairy effluent treatment. *Process Safety and Environmental Protection*, 111, 122-127.
- Bayramoglu, M., Kobya, M., Can, O. T., & Sozbir, M. (2004). Operating cost analysis of electrocoagulation of textile dye wastewater. *Separation and Purification Technology*, 37(2), 117-125.
- Belkacem, M., Khodir, M., & Abdelkrim, S. (2008). Treatment characteristics of textile wastewater and removal of heavy metals using the electroflotation technique. *Desalination*, 228(1-3), 245-254.

- Bennajah, M., Maalmi, M., Darmane, Y., & Touhami, M. E. (2010). Defluoridation of drinking water by electrocoagulation/electroflotation: kinetic study. *Journal of Urban and Environmental Engineering*, 4(1), 37-45.
- Berthouex, P. M., & Brown, L. C. (2002). *Statistics for environmental engineers*.
- Chen, G., Chen, X., & Yue, P. L. (2000). Electrocoagulation and electroflotation of restaurant wastewater. *Journal of environmental engineering*, 126(9), 858-863.
- Ciblak, A., Mao, X., Padilla, I., Vesper, D., Alshawabkeh, I., & Alshawabkeh, A. N. (2012). Electrode effects on temporal changes in electrolyte pH and redox potential for water treatment. *Journal of Environmental Science and Health, Part A*, 47(5), 718-726.
- da Mota, I. D. O., de Castro, J. A., de Góes Casqueira, R., & de Oliveira Junior, A. G. (2015). Study of electroflotation method for treatment of wastewater from washing soil contaminated by heavy metals. *Journal of Materials Research and Technology*, 4(2), 109-113.
- Daneshvar, N., Oladegaragoze, A., & Djafarzadeh, N. (2006). Decolorization of basic dye solutions by electrocoagulation: an investigation of the effect of operational parameters. *Journal of hazardous materials*, 129(1-3), 116-122.
- Dupli Color. (2018). *SDS BUN0100, Universal Gloss Black Perfect Match Dupli-Color Products Company*. Retrieved from <https://www.paintdocs.com/docs/webPDF.jsp?SITEID=DUPLI&prodno=BUN0100&doctype=SDS&lang=2> (Accessed 11 January 2018)
- EnviroChemie. (2014). *Product information: Compact electroflotation - an energy-saving and resource-saving alternative for water treatment*. Retrieved from https://envirochemie.com/cms/upload/news/20140616gb/Compact_electroflotation.pdf (Accessed 11 January 2018).
- Hassani, G., Alinejad, A., Sadat, A., Esmaili, A., Ziaei, M., Bazrafshan, A. A., & Sadat, T. (2016). Optimization of landfill leachate treatment process by electrocoagulation,

electroflotation and sedimentation sequential method. *International Journal of Electrochemical Science*, *11*, 6705-6718.

Hakizimana, J. N., Najid, N., Gourich, B., Vial, C., Stiriba, Y., & Naja, J. (2017). Hybrid electrocoagulation/electroflotation/electrodisinfection process as a pretreatment for seawater desalination. *Chemical Engineering Science*, *170*, 530-541.

HANNA instruments (2014). *HI 98703 Portable Turbidimeter* Retrieved from https://hannainst.com/downloads/dl/file/id/1293/man98703_06_14_new.pdf (Accessed 11 April 2018).

Holt, P. K., Barton, G. W., Wark, M., & Mitchell, C. A. (2002). A quantitative comparison between chemical dosing and electrocoagulation. *Colloids and Surfaces A: Physicochemical and Engineering Aspects*, *211*(2), 233-248.

Jiménez, C., Talavera, B., Saez, C., Cañizares, P., & Rodrigo, M. A. (2010). Study of the production of hydrogen bubbles at low current densities for electroflotation processes. *Journal of chemical technology and biotechnology*, *85*(10), 1368-1373.

Khelifa, A., Moulay, S., & Naceur, A. W. (2005). Treatment of metal finishing effluents by the electroflotation technique. *Desalination*, *181*(1-3), 27-33.

Kobyas, M., Demirbas, E., Can, O. T., & Bayramoglu, M. (2006). Treatment of levafix orange textile dye solution by electrocoagulation. *Journal of hazardous materials*, *132*(2-3), 183-188.

Kolesnikov, V. A., Il'in, V. I., Brodskiy, V. A., & Kolesnikov, A. V. (2017). Electroflotation during wastewater treatment and extraction of valuable compounds from liquid technogenic waste: A review. *Theoretical Foundations of Chemical Engineering*, *51*(4), 369-383.

Kyzas, G. Z., & Matis, K. A. (2016). Electroflotation process: A review. *Journal of Molecular Liquids*, *220*, 657-664.

- Mahvi, A. H., Ebrahimi, S. J. A. D., Mesdaghinia, A., Gharibi, H., & Sowlat, M. H. (2011). Performance evaluation of a continuous bipolar electrocoagulation/electrooxidation–electroflotation (ECEO–EF) reactor designed for simultaneous removal of ammonia and phosphate from wastewater effluent. *Journal of hazardous materials*, 192(3), 1267-1274.
- Mansour, L. B., & Chalbi, S. (2006). Removal of oil from oil/water emulsions using electroflotation process. *Journal of Applied Electrochemistry*, 36(5), 577-581.
- Matis, K. A. (Ed.). (1994). *Flotation science and engineering*. CRC Press, New York.
- Meas, Y., Ramirez, J. A., Villalon, M. A., & Chapman, T. W. (2010). Industrial wastewaters treated by electrocoagulation. *Electrochimica Acta*, 55(27), 8165-8171.
- Mendelev University Science Park. (n.d.) *Table.1. Electroflotation system capability*. Retrieved from <http://enviropark.ru/course/category.php?id=10> (Accessed 11 January 2018).
- Merzouk, B., Madani, K., & Sekki, A. (2010). Using electrocoagulation–electroflotation technology to treat synthetic solution and textile wastewater, two case studies. *Desalination*, 250(2), 573-577.
- Metcalf & Eddy, Burton, F. L., Stensel, H. D., & Tchobanoglous, G. (2003). *Wastewater engineering: treatment and reuse*. McGraw Hill, Boston.
- Mollah, M. Y., Pathak, S. R., Patil, P. K., Vayuvegula, M., Agrawal, T. S., Gomes, J. A., ... & Cocke, D. L. (2004). Treatment of orange II azo-dye by electrocoagulation (EC) technique in a continuous flow cell using sacrificial iron electrodes. *Journal of hazardous materials*, 109(1-3), 165-171.
- Myers, R. H., Montgomery, D. C., & Anderson-Cook, C. M. (2009). *Response surface methodology: process and product optimization using designed experiments*. Wiley, Hoboken.

- Nahui, F. N. B., Nascimento, M. R., Cavalcanti, E. B., & Vilar, E. O. (2008). Electroflotation of emulsified oil in industrial wastes evaluated with a full factorial design. *Brazilian Journal of Chemical Engineering*, 25(3), 435-442.
- Orssatto, F., Ferreira Tavares, M. H., Manente da Silva, F., Eyng, E., Farias Biassi, B., & Fleck, L. (2017). Optimization of the pretreatment of wastewater from a slaughterhouse and packing plant through electrocoagulation in a batch reactor. *Environmental technology*, 38(19), 2465-2475.
- Ozyonar, F. (2016). Treatment of Train Industry Oily Wastewater by Electrocoagulation with Hybrid Electrode Pairs and Different Electrode Connection Modes. *Int. J. Electrochem. Sci*, 11, 1456-1471.
- Perfil'eva, A. V., Brodskii, V. A., Il'in, V. I., & Kolesnikov, V. A. (2016). Effect of the composition of the medium and electroflotation processing parameters on extraction efficiency of chromium (III) dispersed phase from aqueous solutions. *Russian Journal of Applied Chemistry*, 89(3), 388-393.
- Poon, C. P. (1997). Electroflotation for groundwater decontamination. *Journal of hazardous materials*, 55(1-3), 159-170.
- Rahmani, A. R., Nematollahi, D., Godini, K., & Azarian, G. (2013). Continuous thickening of activated sludge by electro-flotation. *Separation and Purification Technology*, 107, 166-171.
- Rawlings, J. O., Pantula, S. G., & Dickey, D. A. (2001). *Applied regression analysis: a research tool*. Springer, New York.
- Salihoglu, G., & Salihoglu, N. K. (2016). A review on paint sludge from automotive industries: Generation, characteristics and management. *Journal of environmental management*, 169, 223-235.
- Symes, D., Al-Duri, B., Bujalski, W., & Dhir, A. (2013). Cost-effective design of the alkaline electrolyser for enhanced electrochemical performance and reduced electrode degradation. *International Journal of Low-Carbon Technologies*, 10(4), 452-459.

- Tumsri, K., & Chavalparit, O. (2011). Optimizing electrocoagulation-electroflotation process for algae removal. In *2nd International Conference on Environmental Science and Technology IPCBEE* (Vol. 6).
- Vesilind, P. A., Morgan, S. M., & Heine, L. G. (2010). *Introduction to Environmental Engineering-SI Version*. CT Cengage Learning, Stamford.
- Vu, T. P., Vogel, A., Kern, F., Platz, S., Menzel, U., & Gadow, R. (2014). Characteristics of an electrocoagulation–electroflotation process in separating powdered activated carbon from urban wastewater effluent. *Separation and Purification Technology*, *134*, 196-203.
- Water Environment Federation (WEF), & American Public Health Association. (2005). Standard methods for the examination of water and wastewater. *American Public Health Association (APHA): Washington, DC, USA*.
- Xu, Y., Shang, J. Q., Yono, F. W., George, G., Coleman, D. P., Sioshansi, M., & Sullivan, S. (2009). Electrokinetic Flotation of Process Water from Paint Booths. *Water Quality Research Journal of Canada (Canadian Association on Water Quality)*, *44*(2) 189-200.
- Zhao, S., Huang, G., Cheng, G., Wang, Y., & Fu, H. (2014). Hardness, COD and turbidity removals from produced water by electrocoagulation pretreatment prior to reverse osmosis membranes. *Desalination*, *344*, 454-462.
- Zhou, W., Gao, L., Cheng, W., Chen, L., Wang, J., Wang, H., ... & Liu, T. (2016). Electro-flotation of *Chlorella* sp. assisted with flocculation by chitosan. *Algal research*, *18*, 7-14.

CHAPTER 5 Experimental Study of Flow Characteristics in Electroflotation Reactor

5.1 Introduction

Study of residence time distribution of reactors provides tools to recognize and define various hydrodynamic factors regarding design and control of water and wastewater treatment processes. In design, reactors are usually treated as either a perfect continuous-flow stirred tank reactor (CSTR) or a plug-flow reactor (PFR), whereas in reality non-ideal behaviors and deviations are observed. The distribution of residence time in a reactor and the model to describe the flow and quality of mixing system are considered in defining the deviation from the ideal reactors (Fogler, 1999). This deviation, caused by channeling and recirculation of fluid, or formation of stagnant regions, results in the ineffective contact and lower performance of the process (Levenspiel, 1999).

Electroflotation is a process used to remove suspended particles from water using the gas bubbles generated from the water electrolysis. During the process, bubbles generated by electrolysis (H_2 , O_2 , etc.) attach to suspended solids in water and ascend to the surface and can be skimmed off. While several process variables, such as applied current density, electrodes, pollutant loading, and hydraulic residence time, are recognized to affect the electroflotation process, the reactor configuration including the geometry, inlet and outlet, as well as hydrodynamics and flow condition inside the reactor are significant influencing factors as well. Studies investigating these factors in electroflotation reactors are limited. Kumar and Goel (2010) performed the tracer test on a relatively small continuous-flow electrocoagulation reactor with about 5 L volume and under hydraulic retention time of 2 hours, found that the reactor behavior was close to continuous stirred-tank reactor, CSTR. However, the effects of different hydraulic retention times or electroflotation gas bubbles on the residence time distribution were not investigated in their study. The residence time distribution studies have been performed on other types of wastewater treatment reactors that implement electrolytic flotation as well (Hansen et al., 2008; Sendhil et al., 2012; Rincon, 2011). Nevertheless, the geometry of these reactors and their flow pattern are different from the electroflotation reactor used in this study.

This study aims to investigate the hydrodynamics and flow characteristics of the electroflotation reactor and to find the effects of different factors on the residence time distribution.

5.2 Residence Time Distribution (RTD)

The residence time of a reactor is the time an element of the flow spends in the reactor or the time-span between entering and exiting the reactor. Caused by the flow patterns inside a reactor, different elements of the fluid have different residence times and consequently, there is a residence time distribution (RTD).

Experimentally, the residence time distribution is established by injecting an inert tracer into the influent of a reactor and measuring the tracer concentration in the effluent over time, Figure 5.1 (Fogler, 1999).

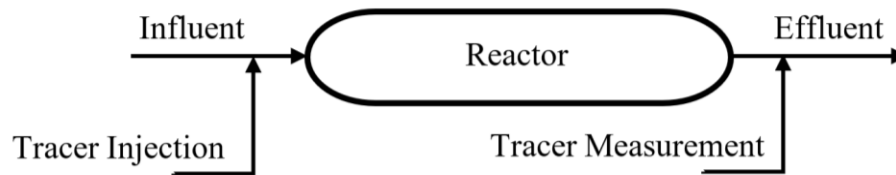


Figure 5.1: Schematic of Residence Time Distribution (RTD) test

The distribution of residence time of the effluent can be obtained by data analysis, known as the exit age distribution, E , or the residence time distribution curve, with unit $[T^{-1}]$. For convenience, E is usually characterized so the area under the RTD curve is one (Eq. 5.1) (Levenspiel, 1999).

$$\int_0^{\infty} E dt = 1 \quad (5.1)$$

There are two most practiced experimental methods of obtaining the RTD curve: pulse injection and step injection.

5.2.1 Pulse Method

In the pulse method, a certain amount of tracer, M , mg, is injected in the influent of the reactor in a time period as short as possible; and the concentration of tracer is measured and recorded in the effluent over time. The function representing the effluent concentration is called $C(t)$ function, as depicted in Figure 5.2.

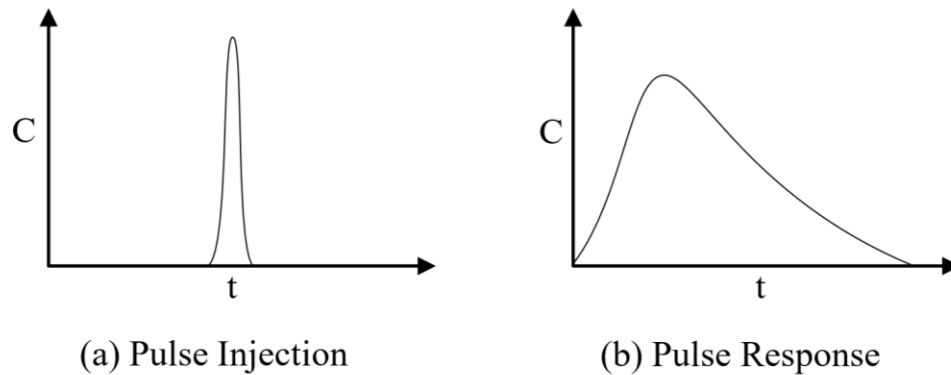


Figure 5.2: (a) Injection and (b) response curve in pulse method

From mass balance, the following equations can be produced (Levenspiel, 1999):

$$A = \int_0^{\infty} C \, dt = \sum_i C_i \Delta t_i = \frac{M}{Q} \quad \left[\frac{\text{mg} \cdot \text{min}}{\text{L}} \right] \quad (5.2)$$

$$\bar{t} = \frac{\int_0^{\infty} tC \, dt}{\int_0^{\infty} C \, dt} \cong \frac{\sum_i t_i C_i \Delta t_i}{\sum_i C_i \Delta t_i} = \frac{V}{Q} \quad [\text{min}] \quad (5.3)$$

where,

t : time, min

A : Area under the C_{pulse} curve, mg.min/L

\bar{t} : Mean of the C_{pulse} curve, min

M : amount of tracer, mg

C : Concentration of tracer, mg/L

Q : Influent flowrate, L/min

V : Volume of reactor, L

To find the $E(t)$ function and curve, the tracer concentration needs to be adjusted so that the area under the C_{pulse} curve becomes unity. Therefore,

$$E = \frac{C_{pulse}}{M/Q} \quad (5.4)$$

While studying RTD curves from different experiments with different retention times, it is helpful to eliminate the effect of different retention times. This can be achieved by introducing a dimensionless time parameter, θ , calculated from the following equation:

$$\theta = \frac{t}{\bar{t}} \quad (5.5)$$

5.2.2 Step Method

Another method commonly adopted to obtain the RTD curve of a reactor is the step introduction of the tracer. In this method, at time equals to zero, the influent into the reactor is adjusted to a specific and constant tracer concentration, C_{max} (mg/L), and the concentration is measured in the effluent, C_{step} , as shown in Figure 5.3.

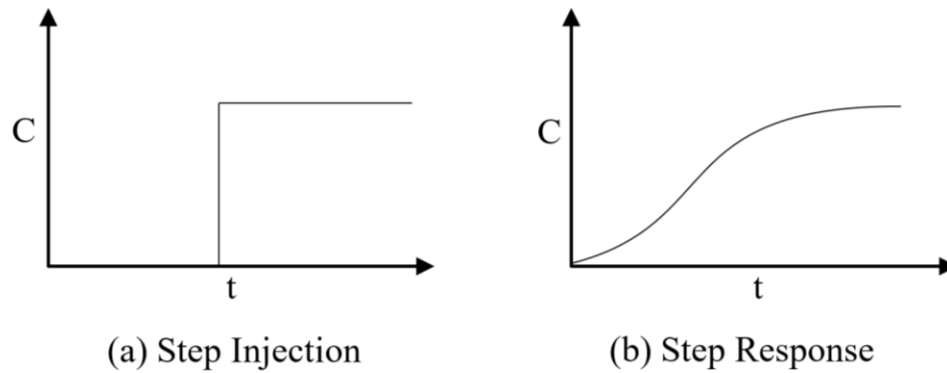


Figure 5.3: (a) Injection and (b) response curve in step method

The relationship between the influent and effluent concentrations can be defined as follows (Levenspiel, 1999):

$$C_{max} = \frac{\dot{m}}{Q} \quad \left[\frac{mg}{L} \right] \quad (5.6)$$

$$C_{max} \bar{t} = \frac{\dot{m}V}{Q^2} \quad \left[\frac{mg \cdot min}{L} \right] \quad (5.7)$$

$$\bar{t} = \frac{\int_0^{C_{max}} t dC_{step}}{\int_0^{C_{max}} dC_{step}} = \frac{1}{C_{max}} \int_0^{C_{max}} t dC_{step} \quad (5.8)$$

where,

\dot{m} : influent flowrate of tracer, mg/min

t : time, min

C_{step} : measured concentration in effluent, mg/L

\bar{t} : mean of the C_{step} curve, min

C_{max} : concentration of tracer in influent, mg/L

Q : influent flowrate, L/min

V : volume of reactor, L

The dimensionless effluent concentration curve against time, $F(t)$, can be established by dividing the concentration values, C_{step} , by the influent concentration, C_{max} , Eq. 5.9.

$$F(t) = \frac{C_{step}}{C_{max}} \quad (5.9)$$

The relationship between $E(t)$ and $F(t)$ is given by Eqs. 5.10 and 5.11 and can be seen in Figure 5.4.

$$F(t) = \int_0^t E(t)dt \quad (5.10)$$

$$E(t) = \frac{dF(t)}{dt} \quad (5.11)$$

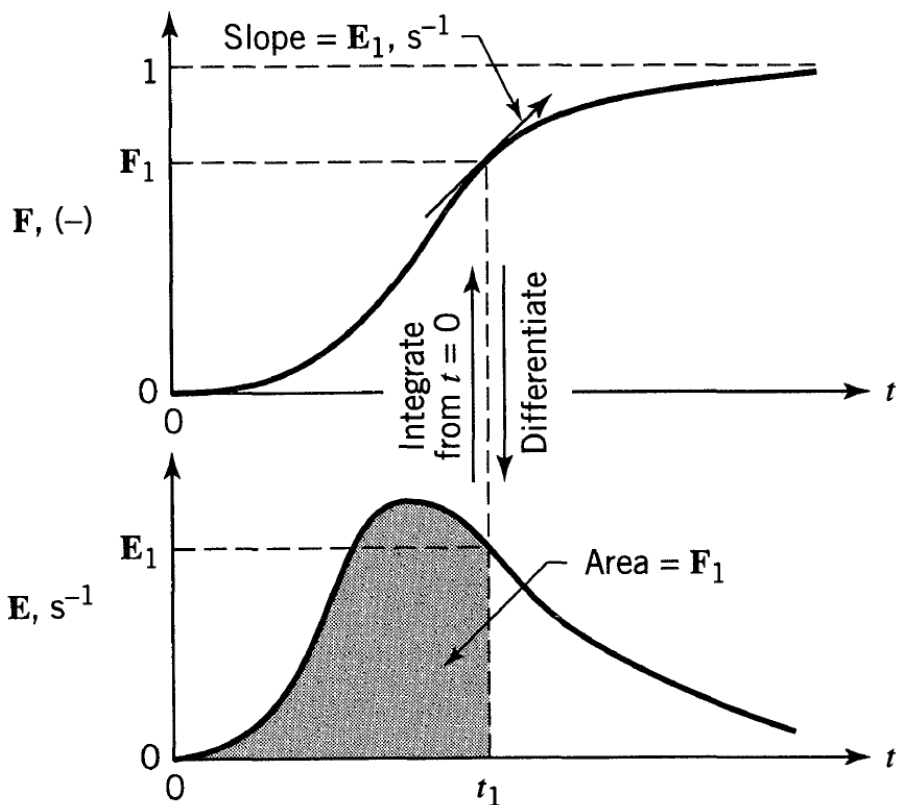


Figure 5.4: Relationship between $E(t)$ and $F(t)$ (Levenspiel, 1999)

In this study, the step method was used to investigate the flow in the electroflotation reactor and to define the residence time distribution curves.

The relationships presented in this study (Eqs. 5.1 to 5.11) assume the closed boundary condition, i.e., the flow enters and exits the reactor only once and there is no external recirculation. Due to the presence of dead or stagnant volume in the reactor, the calculated mean residence time, \bar{t} , is smaller than the theoretical hydraulic retention time, HRT. The percentage of the dead or stagnant volume, $V_D\%$, can be calculated from Eq. 5.12,

$$V_D\% = \frac{HRT - \bar{t}}{HRT} \times 100 \quad (5.12)$$

Other parameters can be extracted from the RTD data and used to analyze and compare the tracer test results. Variance (also known as square of the standard deviation), σ^2 , is the second moment about the mean value of the retention time, \bar{t} , Eq. 5.13 (Fogler, 1999).

$$\sigma^2 = \int_0^{\infty} (t - \bar{t})^2 E(t) dt \quad (5.13)$$

This parameter is an indicator of the spread of the RTD, i.e., the higher values represent the higher distribution spread.

Another useful parameter is the skewness, s^3 , which is the third moment about the mean value of the retention time, \bar{t} , and is defined in Eq. 5.14 (Fogler, 1999).

$$s^3 = \frac{1}{\sigma^{3/2}} \int_0^{\infty} (t - \bar{t})^3 E(t) dt \quad (5.14)$$

The higher the value of the s^3 , the more the distribution is skewed from the mean value of the retention time, \bar{t} .

Other basic fluid mechanics relationships used in this study are as follows:

$$HRT = \frac{V}{Q} \quad (5.15)$$

where,

HRT: Hydraulic retention time, min

$$V = V_D + V_A \quad (5.16)$$

where,

V_D : dead or stagnant volume of reactor, L

V_A : active volume of reactor, L

5.3 Materials and Methods

The experimental system consisted of a feed tank and mixer, feed pump, electroflotation tank, electrodes module and DC power supply. By adjusting the flowrate, different hydraulic retention times were achieved, and their effects were investigated. A magnetic-drive centrifugal pump (model Iwaki # MD-15RT-115NL) was used as the feed pump in this study and the flowrate was adjusted using a combination of in-line valve and by-passing. Furthermore, the effect of gas bubbles on the residence time distribution was examined by performing the experiments in two states, i.e., the DC power supply being on and off (EF ON/EF OFF).

5.3.1 The Reactor

The experiments on the residence time distribution were conducted on the reactor used for the electroflotation of auto paint wastewater, as described in Chapter 4, Figure 4.1. The reactor was made of 12-mm-thick Plexiglass® plate with the inner dimensions of 80×32×25 cm and the effective operational volume of 38.4 L. To have a uniform distribution of flow, the inlet and outlet weirs were installed for the influent and effluent control of the reactor. Also, a vertical baffle was installed near the end section of the reactor, which improved the separation process and prevented the floated particles from entering the effluent and being washed out of the reactor.

5.3.2 Electrodes

The electrode module made of SS316 plates was used in this study, as presented in Chapter 4. The electrodes were connected to a DC supply for electroflotation. The desired DC current was achieved by adjusting the applied voltage to the system.

5.3.3 Tracer Fluid

As mentioned in section 5.2.2, the step method was implemented to find the residence time distribution curves. The tracer fluid was a solution of NaCl (table salt) with a specific concentration. The concentrations of the solution in the influent and effluent of the reactor were measured by the electrical conductivity. This method has been used by other researchers (Essadki et al., 2011; Chawaloesphonsiya et al., 2017; Jeantet et al., 2008; Yousef et al., 2017; Szpyrkowicz, 2005).

To define the relationship between the salt concentration and electrical conductivity, several solutions with different NaCl concentrations were prepared and their corresponding electrical conductivities were measured. Then, the calibration curve was established by the linear regression of the salt concentration and the electrical conductivity of the fluid. Figure 5.5 shows the calibration curve and the equation of the relationship between the NaCl concentration and electrical conductivity of the fluid. The R^2 of the fitted line was 0.9991.

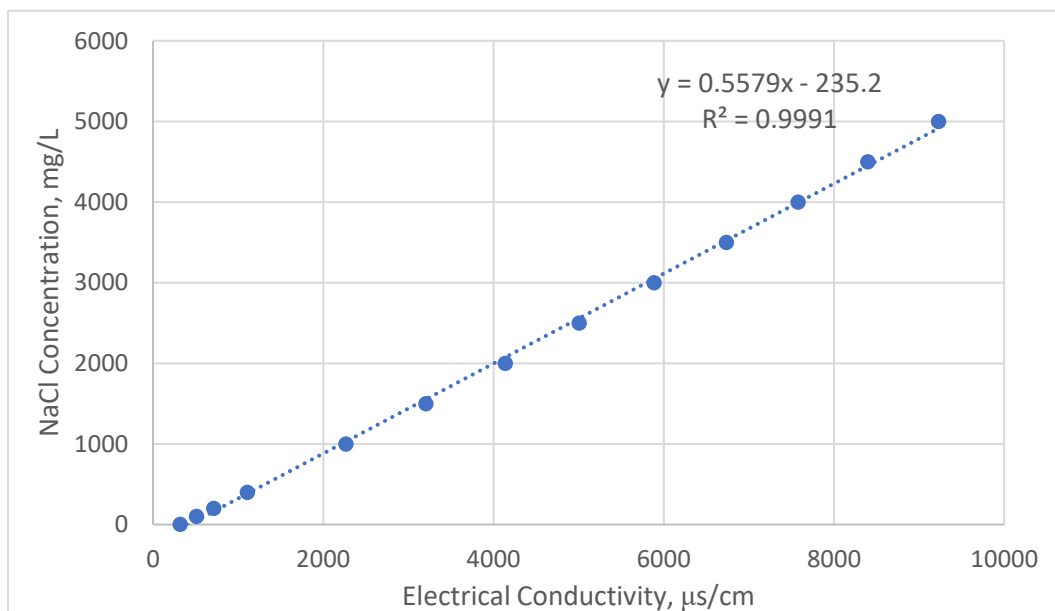


Figure 5.5: Relationship between the NaCl concentration and electrical conductivity

5.3.4 Measurement methods

The measurement of the NaCl concentration was performed through the electrical conductivity of the fluid. In this study, an EC Meter (HI8733, HANNA instruments) was used to measure the electrical conductivity. With a four-ring probe, the conductivity readings were adjusted with Automatic Temperature Compensation (ATC).

5.4 Operating Condition

The tracer fluid was prepared by adding the predetermined quantity of NaCl to tap water before starting each experiment. In the beginning, the reactor was operated with tap water. At the initial time ($t = 0$), the influent was switched to the tracer fluid, then the electrical conductivity, EC, was measured at the constant time intervals. The experiments were carried out until the concentration of the effluent, C_{step} , reached equilibrium with that of the influent, C_{max} .

The study on the Residence Time Distribution, RTD was conducted under three hydraulic retention times (HRT), i.e., 7.4, 8.5 and 15.3 minutes, which were selected according to the optimum retention times of the electroflotation system in treatment of auto paint wastewater. This allowed to examine the effect of retention time on the RTD curves and flow characteristics in the reactor. To evaluate the effect of the produced gas bubbles during the electroflotation process, the RTD experiments were performed under two modes, i.e., EF: ON and EF: OFF.

The NaCl concentration in the influent was 3100-3300 mg/L and the applied current density was 112 A/m². Table 5.1 presents a summary of the process variables.

Table 5.1: Process variables studied in Residence Time Distribution experiments

Parameter	Unit	Values
Hydraulic Retention Time (HRT)	min	7.4, 8.5, 15.3
Applied Current Density	A/m ²	112
Influent Concentration of NaCl	mg/L	3100-3300

5.5 Results and Discussion

The experiments using the step method residence time distribution were conducted at three HRTs and two states of electroflotation | (ON and OFF). Results of these experiments are presented in Tables C.1 to C.6 in Appendix C. The NaCl concentrations were derived from the calibration curve of EC versus NaCl concentration. The $F(t)$ values were calculated from Eq. 5.9. $F(t)$ curves of the electroflotation reactor are presented in Figures 5.6 to 5.8.

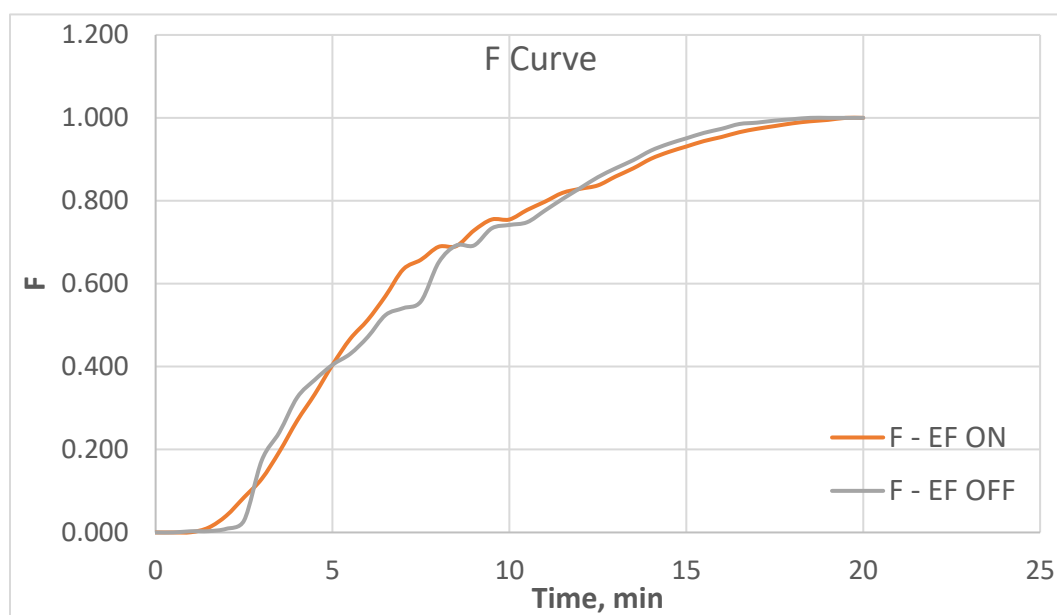


Figure 5.6: $F(t)$ curve of the RTD experiments of the electroflotation reactor HRT=7.4 min

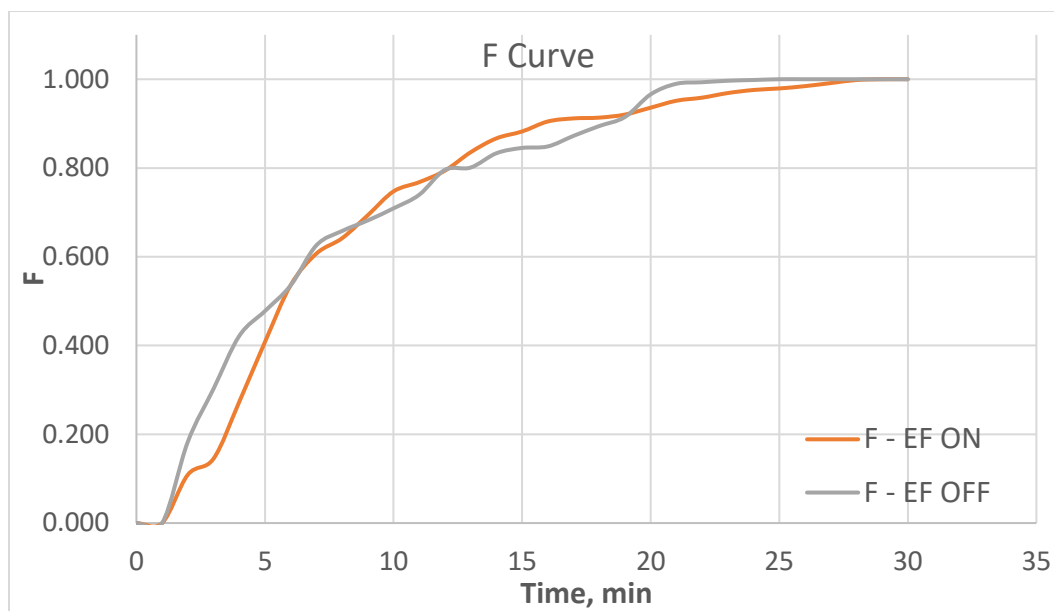


Figure 5.7: F(t) curve of the RTD experiments of the electroflotation reactor HRT=8.5 min

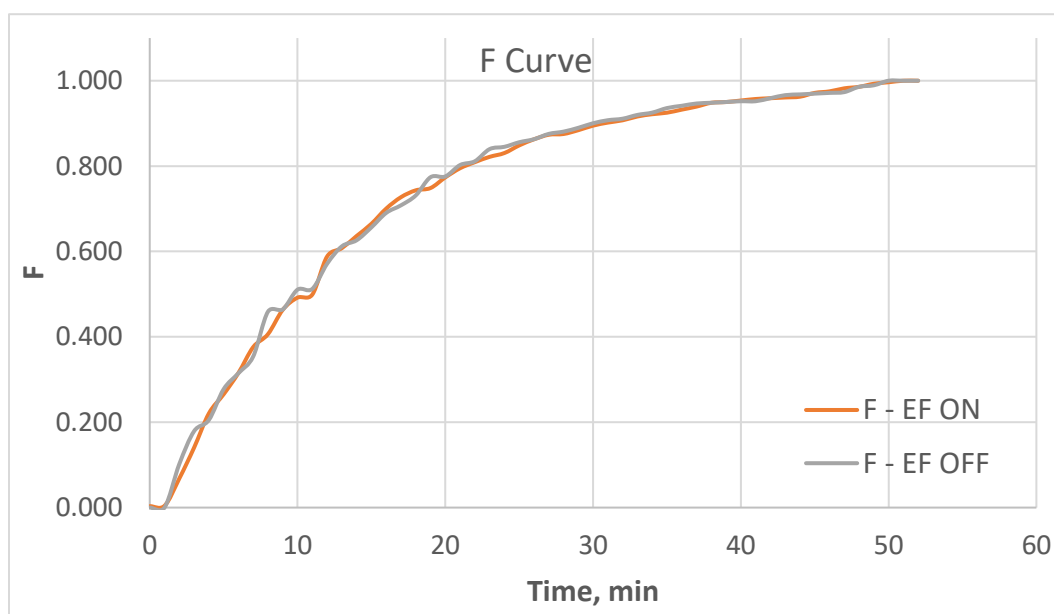
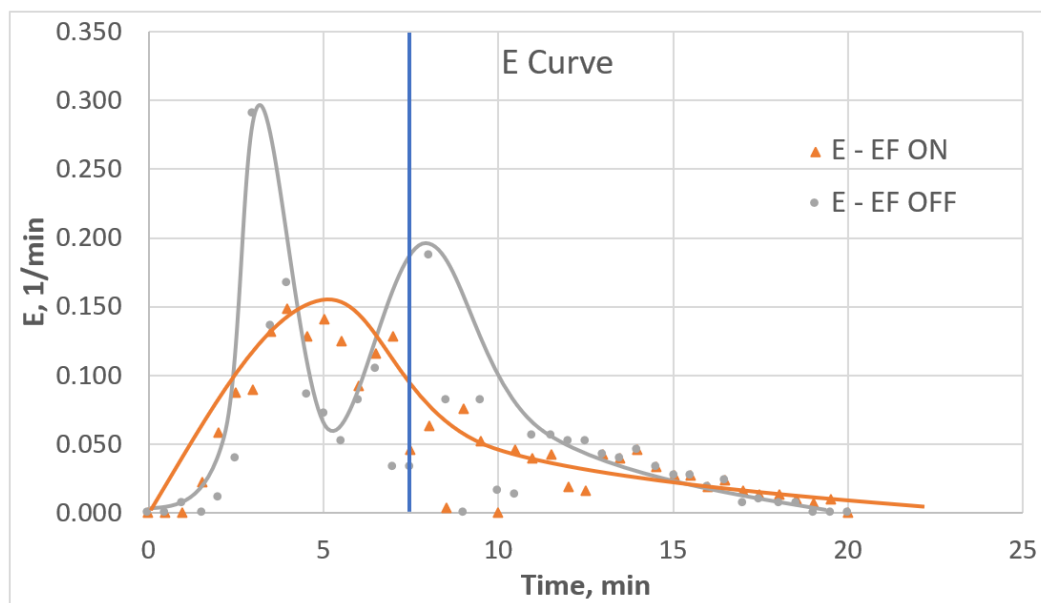


Figure 5.8: F(t) curve of the RTD experiments of the electroflotation reactor HRT=15.3 min

By definition, Eq. 5.10, the $F(t)$ curves integrate the tracer concentration variations. Therefore, they usually look smooth and hide real effects; while these effects are more evident in the $E(t)$ curves (Levenspiel, 1999). Hence, it is helpful to derive the $E(t)$ curves.

Using Eq. 5.11, the $E(t)$ values were determined. The approximate trendline curves are depicted in Figures 5.9 to 5.11.



**Figure 5.9: $E(t)$ curve of the RTD experiments of the electroflotation reactor
HRT=7.4 min**

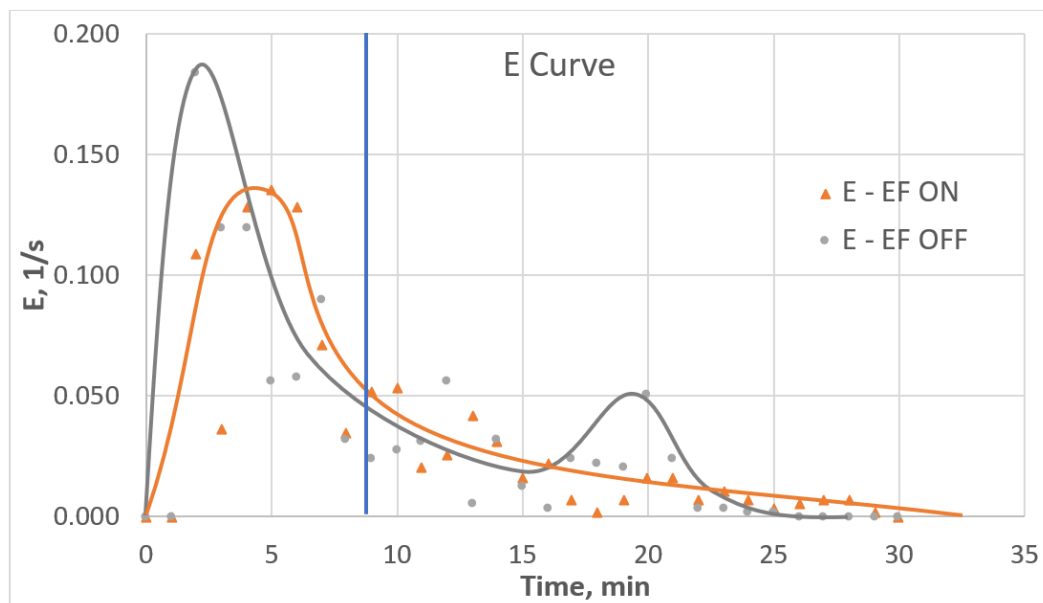


Figure 5.10: $E(t)$ curve of the RTD experiments of the electroflotation reactor HRT=8.5 min

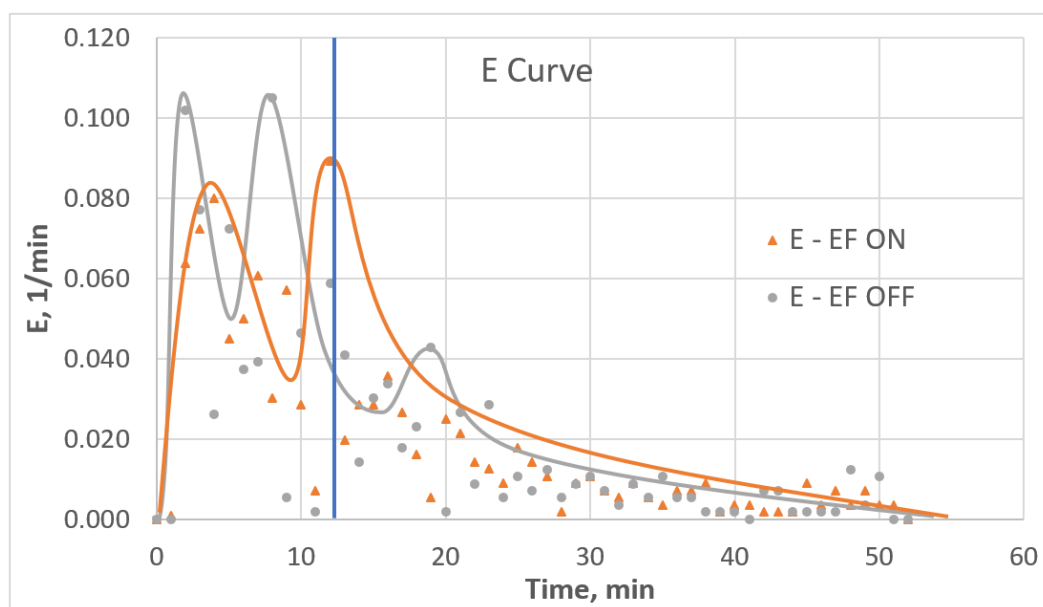


Figure 5.11: $E(t)$ curve of the RTD experiments of the electroflotation reactor HRT=15.3 min

Comparing the $E(t)$ curves of Figures 5.9 to 5.11, it was noted that the $E(t)$ curves of EF:OFF mode had higher peaks compared with the EF:ON curves. For instance, at HRT: 7.4 min (Figure 5.9), the peak value for EF:OFF curve is approximately 0.300 1/min which was almost twice as much as the peak value of EF:ON mode, 0.150 1/min. When HRT was 8.5 min (Figure 5.10), the peak values for EF:OFF and EF:ON mode were approximately 1.8 and 1.3 1/min, respectively. Similarly, the peak value of EF:OFF mode for experiment with HRT 15.3 min (Figure 5.11) was approximately 1.05 1/min, while it was 0.09 1/min for the EF:ON mode. It was observed that the differences between the peak values of EF:OFF and ON modes were greater in the experiments with lower HRTs, when the volumetric flowrates were higher. The higher peak values are the indicator of plug-flow behavior and therefore, it can be concluded that under the EF:OFF mode, the flow regime inside the electroflotation reactor was closer to the plug flow.

Another observation was that the peaks of $E(t)$ curves of EF:ON experiments were closer to the retention time values (vertical blue line) in all experiments, as presented in Figure 5.9 to 5.11. This is related to the topic of “earliness” of $E(t)$ peaks and more discussion on this phenomenon is presented in section 5.5.4.

Also, it was noted that some of the $E(t)$ curves had multiple peaks. The $E(t)$ curves of EF:OFF mode experiments at HRTs 7.4, 8.5 and 15.3 min had multiple curves while for experiments of EF:ON mode, the multiple peak happened only at higher HRT, i.e., HRT: 15.3 min, when the volumetric flowrate was low. The multiple peaks in the $E(t)$ curves were the indication of internal recirculation (Levenspiel, 2011). The configuration of the EF reactor used in this study, arrangement of the inlet and outlet, and especially the vertical baffle close to the exit of the reactor were the possible causes of the flow recirculation. Figure 5.12 illustrates the possible recirculation regions in the reactor.

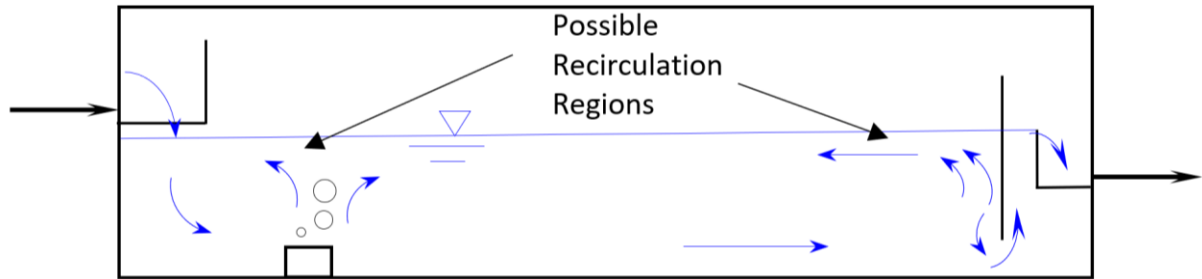


Figure 5.12: Possible regions of the flow recirculation in the EF reactor

Another reason could be that the flow rate of the influent was uneven, caused by the feed pump and piping arrangement. The resultant variable flow velocity could cause axial dispersion in the reactor and create multiple peaks (Metcalf and Eddy, 2003).

The mean residence time of the EF reactor was calculated using Eq. 5.8. The results are presented in Table 5.2.

Table 5.2: Theoretical and calculated mean residence time of the reactor under different conditions

Experiment No.	HRT, min	Electroflotation Mode	Mean Residence Time (\bar{t}), min
1	7.4	ON	7.1
2	8.5	ON	7.8
3	15.3	ON	13.5
4	7.4	OFF	7.2
5	8.5	OFF	7.4
6	15.3	OFF	13.3

The calculated residence times were smaller than the theoretical values, HRT; which was attributed to the presence of dead volumes not contributing to the flow passing through the reactor. The percentage of the dead volume of the reactor was calculated using Eq. 5.12. The results are presented in Table 5.3.

Table 5.3: Percent dead volume of the electroflotation reactor under different conditions

Experiment No.	HRT, min	Electroflotation Mode	Dead volume (V_D), %
1	7.4	ON	4.1
2	8.5	ON	8.2
3	15.3	ON	11.8
4	7.4	OFF	2.7
5	8.5	OFF	12.9
6	15.3	OFF	13.3

In experiments No 1 and No 4, at HRT 7.4 min, the calculated residence time, \bar{t} , was 7.1 and 7.2 min for EF ON and OFF modes, respectively. At the HRT 15.3 min, the \bar{t} values

were 13.5 and 13.3 min for EF ON and OFF modes, respectively. Also, the percentage of the stagnant or dead volume ranged from 2.7 to 13.1 in different experiments.

5.5.1 Effect of Hydraulic Retention Time

Figures 5.13 and 5.14 depict the $F(t)$ curves of RTD experiments at different hydraulic retention times.

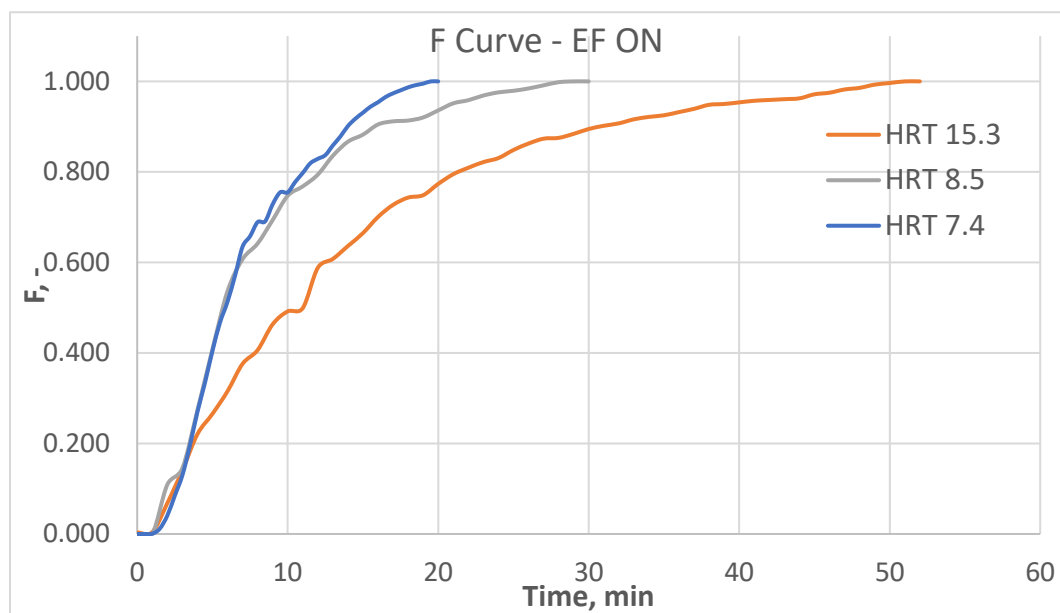


Figure 5.13: $F(t)$ curve of the RTD experiments of the electroflotation reactor EF:ON

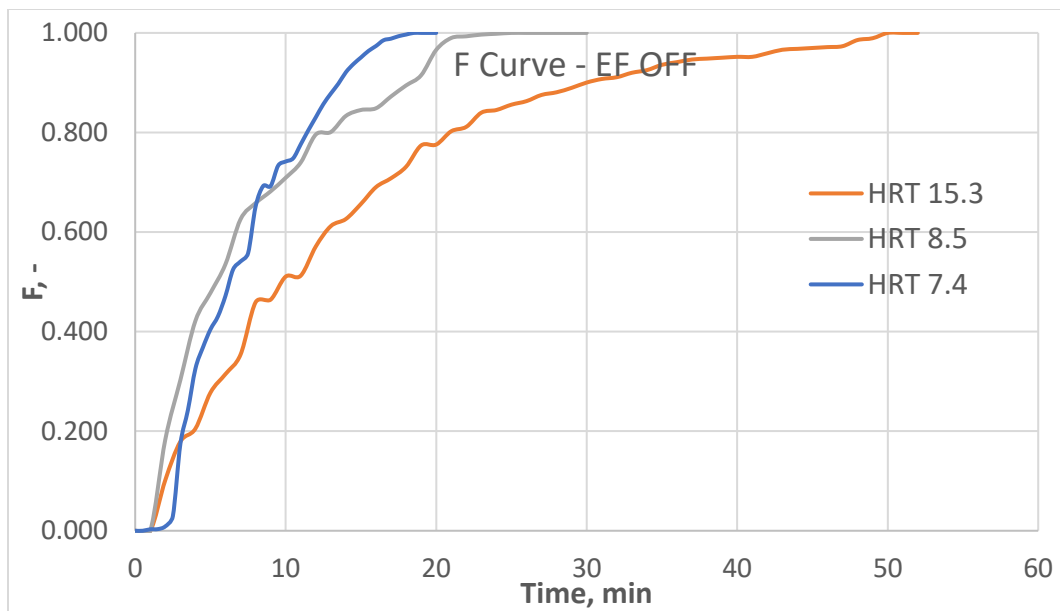


Figure 5.14: F(t) curve of the RTD experiments of the electroflotation reactor EF:OFF

The corresponding E(t) curves (trendline) are presented in Figures 5.15 and 5.16.

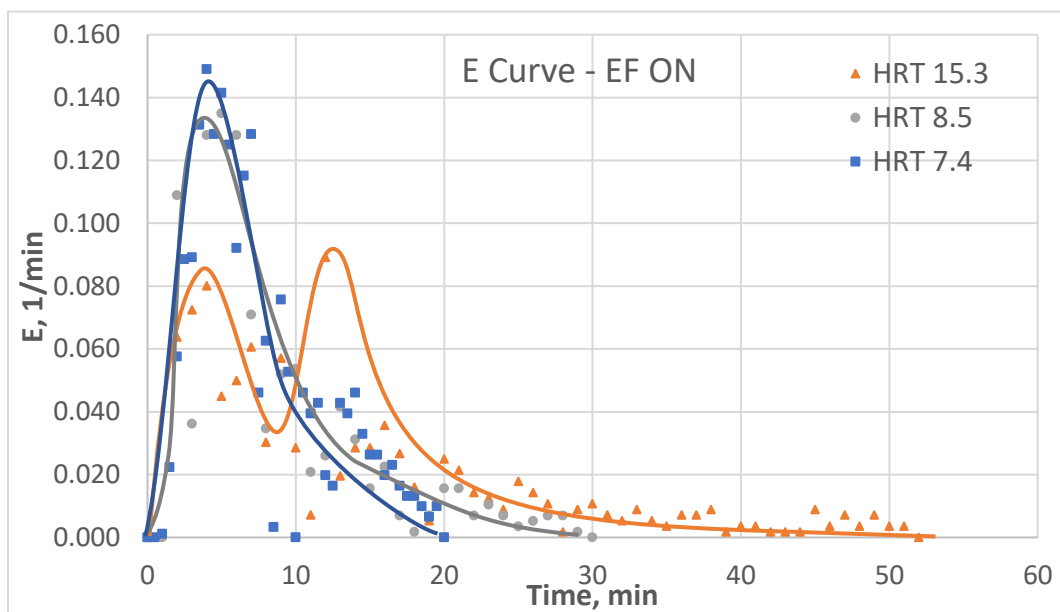


Figure 5.15: E(t) curve of the RTD experiments of the electroflotation reactor EF:ON

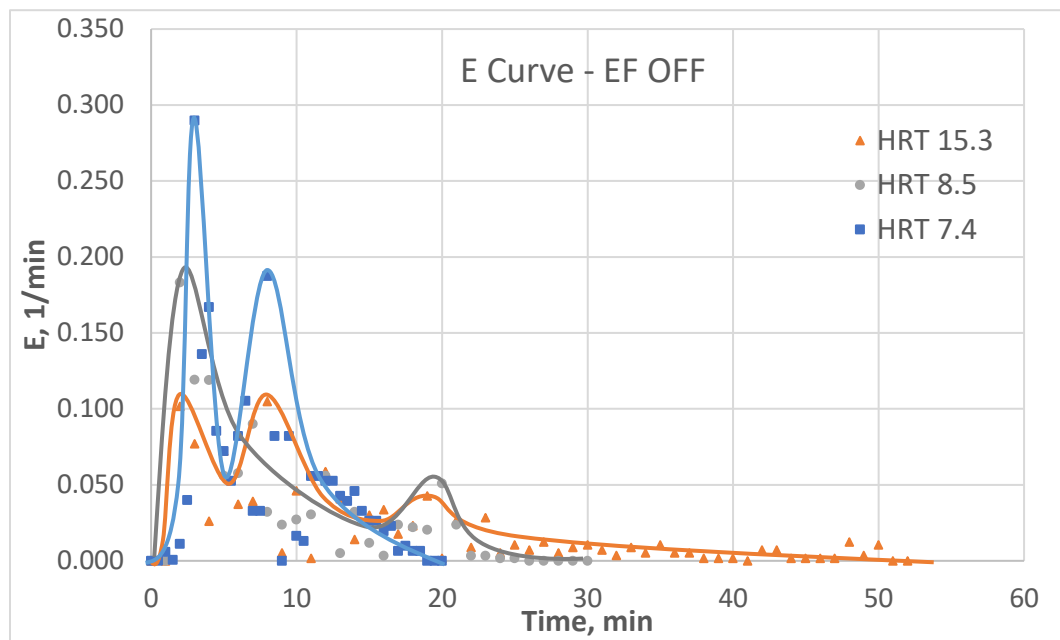


Figure 5.16: E(t) curve of the RTD experiments of the electroflotation reactor EF:OFF

It was observed that, in Figures 5.15 and 5.16, the E(t) curves of shorter HRTs, had higher peaks, especially for experiments performed under the EF:OFF mode. As mentioned before, the higher peaks are indicator of the plug-flow regime. In other words, with the increase of reactor retention time, the flow regime deviated from plug flow. Since the curves in each graph were from experiments with different hydraulic retention times, it was difficult to analyze and compare them with respect to time. Hence, a dimensionless time parameter was introduced for analysis. The dimensionless time, θ , was defined as the time divided by the mean residence time of the reactor and calculated from Eq. 5.5. The values of θ were plotted versus the F(t) and E(t) curves (trendline) and are depicted in Figures 5.17 to 5.20.

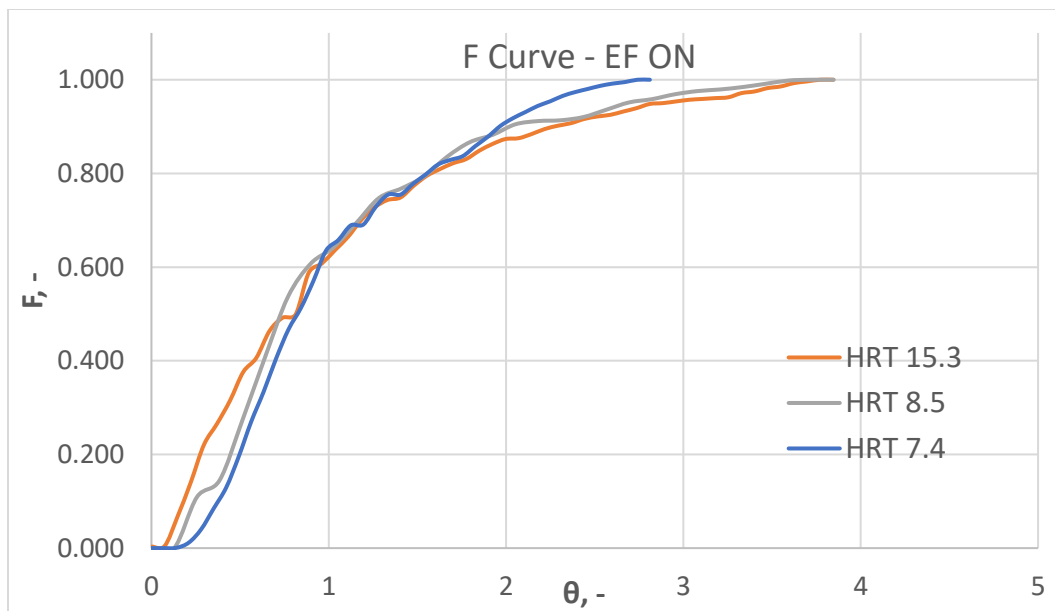


Figure 5.17: F(t) curve of the RTD experiments vs θ , EF: ON

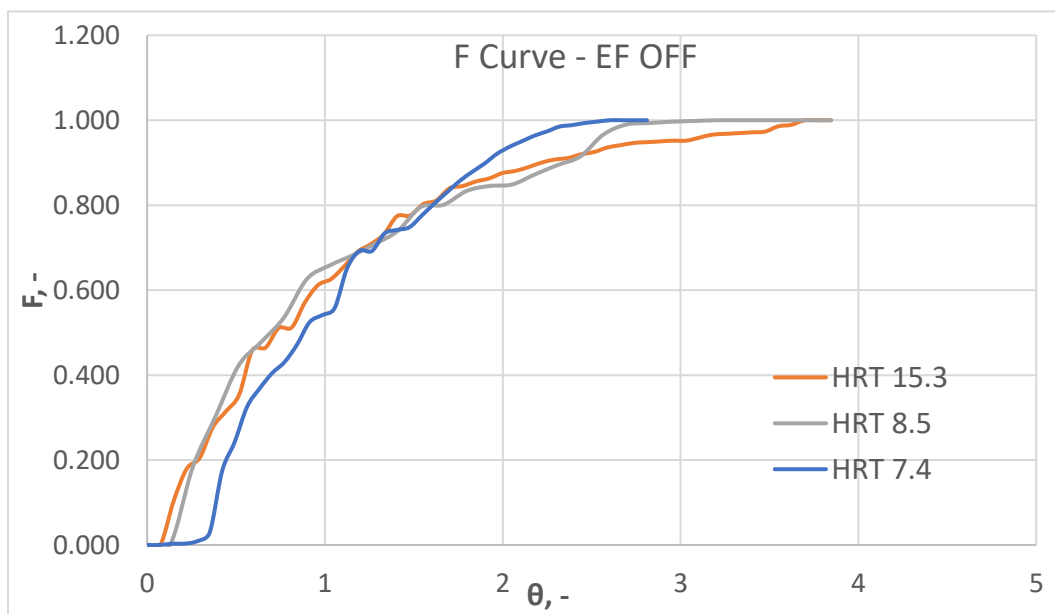


Figure 5.18: F(t) curve of the RTD experiments vs θ , EF: OFF

From F(t) curves, shown in Figures 5.17 and 5.18, it was noticed that with the decrease of HRT (increase of the flowrate), the effluent concentration reached the influent

concentration, C_{max} , earlier, and curves had steeper slope, with the behavior closer to plug-flow reactors, regardless the EF was ON or OFF. The higher velocity of the fluid at lower HRT was the reason for this behavior. The higher velocity and momentum of the fluid reduced the mixing effect inside the reactor and advanced the piston-flow behavior.

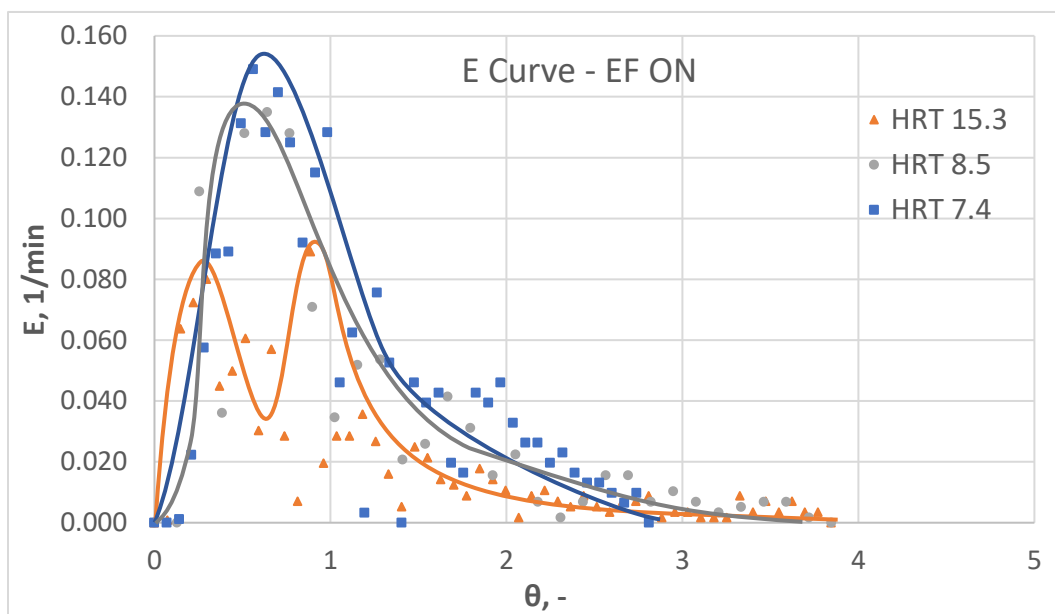


Figure 5.19: E(t) curve of the RTD experiments vs θ , EF: ON

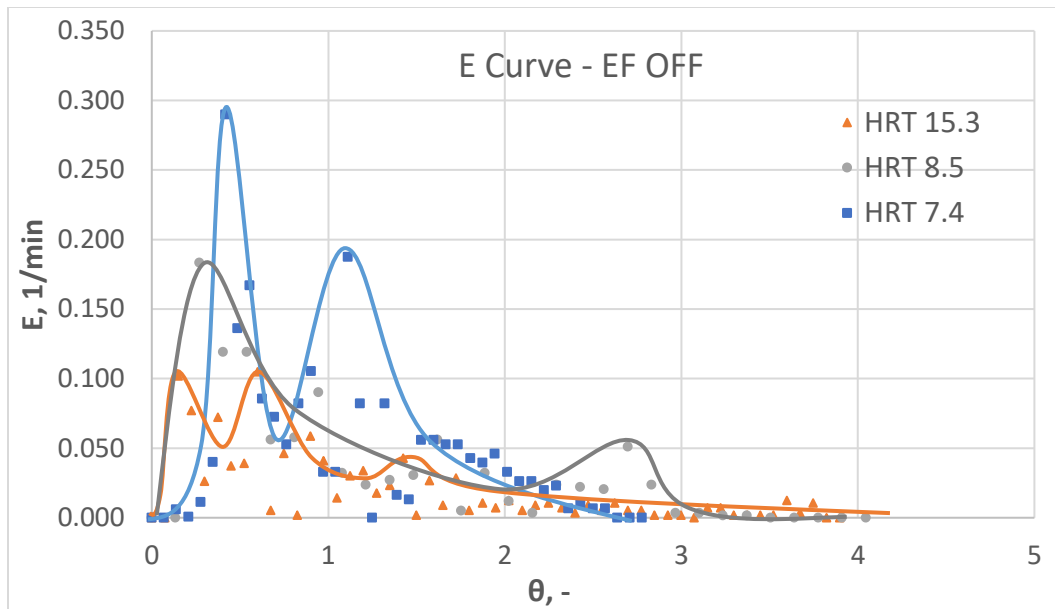


Figure 5.20: E(t) curve of the RTD experiments vs θ , EF: OFF

Comparing the E(t) curves of different HRTs in Figures 5.19 and 5.20, it was noticed that the curves of longer HRTs had wider spread over horizontal dimensionless time axis and took longer to reach zero, especially for the experiments conducted under the EF:OFF mode. For instance, under the EF:OFF mode (Figure 5.20), at HRTs 7.4, 8.5 and 15.3 min, the E(t) value reached zero at approximate θ values of 2.7, 3.5 and 4.1, respectively. This phenomenon is related to the topic of “tailing” of E(t) curves which is more discussed in section 5.5.4.

Further, the higher peaks at lower HRTs were observed in E(t) curves, as shown in Figures 5.19 and 5.20. Once again, this could be attributed to the plug-flow performance of the reactor when the HRT was lower, and the volumetric flow velocity was higher in the reactor. The same trend has been reported by other authors (Torres et al., 1998; Johansen and Hereide, 2013).

The smaller dead volume and consequently, greater active volume, resulted in the higher mean residence time of the reactor. The dead volume and mean residence time of the EF reactor in different conditions are presented in Figures 5.21 and 5.22, respectively.

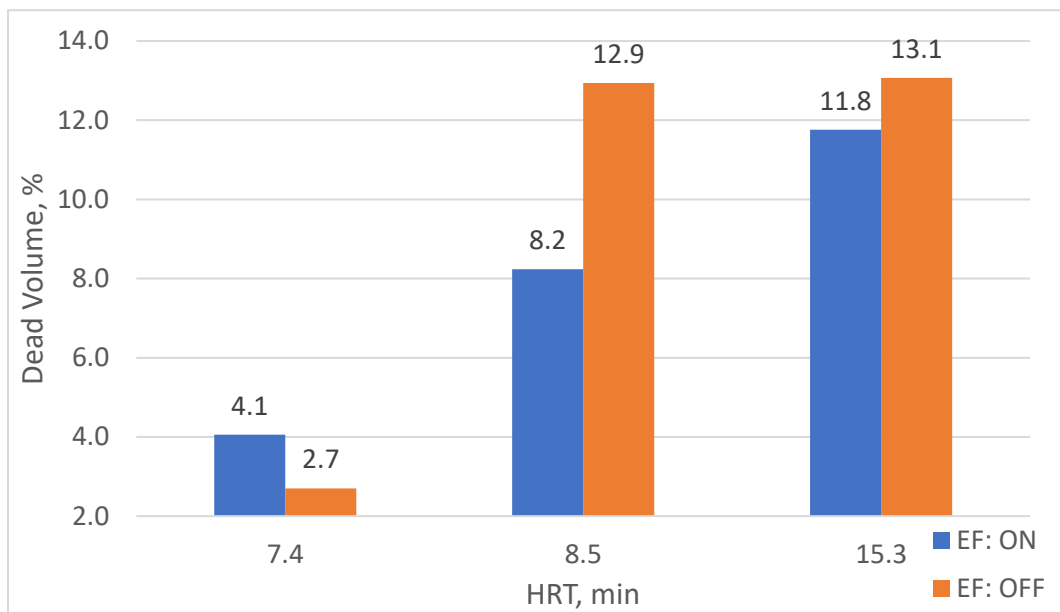


Figure 5.21: Dead volume of the EF reactor in different conditions

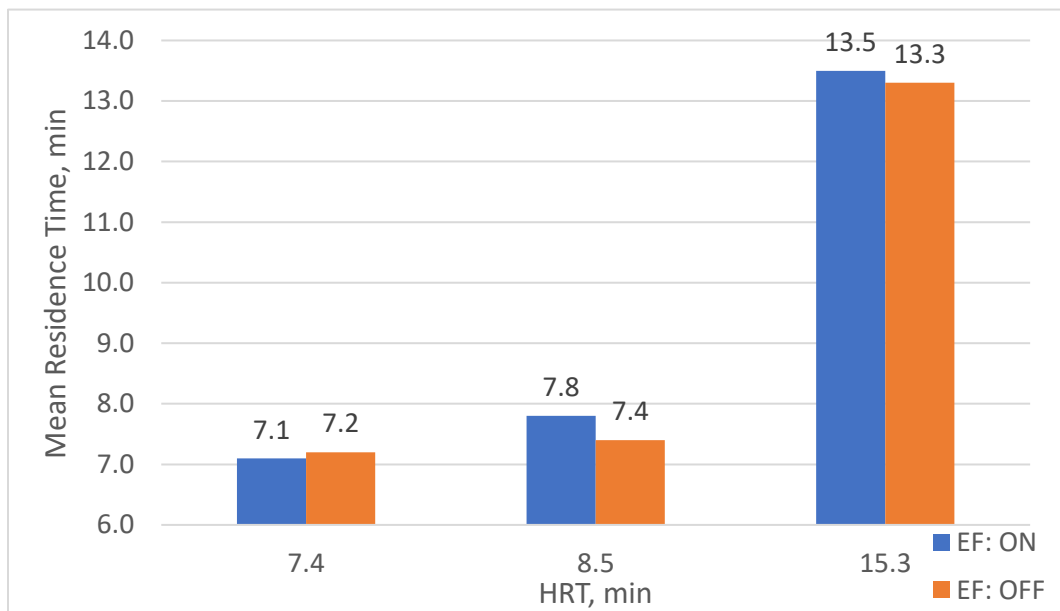


Figure 5.22: Mean residence time of the EF reactor in different conditions

As presented in Figure 5.21, the stagnant or dead volume of the reactor increased with the increase of the HRT. The dead volume values of the reactor at HRTs 7.4, 8.5 and 15.3 min, when the EF was ON, were 4.1, 8.2 and 11.8 percent, respectively. Smaller dead volume was equivalent to larger active volume (Eq. 5.16). Therefore, with the decrease of HRT values, the calculated mean residence time, \bar{t} , became closer to the theoretical residence time, HRT (at dead volume = 0, $\bar{t} = \text{HRT}$).

As defined in section 5.2.2, σ^2 and s^3 are two parameters to quantitatively evaluate and compare the RTD curves. The variance, σ^2 , represents the spread of the distribution curve and s^3 is an indicator of the skewness of the curve with respect to the mean value, \bar{t} . The values of these parameters under different experimental conditions were calculated using Eqs. 5.13 and 5.14. The results are presented in Figures 5.23 and 5.24.

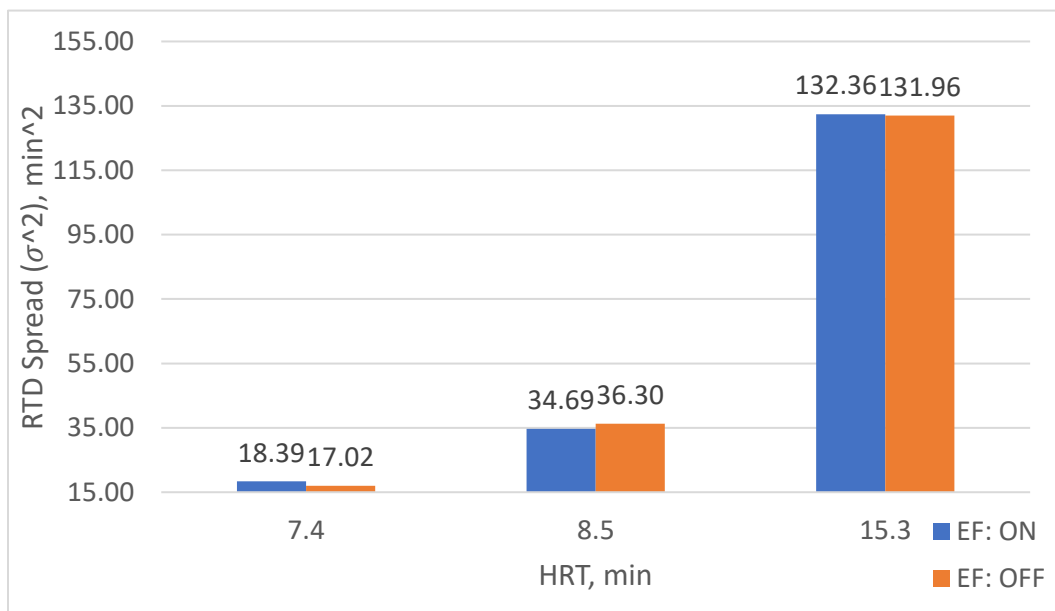


Figure 5.23: RTD spread parameter, σ^2 , in different conditions

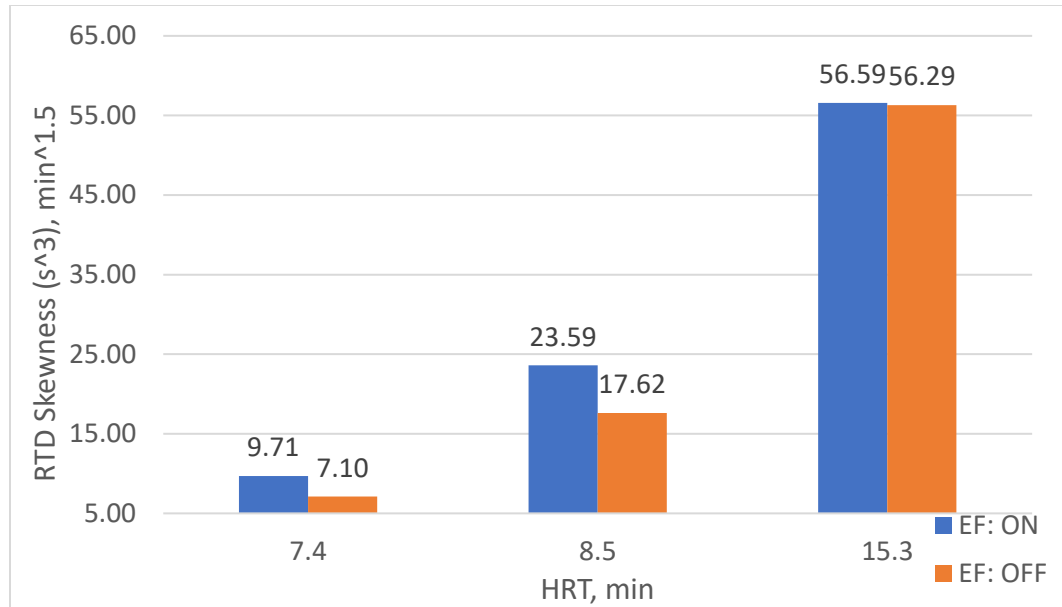


Figure 5.24: RTD skewness parameter, s^3 , in different conditions

With respect to the spread parameter, σ^2 , it was noticed, in Figure 5.23, that the increase of HRT had a major impact on the spread of the RTD values. For instance, in the situation when the EF was ON, the σ^2 values were 18.39, 34.69 and 132.36 min^2 at the HRT of 7.4, 8.5 and 15.3 min, respectively. Similarly, as shown in Figure 5.24, the values of the skewness parameter, s^3 , increased with the increase of the HRT, e.g., under the EF: ON mode and at the HRT: 7.4 min, the skewness parameter was 9.71 $\text{min}^{1.5}$. The s^3 values at the HRTs 8.5 and 15.2 min were 23.59 and 56.59 $\text{min}^{1.5}$, respectively. It means that the E(t) curves were more symmetrical at lower HRTs, when the velocity of the fluid was higher in the EF reactor (lower HRT ~ higher flowrate ~ higher velocity).

5.5.2 Effect of Gas Bubbles

In F(t) curves of the RTD experiments for different HRTs, Figures 5.6 to 5.8, it can be seen that when the EF is OFF, the effluent tracer concentrations reach equilibrium to the influent concentrations (at $F = 1$) earlier, compared to the EF: ON mode. This can be explained by the fact that the gas bubbles generated by the EF process, create internal

turbulence and mixing, hence interrupting the ideal plug-flow behavior of the reactor. The mixing effect of gas bubbles is also reflected in the $E(t)$ curves, as shown in Figures 5.9 to 5.11. It is noted that the $E(t)$ curves under the EF-OFF mode have higher peaks, compared to the E curves of the EF-ON experiments.

As presented in Table 5.3, under the EF: ON mode, the gas bubbles turbulence and mixing effect, move the flow towards the reactor corners, reducing the short-circuiting and decreasing the dead volume of the reactor, especially at the higher HRTs, i.e., 8.5 and 15.3 min. At HRT 7.4 min, due to the prevailing effects of the higher velocity and momentum of the flow, the gas-bubbles mixing effect is not observed.

The dead volume and mean residence time values, presented in Figures 5.21 and 5.22, are evaluated. It is noted that at the HRTs 8.5 and 15.3 min, under the EF: ON mode, the mean residence time is higher compared to the EF: OFF mode. For instance, at the HRT: 8.5 min, the mean residence time under the EF: ON and EF: OFF modes are 7.8 and 7.4 min, respectively. The dead volume, at the HRT: 8.5 min, under the EF: ON and EF: OFF modes are 8.2% and 12.9%, respectively.

Similarly, at the HRT: 15.3 min, the dead volume is 11.8% under the EF: ON mode, and 13.1% under the EF: OFF mode. This is equivalent to 13.5 and 13.3 min residence time under the EF: ON and EF: OFF modes, respectively.

Overall, the results show that at higher HRTs (lower flowrates), the electroflotation gas bubbles create mixing effects, leading to lower dead volumes and higher residence times in the EF reactor.

Examining the σ^2 values in Figure 5.23 (the σ^2 values at EF: ON and EF: OFF modes), no meaningful trend about the effect of EF gas bubbles is identified. For example, the σ^2 values at HRT 15.3 min are 132.36 and 131.96 min^2 at EF: ON and EF: OFF modes, respectively. However, from Figure 5.24 (the s^3 values at EF: ON and EF: OFF modes), it is noted that at the HRTs 7.4 and 8.5 min, the gas bubbles produced during the electroflotation process (EF: ON mode) enhance the skewness of the RTD curves with

respect to the mean value. For instance, the s^3 values at HRT 8.5 min are 23.59 and 17.62 $\text{min}^{1.5}$ at EF: ON and EF: OFF modes, respectively.

Hence, it can be stated that the EF gas generation, makes the $E(t)$ curve more asymmetrical and farther from the ideal plug-flow reactor. Therefore, in the design and evaluation of the electroflotation reactor, the flow regime should not be considered as an ideal plug flow.

5.5.3 Electroflotation Process Modelling

Modelling wastewater treatment processes is beneficial in scale up as well as representing and predicting the process and involves incorporating hydrodynamic features of reactors along with process kinetics. Continuous-flow reactors are usually divided into two main categories, i.e., complete-mix reactors and plug-flow reactors. It is assumed in the complete-mixed reactors that as wastewater enters the reactor, the complete mixing happens immediately and consistently. Complete-mix reactors usually are in circular or rectangular shape and include a mixing device. On the other hand, in an ideal plug-flow reactor, no longitudinal mixing occurs, and the reactor has higher length-to-width ratio compared with the complete-mix reactors (Metcalf and Eddy, 2003). Considering the geometry of the electroflotation reactor employed in this study and also the results of residence time distribution study, the plug-flow model was selected to describe the reactor. Caused by the presence of stagnant regions in the reactor, channelling, etc., it was shown that the flow regime was not ideal in the reactor. Therefore, a nonideal plug-flow model can describe the flow pattern and process of the electroflotation reactor used in this study. Dispersion model and tank-in-series model are two common (and roughly equivalent) models used by researchers and engineers to describe the deviation from plug-flow (Levenspiel, 1999). Based on the results of tracer tests and the available data for the modelling, the axial dispersion model was decided to model the process in the electroflotation reactor.

Process Kinetics and Dispersion

The axial dispersion model overlays a diffusion-like longitudinal spreading process on plug-flow regime and is characterized by dispersion coefficient, D (m^2/s). The higher values of dispersion coefficient represent the rapid spreading process in reactor and dispersion coefficient of zero is equivalent to plug flow. $(\frac{D}{uL})$ is a dimensionless group used to introduce the spread in reactor, where u is fluid velocity (m/s) and L is length of the reactor (m).

Equation of mass balance in a plug-flow reactor with axial dispersion is as follows:

$$\text{input} = \text{output} + \text{disappearance by reaction} + \text{accumulation} \quad (5.17)$$

at steady-state condition:

$$(\text{Out-in})_{\text{bulk flow}} + (\text{Out-in})_{\text{axial dispersion}} + \text{disappearance by reaction} + \text{accumulation} = 0 \quad (5.18)$$

Figure 5.25 presents variables of a closed reactor with reaction and dispersion.

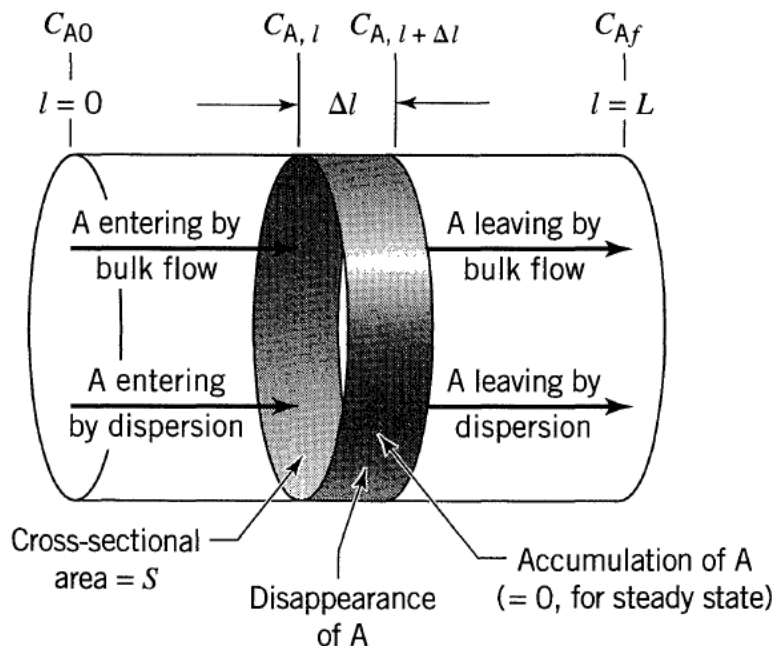


Figure 5.25: Variables for a closed plug-flow reactor with reaction and dispersion (Levenspiel, 1999)

While C_A is pollutant concentration, C_{A0} is influent concentration, C_{Af} is effluent concentration, L is length of reactor, V is volume of reactor, S is cross-sectional area of reactor, u is flow velocity, r_A is reaction rate, k is rate constant and n is reaction order, following equations can be established for terms of Eq. (5.18) (Levenspiel, 1999):

$$\text{entering by bulk flow} = C_{A,l} \cdot u \cdot S \quad (\text{mol/s}) \quad (5.19)$$

$$\text{leaving by bulk flow} = C_{A,l+\Delta l} \cdot u \cdot S \quad (5.20)$$

$$\text{entering by axial dispersion} = -\left(DS \frac{dC_A}{dl}\right)_{l+\Delta l} \quad (5.21)$$

$$\text{leaving by axial dispersion} = -\left(DS \frac{dC_A}{dl}\right)_l \quad (5.22)$$

$$\text{disappearance by reaction} = (-r_A)V = (-r_A)S \Delta l \quad (\text{mol/s}) \quad (5.23)$$

Entering these terms in Eq. (5.18):

$$u \frac{(C_{A,l+\Delta l} - C_{A,l})}{\Delta l} - D \frac{\left[\left(\frac{dC_A}{dl}\right)_{l+\Delta l} - \left(\frac{dC_A}{dl}\right)_l\right]}{\Delta l} + (-r_A) = 0 \quad (5.24)$$

taking limits $\Delta l \rightarrow 0$:

$$u \frac{dC_A}{dl} - D \frac{d^2C_A}{dl^2} + (k_A^n) = 0 \quad (5.25)$$

and in dimensionless form where $z = l/L$ and $\tau = \bar{t}$:

$$\frac{D}{uL} \frac{d^2C_A}{dz^2} - u \frac{dC_A}{dz} - k_\tau C_A^n = 0 \quad (5.26)$$

Figure 5.26 represents a graphical solution of Eq. (5.26) for second-order reaction in closed reactors.

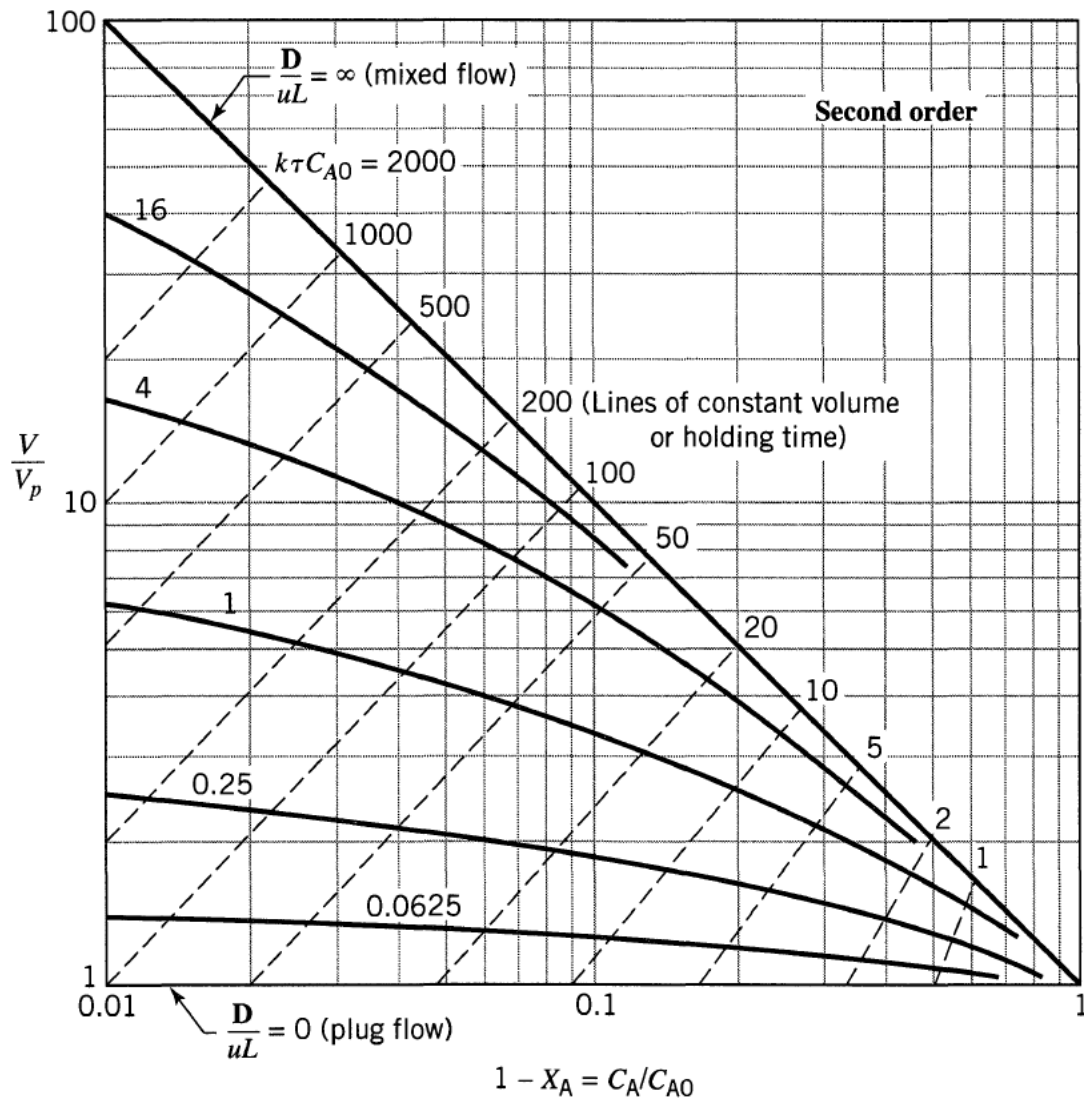


Figure 5.26: Graphical solution of axial dispersion model for second-order reactions (Levenspiel, 1999)

In order to use this graphical solution, values of D/uL and $k\tau C_{A0}$ terms need to be determined. The value of D/uL can be calculated from Eq. (5.27) (Levenspiel, 1999):

$$\sigma_{\theta}^2 = \frac{\sigma_{\bar{t}}^2}{\bar{t}^2} = 2 \left(\frac{D}{uL} \right) - 2 \left(\frac{D}{uL} \right)^2 [1 - e^{-uL/D}] \quad (5.27)$$

To solve this equation and find D/uL , $\sigma_{\bar{t}}^2$ and \bar{t}^2 values of residence time distribution (RTD) experiments of the current chapter were used. The continuous-flow treatment

experiments of Chapter 4 were conducted under retention times of 4, 6 and 8 min, and the calculated mean residence time of RTD experiments were 7.1, 7.8 and 13.5 min (Table 5.2). Therefore, results of experiments with calculated residence time of 7.1 and 7.8 were selected to validate the process model as 7.1-7.8 min range was valid for both the treatment and RTD experiments.

In $k\tau C_{A0}$ term, k is reaction rate constant, τ is mean residence time and C_{A0} is the influent TSS concentration in this study. In Chapter 3, kinetics of treatment of auto paint wastewater using electroflotation was studied. The second-order kinetics was selected to better describe the process and the rate constants were calculated. The empirical equation (Eq. 3.17) relating the rate constant, k , to the initial TSS concentration, C_0 , and current density, J , was as follows:

$$k = 13.27 - 0.01789 C_0 + 0.2345 J \quad (3.17)$$

This equation was established based on the experiments conducted under current density range of 11-44 A/m², while, the treatment studies in Chapter 4 were conducted with current density of 50, 75 and 100 A/m². Therefore, in this section, only the k values for current density of 50 A/m² were extrapolated from Eq. (3.17) and experimental results of treatment tests with current density of 50 A/m² were used for the model validation.

In Chapter 4 and using multiple linear regression, Eq. (4.18) was developed for %removal of TSS, Y , with independent variables of the applied current density (J , A/m²), HRT (t , min) and influent TSS concentration (C , mg/L):

$$Y = 56.86 + 0.2145 J + 2.675 t - 0.01723 C \quad (4.18)$$

This equation was used to calculate the effluent TSS to be compared with the results of the process model. In summary, the combinations of following data were utilized to validate the model:

- Influent TSS: 175, 531 and 1108 mg/L

- Calculated mean residence time: 7.1 and 7.8 min
- Current density: 50 A/m²

The calculated parameters and results of the process model are summarized in Table 5.4.

Table 5.4: Parameters and results of the process model

TSS _{in} (C ₀) mg/L	Residence time (\bar{t}), min	Current density (J), A/m ²	$\sigma_{\bar{t}}^2$, min ²	\bar{t}^2 , min ²	σ_{θ}^2 , -	k, L/mg.min	$k\tau C_{A0}$	Du/L	TSS _{out} <u>model</u> , mg/L	TSS _{out} <u>Regression</u> Eq. 4.18, mg/L
175	7.1	50	18.39	50.41	0.36	0.0022	2.7	0.24	47	29
531	7.1	50	18.39	50.41	0.36	0.0015	5.8	0.24	117	120
1108	7.1	50	18.39	50.41	0.36	0.0005	4.1	0.24	321	360
175	7.8	50	34.69	60.84	0.57	0.0022	3.0	0.51	56	25 ¹
531	7.8	50	34.69	60.84	0.57	0.0015	6.4	0.51	112	110 ²
1108	7.8	50	34.69	60.84	0.57	0.0005	4.5	0.51	310	340 ³

1. The experimental value of TSS_{out} was 26±1 mg/L.
 2. The experimental value of TSS_{out} was 102±2mg/L.
 3. The experimental value of TSS_{out} was 346±2 mg/L.

As it can be noted, the model provided acceptable results, especially for the midrange values of influent TSS, i.e., 531 mg/L. For instance, the effluent TSS from the model was 117 mg/L and from the empirical equation was 120 mg/L, under influent TSS 531 mg/L, residence time 7.1 min and current density 50 A/m². This was significant because the midrange values were selected based on the normal and most probable TSS values in the real situation of auto paint booths. It should also be emphasized that these results were obtained by combining the empirical models of kinetic study of Chapter 3, TSS removal of Chapter 4, RTD tests of the current chapter, as well as the process model, and measured the accuracy and practical applicability of these equations and models.

5.5.4 Discussion

The ideal and actual $E(t)$ curves of a plug-flow reactor are presented in Figure 5.27.

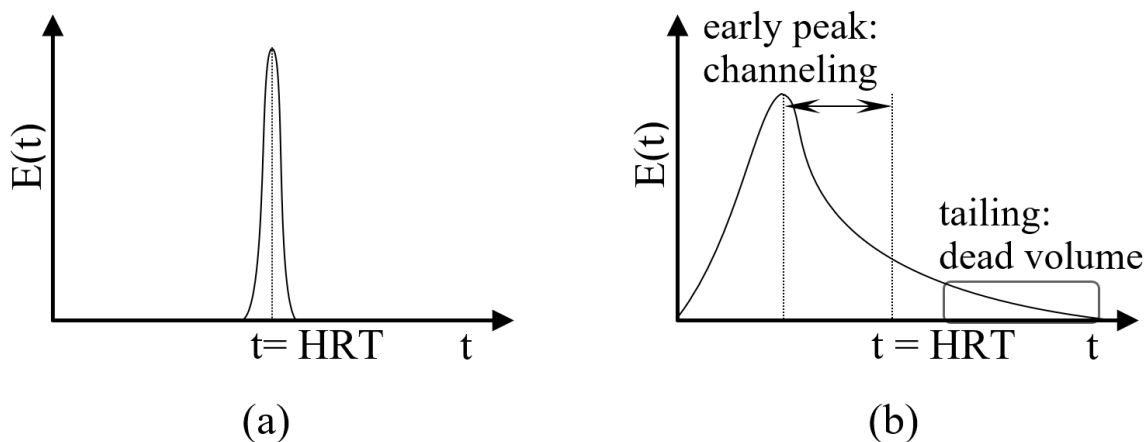


Figure 5.27: (a) Ideal plug-flow E curve; (b) Actual plug-flow E curve

The presence of stagnant and dead regions in the reactor, resulted in tailing in $E(t)$ curve, Figure 5.27(b). Comparing the $E(t)$ curves of different HRTs in Figures 5.19 and 5.20, the longer tailings were identified in the higher HRT curves. This was in agreement with the skewness values, Figure 5.24, and dead volumes, Figure 5.21, of the reactor at different HRTs, i.e., the decrease of HRT resulted in the decrease of the $E(t)$ curve

tailing, the skewness and the dead volume of the reactor; which was equivalent to the mean residence time improvement.

In the removal process of the electroflotation reactor, the suspended paint particles collide with the gas bubbles, bubble-particle attachments occur, and they slowly ascend to the surface to be removed. Each stage of this process requires adequate time to complete. Hence, improvement of the mean residence time leads to the higher removal rate of the suspended particles in the reactor.

According to the above discussions, it can be stated that the shorter HRTs, in terms of the flow characteristics, provide the improved mean residence time and consequently, generate the better performance and higher treatment efficiency of the electroflotation reactor. This is useful in the scale-up and design of the reactor. For example, in Chapter 4, section 4.4.1, two optimum condition scenarios of the treatment of the auto paint wastewater with the initial TS 1500 mg/L were identified, i.e., (1) current density 100 A/m² and HRT 6 min; (2) current density 75 A/m² and HRT 8 min. The results of residence time distribution study recommend the scenario (1) with the shorter HRT, 6 min. The shorter HRT provides the better flow characteristics and, in terms of the hydrodynamics, the higher removal rate.

Although the electroflotation process is the focus of this study, investigation of the flow characteristics in the EF-OFF mode provides valuable insight into the impacts of the EF gas bubbles on the hydrodynamics of the reactor.

In theory, the peak of E(t) curve of a plug-flow reactor happens at the value of hydraulic retention time, Figure 5.27(a). In Figures 5.9 to 5.11, it was noted that the E-curve peaks were earlier than the HRT values (the vertical blue lines), especially in EF: OFF mode experiments. The early peak in the E(t) curve, Figure 5.27(b), is an indication of fast-moving flow exiting the reactor (channeling) and the channeling creates ineffective and inadequate retention time of the paint particles in the reactor. It was shown that (Figures 5.9 to 5.11) the EF gas bubbles reduced this adverse effect. As discussed in section 5.5.3, the EF gas bubbles increased the mean residence time of the reactor by decreasing the dead volume as well. Further, under the EF-OFF mode, the multiple peaks and

unfavorable internal recirculation were observed at all HRTs; while under the EF-ON mode, the multiple peaks only occurred at the high HRT, 15.3 min (low flowrate).

Therefore, it was concluded that, in terms of the reactor hydrodynamics, the gas bubble generation during the electroflotation, reduced the adverse effects of channeling, increased the mean residence time, inhibited the internal recirculation and overall, hydrodynamically, improved the performance and treatment efficiency of the system.

5.6 Conclusions

The step-method residence time distribution experiments with NaCl as the tracer, were performed on the electroflotation reactor to investigate the flow pattern and characteristics in the reactor and find the parameters (e.g., actual mean residence time), which are essential in the design and control of the process. Moreover, the effects of different HRTs, i.e., 7.4, 8.5 and 15.3 min and EF gas bubbles on the RTD parameters were investigated.

By measuring the electrical conductivity of the reactor effluent and using the prepared calibration curve, the NaCl concentrations were used to calculate the RTD parameters and generate the $F(t)$ and $E(t)$. The results showed that all $E(t)$ curves of the EF-OFF mode exhibited multiple peaks resulting from internal flow circulation in the reactor, which was caused by the vertical baffle in the reactor

Because of stagnant regions in the reactor, the calculated mean residence times, \bar{t} , were smaller than the theoretical hydraulic retention times, HRTs. Under the EF-ON mode, the mean residence times were 7.1, 7.8 and 13.5 min, versus the calculated HRTs 7.4, 8.5 and 15.3 min, respectively. To examine the effect of different HRTs (7.4, 8.5 and 15.3 min) on RTD curves, a dimensionless time parameter, θ , was introduced and the $F(t)$ and $E(t)$ curves were plotted against the θ values. It was concluded that with the decrease of HRT (increased flowrate), the actual mean residence time, \bar{t} , became closer to the theoretical residence time, HRT. This should be considered in the design of a full-scale electroflotation reactor, i.e., selecting the shorter HRT for the reactor to achieve better flow characteristics and the higher removal rate.

The RTD experiments were performed under the current ON and OFF modes. It was realized that at the lower flowrates, i.e., higher HRTs, the gas bubbles created turbulence and mixing, resulting in the lower dead volumes and higher residence times in the EF reactor. The gas bubbles produced during the electroflotation reduced the channeling and internal recirculation, improved the mean residence time, and improved the performance and treatment efficiency of the reactor.

The variance, σ^2 and skewness, s^3 , parameters of the RTD curves under the different conditions were calculated. Both parameters increased with the increase of the HRT. It meant that with the increase of HRT, the flow regime inside the reactor deviated from the ideal plug-flow behavior.

The process model was developed incorporating empirical equations of rate constant, removal rate and hydrodynamics of the reactor. Comparing the results, it was concluded that the model was able to predict the effluent TSS concentration of electroflotation system with acceptable accuracy, especially for the midrange TSS values.

Acknowledgements

This study has been supported by the University of Western Ontario and the Natural Sciences and Engineering Research Council of Canada, NSERC.

References

- Chawaloesphonsiya, N., Prommajun, C., Wongwailikhit, K., & Painmanakul, P. (2017). Comparison of cutting-oil emulsion treatment by electrocoagulation–flotation in bubble column and airlift reactors. *Environmental technology*, 38(10), 1295-1304.
- Essadki, A. H., Gourich, B., Vial, C., & Delmas, H. (2011). Residence time distribution measurements in an external-loop airlift reactor: Study of the hydrodynamics of the liquid circulation induced by the hydrogen bubbles. *Chemical engineering science*, 66(14), 3125-3132.
- Fogler, H. S. (1999). *Elements of chemical reaction engineering* (3rd ed). Prentice Hall PTR; London: Prentice-Hall, Upper Saddle River, N.J
- Hansen, H. K., Nuñez, P., & Jil, C. (2008). Removal of arsenic from wastewaters by airlift electrocoagulation. Part 2: continuous reactor experiments. *Separation Science and Technology*, 43(14), 3663-3675.
- Jeantet, R., Ducept, F., Dolivet, A., Méjean, S., & Schuck, P. (2008). Residence time distribution: a tool to improve spray-drying control. *Dairy Science & Technology*, 88(1), 31-43.
- Johansen, A. & Hereide, Y. M. (2013). *Felles-lab RE7: Residence Time distribution Report*. NTNU, Trondheim, Norway. Retrieved from <https://dvikan.no/ntnu-studentserver/reports/ResidenceTimeDistribution-report.pdf> (Accessed 10 March 2018).
- Kumar, N. S., & Goel, S. (2010). Factors influencing arsenic and nitrate removal from drinking water in a continuous flow electrocoagulation (EC) process. *Journal of hazardous materials*, 173(1-3), 528-533.
- Levenspiel, O. (1999). *Chemical reaction engineering* (3rd ed). Wiley, New York
- Levenspiel, O. (2011). *Tracer technology: modeling the flow of fluids* (Vol. 96). Springer Science & Business Media.

Metcalf & Eddy, Burton, F. L., Stensel, H. D., & Tchobanoglous, G. (2003). *Wastewater engineering: treatment and reuse*. McGraw Hill.

Rincon, G. (2011). Kinetics of the electrocoagulation of oil and grease.

Sendhil, J., Muniswaran, P. K. A., & Basha, C. A. (2012). Residence time distribution studies in flow through tubular electrochemical reactor. *International Journal of Engineering*, 1(7), 52-62.

Szpyrkowicz, L. (2005). Hydrodynamic effects on the performance of electro-coagulation/electro-flotation for the removal of dyes from textile wastewater. *Industrial & engineering chemistry research*, 44(20), 7844-7853.

Torres, A. P., Oliveira, F. A. R., & Fortuna, S. P. (1998). Residence time distribution of liquids in a continuous tubular thermal processing system part I: Relating RTD to processing conditions. *Journal of Food Engineering*, 35(2), 147-163.

Youssef, Z., Ducept, F., Bennaceur, H., Malinowska, B., Almeida, G., Perre, P., & Flick, D. (2017). Residence time distribution in a biomass pretreatment reactor: Experimentation and modeling. *Chemical Engineering Research and Design*, 125, 233-244.

CHAPTER 6 Summary, Conclusions and Recommendations

Electroflotation (EF) is a wastewater treatment process to separate suspended particles from water using the gas bubbles produced via the water electrolysis. This dissertation aimed on the fundamental principles and applications of electroflotation process in treatment of industrial wastewaters and the main focus was on treatment of automotive paint wastewater.

6.1 Summary

The thesis included four parts in manuscript style. In the first part (Chapter 2), applications of electroflotation in treatment of industrial wastewaters were comprehensively reviewed, with detailed discussions on fundamentals of electroflotation process, electrode materials and arrangements, electroflotation reactor design and significant process variables.

In the second part (Chapter 3), kinetics of electroflotation process was examined and the statistical analysis of the available data from batch tests of electroflotation treatment of auto paint wastewaters was conducted. The theories of kinetic rates were presented and the first-order and second-order models of electroflotation were established. Using different statistical methods, e.g., “Best Subsets Regression” and “Stepwise Regression Analysis”, the most influencing factors in treatment of auto paint wastewater were determined. The Response Surface Methodology, ANOVA and Regression Analysis were implemented to examine the experimental data of each auto paint wastewater and the empirical equations of treatment efficiency as a function of the time and current density were generated.

In the third part (Chapter 4), the treatment study of auto paint wastewater using electroflotation method in a continuous-flow reactor was conducted. The electroflotation reactor and electrodes module were designed and constructed. An experimental plan was developed and executed, and the effects of different process variables, i.e., applied current density, reactor retention time and initial concentration of total solids on the

system performance were investigated. The electrochemistry of system was discussed; and the values of specific energy consumption of the electroflotation process in different experimental conditions were calculated and assessed. The Response Surface Methodology and Multiple Linear Regression methods were employed to statistically analyze the experimental data and to generate the empirical equations of the treatment process.

In the fourth part (Chapter 5), an experimental investigation was conducted on the flow characteristics and hydrodynamics of the electroflotation reactor and the factors influencing the residence time distribution. The experimental system comprised a feed tank, pump, electroflotation reactor, electrodes module and DC power supply. Step-method residence time distribution tests with NaCl as the tracer were conducted under different hydraulic retention times and bubble-generation modes, i.e., DC power ON/OFF modes. The values of $F(t)$, $E(t)$, dead volume, variance and skewness parameters were calculated for different conditions and the effects of retention time and electroflotation gas bubbles on hydrodynamics of the reactor were evaluated. The results were used to provide practical recommendations on hydrodynamic design of the electroflotation reactor for optimization

6.2 Conclusions

6.2.1 Literature Review

- The electroflotation technology has shown to be effective for treatment of industrial effluents, e.g., tannery wastewater, food processing effluents, textile effluents, etc.
- The commercialized electroflotation units were installed and successfully operated for treatment of industrial effluents in different countries, indicating more full-scale constructions in the future.

6.2.2 Kinetic Study

- The kinetic study was conducted on the available experimental data of batch electroflotation treatment of auto paint wastewater. The results revealed that the second-order kinetics was a better fit to the process. The reaction rate constants increased with increasing current density.
- Through statistical analysis, the applied current density and initial TSS concentration were found as the most important influencing factors in treatment process. Using the Response Surface Methodology (RSM), the equations of the removal rate of TSS (as the response) for each wastewater sample were established, with the reaction time and the applied current density as the predictors.
- Among the statistical tools (response surface analysis and the stepwise regression) the stepwise regression method generated improved empirical equations with adequate precision. The reaction time proved to be an important variable in stepwise method equations.

6.2.3 Continuous-Flow Treatment Study

- The efficiency of continuous-flow electroflotation reactor with the effective volume of 38.4 L and stainless steel electrodes, in treatment of auto paint wastewater was studied. The effect of process variables, i.e., influent TS concentration (500-3000 mg/L), current density (50-100 A/m²) and retention time (4-8 min) on treatment performance were examined. The optimum operating conditions were determined. The maximum TSS removal rate was 95%.
- It was noted that with the increase of influent TS, the treatment efficiency decreased, e.g., under current density 100 A/m² and HRT 8 min, the treatment efficiency for influent TS of 500 was 95% and for influent TS of 3000 mg/L was 85%. The removal rate increased with increasing applied current density, e.g., the

TSS removal rates under current densities of 50 A/m^2 was 69% and under current density of 75 A/m^2 was 74% with influent TS of 3000 mg/L and HRT of 8 min. The mechanism was explained by Faraday's law. The system efficiency increased with increasing hydraulic retention time.

- The electrochemistry of the process and the pH-increase of the wastewater were discussed and justified. The specific energy consumptions of the system were calculated and realized to be among the lowest in comparison with the commercial systems.
- A full quadratic model with regression coefficients was designated to produce the empirical equations. Multiple linear regression showed better results in describing the process. The independent variables were HRT, influent TSS and applied current density and the response was TSS removal efficiency.

6.2.4 Hydrodynamic Study

- The step-method tracer tests with NaCl as the tracer were conducted and the effects of various HRT values (7.4-15.3 min) and electroflotation gas bubbles (DC Power ON/OFF) on the residence time distribution, RTD, parameters were examined. The RTD curves were plotted and showed multiple peaks under EF-OFF mode. The geometry of the reactor suggested to cause recirculation and creating multiple peaks.
- The mean residence times were calculated and noted to be smaller than the theoretical retention times, e.g., under the EF-ON mode, the mean residence times were 7.1 and 13.5 min at retention times of 7.4 and 15.3 min, respectively.
- Observing the RTD curves, it was determined that with the decrease of retention time, the actual mean residence time became closer to the theoretical residence time, i.e., regarding the hydrodynamics, shorter retention times of the reactor resulted in lower dead volume and better performance of the reactor.

- The gas bubbles generated by electrolysis reduced the channeling and internal recirculation and improved the mean residence time of the reactor.

6.3 Recommendations

The results of this study indicated the EF treatment of auto paint wastewater in a designed continuous-flow electroflotation reactor. Further, the hydrodynamic study provided guidelines for the electroflotation reactor design. The recommended areas for future researches are as follows:

- The designed and constructed reactor showed excellent hydrodynamic performance, i.e., effective electrodes, inlet and outlet weirs and internal baffle. This design can be implemented for treatment of other types of industrial wastewaters, e.g., oil sands tailings slurries.
- In electroflotation process, the removal mechanism is through attachment (“adsorption”) of suspended particle to bubble surfaces. Theoretical and experimental studies should be performed to model this mechanism. The author suggests that the process is analogous to adsorption process and therefore, adsorption isotherms, e.g., Freundlich, Langmuir, etc., should be evaluated.
- Computational Fluid Dynamics, CFD, should be employed to model the flow regime inside the reactor, find the flow patterns, velocity fields and stagnant regions. Results of the CFD studies can be validated with the experimental RTD tests results and then, be used to further improve the reactor design.
- The continuous-flow experiments were conducted in a reactor with stainless steel electrodes. While the results were promising, performance of other electrode materials, e.g., DSA electrodes should be examined as well. Also, effects of using electrodes with larger surface areas should be studied.
- The cost-benefit analysis of the system in full scale should be conducted and the results should be compared with alternative flotation processes as well as chemical methods. The capital costs and operating costs need to be taken into consideration.

Appendix A

Table A.1: Summary of operating parameters (Shang, 2004)

	ID		ID
		Initial TSS (mg/L)	
		%Removal	
		Current Density, J (A/m²)	
		Rate Constant, k × 10⁴	
		pH	
		Zeta-potential (mV)	
		Conductivity (μS/Cm)	
ClearCoat_TS4669	ClearCoat_TS4669	759	759
		93	93
		11	11
		5	5
		7.7	7.7
		-4.36	-4.36
		1668	1668

ClearCoat_TS1992	ClearCoat_TS4669	ClearCoat_TS4669	ID
563	759	759	Initial TSS (mg/L)
91	94	94	%Removal
11	44	33	Current Density, J (A/m ²)
5	7	6	Rate Constant, k × 10 ⁴
8.4	7.7	7.7	pH
-3.43	-4.36	-4.36	Zeta-potential (mV)
1233	1668	1668	Conductivity (μS/Cm)

ClearCoat_TS1992	ClearCoat_TS1992	ClearCoat_TS1992	ID
563	563	563	Initial TSS (mg/L)
96	96	94	%Removal
44	33	22	Current Density, J (A/m ²)
11	11	7	Rate Constant, k × 10 ⁴
8.4	8.4	8.4	pH
-3.43	-3.43	-3.43	Zeta-potential (mV)
1233	1233	1233	Conductivity (μS/Cm)

Primer_TS1432	Primer_TS1432	Primer_TS1432	ID
156	156	156	Initial TSS (mg/L)
90	88	84	%Removal
33	22	11	Current Density, J (A/m ²)
18	18	11	Rate Constant, k × 10 ⁴
8.8	8.8	8.8	pH
-3.88	-3.88	-3.88	Zeta-potential (mV)
1024	1024	1024	Conductivity (μS/Cm)

Primer_TS2374	Primer_TS2374	Primer_TS1432	ID
383	383	156	Initial TSS (mg/L)
94	91	90	%Removal
22	11	44	Current Density, J (A/m ²)
14	7	18	Rate Constant, k × 10 ⁴
8.7	8.7	8.8	pH
-1.94	-1.94	-3.88	Zeta-potential (mV)
2060	2060	1024	Conductivity (μS/Cm)

MixedPaint_TS2789	Primer_TS2374	Primer_TS2374	ID
562	383	383	Initial TSS (mg/L)
88	96	96	%Removal
11	44	33	Current Density, J (A/m ²)
4	18	17	Rate Constant, k × 10 ⁴
7.8	8.7	8.7	pH
-8.13	-1.94	-1.94	Zeta-potential (mV)
1287	2060	2060	Conductivity (μS/Cm)

MixedPaint_TS2789	MixedPaint_TS2789	MixedPaint_TS2789	MixedPaint_TS2789	ID
562	562	562	562	Initial TSS (mg/L)
97	97	97	96	%Removal
44	33	33	22	Current Density, J (A/m ²)
17	13	13	9	Rate Constant, k × 10 ⁴
7.8	7.8	7.8	7.8	pH
-8.13	-8.13	-8.13	-8.13	Zeta-potential (mV)
1287	1287	1287	1287	Conductivity (μS/Cm)

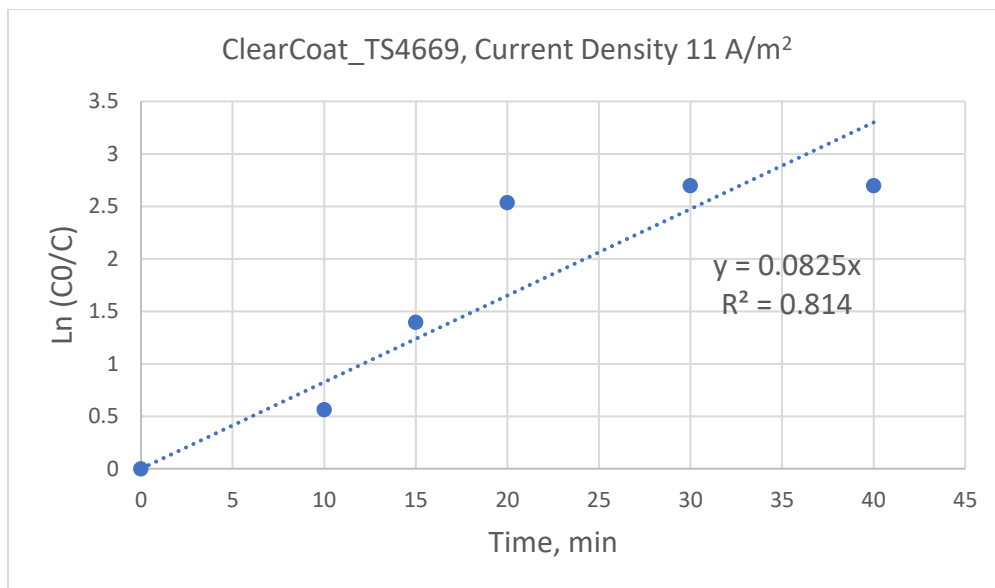


Figure A.1: ClearCoat_TS4669 Wastewater, Current Density 11 (A/m²): First-order Rate Constant (k = slope)

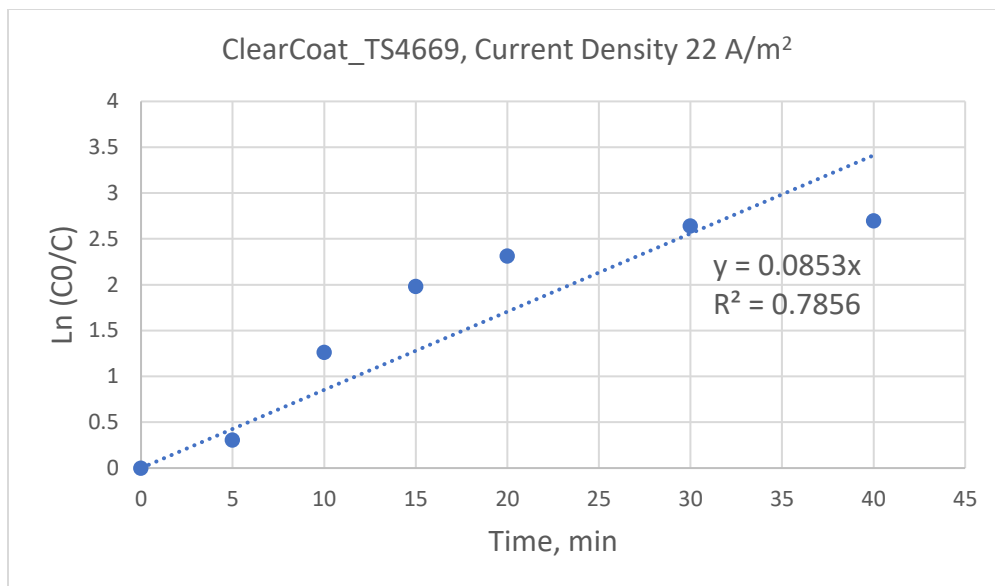


Figure A.2: ClearCoat_TS4669 Wastewater, Current Density 22 (A/m²): First-order Rate Constant ($k = \text{slope}$)

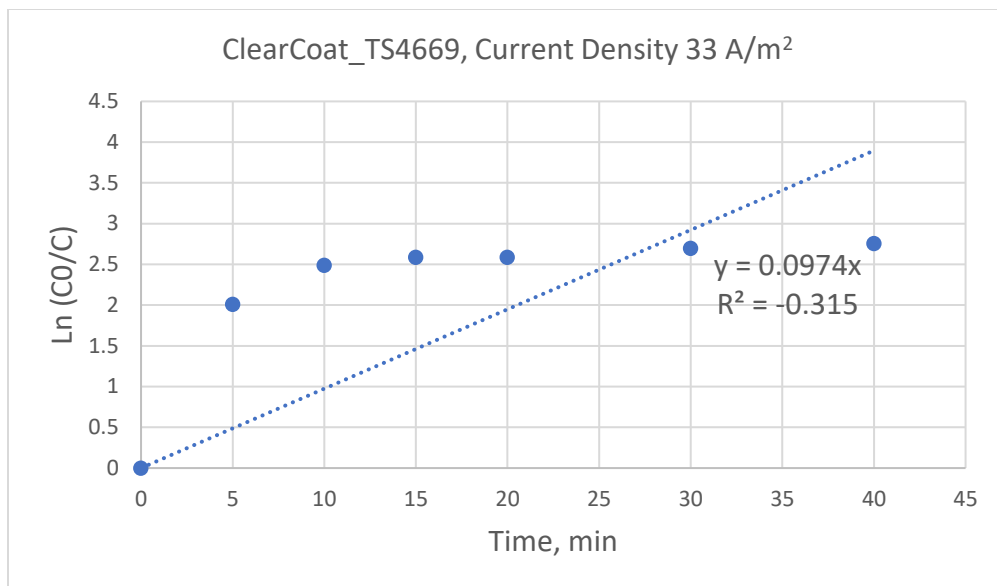


Figure A.3: ClearCoat_TS4669 Wastewater, Current Density 33 (A/m²): First-order Rate Constant (k = slope)

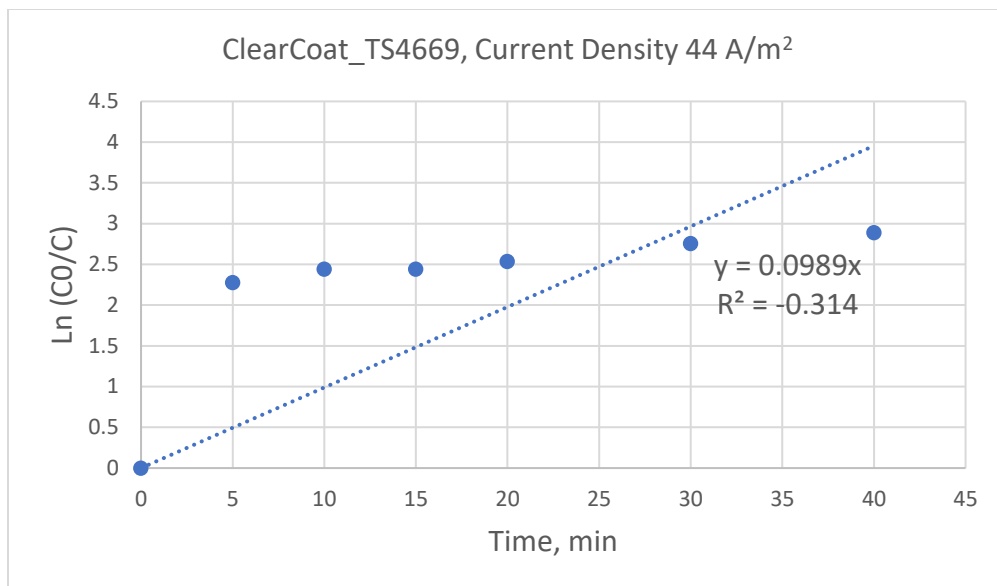


Figure A.4: ClearCoat_TS4669 Wastewater, Current Density 44 (A/m²): First-order Rate Constant (k = slope)

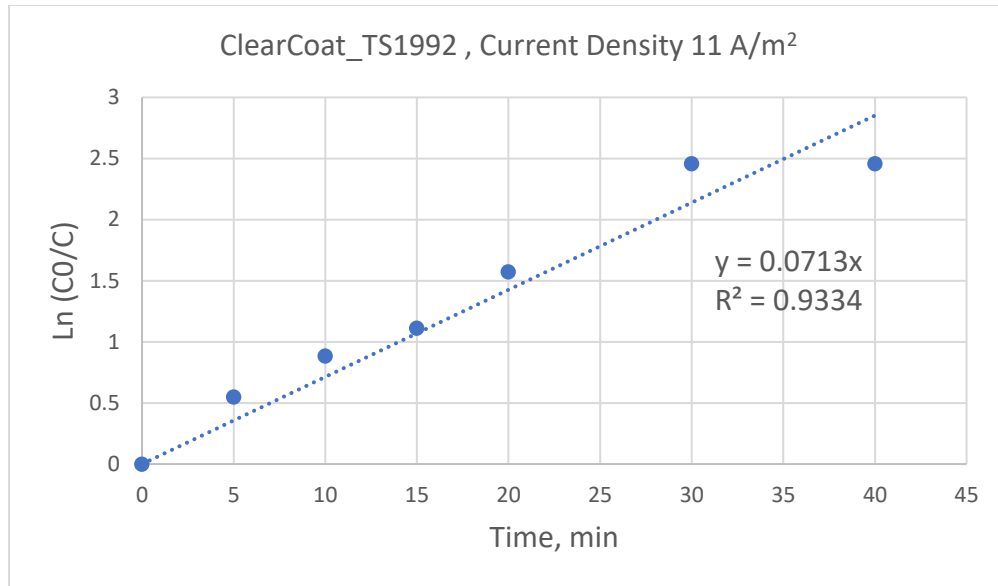


Figure A.5: ClearCoat_TS1992 Wastewater, Current Density 11 (A/m²): First-order Rate Constant ($k = \text{slope}$)

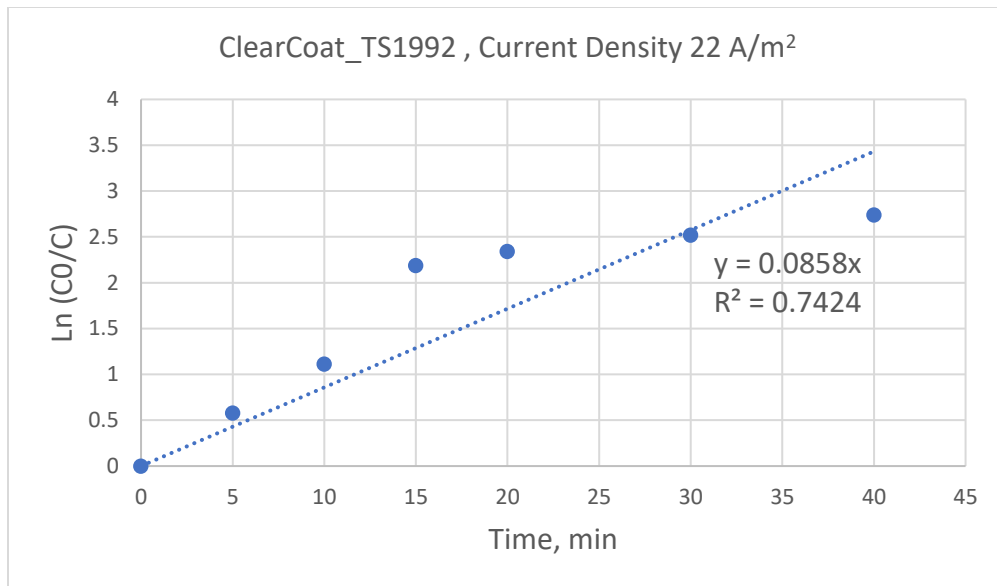


Figure A.6: ClearCoat_TS1992 Wastewater, Current Density 22 (A/m²): First-order Rate Constant (k = slope)

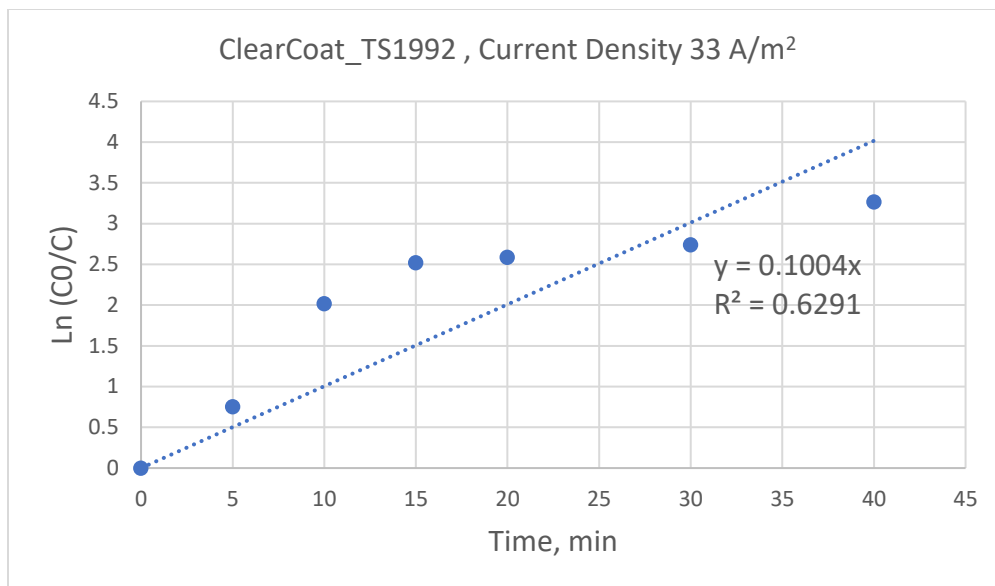


Figure A.7: ClearCoat_TS1992 Wastewater, Current Density 33 (A/m²): First-order Rate Constant (k = slope)

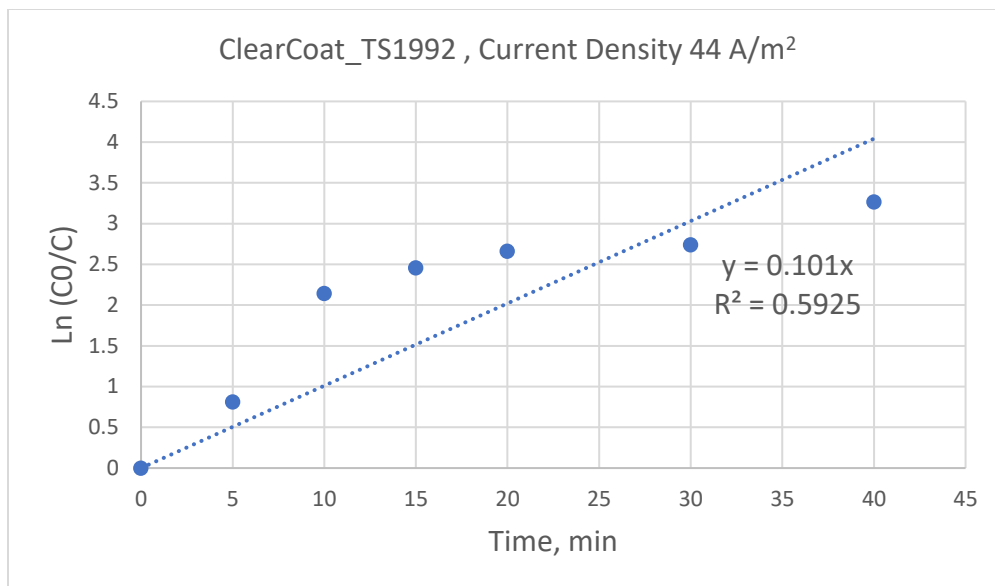


Figure A.8: ClearCoat_TS1992 Wastewater, Current Density 44 (A/m²): First-order Rate Constant (k = slope)

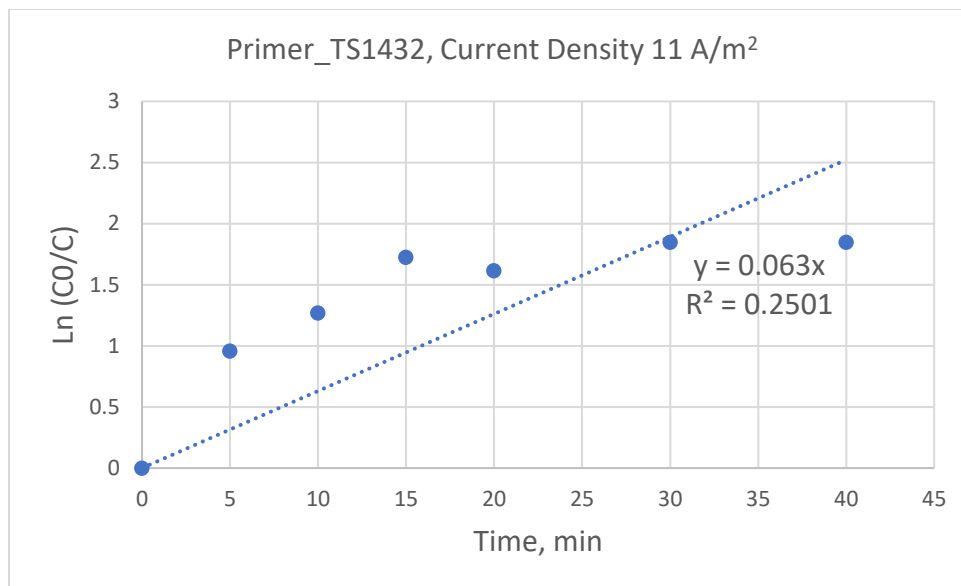


Figure A.9: Primer_TS1432 Wastewater, Current Density 11 (A/m²): First-order Rate Constant ($k = \text{slope}$)

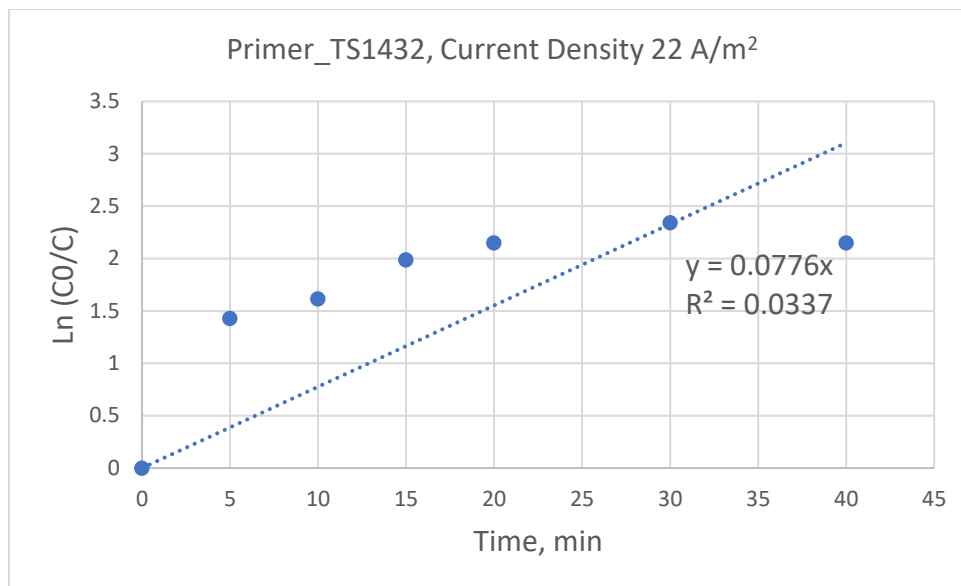


Figure A.10: Primer_TS1432 Wastewater, Current Density 22 (A/m²): First-order Rate Constant (k = slope)

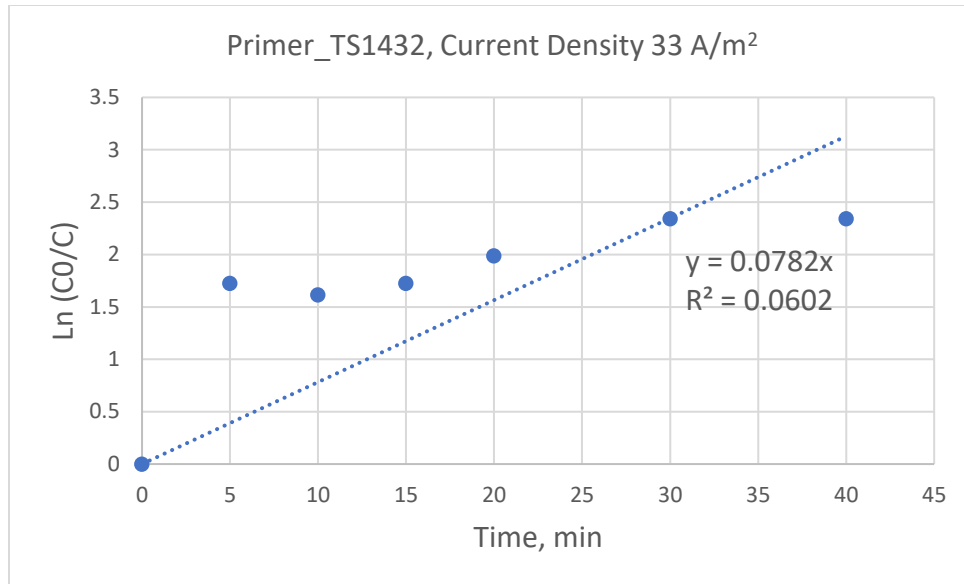


Figure A.11: Primer_TS1432 Wastewater, Current Density 33 (A/m²): First-order Rate Constant (k = slope)

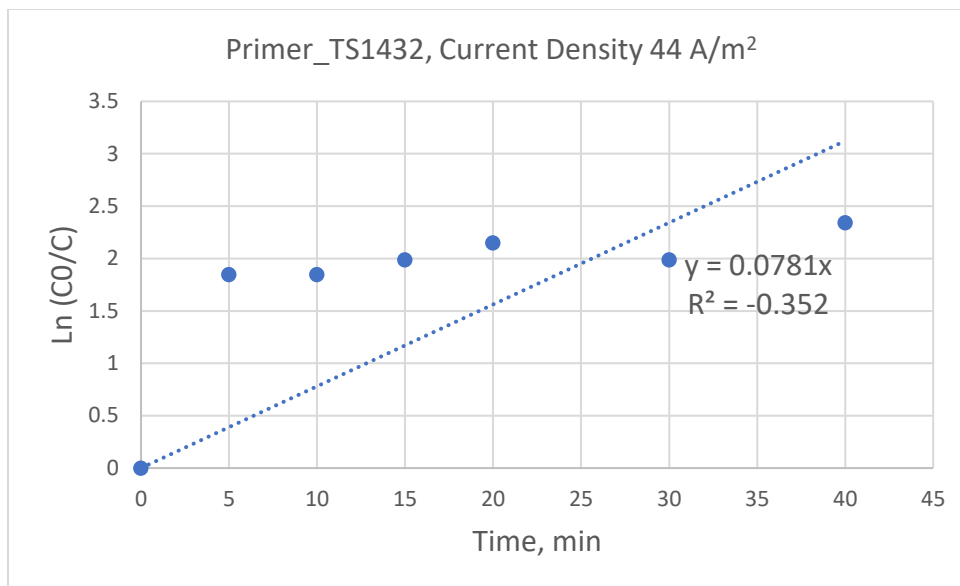


Figure A.12: Primer_TS1432 Wastewater, Current Density 44 (A/m²): First-order Rate Constant (k = slope)

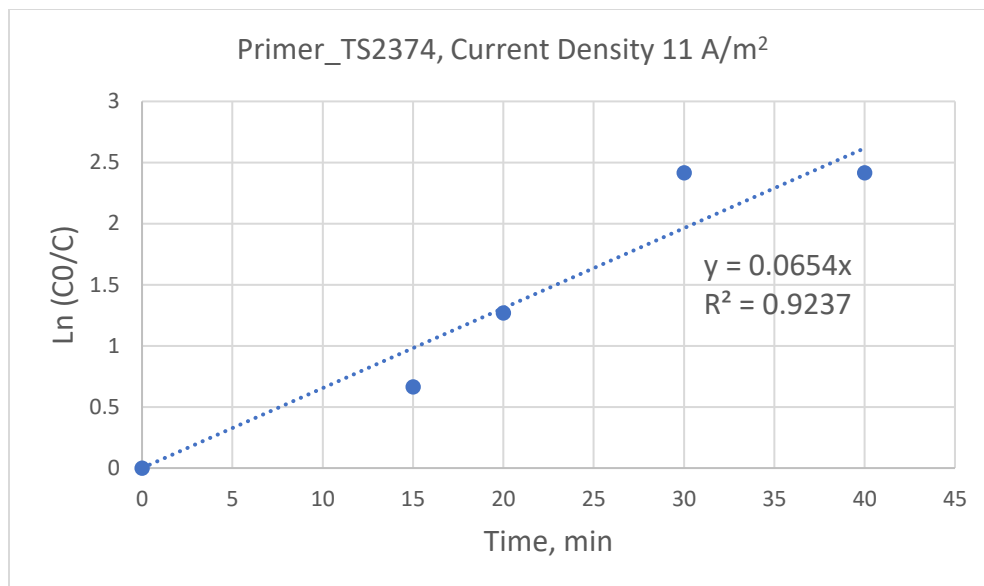


Figure A.13: Primer_TS2374 Wastewater, Current Density 11 (A/m²): First-order Rate Constant (k = slope)

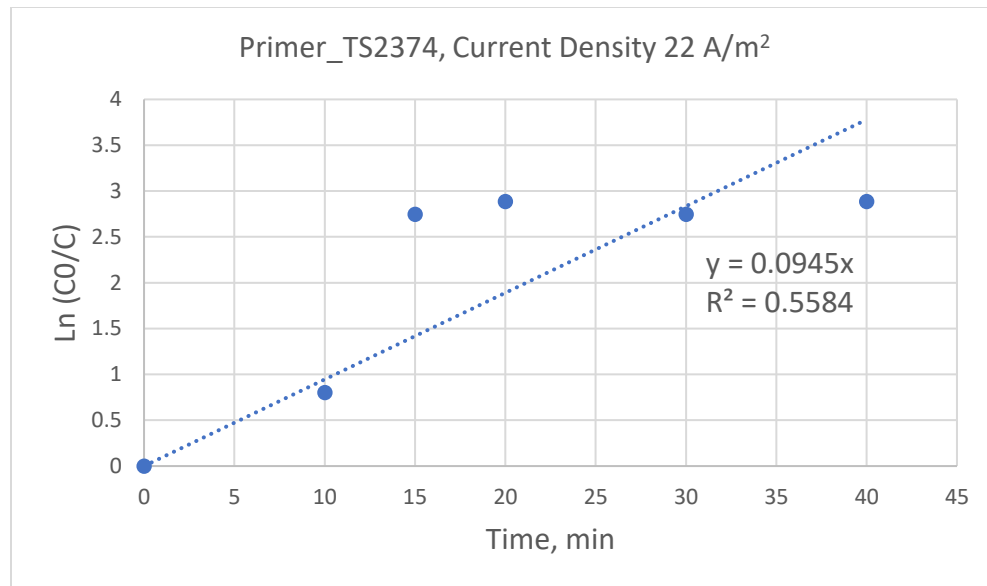


Figure A.14: Primer_TS2374 Wastewater, Current Density 22 (A/m²): First-order Rate Constant (k = slope)

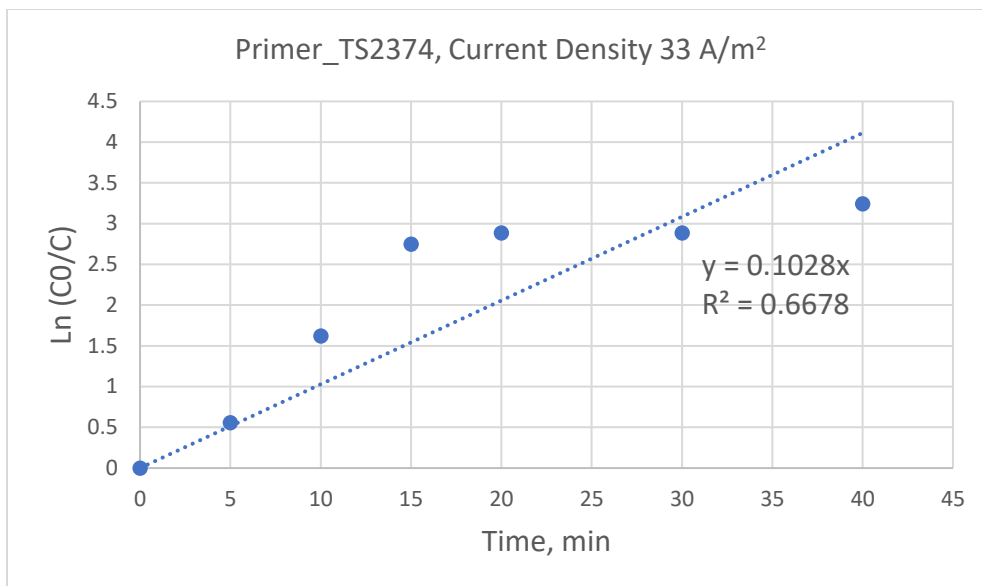


Figure A.15: Primer_TS2374 Wastewater, Current Density 33 (A/m²): First-order Rate Constant (k = slope)

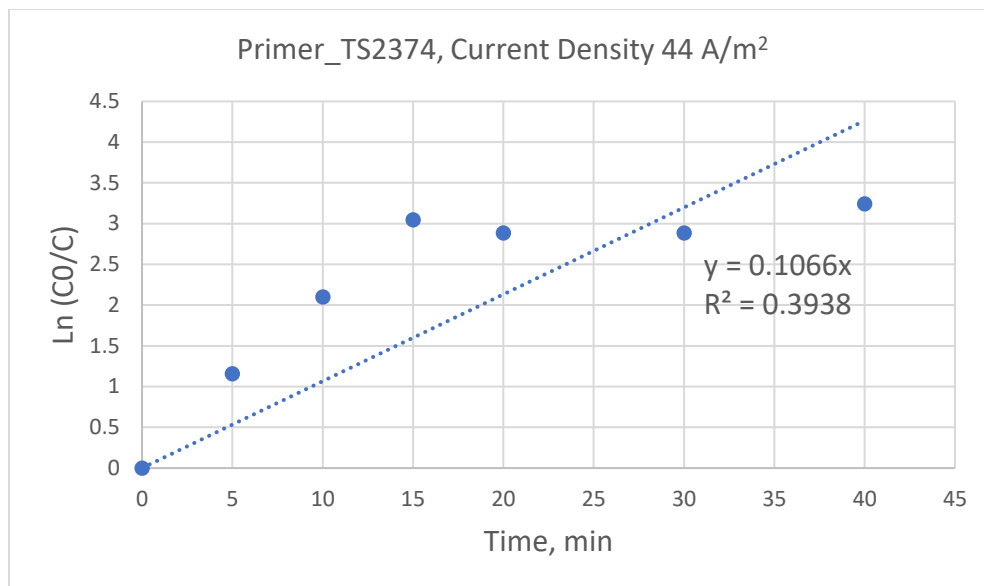


Figure A.16: Primer_TS2374 Wastewater, Current Density 44 (A/m²): First-order Rate Constant ($k = \text{slope}$)

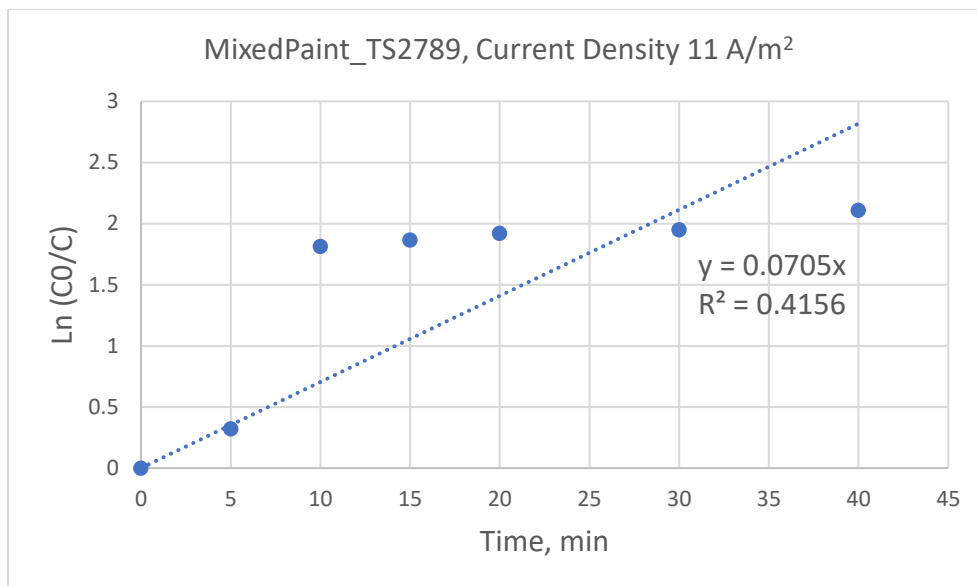


Figure A.17: MixedPaint_TS2789 Wastewater, Current Density 11 (A/m²): First-order Rate Constant (k = slope)

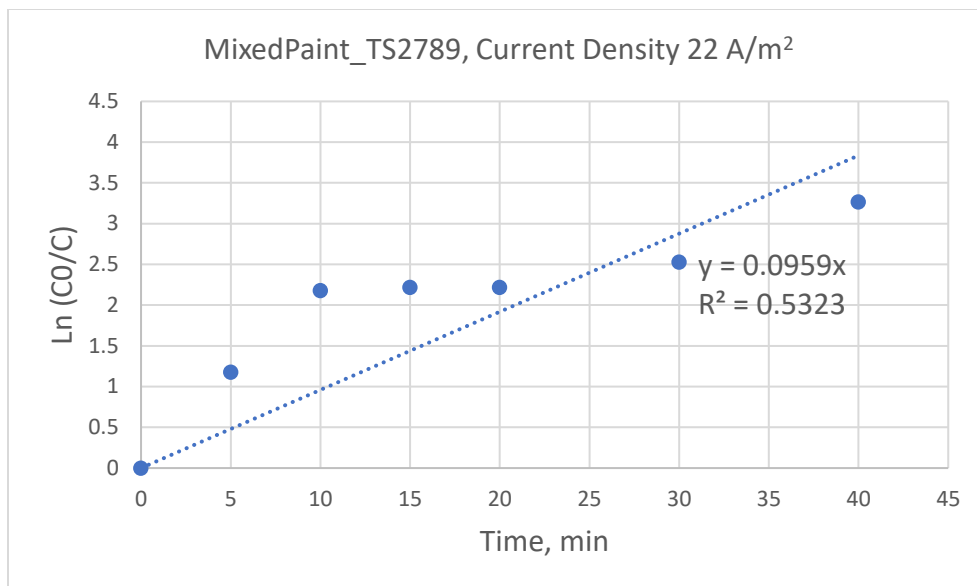


Figure A.18: MixedPaint_TS2789 Wastewater, Current Density 22 (A/m²): First-order Rate Constant (k = slope)

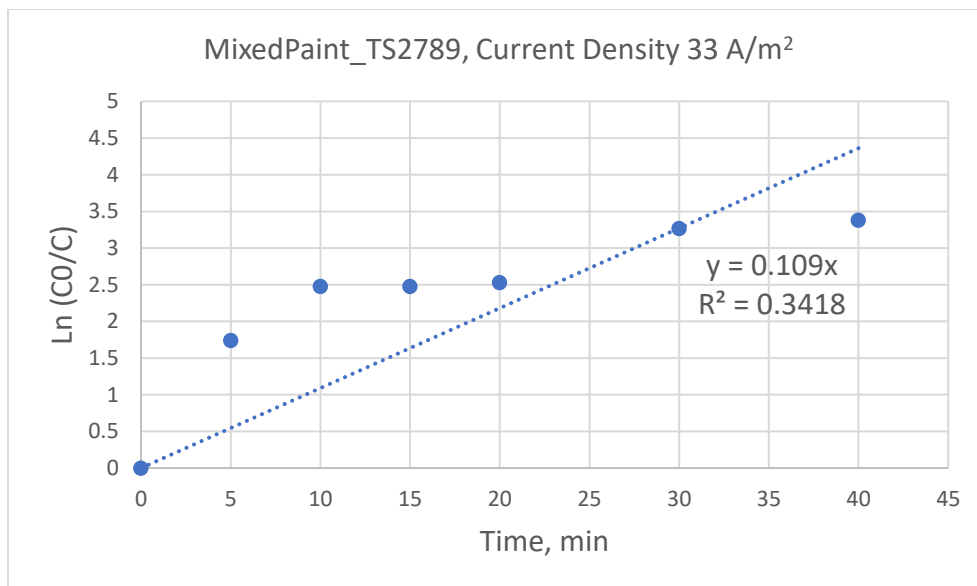


Figure A.19: MixedPaint_TS2789 Wastewater, Current Density 33 (A/m²): First-order Rate Constant (k = slope)

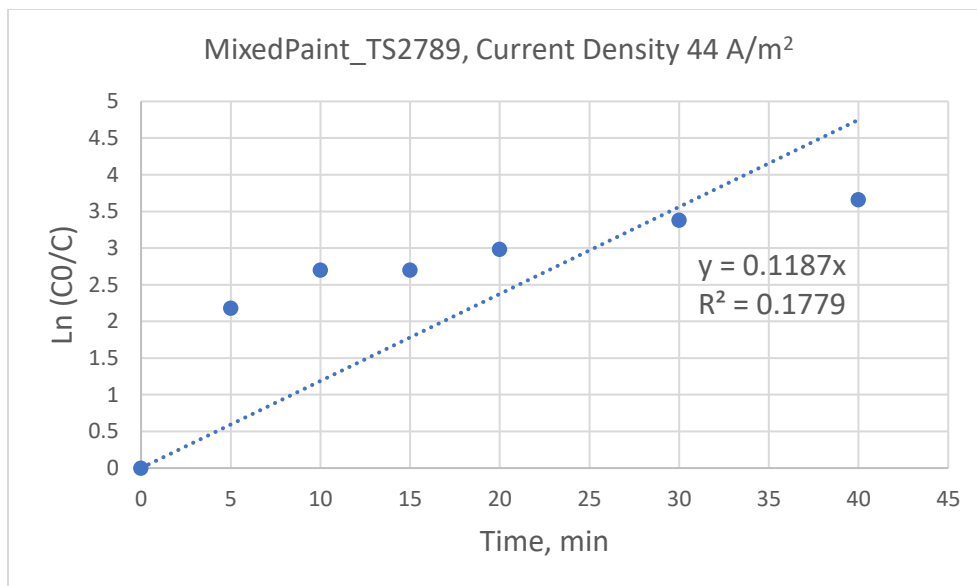


Figure A.20: MixedPaint_TS2789 Wastewater, Current Density 44 (A/m²): First-order Rate Constant (k = slope)

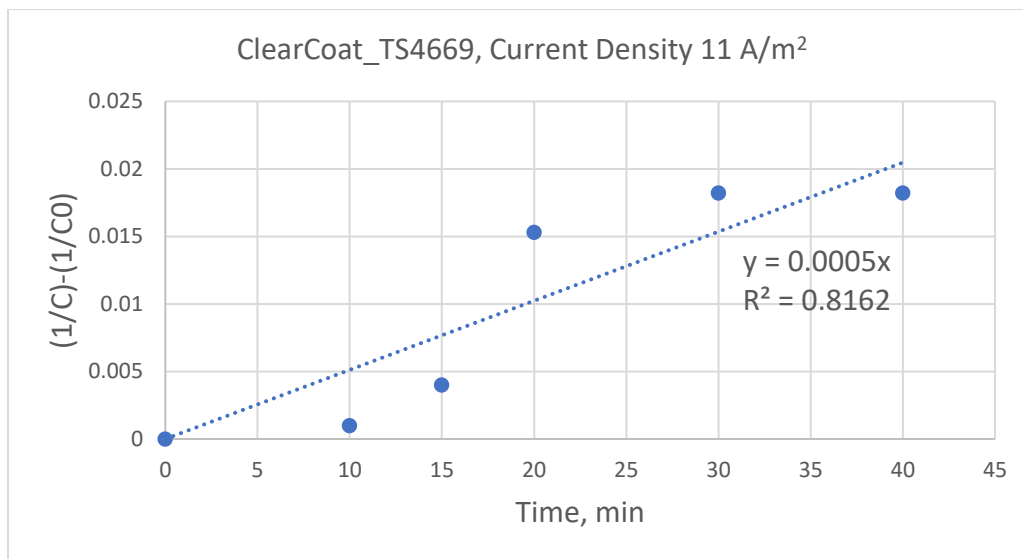


Figure A.21: ClearCoat_TS4669 Wastewater, Current Density 11 (A/m²): Second-order Rate Constant (k = slope)

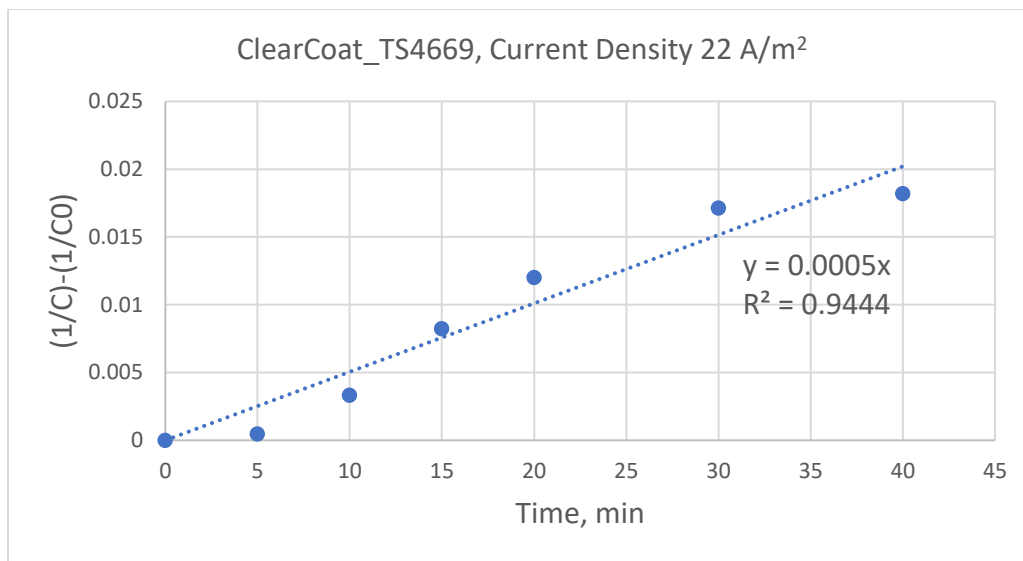


Figure A.22: ClearCoat_TS4669 Wastewater, Current Density 22 (A/m²): Second-order Rate Constant (k = slope)

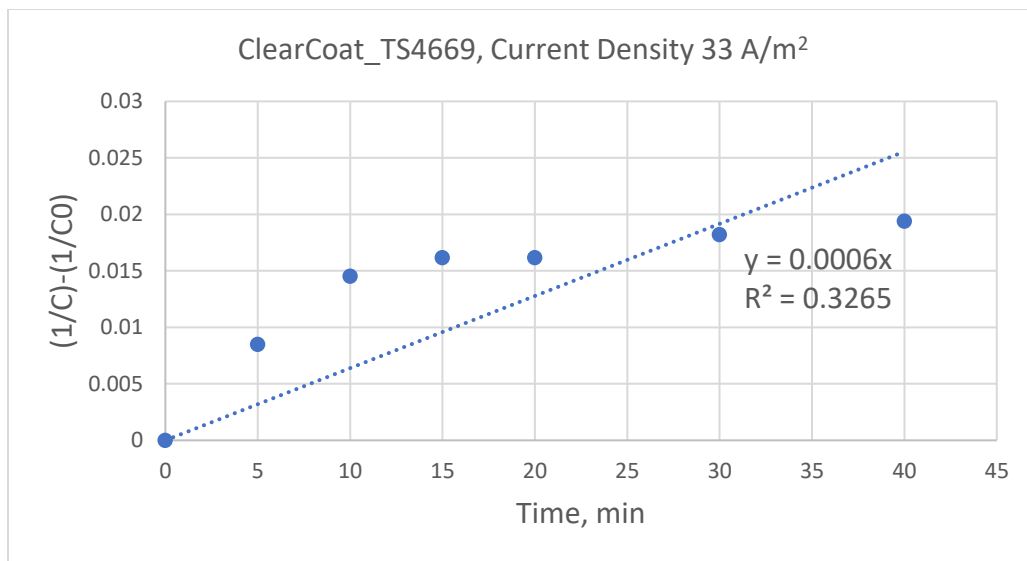


Figure A.23: ClearCoat_TS4669 Wastewater, Current Density 33 (A/m²): Second-order Rate Constant (k = slope)

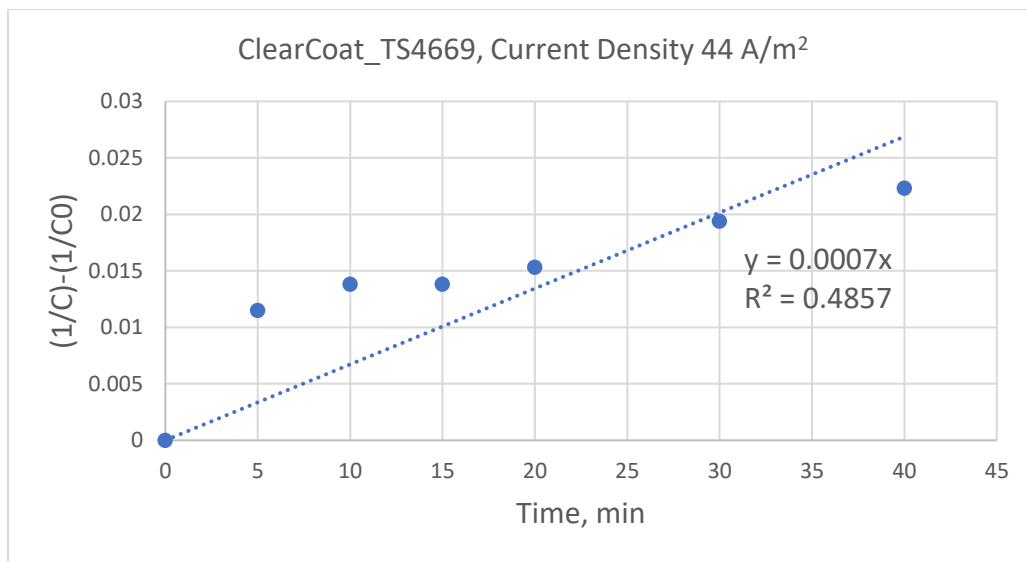


Figure A.24: ClearCoat_TS4669 Wastewater, Current Density 44 (A/m²): Second-order Rate Constant (k = slope)

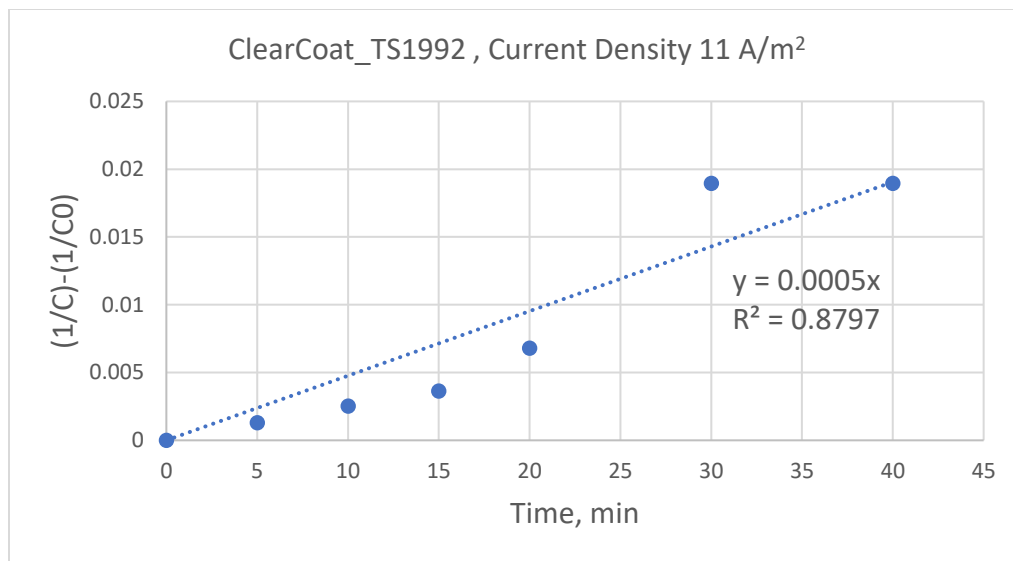


Figure A.25: ClearCoat_TS1992 Wastewater, Current Density 11 (A/m²): Second-order Rate Constant (k = slope)

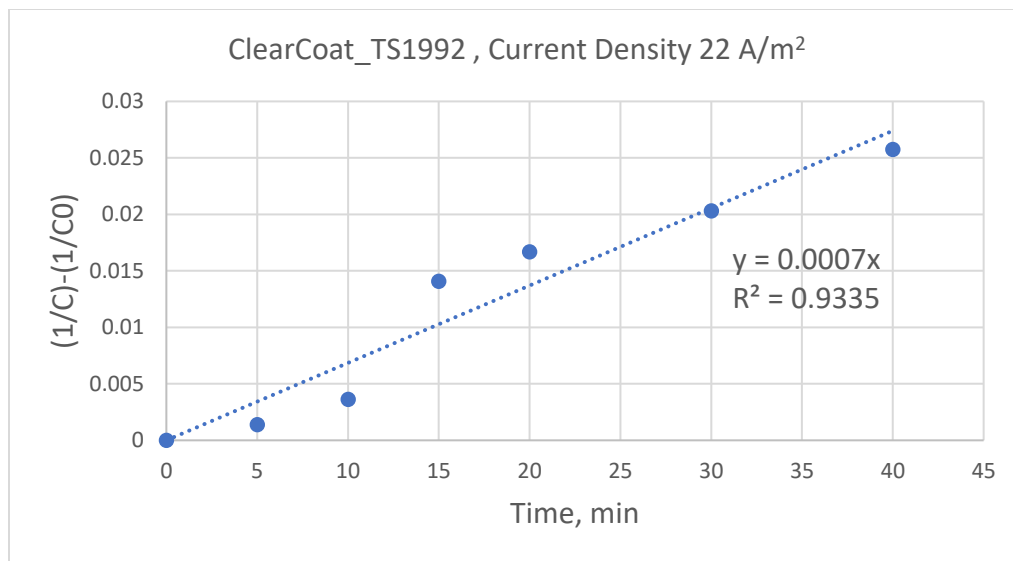


Figure A.26: ClearCoat_TS1992 Wastewater, Current Density 22 (A/m²): Second-order Rate Constant (k = slope)

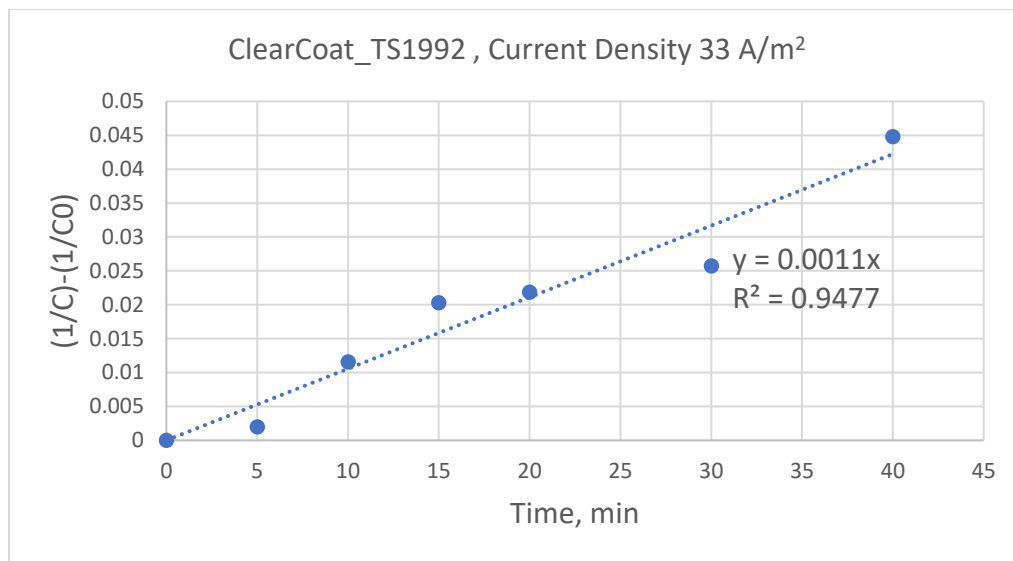


Figure A.27: ClearCoat_TS1992 Wastewater, Current Density 33 (A/m²): Second-order Rate Constant (k = slope)

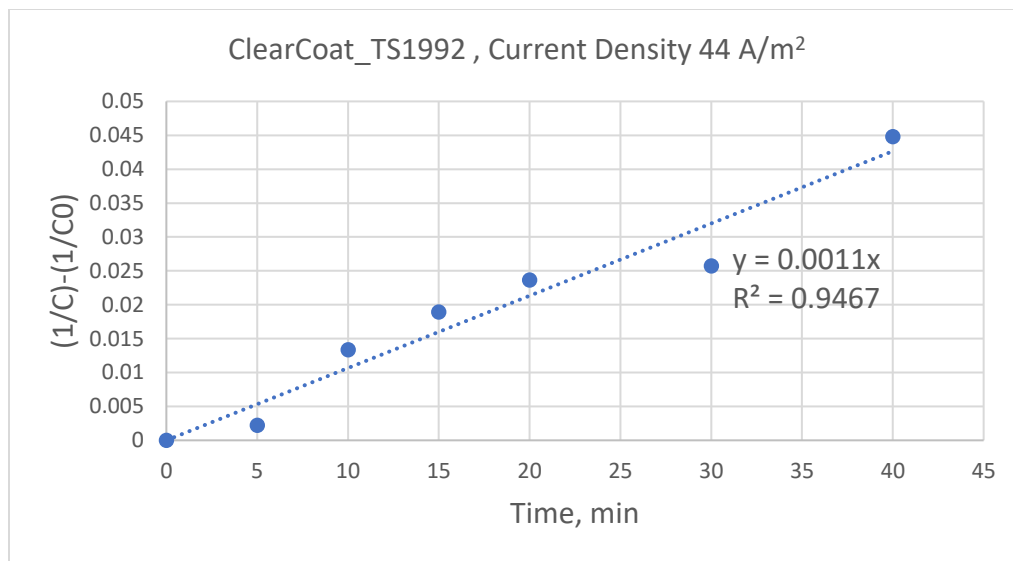


Figure A.28: ClearCoat_TS1992 Wastewater, Current Density 44 (A/m²): Second-order Rate Constant (k = slope)

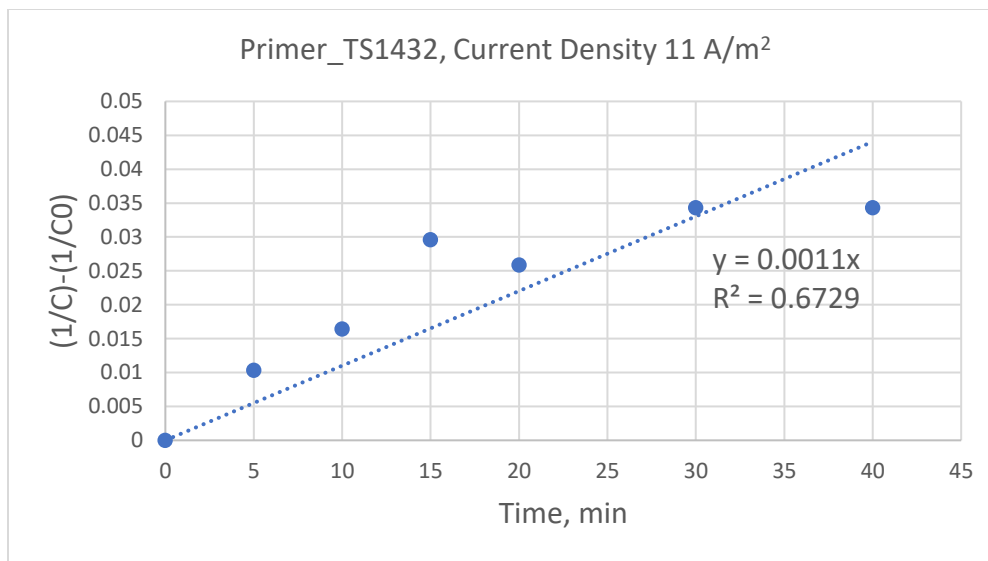


Figure A.29: Primer_TS1432 Wastewater, Current Density 11 (A/m²): Second-order Rate Constant (k = slope)

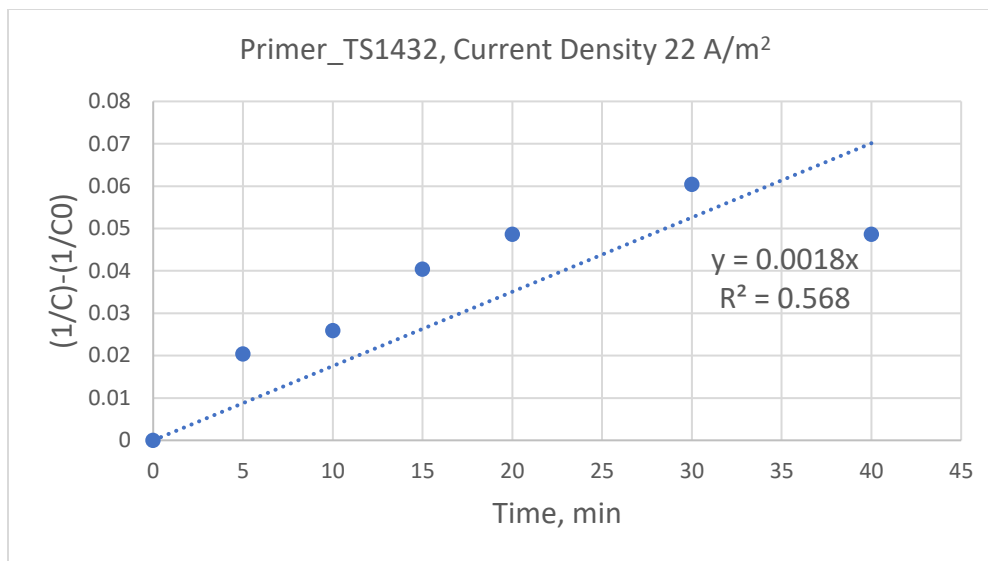


Figure A.30: Primer_TS1432 Wastewater, Current Density 22 (A/m²): Second-order Rate Constant (k = slope)

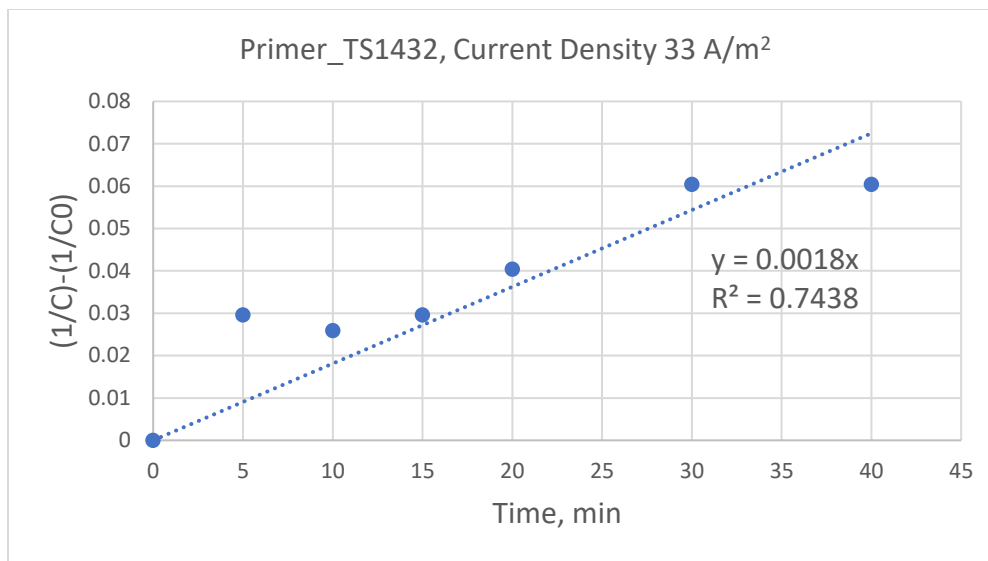


Figure A.31: Primer_TS1432 Wastewater, Current Density 33 (A/m²): Second-order Rate Constant (k = slope)

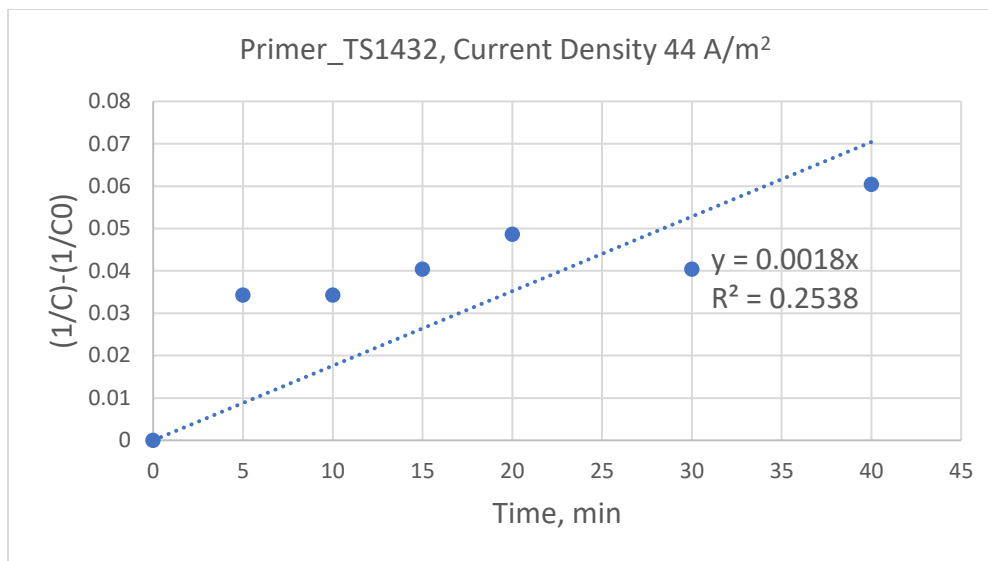


Figure A.32: Primer_TS1432 Wastewater, Current Density 44 (A/m²): Second-order Rate Constant (k = slope)

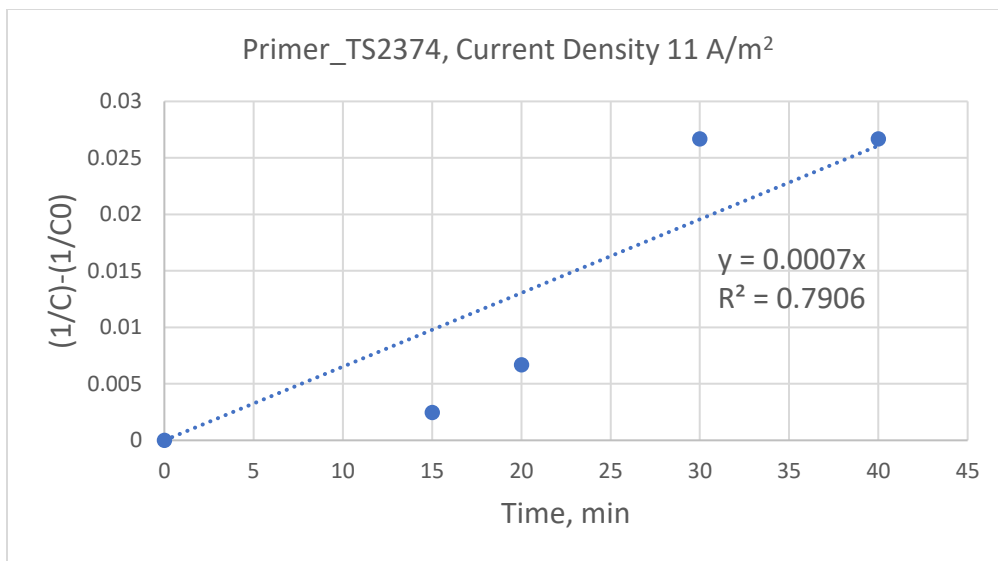


Figure A.33: Primer_TS2374 Wastewater, Current Density 11 (A/m²): Second-order Rate Constant (k = slope)

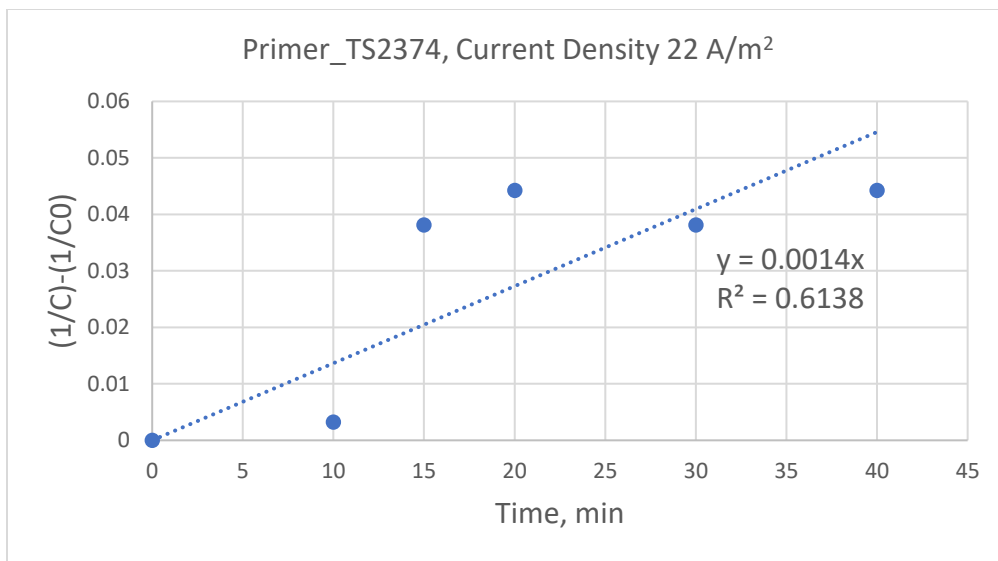


Figure A.34: Primer_TS2374 Wastewater, Current Density 22 (A/m²): Second-order Rate Constant (k = slope)

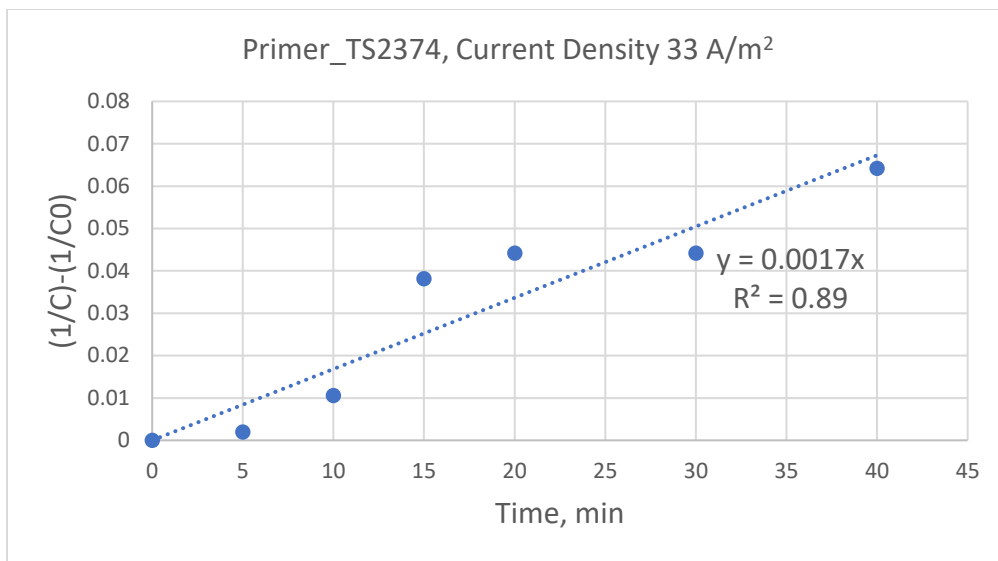


Figure A.35: Primer_TS2374 Wastewater, Current Density 33 (A/m²): Second-order Rate Constant (k = slope)

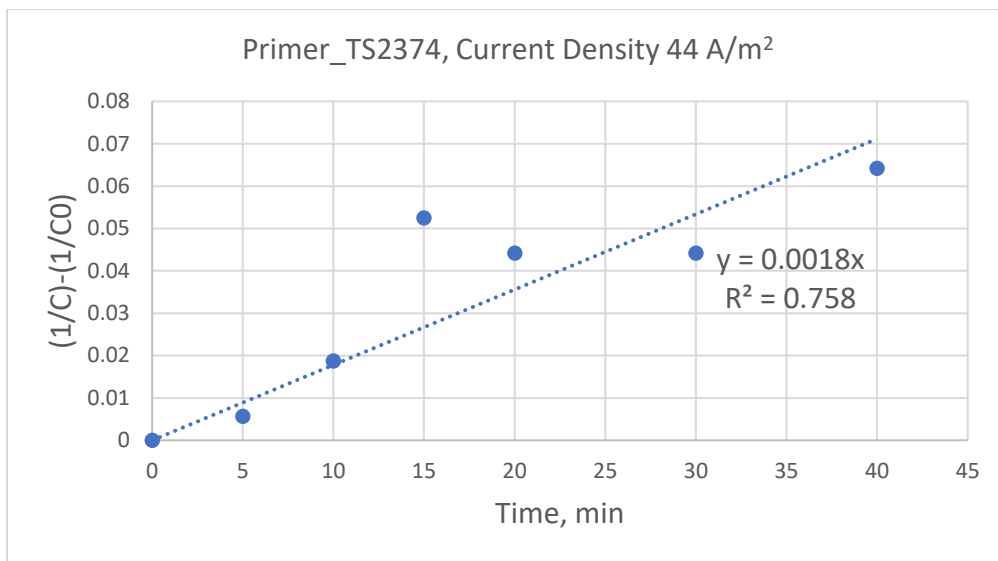


Figure A.36: Primer_TS2374 Wastewater, Current Density 44 (A/m²): Second-order Rate Constant (k = slope)

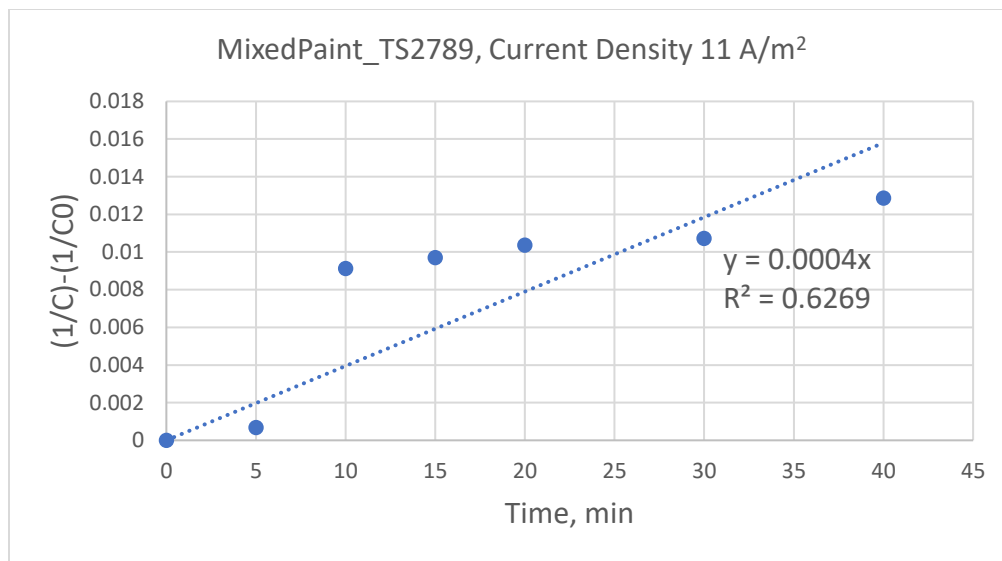


Figure A.37: MixedPaint_TS2789 Wastewater, Current Density 11 (A/m²): Second-order Rate Constant (k = slope)

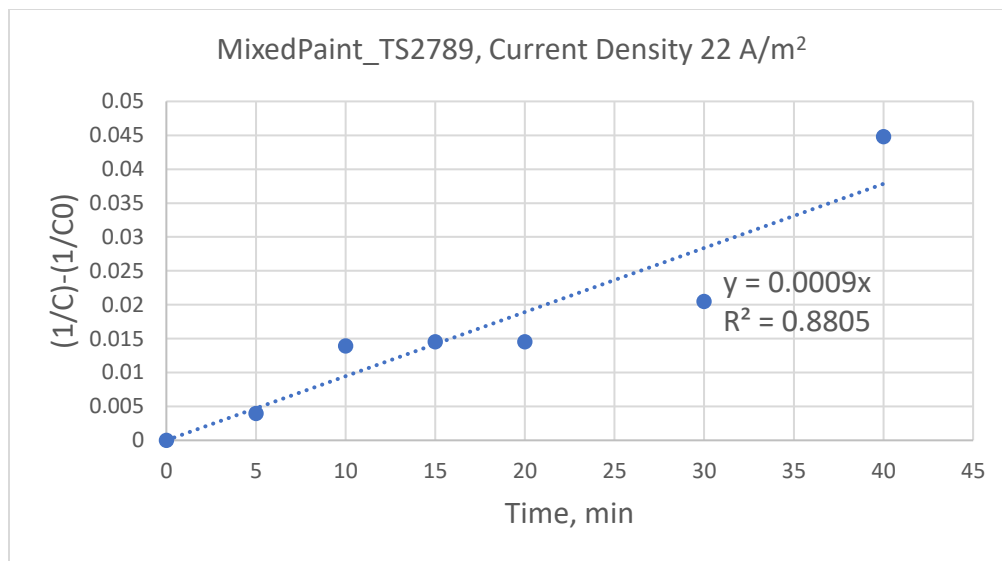


Figure A.38: MixedPaint_TS2789 Wastewater, Current Density 22 (A/m²): Second-order Rate Constant (k = slope)

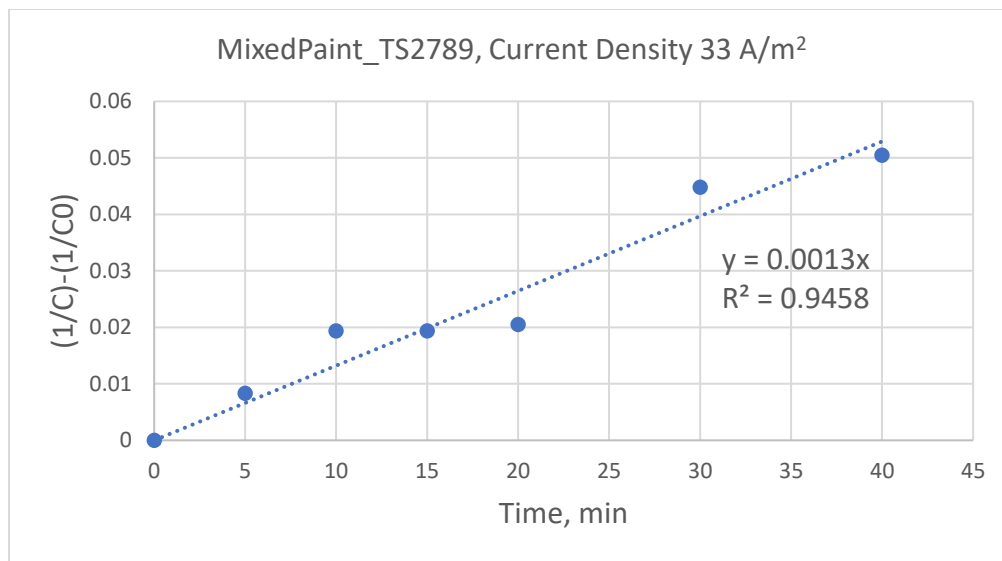


Figure A.39: MixedPaint_TS2789 Wastewater, Current Density 33 (A/m²): Second-order Rate Constant (k = slope)

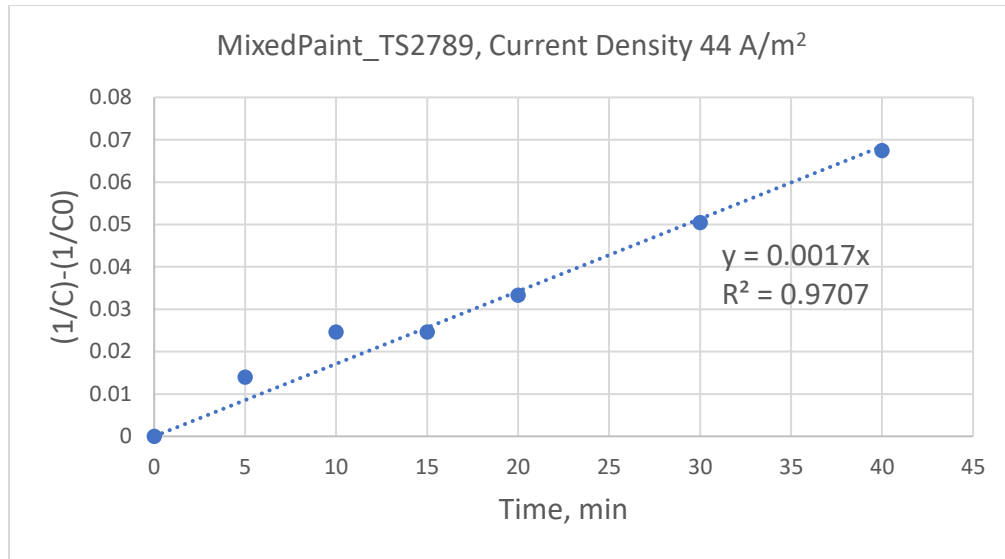


Figure A.40: MixedPaint_TS2789 Wastewater, Current Density 44 (A/m²): Second-order Rate Constant (k = slope)

Appendix B

Table B.1: TSS values in different conditions

Run No.	initial TS (mg/L)	Applied Current Density(A/m ²)	Hydraulic Retention Time (min)	TSS _{eff} 1 (mg/L)	TSS _{eff} 2 (mg/L)	TSS _{eff} 3 (mg/L)
1	500	50	4	37	41	39
2	500	75	4	25	23	27
3	500	100	4	24	25	25
4	500	50	6	38	37	41
5	500	75	6	24	25	24
6	500	100	6	18	18	17
7	500	50	8	25	26	26
8	500	75	8	15	14	15
9	500	100	8	10	9	9
10	1500	50	4	154	160	160
11	1500	75	4	146	143	142
12	1500	100	4	128	128	127
13	1500	50	6	118	117	115
14	1500	75	6	113	115	114
15	1500	100	6	88	88	87
16	1500	50	8	104	102	100
17	1500	75	8	66	65	69
18	1500	100	8	46	47	47
19	3000	50	4	478	473	477

Run No.	initial TS (mg/L)	Applied Current Density(A/m ²)	Hydraulic Retention Time (min)	TSS _{eff} 1 (mg/L)	TSS _{eff} 2 (mg/L)	TSS _{eff} 3 (mg/L)
20	3000	75	4	373	378	375
21	3000	100	4	331	324	323
22	3000	50	6	449	443	442
23	3000	75	6	298	303	296
24	3000	100	6	279	278	279
25	3000	50	8	347	347	344
26	3000	75	8	287	289	296
27	3000	100	8	160	164	167

Table B.2: Conductivity values in different conditions

Run No.	initial TS (mg/L)	Applied Current Density(A/m ²)	Hydraulic Retention Time (min)	Conductivity _{eff 1} (μS/cm)	Conductivity _{eff 2} (μS/cm)	Conductivity _{eff 3} (μS/cm)
1	500	50	4	342	345	345
2	500	75	4	347	345	344
3	500	100	4	340	346	351
4	500	50	6	340	347	344
5	500	75	6	342	347	346
6	500	100	6	341	346	356
7	500	50	8	345	342	344
8	500	75	8	346	347	347
9	500	100	8	346	352	353
10	1500	50	4	1093	1084	1086
11	1500	75	4	1089	1090	1089
12	1500	100	4	1091	1090	1094
13	1500	50	6	1079	1089	1096
14	1500	75	6	1092	1085	1095
15	1500	100	6	1094	1091	1102
16	1500	50	8	1092	1095	1079
17	1500	75	8	1086	1101	1094
18	1500	100	8	1092	1112	1102
19	3000	50	4	2330	2345	2337
20	3000	75	4	2327	2345	2349

Run No.	initial TS (mg/L)	Applied Current Density(A/m ²)	Hydraulic Retention Time (min)	Conductivity _{eff} 1 (μS/cm)	Conductivity _{eff} 2 (μS/cm)	Conductivity _{eff} 3 (μS/cm)
21	3000	100	4	2335	2345	2358
22	3000	50	6	2339	2337	2340
23	3000	75	6	2356	2347	2330
24	3000	100	6	2350	2355	2354
25	3000	50	8	2336	2346	2339
26	3000	75	8	2351	2349	2357
27	3000	100	8	2353	2362	2385

Table B.3: pH values in different conditions

Run No.	initial TS (mg/L)	Applied Current Density(A/m ²)	Hydraulic Retention Time (min)	pH _{eff} 1	pH _{eff} 2	pH _{eff} 3
1	500	50	4	6.90	6.91	6.93
2	500	75	4	6.98	6.99	6.99
3	500	100	4	7.10	7.15	7.16
4	500	50	6	6.95	6.91	6.92
5	500	75	6	7.08	7.07	7.08
6	500	100	6	7.30	7.35	7.36
7	500	50	8	6.98	6.95	6.96
8	500	75	8	7.21	7.22	7.22
9	500	100	8	7.76	7.77	7.73
10	1500	50	4	6.65	6.66	6.69
11	1500	75	4	6.75	6.74	6.74
12	1500	100	4	6.89	6.88	6.86
13	1500	50	6	6.71	6.68	6.70
14	1500	75	6	6.76	6.83	6.83
15	1500	100	6	7.03	7.10	7.06
16	1500	50	8	6.77	6.72	6.74
17	1500	75	8	6.94	6.95	6.94
18	1500	100	8	7.38	7.41	7.43
19	3000	50	4	6.61	6.63	6.61
20	3000	75	4	6.66	6.70	6.67
21	3000	100	4	6.78	6.82	6.82

Run No.	initial TS (mg/L)	Applied Current Density(A/m ²)	Hydraulic Retention Time (min)	pH _{eff} 1	pH _{eff} 2	pH _{eff} 3
22	3000	50	6	6.65	6.63	6.62
23	3000	75	6	6.74	6.77	6.75
24	3000	100	6	7.01	7.02	7.00
25	3000	50	8	6.66	6.63	6.65
26	3000	75	8	6.97	6.90	6.87
27	3000	100	8	7.42	7.37	7.36

Table B.4: Turbidity values in different conditions

Run No.	initial TS (mg/L)	Applied Current Density(A/m ²)	Hydraulic Retention Time (min)	Turbidity _{eff 1} (NTU)	Turbidity _{eff 2} (NTU)	Turbidity _{eff 3} (NTU)
1	500	50	4	91	95	92
2	500	75	4	46	44	53
3	500	100	4	45	45	50
4	500	50	6	91	93	94
5	500	75	6	44	40	47
6	500	100	6	33	29	30
7	500	50	8	53	55	46
8	500	75	8	26	23	22
9	500	100	8	11	10	11
10	1500	50	4	422	430	425
11	1500	75	4	373	360	368
12	1500	100	4	303	302	300
13	1500	50	6	260	262	268
14	1500	75	6	249	248	259
15	1500	100	6	170	171	170
16	1500	50	8	215	214	214
17	1500	75	8	118	115	110
18	1500	100	8	70	74	70
19	3000	50	4	1523	1517	1512
20	3000	75	4	1023	1031	1020
21	3000	100	4	815	818	810

Run No.	initial TS (mg/L)	Applied Current Density(A/m ²)	Hydraulic Retention Time (min)	Turbidity _{eff} 1 (NTU)	Turbidity _{eff} 2 (NTU)	Turbidity _{eff} 3 (NTU)
22	3000	50	6	1364	1360	1355
23	3000	75	6	705	710	717
24	3000	100	6	638	638	637
25	3000	50	8	892	899	896
26	3000	75	8	671	690	680
27	3000	100	8	283	288	291

Appendix C

Table C.1: RTD experiment results for HRT=7.4 min and Electroflotation=ON: EC, concentration, F(t) and E(t) values at different times

Time, min	EC, $\mu\text{S}/\text{cm}$	NaCl Concentration, mg/L	F(t), -	E(t), min^{-1}
0	298	0	0.000	0.000
0.5	302	0	0.000	0.000
1	302	2	0.001	0.001
1.5	493	40	0.012	0.022
2	668	137	0.041	0.058
2.5	937	288	0.085	0.089
3	1208	439	0.129	0.089
3.5	1607	661	0.195	0.131
4	2060	914	0.270	0.149
4.5	2450	1132	0.334	0.128
5	2880	1372	0.404	0.141
5.5	3260	1584	0.467	0.125
6	3540	1740	0.513	0.092
6.5	3890	1935	0.571	0.115
7	4280	2153	0.635	0.128
7.5	4420	2231	0.658	0.046
8	4610	2337	0.689	0.063
8.5	4620	2342	0.691	0.003
9	4850	2471	0.729	0.076
9.5	5010	2560	0.755	0.053
10	5010	2560	0.755	0.000
10.5	5150	2638	0.778	0.046
11	5270	2705	0.798	0.039
11.5	5400	2777	0.819	0.043

Time, min	EC, $\mu\text{S}/\text{cm}$	NaCl Concentration, mg/L	F(t), -	E(t), min^{-1}
12	5460	2811	0.829	0.020
12.5	5510	2839	0.837	0.016
13	5640	2911	0.859	0.043
13.5	5760	2978	0.878	0.039
14	5900	3056	0.901	0.046
14.5	6000	3112	0.918	0.033
15	6080	3157	0.931	0.026
15.5	6160	3201	0.944	0.026
16	6220	3235	0.954	0.020
16.5	6290	3274	0.965	0.023
17	6340	3302	0.974	0.016
17.5	6380	3324	0.980	0.013
18	6420	3347	0.987	0.013
18.5	6450	3363	0.992	0.010
19	6470	3374	0.995	0.007
19.5	6500	3391	1.000	0.010
20	6500	3391	1.000	0.000

**Table C.2: RTD experiment results for HRT=7.4 min and Electroflotation=OFF:
EC, concentration, F(t) and E(t) values at different times**

Time, min	EC, $\mu\text{S}/\text{cm}$	NaCl Concentration, mg/L	F(t), -	E(t), min^{-1}
0	340	0	0.000	0.000
0.5	343	0	0.000	0.000
1	322	10	0.003	0.006
1.5	324	11	0.003	0.001
2	392	30	0.009	0.011
2.5	597	98	0.029	0.040
3	1478	589	0.174	0.290
3.5	1892	820	0.242	0.136
4	2400	1104	0.325	0.167
4.5	2660	1249	0.368	0.086
5	2880	1372	0.404	0.072
5.5	3040	1461	0.431	0.053
6	3290	1600	0.472	0.082
6.5	3610	1779	0.525	0.105
7	3710	1835	0.541	0.033
7.5	3810	1890	0.557	0.033
8	4380	2208	0.651	0.188
8.5	4630	2348	0.692	0.082
9	4630	2348	0.692	0.000
9.5	4880	2487	0.733	0.082
10	4930	2515	0.742	0.016
10.5	4970	2538	0.748	0.013
11	5140	2632	0.776	0.056
11.5	5310	2727	0.804	0.056
12	5470	2817	0.831	0.053
12.5	5630	2906	0.857	0.053
13	5760	2978	0.878	0.043

Time, min	EC, $\mu\text{S}/\text{cm}$	NaCl Concentration, mg/L	F(t), -	E(t), min^{-1}
13.5	5880	3045	0.898	0.039
14	6020	3123	0.921	0.046
14.5	6120	3179	0.937	0.033
15	6200	3224	0.951	0.026
15.5	6280	3268	0.964	0.026
16	6340	3302	0.974	0.020
16.5	6410	3341	0.985	0.023
17	6430	3352	0.988	0.007
17.5	6460	3369	0.993	0.010
18	6480	3380	0.997	0.007
18.5	6500	3391	1.000	0.007
19	6500	3391	1.000	0.000
19.5	6500	3391	1.000	0.000
20	6500	3391	1.000	0.000

Table C.3: RTD experiment results for HRT=8.5 min and Electroflotation=ON: EC, concentration, F(t) and E(t) values at different times

Time, min	EC, $\mu\text{S}/\text{cm}$	NaCl Concentration, mg/L	F(t), -	E(t), min^{-1}
0	320	0	0.000	0.000
1	406	0	0.000	0.000
2	1051	351	0.109	0.109
3	1260	468	0.145	0.036
4	2000	881	0.273	0.128
5	2780	1316	0.408	0.135
6	3520	1729	0.536	0.128
7	3930	1957	0.607	0.071
8	4130	2069	0.642	0.035
9	4430	2236	0.694	0.052
10	4740	2409	0.747	0.054
11	4860	2476	0.768	0.021
12	5010	2560	0.794	0.026
13	5250	2694	0.836	0.042
14	5430	2794	0.867	0.031
15	5520	2844	0.882	0.016
16	5650	2917	0.905	0.022
17	5690	2939	0.912	0.007
18	5700	2945	0.913	0.002
19	5740	2967	0.920	0.007
20	5830	3017	0.936	0.016
21	5920	3068	0.952	0.016
22	5960	3090	0.958	0.007
23	6020	3123	0.969	0.010
24	6060	3146	0.976	0.007
25	6080	3157	0.979	0.003
26	6110	3174	0.984	0.005

Time, min	EC, $\mu\text{S}/\text{cm}$	NaCl Concentration, mg/L	F(t), -	E(t), min^{-1}
27	6150	3196	0.991	0.007
28	6190	3218	0.998	0.007
29	6200	3224	1.000	0.002
30	6200	3224	1.000	0.000

**Table C.4: RTD experiment results for HRT=8.5 min and Electroflotation=OFF:
EC, concentration, F(t) and E(t) values at different times**

Time, min	EC, $\mu\text{S}/\text{cm}$	NaCl Concentration, mg/L	F(t), -	E(t), min^{-1}
0	298	0	0.000	0.000
1	299	0	0.000	0.000
2	1499	601	0.183	0.183
3	2200	992	0.303	0.119
4	2900	1383	0.422	0.119
5	3230	1567	0.478	0.056
6	3570	1757	0.536	0.058
7	4100	2052	0.626	0.090
8	4290	2158	0.658	0.032
9	4430	2236	0.682	0.024
10	4590	2326	0.709	0.027
11	4770	2426	0.740	0.031
12	5100	2610	0.796	0.056
13	5130	2627	0.801	0.005
14	5320	2733	0.833	0.032
15	5390	2772	0.845	0.012
16	5410	2783	0.849	0.003
17	5550	2861	0.872	0.024
18	5680	2934	0.895	0.022
19	5800	3001	0.915	0.020
20	6100	3168	0.966	0.051
21	6240	3246	0.990	0.024
22	6260	3257	0.993	0.003
23	6280	3268	0.997	0.003
24	6290	3274	0.998	0.002
25	6300	3280	1.000	0.002
26	6300	3280	1.000	0.000

Time, min	EC, $\mu\text{S}/\text{cm}$	NaCl Concentration, mg/L	F(t), -	E(t), min^{-1}
27	6300	3280	1.000	0.000
28	6300	3280	1.000	0.000
29	6300	3280	1.000	0.000
30	6300	3280	1.000	0.000

**Table C.5: RTD experiment results for HRT=15.3 min and Electroflotation=ON:
EC, concentration, F(t) and E(t) values at different times**

Time, min	EC, $\mu\text{S/cm}$	NaCl Concentration, mg/L	F(t), -	E(t), min^{-1}
0	440	10	0.003	0.000
1	445	13	0.004	0.001
2	803	213	0.068	0.064
3	1209	439	0.140	0.072
4	1658	690	0.220	0.080
5	1910	830	0.265	0.045
6	2190	987	0.315	0.050
7	2530	1176	0.376	0.061
8	2700	1271	0.406	0.030
9	3020	1450	0.463	0.057
10	3180	1539	0.492	0.029
11	3220	1561	0.499	0.007
12	3720	1840	0.588	0.089
13	3830	1902	0.608	0.020
14	3990	1991	0.636	0.029
15	4150	2080	0.665	0.029
16	4350	2192	0.700	0.036
17	4500	2275	0.727	0.027
18	4590	2326	0.743	0.016
19	4620	2342	0.749	0.005
20	4760	2420	0.774	0.025
21	4880	2487	0.795	0.021
22	4960	2532	0.809	0.014
23	5030	2571	0.822	0.012
24	5080	2599	0.831	0.009
25	5180	2655	0.848	0.018
26	5260	2699	0.863	0.014

Time, min	EC, $\mu\text{S}/\text{cm}$	NaCl Concentration, mg/L	F(t), -	E(t), min^{-1}
27	5320	2733	0.873	0.011
28	5330	2738	0.875	0.002
29	5380	2766	0.884	0.009
30	5440	2800	0.895	0.011
31	5480	2822	0.902	0.007
32	5510	2839	0.907	0.005
33	5560	2867	0.916	0.009
34	5590	2883	0.922	0.005
35	5610	2895	0.925	0.004
36	5650	2917	0.932	0.007
37	5690	2939	0.939	0.007
38	5740	2967	0.948	0.009
39	5750	2973	0.950	0.002
40	5770	2984	0.954	0.004
41	5790	2995	0.957	0.004
42	5800	3001	0.959	0.002
43	5810	3006	0.961	0.002
44	5820	3012	0.963	0.002
45	5870	3040	0.971	0.009
46	5890	3051	0.975	0.004
47	5930	3073	0.982	0.007
48	5950	3084	0.986	0.004
49	5990	3107	0.993	0.007
50	6010	3118	0.996	0.004
51	6030	3129	1.000	0.004
52	6030	3129	1.000	0.000

**Table C.6: RTD experiment results for HRT=15.3 min and Electroflotation=OFF:
EC, concentration, F(t) and E(t) values at different times**

Time, min	EC, $\mu\text{S}/\text{cm}$	NaCl Concentration, mg/L	F(t), -	E(t), min^{-1}
0	345	0	0.000	0.000
1	349	0	0.000	0.000
2	994	319	0.102	0.102
3	1427	561	0.179	0.077
4	1574	643	0.205	0.026
5	1980	869	0.277	0.072
6	2190	987	0.315	0.037
7	2410	1109	0.354	0.039
8	3000	1439	0.459	0.105
9	3030	1455	0.464	0.005
10	3290	1600	0.511	0.046
11	3300	1606	0.512	0.002
12	3630	1790	0.571	0.059
13	3860	1918	0.612	0.041
14	3940	1963	0.626	0.014
15	4110	2058	0.656	0.030
16	4300	2164	0.690	0.034
17	4400	2220	0.708	0.018
18	4530	2292	0.731	0.023
19	4770	2426	0.774	0.043
20	4780	2432	0.776	0.002
21	4930	2515	0.802	0.027
22	4980	2543	0.811	0.009
23	5140	2632	0.840	0.028
24	5170	2649	0.845	0.005
25	5230	2683	0.856	0.011
26	5270	2705	0.863	0.007

Time, min	EC, $\mu\text{S}/\text{cm}$	NaCl Concentration, mg/L	F(t), -	E(t), min^{-1}
27	5340	2744	0.875	0.012
28	5370	2761	0.881	0.005
29	5420	2789	0.890	0.009
30	5480	2822	0.900	0.011
31	5520	2844	0.907	0.007
32	5540	2856	0.911	0.004
33	5590	2883	0.920	0.009
34	5620	2900	0.925	0.005
35	5680	2934	0.936	0.011
36	5710	2950	0.941	0.005
37	5740	2967	0.947	0.005
38	5750	2973	0.948	0.002
39	5760	2978	0.950	0.002
40	5770	2984	0.952	0.002
41	5770	2984	0.952	0.000
42	5810	3006	0.959	0.007
43	5850	3029	0.966	0.007
44	5860	3034	0.968	0.002
45	5870	3040	0.970	0.002
46	5880	3045	0.972	0.002
47	5890	3051	0.973	0.002
48	5960	3090	0.986	0.012
49	5980	3101	0.989	0.004
50	6040	3135	1.000	0.011
51	6040	3135	1.000	0.000
52	6040	3135	1.000	0.000

Curriculum Vitae

Name: Syed Reza Mohtashami

Post-secondary Education and Degrees: Western University
London, Ontario, Canada
2014-2018 Ph.D.

Shiraz University
Shiraz, Fars, Iran
2010 M.Sc.

Shiraz University
Shiraz, Fars, Iran
2005 B.Sc.

Honours and Awards: WGRS – ENGINEERING Scholarship
Western University
2014-2018

University Scholarship
Shiraz University
2010

Related Work Experience Teaching and Research Assistant
Western University
2014-2018

Project Manager and Design Engineer
MSE Company and JKS Consultant Company, Iran
2010-2014

Publications:

Mohtashami, R., Shang, J. Q., & Xu, Y. (2018). Treatment of Automotive Paint Wastewater Using Electroflotation: Kinetic Study, Influencing Factors and Data Analysis. *Environmental Processes*, 1-15.

Mohtashami, S. R., Karimi Jashni, A., & Bidokhti, T. (2008). Performance of Anaerobic Baffled Reactor (ABR) in landfill leachate treatment. *Water and Wastewater*, 66, 10-8.

Mohtashami, S. R., Karimi Jashni, A. (2008). Biological Treatment of Landfill Leachate Using A Combined Anaerobic/Aerobic System. International Conference of Environmental Engineering and Environmental Issues, Enviro2008, Melbourne, Australia.

Mohtashami, S. R., Taleb Beidokhti, N. (2007). "Air Pollution Resulting from Agricultural Activities in Iran". National Conference of World Environment Day-Iran, Tehran, Iran.

Mohtashami, S. R., Karimi Jashni, A. (2007). "Study of Use of Iodine in Water Treatment". National Conference of World Environment Day-Iran, Tehran, Iran.

Mohtashami, S. R., Karimi Jashni, A. (2006). "Marine Discharge of Wastewater in Coastal Zones, Assessment and Design". 7th International Conference on Coastal, Ports and Marine Structures, ICOPMAS 2006, Tehran, Iran.